

PhD. 25710

Collapse of Masonry Structures



A dissertation submitted to the University of Cambridge
in partial fulfilment of the requirements for the
degree of Doctor of Philosophy

by

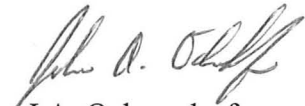
John Allen Ochsendorf



To Professor Jacques Heyman

Declaration

The work described in this dissertation was carried out in the Department of Engineering at the University of Cambridge between September 1998 and April 2002. The author declares that, except for commonly understood and accepted ideas, or where specific reference is made to the work of others, the content of this dissertation is his own work and includes nothing that is the outcome of work done in collaboration. This dissertation has not been submitted previously, in part or in whole, to any university or institution for any degree, diploma, or other qualification. The length of this dissertation is 185 pages and it contains 84 figures and approximately 45,000 words including appendices and references.



J.A. Ochsendorf
May 2002

Acknowledgements

I wish to thank both of my supervisors, Professor Jacques Heyman and Professor Christopher R. Calladine, for guiding my research. I will always value the many hours we spent discussing my ideas, and it has been a wonderful privilege to work with both professors. This project would not have been possible without their assistance.

I am indebted to Professor Santiago Huerta, who inspired my work in new directions and welcomed me as a visiting researcher in the Building Structures Department of the Escuela Técnica Superior de Arquitectura at the Universidad Politécnica de Madrid. Professor Huerta offered constant encouragement as well as his formidable knowledge of the history of masonry mechanics. The final version of the dissertation owes much to Professor Huerta, and in particular, he shared his knowledge of the history of buttress design and collapse based on years of careful research. Thus, much of the historical review of Chapter 2 is derived from Professor Huerta's scholarship and I fully acknowledge his generosity in sharing openly with me. I am extremely grateful for his assistance and his friendship.

Professor José Ignacio Hernando, also of the Universidad Politécnica de Madrid, contributed to the work on the buttress fracture and verified the results with his own linear-programming methods.

Numerous members of the Engineering Department helped me and I would like to thank Dr. Campbell Middleton and Mrs. Rowena Baxter in particular, both of whom I turned to on many occasions. I am also thankful for the laboratory assistance of Mr. Roger Denston and Mr. Martin Toohey.

Mr. S.C. Deshpande of S.E.W.R.I. Consultants Ltd., Mumbai, India, kindly provided the information for the case study on the church at Goa.

Professor Mary J. Sansalone and Mr. Erik Y. Lin carefully read early drafts of the dissertation and the final version is greatly improved as a result of their comments.

I wish to express my gratitude to Mr. Allan McRobie, Professor Thomas Boothby, Dr. Robin Spence, Dr. Steve Denton, Dr. Janet Lees, Professor Fernando Pérez, and Professor Pere Roca for their personal assistance or timely advice at various stages in my research.

I am pleased to acknowledge the National Science Foundation and the J. William Fulbright Foundation of the United States for providing primary financial support. I received additional funding from King's College, the Cambridge Overseas Trust, and the Centre for Latin American Studies at the University of Cambridge.

I am forever indebted to my mentor, Professor Mary J. Sansalone, for her inspiration, guidance, and friendship, which has been central to my personal and intellectual growth for the last ten years. Professor William B. Streett also encouraged my studies at Cambridge and has served as an important role model for me.

I would like to thank all of my friends who have taught me so much about life, and in particular, my fellow King's College scrabblers, William Grundy and Fritha Wolsak, who taught me the importance of the beautiful game. Most of all, I would like to thank my family for their unending support and encouragement.

Abstract

This dissertation examines the collapse of masonry structures in response to large support displacements and horizontal ground accelerations. There are two main classes of masonry structure: arches that thrust, and supporting elements, such as walls and buttresses, which resist the thrust. This dissertation analyses the safety of arches and buttresses and identifies the resulting collapse mechanisms due to support displacements or horizontal accelerations. In particular, this research investigates the stability of a masonry arch supported on buttresses and the conditions necessary for collapse to occur. Engineers are frequently asked to determine the safety of masonry structures that have been severely distorted over the years, often due to subsidence or other long-term movements in the foundations, and this dissertation provides guidance in the assessment of such structures.

The resistance of masonry buttresses to high-level horizontal loads is examined. In the case of failure due to overturning, a fracture will develop in the masonry, significantly reducing the resistance of the buttress. The capacity is further reduced by outward leaning of the buttresses, a common source of distress for masonry structures due to movements in the supporting foundations. Based on these considerations, new measures of safety are proposed for buttresses under horizontal loading.

Outward leaning of the buttresses increases the span of the arch or vault. Spreading supports will cause large deformations in the arch, which increase the horizontal thrust of the arch and may lead to collapse. In addition, lateral ground accelerations can cause the collapse of arches. The influence of seismic action can be approximated to first order by equivalent static analysis to determine the initial collapse mechanism. These problems are analysed for circular masonry arches, and the collapse conditions are identified for various geometries.

The findings are combined to investigate the stability of the masonry arch supported on buttresses. The safety of the system is examined by studying the influence of imposed displacements. As the buttresses lean, the thrust of the vault increases and the resistance of the buttress decreases. The collapse mechanisms are identified for both the static case of leaning buttresses and the dynamic case of horizontal acceleration. This analysis illustrates that the arch will collapse and the buttresses will remain standing in most cases.

Based on these considerations, new methods are proposed for assessing the safety of masonry structures and determining the influence of future movements on the stability of existing masonry structures.

Table of Contents

Declaration.....	i
Acknowledgements	ii
Abstract.....	iii
Table of Contents	iv
Notation.....	vii
List of Tables	x
List of Figures.....	xi
I. INTRODUCTION	1
1 Introduction.....	2
1.1 Introduction.....	2
1.2 Statement of Problem.....	3
1.3 Collapse of Masonry Structures.....	5
1.4 Motivations for Research.....	6
1.5 Summary	7
2 Literature Review	9
2.1 Theory of Masonry Structures	9
2.2 Methods of Analysis	11
2.3 The Masonry Buttress.....	13
2.4 The Masonry Arch	16
2.5 Arches on Buttresses.....	20
2.6 Measures of Safety.....	26
2.7 Summary	27
II. THE MASONRY BUTTRESS.....	29
3 Collapse of Masonry Buttresses.....	30
3.1 Introduction.....	30
3.2 Mechanism of Collapse.....	31
3.3 Proof of Straight Fracture	32
3.4 Equations of Equilibrium.....	36
3.5 Limits on Sliding	40
3.6 Rectangular Buttresses.....	40
3.7 Non-Rectangular Buttresses.....	45
3.8 Experimental Results	48
3.9 Summary	51

4	Leaning Buttresses	53
	4.1 Introduction.....	53
	4.2 Shape of Fracture for Leaning Buttresses	54
	4.3 Leaning Rectangular Buttresses.....	55
	4.4 Thrust Capacity of Leaning Buttresses	59
	4.5 Safety of Buttresses.....	61
	4.6 Safety of Leaning Buttresses	66
	4.7 Comparison of Safety Factors.....	68
	4.8 Summary	72
 III. THE MASONRY ARCH.....		73
5	The Masonry Arch on Spreading Supports	74
	5.1 Introduction.....	74
	5.2 Least Thickness Analysis.....	75
	5.3 Thrust of Arches	80
	5.4 Failure Mechanism for Spreading Supports	84
	5.5 Spread Limits at Collapse	88
	5.6 Effect of Voussoir Size	90
	5.7 Experimental Results	93
	5.8 Summary	95
6	The Masonry Arch under Constant Lateral Acceleration.....	98
	6.1 Introduction.....	98
	6.2 Method of Analysis.....	99
	6.3 Collapse Mechanisms	102
	6.4 Critical Hinge Locations.....	107
	6.5 Thrust at Collapse	108
	6.6 Effect of Voussoir Size	109
	6.7 Summary	110
 IV. THE BUTTRESSED ARCH.....		111
7	Collapse of Buttressed Arches	112
	7.1 Introduction.....	112
	7.2 Geometry of Buttressed Arches	114
	7.3 Arch on Leaning Buttresses	115
	7.4 Collapse Due to Horizontal Acceleration	121
	7.5 Discussion	126
	7.6 Summary	127

8	Safety of Buttressed Arches	129
	8.1 Introduction.....	129
	8.2 Case Study: Church at Old Goa, India.....	129
	8.3 Load Factor for Collapse	134
	8.4 Pressure Point Factor	135
	8.5 Safety Assessment of an Arch on Leaning Buttresses.....	137
	8.6 Seismic Safety.....	140
	8.7 Maintenance and Repair	146
	8.8 Summary	147
 V. CONCLUSIONS.....		148
9	Conclusions.....	149
	9.1 Summary of Results.....	149
	9.2 Future Work	151
 VI. APPENDICES		153
	A) Computer Programs	154
	A.1 ArchSpread.....	154
	A.2 ArchTilt.....	161
	A.3 ArchLean.....	164
	A.4 ButtressTilt.....	171
	A.5 SolidTilt	174
	B) Experimental Descriptions.....	177
	B.1 Description of Model Blocks	177
	B.2 Construction of Model Buttresses	177
	B.3 Predictions for Buttress Experiments.....	177
	C) References.....	179

Notation

The following is a list of abbreviations used in this dissertation:

- b = width of buttress at base
- d = rise of arch from intrados hinge to apex (crown) hinge at extrados
- e = vertical height of buttress fracture from the overturning hinge
- f_s = assumed static coefficient of friction for stone on stone (~ 0.7)
- g = acceleration of gravity (9.81 m/s^2)
- h = height of applied force from base of buttress
- h_b = total height of a rectangular buttress
- H = horizontal force applied to a buttress due to the thrust of an arch
- H_a = applied horizontal force
- H_{cr} = horizontal force to initiate the fracture in a buttress
- H_{max} = the maximum thrust provided by an arch
- H_{min} = the minimum thrust provided by an arch
- $H_{reduction}$ = the reduction in thrust capacity of a buttress due to leaning
- H_s = horizontal force to overturn a solid (unfractured) buttress
- H_u = horizontal force causing failure of the buttress
- H_ϕ = horizontal force causing failure of a buttress leaning by an angle ϕ
- $H_{s\phi}$ = horizontal force to overturn a solid buttress leaning by an angle ϕ
- $H_{\phi cr}$ = horizontal force to initiate the fracture in a leaning buttress
- I = location of instantaneous centre for the central portion of an arch mechanism
- l_a = horizontal centroid of half of arch measured from intrados hinge
- L = span of arch

- M_i = weight of individual arch segments between hinges in an assumed mechanism
 M_s = stabilising moment due to the weight of the buttress and the vertical force about the point of possible overturning
 $M_{s\phi}$ = stabilising moment due to the weight of the buttress and the vertical force about the point of possible overturning for a leaning buttress
 t = radial thickness of a circular arch
 R = radius of a circular arch measured to the centre-line of the arch
 SF_{load} = load factor of safety
 $SF_{pressurepoint}$ = pressure point factor of safety
 $SF_{Rankine}$ = Rankine's measure of buttress safety based on eccentricity of thrust at base
 V = vertical force applied to a buttress (due to weight of half of the arch)
 W = weight of the buttress above the section being considered
 W_b = total weight of the buttress
 W_c = weight of ineffective, fractured region of a buttress
 W_o = weight of the unfractured, upper portion of the buttress
 x, y = system of Cartesian space coordinates
 x_b = horizontal centroid of solid buttress measured from point of overturning
 y_b = vertical centroid of a solid buttress measured from the base
 \bar{y} = vertical centroid of solid buttress measured from base including all vertical load, such as the weight of the vault, V
 α = half angle of embrace of a circular arch
 α_{max} = maximum possible half angle of embrace for a given thickness ratio before a circular arch will collapse at the minimum thickness limit
 β = angle of intrados hinges in a circular masonry arch measured from the apex
 β_o = initial intrados hinge location for a slight spreading of the supports

- M_i = weight of individual arch segments between hinges in an assumed mechanism
 M_s = stabilising moment due to the weight of the buttress and the vertical force about the point of possible overturning
 $M_{s\phi}$ = stabilising moment due to the weight of the buttress and the vertical force about the point of possible overturning for a leaning buttress
 t = radial thickness of a circular arch
 R = radius of a circular arch measured to the centre-line of the arch
 SF_{load} = load factor of safety
 $SF_{pressurepoint}$ = pressure point factor of safety
 $SF_{Rankine}$ = Rankine's measure of buttress safety based on eccentricity of thrust at base
 V = vertical force applied to a buttress (due to weight of half of the arch)
 W = weight of the buttress above the section being considered
 W_b = total weight of the buttress
 W_c = weight of ineffective, fractured region of a buttress
 W_o = weight of the unfractured, upper portion of the buttress
 x, y = system of Cartesian space coordinates
 x_b = horizontal centroid of solid buttress measured from point of overturning
 y_b = vertical centroid of a solid buttress measured from the base
 \bar{y} = vertical centroid of solid buttress measured from base including all vertical load, such as the weight of the vault, V
 α = half angle of embrace of a circular arch
 α_{max} = maximum possible half angle of embrace for a given thickness ratio before a circular arch will collapse at the minimum thickness limit
 β = angle of intrados hinges in a circular masonry arch measured from the apex
 β_o = initial intrados hinge location for a slight spreading of the supports

- β_u = intrados hinge location at collapse due to spreading of the supports
- ϕ = angle of lean of buttress (in radians typically)
- ϕ_{max} = maximum angle of lean of fractured buttress before overturning (at $H=0$)
- γ = depth-density of buttress (typically in units of kN/m^2)
- Γ = angle of applied acceleration measured from the vertical
- η = pressure point co-ordinate at horizontal section through the buttress
- η_0 = initial pressure point co-ordinate due only to vertical forces ($H=0$)
- η_{cr} = pressure point co-ordinate to initiate a fracture in the buttress
- η_ϕ = pressure point co-ordinate for a buttress leaning by an ϕ
- λ = constant horizontal acceleration factor (multiplied by gravity)
- λ_{min} = minimum constant horizontal acceleration to form a collapse mechanism in a masonry structure
- μ = coefficient of height at which the force is applied to a rectangular buttress
- θ = angle of inclination of the fracture measured from horizontal
- ξ = fracture height divided by height of applied horizontal force for a rectangular buttress
- ψ = ratio of vertical load to the buttress weight for a rectangular buttress

List of Tables

Table 3.1	Experimental results versus predicted results for model buttresses
Table 4.1	Comparison of safety factors for a rectangular buttress
Table 5.1	Historical solutions for minimum thickness of a semicircular arch
Table 5.2	Minimum thickness ratios and hinge locations for varying angles of embrace
Table 5.3	Collapse state for an arch with varying voussoir sizes on spreading supports
Table 5.4	Experimental results versus predicted results for model arches
Table 6.1	Values for the transition between mechanisms for a circular arch under lateral acceleration
Table 6.2	Collapse state for an arch with varying voussoir sizes under lateral acceleration
Table 8.1	Pressure point factor for the church at Goa, India

List of Figures

-
- Figure 1.1 Severe deformations in a barrel vault, Guimarei, Spain
- Figure 1.2 Collapse mechanisms in masonry arch experiments by Danyzy (1732)
- Figure 2.1 Stable state of a cracked voussoir arch
- Figure 2.2 Experiment on rectangular masonry buttress by Vicat (1832)
- Figure 2.3 Overturning force for a masonry buttress, showing possibility for fracture by Dupuit (1870)
- Figure 2.4 Leaning masonry wall with progressive cracking (Heyman 1992)
- Figure 2.5 Deformed arch due to spreading supports (Viollet-le-Duc 1854)
- Figure 2.6 Collapse state of a buttressed arch bridge (Monasterio ca. 1800)
- Figure 2.7 Line of fracture for collapse of a buttressed arch (Persy 1834)
- Figure 2.8 Collapse of a buttressed arch bridge (Walther 1855)
- Figure 2.9 Buttressed arch analyses using discrete element methods
- Figure 2.10 Deformed state of the church at Vezelay (Viollet-le-Duc 1854)
- Figure 2.11 "Kinematic" safety of an arch on spreading supports (Smars 2000)
- Figure 3.1 Buttress collapse by overturning
- Figure 3.2 Assumption of linear stress distribution for buttress fracture analysis
- Figure 3.3 Equilibrium in the lower, fractured region of the buttress
- Figure 3.4 Buttress geometry
- Figure 3.5 Variation in fracture height for rectangular buttresses
- Figure 3.6 Collapse loads for rectangular buttresses under horizontal loads
- Figure 3.7 Possible fracture patterns in Gothic buttresses
- Figure 3.8 Assumed stress distributions in rectangular and T-shaped buttresses
- Figure 3.9 Possible contributions of cross-walls to the buttress
- Figure 3.10 Model experiments on rectangular buttresses
- Figure 3.11 Model experiments on T-shaped buttresses
- Figure 4.1 Experiment on sloping masonry buttress by Vicat (1832)
- Figure 4.2 Geometry of a leaning rectangular buttress on a rotated support
- Figure 4.3 Variation in fracture height for a leaning rectangular buttress ($h_b/b=4$)
- Figure 4.4 Variation in fracture height for a leaning rectangular buttress ($h_b/b=6$)
- Figure 4.5 Thrust capacity for a leaning rectangular buttress
- Figure 4.6 Reaction point at the base of the buttress due to horizontal thrust

- Figure 4.7 Movement of pressure point at the base of buttress as force increases
- Figure 4.8 Influence of leaning on buttress reaction point and capacity
- Figure 4.9 Comparison of safety factors for a rectangular buttress
- Figure 5.1 Definition of geometry for a voussoir masonry arch
- Figure 5.2 Circular arch at minimum thickness ratio
- Figure 5.3 Static equilibrium of a thin voussoir near the intrados hinge
- Figure 5.4 Minimum thickness of circular arches for varying angles of embrace
- Figure 5.5 Minimum thickness of circular arches on log-log scale
- Figure 5.6 Circular arch segment with spreading abutments at minimum thrust
- Figure 5.7 Change in horizontal thrust of a voussoir arch with support movements
- Figure 5.8 Equilibrium of central region of the arch
- Figure 5.9 Horizontal thrust of a circular arch as a function of the intrados hinge
- Figure 5.10 Intrados hinge location corresponding to minimum thrust for circular arches
- Figure 5.11 Algorithm to determine collapse of an arch on spreading supports
- Figure 5.12 Collapse mechanisms and associated horizontal thrust for arches on spreading supports
- Figure 5.13 Thrust increase at collapse for circular arches on spreading supports
- Figure 5.14 Span increase for collapse of circular arches on spreading supports
- Figure 5.15 Summary of intrados hinge movements due to spreading supports
- Figure 5.16 Symmetrical collapse mechanism for an arch on spreading supports
- Figure 5.17 Thrust increase with span increase for varying voussoir sizes
- Figure 5.18 Undeformed model Arch1
- Figure 5.19 Model Arch1 on spreading supports just before collapse
- Figure 5.20 Undeformed model Arch2
- Figure 5.21 Model Arch2 on spreading supports just before collapse
- Figure 6.1 Collapse of masonry arch due to lateral acceleration
- Figure 6.2 Geometry of a masonry arch under lateral acceleration
- Figure 6.3 Equivalent tilted arch and components of work done by acceleration
- Figure 6.4 Minimum thickness arch rotated through an angle Γ
- Figure 6.5 Maximum angle of tilt for circular arches of various thickness ratios
- Figure 6.6 Minimum horizontal acceleration for collapse of a circular arch
- Figure 6.7 Critical hinge locations for a circular arch of various angles of embrace under constant horizontal acceleration

- Figure 6.8 Change in support reactions in arch under constant lateral acceleration
- Figure 7.1 Collapse of a buttressed arch due to a point load and self-weight
- Figure 7.2 Buttressed arches Case A and B
- Figure 7.3 Collapse state for buttressed arch Case A due to leaning buttresses
- Figure 7.4 Collapse state for buttressed arch Case B due to leaning buttresses
- Figure 7.5 Comparison of collapse states due to leaning buttresses
- Figure 7.6 Threshold thickness between weak buttress and strong buttress failure
- Figure 7.7 Possible collapse mechanisms for buttressed arches under horizontal acceleration
- Figure 7.8 Collapse of buttressed arch Case A due to horizontal acceleration
- Figure 7.9 Collapse of buttressed arch Case B due to horizontal acceleration
- Figure 8.1 Church in Old Goa, India presented as a case study
- Figure 8.2 Changing horizontal thrust as the south buttress leans in Goa church
- Figure 8.3 Collapse mechanism of Goa church due to lean of south buttress
- Figure 8.4 Analysis procedure for assessing the safety of an arch supported on leaning buttresses
- Figure 8.5 Three types of failure for an arch supported on leaning buttresses
- Figure 8.6 Comparison of safety factors for the church at Goa, India
- Figure 8.7 Minimum horizontal acceleration to form a collapse mechanism for the church at Goa
- Figure 8.8 Possible collapse mechanisms for the church at Goa due to horizontal acceleration assuming that south buttress remains solid
- Figure 8.9 Possible collapse mechanisms for the church at Goa due to horizontal acceleration assuming that south buttress fractures
- Figure 8.10 Acceleration pulse curve for an assumed mechanism of collapse
- Figure B.1 Block layouts for model buttress experiments of Chapter 3
- Figure B.2 Predicted collapse mechanisms for rectangular buttress experiments
- Figure B.3 Predicted collapse mechanisms for T-shaped buttress experiments

PART I: INTRODUCTION

Chapter 1 Introduction

1.1 Introduction

The safe design of structures is based on a reliable understanding of their collapse state. Modern engineered structures depend on their ductility to warn of impending collapse and to absorb energy in the event of overloading. Having confidence in the failure modes for reinforced concrete and steel structures allows engineers to design and assess the safety of these structures.

Engineers do not have the same confidence in assessing the safety of unreinforced masonry structures. Unlike ductile materials, such as steel or reinforced concrete, masonry does not have the capacity to absorb energy through yielding. The modes of collapse for masonry structures are not well understood, particularly under the influence of seismic loading. Furthermore, engineers have not investigated collapse modes induced by large support displacements that may occur progressively over time, which are a significant concern for historic buildings. This thesis investigates the influence of support displacements and horizontal accelerations on the safety of vaulted masonry buildings.

Existing masonry structures present a serious problem for the structural engineer, who often has no experience with unreinforced masonry structures. For masonry buildings, the applied loads such as wind or snow loading are often small in relation to the weight of the structure, and the deformations due to these applied loads are very small. But in a masonry vault supported on buttresses, the actual distortion of the structure with respect to its as-built shape, can be very large, often exceeding 300 mm in the case of large churches or cathedrals. These distortions tend to increase throughout the life of the structure, usually on account of foundation movements. The collapse condition of such structures may depend on the size of these slowly-increasing displacements, and not on the magnitude of the applied loads. Finally, the safety of traditional masonry structures depends on their stability, rather than on the strength of the material (Heyman 1995). For all of these reasons, structural engineers often have difficulty assessing the safety of historic masonry buildings.



This dissertation proposes new methods for the analysis of masonry structures based on the introduction of displacements and the application of horizontal accelerations. Displacements and accelerations will de-stabilise the system and lead to an unsafe condition in which the structure will collapse. For the approach outlined in this dissertation, the analyst must apply equilibrium, kinematics, and simplifying assumptions about the masonry material.

1.2 Statement of Problem

The collapse of a masonry structure may be caused by one of three general actions:

- 1) applied loading (as in the overloading of a masonry bridge);
- 2) applied displacements (as in the differential settlement of foundations); or
- 3) applied ground accelerations (as in the case of a strong earthquake).

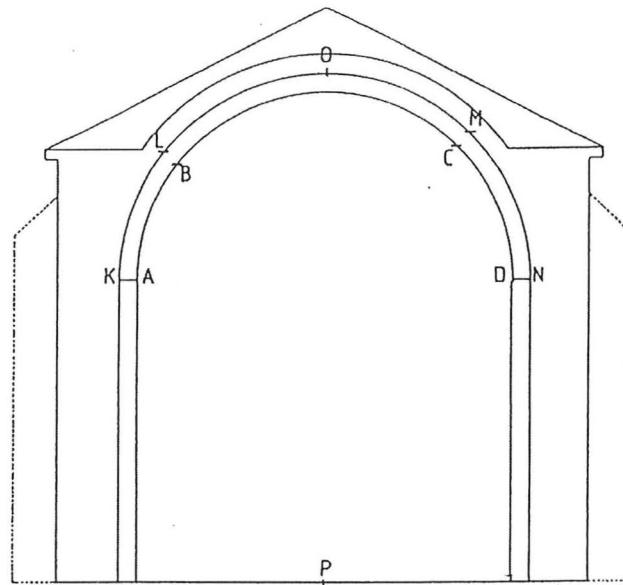
Engineers have already explored the first action in some detail, particularly for masonry bridges. Overloading is generally not a problem for masonry buildings such as vaulted cathedrals. The second action is a very real problem, particularly due to the long-term movements of the deformable foundations of a masonry building. Likewise, ground accelerations as a result of seismic activity are also a significant threat to masonry structures. This dissertation focusses on the second and third actions, and seeks to determine the influence of applied displacements and applied accelerations on the stability of masonry structures.

Traditional masonry structures consist of arches that thrust, and buttresses which resist the thrust. The thrust of the vault will deform the structure, and may cause large displacements in the buttresses, often due to creep in the non-rigid foundations. An example of the deformed state of such a structure is illustrated in Figure 1.1. Most commonly, the buttresses will lean outwards, causing:

- 1) an increase in the span of the vault;
- 2) a sagging deformation in the arch (or vault) to accommodate the span increase, involving a decrease in the rise of the arch; and
- 3) an increase in the arch thrust.

As a result of this change in geometry, the thrust of the arch can increase substantially. The increased thrust can cause further leaning of the buttress, and this geometrical change can eventually lead to collapse. This is a typical pathology in existing masonry

arches and vaults supported on leaning buttresses (Huerta and López 1997; Medero *et al.* 1998; Boothby 2001). Furthermore, the leaning buttresses produce eccentric loads on the foundations, which will lead to increased deformations over time.



(Reproduced by permission of S. Huerta.)

0 1 m

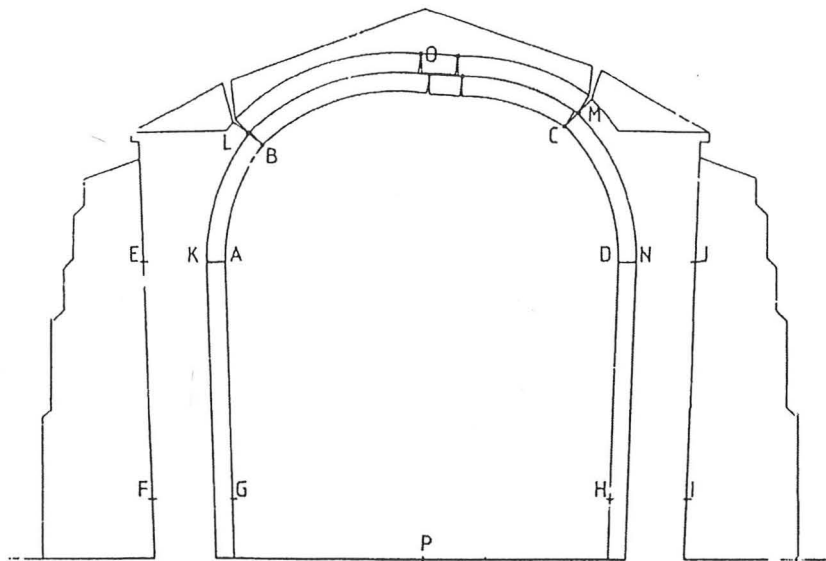


Figure 1.1 Severe deformations in a barrel vault, Guimarei, Spain (Huerta and López 1997). The upper diagram shows the church as built, with buttresses of uniform thickness. The lower diagram shows the current conformation, in which the outer stepped buttresses were added later in an attempt to reinforce the severely deformed church.

This dissertation proposes methods for the collapse analysis of a masonry arch supported on buttresses. This structural form is one of the oldest methods of construction, and it is a common structural system in historic buildings throughout

Europe and much of the world. Yet, engineers have not previously examined the changes in geometry that can lead to the collapse of buttressed arch structures. This dissertation is a first attempt to do so.

1.3 Collapse of Masonry Structures

The collapse of masonry structures is a question of stability, not strength. A simple voussoir arch such as a masonry bridge will fail due to the formation of a mechanism of collapse, and not due to the failure of the material. Thus, masonry structures derive their safety from the *geometry* of the structure, and not from the strength of the material. Danyzy's experiments in France in 1732 illustrated examples of possible collapse mechanisms (Figure 1.2), which form due to hinging between the blocks (Heyman 1995).

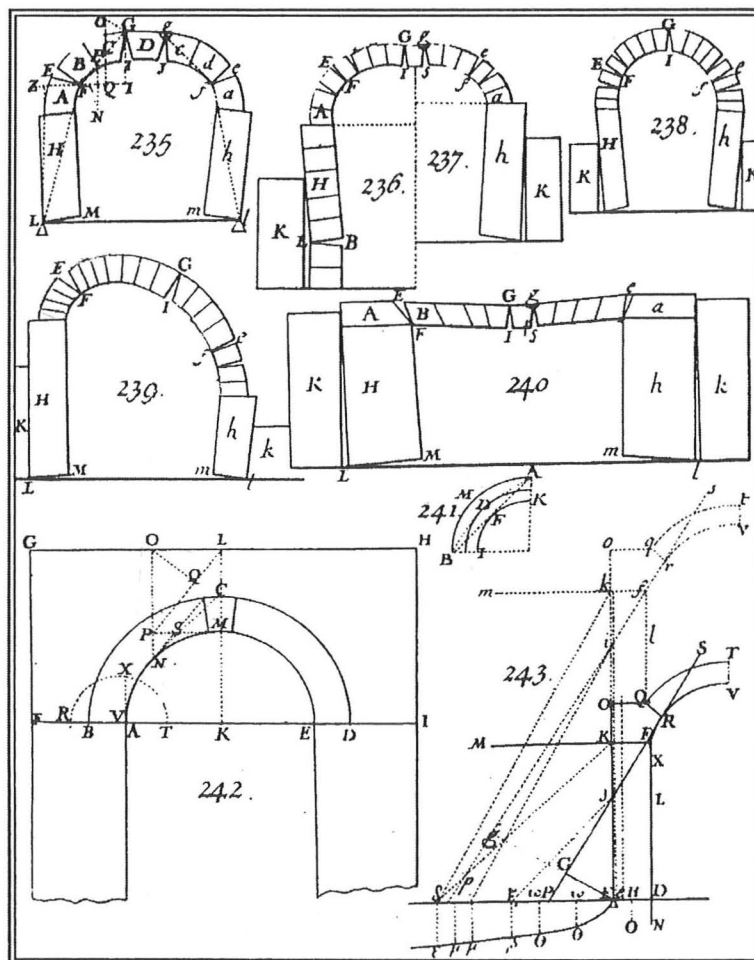


Figure 1.2 Collapse mechanisms in masonry arches from experiments by Danyzy in 1732 (Heyman 1995).

The engineer must assess the capacity of a masonry structure for increased displacements, in addition to increased loads. For masonry bridges, and for particular masonry buildings, large applied loads may cause collapse. But for masonry buildings in general, and masonry vaults in particular, engineers must also determine the applied displacements which would cause collapse. However, researchers have neither investigated the de-stabilising effects of progressive geometry changes nor developed measures of structural safety based on the effects of increased support displacements.

Heyman discusses the tendency of masonry buildings to drift over time, and summarises the problem with the statement: "...the overall dimensions of a masonry structure can only grow, never decrease" (Heyman 1995). For the current analysis, it is sufficient to state that the displacements are imposed on the structure by a hostile environment. This dissertation is not primarily concerned with the source of these displacements -- usually creep in the foundations -- rather it seeks to find the magnitude of displacements to cause collapse. Although the applied load does not change, imposed displacements can lead to the collapse of masonry structures. The engineer must understand the prior movements in a masonry structure and investigate the implications of increased displacements.

1.4 Motivations for Research

This research was motivated by three primary factors:

- 1) The growing significance of historic masonry structures, whose economic and cultural importance is vital throughout Europe. In 1997, the partial collapse of the masonry vault in the Basilica of St. Francis in Assisi, Italy caused the loss of human life, irreplaceable artwork, and tourist revenue (Crocì 1998).
- 2) To date, researchers have not developed satisfactory methods to determine the collapse state and to assess the safety of masonry buildings. In particular, researchers have not explored the load-capacity of masonry buttresses, and the general conditions which will cause masonry vaulted structures to collapse.
- 3) Researchers have not sufficiently examined the effect of geometry changes or imposed accelerations on masonry structures. Research efforts have emphasised the load capacity of masonry structures, rather than their capacity to sustain imposed displacements or for ground accelerations.

In attempting to address these problems, the current study aims to develop new methods for assessing the structural safety of masonry arches supported on buttresses.

1.5 Summary

This dissertation investigates the collapse of masonry arches supported on buttresses. The analysis begins with Heyman's general principles of limit analysis, and extends the approach to consider the collapse conditions for masonry buttresses and the influence of progressive displacements as well as horizontal acceleration for masonry arches. This dissertation aims at determining the magnitude of displacements necessary for the collapse of buttresses, arches, and buttressed arches. In addition, a method for assessing the seismic resistance of masonry structures is proposed, based on the minimum value of horizontal acceleration to form a collapse mechanism.

Chapter 2 reviews the relevant literature and discusses the current state of the structural analysis of masonry structures. Previous work on the resistance of buttresses and the collapse of buttressed arches is reviewed and assessed.

Chapter 3 determines the resistance of an isolated masonry buttress to lateral loads, and investigates the factors influencing the load capacity of a buttress. The failure of a buttress under lateral loads is characterised by a fracture, which separates the buttress and reduces the resistance of the buttress. A method is proposed for predicting this surface of fracture and computing the resistance of buttresses to lateral loads.

Chapter 4 examines the influence of leaning on the lateral force which the buttress can provide. The vertical buttress provides the maximum resistance, and as the buttress rotates away from the applied load, the capacity of the buttress decreases. In addition, this chapter proposes new measures of safety for masonry buttresses under lateral loads, taking into account the influence of leaning.

Chapter 5 analyses the collapse conditions for an isolated circular masonry arch on spreading supports. This is equivalent to the case of a masonry arch supported on progressively leaning buttresses, in which the lean of the buttress causes the span of the arch to increase. For this problem, the lean of the buttress is assumed as given, and is

slowly increased until the arch collapses. The aim is to determine the increase in horizontal thrust as the arch is deformed until collapse.

Chapter 6 determines the minimum constant lateral acceleration to cause collapse of the circular masonry arch under its own weight. This is equivalent to an idealised seismic loading, and can be used to estimate the magnitude of peak ground acceleration necessary to form a collapse mechanism.

Chapter 7 investigates the collapse state for a masonry arch supported on buttresses. This chapter combines the results of Chapters 3, 4, 5, and 6 to investigate the stability of a circular arch supported on masonry buttresses. The influence of buttress leaning is determined, and the collapse state for various configurations is illustrated. The same structural configurations are analysed for constant lateral acceleration and the collapse state is identified. The aim is to determine the general patterns of behaviour and the likely failure modes for buttressed arches.

Chapter 8 proposes measures for the structural safety of buttressed arches. Based on the findings of the earlier chapters, new methods are proposed for assessing the safety of existing buttressed arches. To illustrate the methods, a simple case study is introduced and discussed.

Chapter 9 provides general conclusions and outlines future work in this field.

Chapter 2 Literature Review

2.1 Theory of Masonry Structures

There are two dominant theories for the structural analysis of masonry: elastic analysis and limit analysis. Both theories require the analyst to make assumptions about the material properties and support conditions. However, classic elastic analysis requires numerous assumptions, many of which are not justifiable for masonry structures. Limit analysis of masonry structures requires only three simplifying assumptions, which reflect the true nature of unreinforced masonry, and can be easily verified if necessary (Heyman 1966, 1995, 1998).

2.1.1 Limit Analysis of Masonry Structures

The three well-known assumptions required to apply limit analysis to masonry are:

- 1) masonry is rigid;
- 2) masonry has no tensile strength; and
- 3) sliding failure does not occur.

The first assumption is reasonable because the stresses in traditional masonry structures are exceedingly low; typically at least an order of magnitude below the failure stress of the material. Furthermore, the strains are exceedingly small and the material deformation is an order of magnitude or more below the deformations imposed by the environment. The second assumption is slightly conservative, but is accurate. Stone is very weak in tension, and mortar joints do not provide significant tensile resistance between stones. The final assumption is generally true, since the very high friction between stones is sufficient to prevent sliding in most cases. Naturally, there are some exceptions to these assumptions, and the analyst must check their validity in each particular case (Heyman 1995). These three assumptions lead to simple computations which provide accurate predictions of the actual behaviour of masonry structures.

The simplest problem in masonry structure is the arch. The thrust of the arch may lead to small changes in the support conditions and a small increase in the length of the span. The arch must adapt to this small increase in span by forming hinges, or cracks,

between the individual voussoirs (as in Figure 2.1). This is the stable state of a masonry arch, and cracking is the natural way that masonry adjusts to small and inevitable changes in the boundary conditions. Figure 2.1 illustrates a voussoir arch, which has responded to a small increase in the span length by forming three hinges. The voussoirs are considered to be rigid, and the structure is safe as long as a "line of thrust" can be found within the masonry. The line of thrust represents the line of forces within the arch due to the applied loads, which will be discussed in detail in Chapter 5. In Figure 2.1 the line of thrust is illustrated as a dashed line, where the applied load is simply the self-weight of the arch.

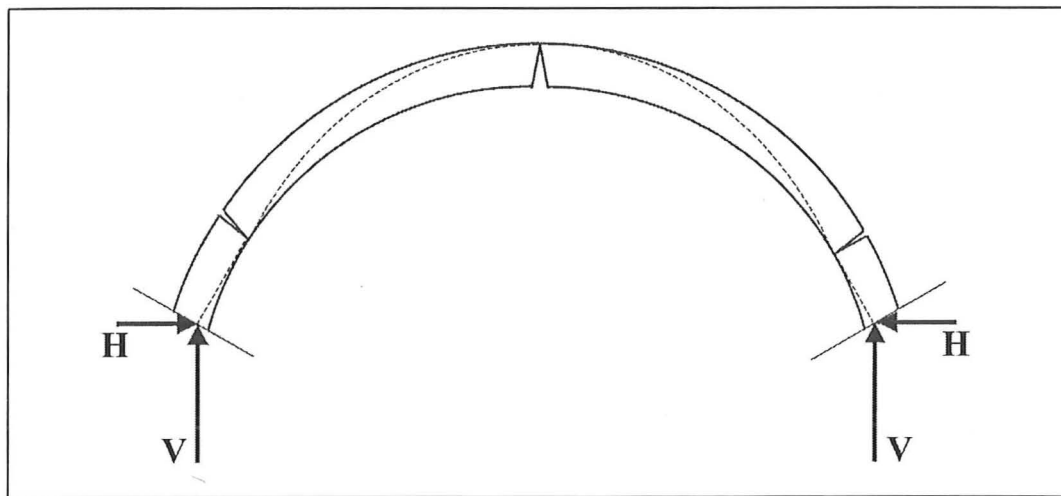


Figure 2.1 Stable state of a cracked voussoir arch (after Heyman 1995).

The three-hinged arch is statically determinate, and the thrust of the arch can be determined uniquely for the given geometry from statical equilibrium. There is no question of being able to compute the exact stresses in the masonry. Importantly, limit analysis procedures begin with the *deformed* shape of the structure, i.e. the current configuration of the structure, and seek to demonstrate its safety.

2.1.2 Elastic analysis of masonry structures

Since Navier (1826) introduced the idea of elastic analysis to determine the stress state in statically indeterminate structures, engineers have applied elastic analysis to the design and assessment of structures. Elastic analysis assumes that the material is a continuum, which behaves as a linear-elastic solid. The method is inappropriate for assessing masonry structures for the following reasons:

- 1) The deformations in masonry structures are not due to *elastic* deformations of the masonry material, and cannot be predicted satisfactorily by an elastic analysis.
- 2) The exact stress state is unknowable in a masonry structure, due to the unknown loading history, boundary conditions, and material properties.
- 3) The material is heterogeneous, and is separated by joints and fractures throughout, making it unreasonable to model as an elastic continuum.

For example, the hinged masonry arch in Figure 2.1 cannot be explained by use of linear elastic analysis, though it is among the simplest and most common problems in masonry structure. In 1927, a Harvard professor of engineering argued against the use of elastic analysis for masonry, writing "to apply the elastic theory even to the reinforced concrete arch is illusory, and a vain seeking after exactness where exactness is impossible" (Swain 1927, p. 423).

Swain's comments foreshadow the theorems of limit analysis, which were developed and refined in the 20th century (Heyman 1998). This thesis will follow in the tradition of limit analysis by using equilibrium, combined with kinematic analysis of mechanisms, to examine the safety of masonry structures. The problem is to define the stability conditions for rigid-block structures using conventional structural mechanics.

2.2 Methods of Analysis

To investigate the de-stabilising influence of displacements on masonry structures, limit analysis provides a theoretical basis (Heyman 1966, 1995). For a given configuration, the stability of a masonry structure can be demonstrated by drawing a thrust line that lies wholly within the masonry. Moseley (1843) and Milankovitch (1907) defined the principles of the thrust line in rigorous detail. The thrust line is constructed by considering slices of the masonry whose weight acts on the thrust line, similar to weights on a hanging chain, as in the case of a funicular polygon. (See Heyman 1995 for a full discussion of the hanging chain and its relevance to the arch.) Thrust lines can be drawn by use of graphic statics, as well as by the deployment of basic computer programs. A thrust line represents one possible line of forces in the structure, and the shape of the line is dependent on the theoretical slices considered

(Milankovitch 1907). The slices considered should reflect the construction of the masonry. In masonry arches it is logical to slice the arch radially, dividing the arch into voussoirs in the same way that many arches are constructed. For masonry buttresses it is logical to slice the buttress horizontally, dividing the buttress in elevation since buttresses are typically built in horizontal courses of masonry. Most importantly, a thrust line must be demonstrated to lie within the masonry, and the analyst must apply the loads that can influence the thrust line.

Many researchers are now applying advanced finite-element formulations, such as the distinct element method or the discrete element method, to model the discontinuous nature of masonry structures (Mamaghani *et al.* 1999). One well-known example is UDEC, a commercially available program used widely in geotechnical engineering for analysing discontinuous rock masses (UDEC 2000). Such finite-element formulations can be used to model individual blocks, assumed to be elastic or rigid, which are connected by "contact elements". These programs are capable of computing large displacements in discontinuous media, and can model the complete detachment of discrete bodies. The method can be used to predict collapse mechanisms; but the results are extremely sensitive to assumptions about the material properties of the "contact elements", which are essentially unknowable for a real structure. This dissertation proposes an alternative analysis method, which is based on traditional mechanics of rigid bodies and uses much simpler assumptions about the material properties.

In the field of mechanics, it is straightforward to analyse the structure by using rigid-block analysis based on equilibrium and compatibility for a known mechanism. Work calculations can be carried out to verify the stability of the structure and determine the critical collapse mechanism. The analyst must investigate alternative kinematically admissible mechanisms of collapse, and determine which of them is the governing collapse mechanism. For the relatively simple structures in this dissertation, MATLAB programs have been written to analyse rigid-block structures. Copies of the programs are included in Appendix A.

2.3 The Masonry Buttress¹

The design of masonry buttresses was a primary concern for medieval and Renaissance builders. Before the advent of theoretical structural mechanics, builders could safely design vaults and arches in a wide variety of forms, provided the buttresses could support the thrust of the arch. Buttress design was a more difficult problem, and insufficient buttressing could lead to catastrophic collapse of the structure. Huerta (1990, 1999), Sanabria (1982), Heyman (1982, 1995), and others have discussed the great importance of the proper design of buttressing. A significant proportion of the medieval design rules for masonry structures were concerned with the sizing of the buttresses.

Despite the historical importance of buttress design, researchers have not focussed sufficient attention on the capacity of masonry buttresses to resist horizontal loads. The buttress problem is one of simple statics: the overturning moment produced by the thrust of the vault about a point of rotation must be equilibrated by the stabilising moment of the effective mass of the buttress. Engineers often assume that buttresses are monolithic, with the entire mass of the buttress resisting the lateral forces. This was the usual assumption from the earliest scientific design of buttresses (La Hire 1712; Bélidor 1729), and the assumption continues to be applied today (Boothby 1994; Gilbert and Melbourne 1994). However, a masonry buttress is actually a series of individual stones placed roughly in horizontal courses. The material can only transmit compressive forces, and tensile forces will separate the stones. At the limit of overturning, a region of the buttress will fracture and become ineffective, thereby reducing the capacity of the buttress.

For collapse due to overturning, a masonry buttress will not act as a monolithic mass, and the analyst must consider the formation of a fracture at the collapse state. Several researchers considered this possibility in the 19th century: Monasterio (ca. 1800), Gauthey (1809), Audoy (1820), and Dupuit (1870), each of whom identified the problem but did not resolve it. Navier (1826) concluded that the critical fracture was a straight line inclined at 45° , though he did not justify the use of a straight fracture.

¹ The historical review of the analysis of masonry buttresses and buttressed arches is presented here with kind permission of Professor Santiago Huerta. Professor Huerta has researched this topic for many years and he generously shared his knowledge and the primary documents discussed here.

Experiments by Seguin (1826) and Vicat (1832) showed that a surface of fracture forms when a masonry buttress overturns due to steadily increasing lateral loads. The result of Vicat's experiments on masonry bridge towers is presented in Figure 2.2, and the resulting fracture in the buttress significantly reduces its effective mass. Vicat's experiment investigated the use of masonry piers as the towers and the anchorage blocks, simultaneously, for suspension bridges. The resulting load due to the cable is equivalent to an inclined load applied at the top of the masonry pier, which is similar to the thrust from an arch.

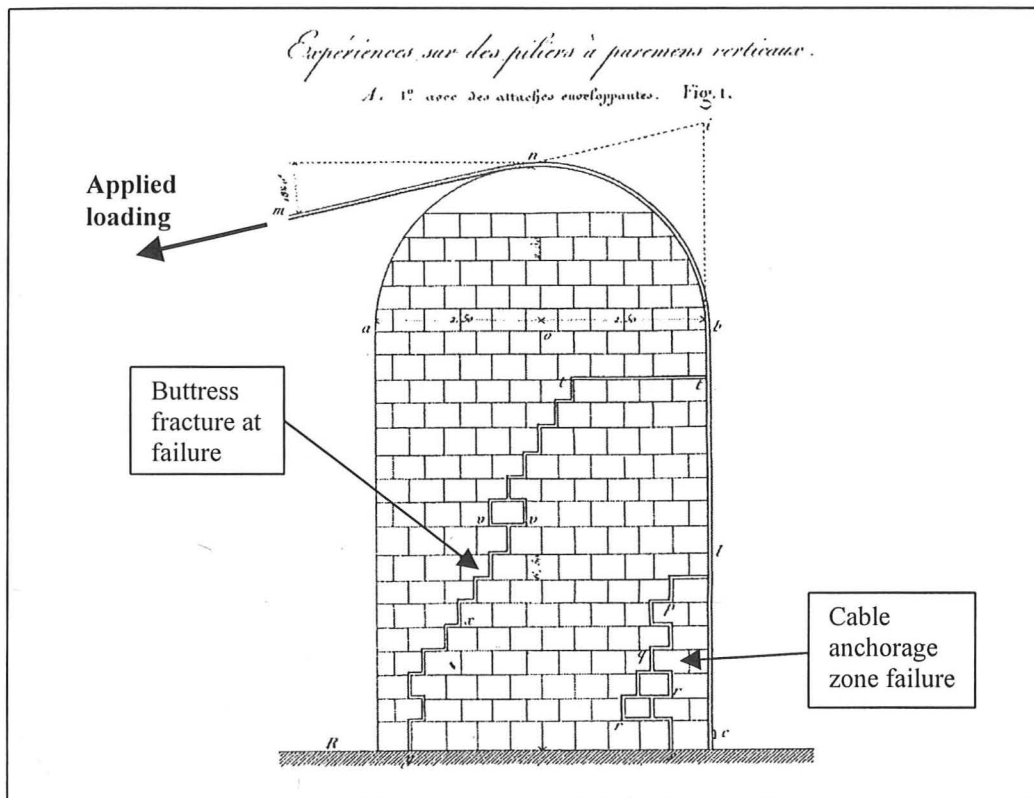


Figure 2.2 Experiment on masonry pier for a suspension bridge showing fracture at collapse (Vicat 1832). The cable "pulls" the buttress over in the same way that a horizontal thrust from an arch or vault would "push" against the buttress.

Dupuit (1870) defines the problem clearly: see Figure 2.3. The overturning force for a solid buttress can be determined from equilibrium (as a single block pivoting about one corner). This force is assumed to cause a fracture (line CS in the diagram on the left) in the masonry when the thrust line exits the middle third of the rectangular cross-section. A new thrust is calculated to equilibrate the fractured buttress, and this lower value of thrust results in a new fracture (line FE in the diagram on the right). By iterating until the thrust is in equilibrium with the overturning force and the fracture

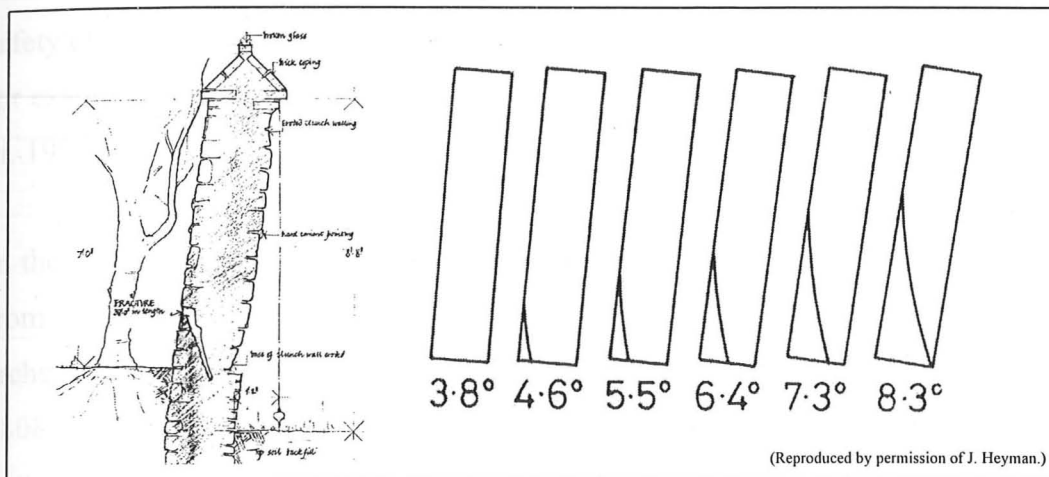


Figure 2.4 Leaning masonry wall with progressive cracking until collapse (Heyman 1992).

2.4 The Masonry Arch

2.4.1 Masonry arch bridges

Engineering researchers have studied masonry arches in great detail in recent years, in an effort to assess and repair existing motorway bridges (Harvey 1988; Melbourne 1995; Hughes and Blackler 1997; Ng *et al.* 1999). The analysis of masonry bridges is a special problem: historic masonry structures are now required to carry much heavier loads than the original builders envisioned, and engineers must determine the safe load capacity of the bridges. This is a highly specialised area of research, which presents a series of specific problems and will not be directly addressed here. However, some of the findings of this dissertation, particularly on the safety of buttresses, are relevant to the collapse state of masonry arch bridges.

2.4.2 The masonry arch on spreading supports

Researchers have hitherto devoted little attention to the study of masonry arches supported on tall buttresses, which is a common structural system in churches and other historic buildings. For such structures, the self-weight of the structure is typically much greater than any live loading on top of the arches. It is unlikely that a very large concentrated load will be applied to the top of a masonry arch in a historic building. As opposed to vertical loading, imposed displacements due to progressive geometry changes in the buttresses are the greatest threat to the stability of arches in buildings. Despite this, few researchers have investigated the influence of displacements on the stability of masonry arches. Almost all recent studies on the

safety of arches have been concerned with the stability under applied point loads. (See for example Heyman 1969, 1980; Harvey 1988; Boothby *et al.* 1992; and Lucchesi *et al.* 1997 for the conventional analysis of masonry arches subjected to vertical loads.)

In the past, numerous studies have been made of the possible mechanisms resulting from imposed displacements. In 1732, Danyzy carried out a series of experiments on arches and investigated the influence of displacements on stability (Heyman 1998). In 1808, Schulz published various mechanisms of collapse for an arch supported on buttresses (Kurrer 1997). Viollet-le-Duc investigated the collapse state of the grossly deformed vault in the church at Vézelay, France, but he did not consider the general problem of arches on spreading supports: see Figure 2.5.

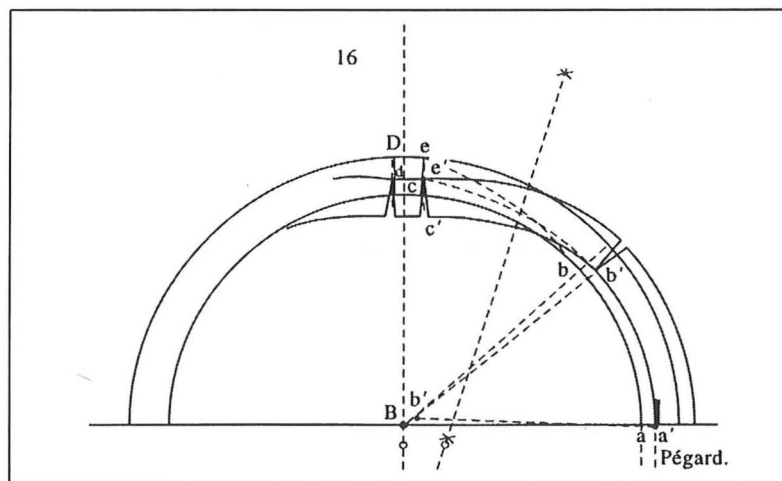


Figure 2.5. Deformed arch in the church at Vézelay, France due to spreading supports (Viollet-le-Duc 1854). (See also Figure 2.10 later in this chapter.)

More recently, Smars (2000) has studied the stability of arches and vaults, considering the influence of displacements. Smars identified the domain of statically admissible movements for a chosen mechanism in a semi-circular voussoir arch. However, he did not investigate the possibility that the hinges might move as the arch supports spread apart. Chapter 5 demonstrates that various collapse mechanisms are possible for the arch on spreading abutments, and that the analyst must consider the possibility of the hinges moving location.

Although these isolated studies have considered the influence of movements, none of the authors has investigated the implications of movements on the horizontal thrust of

the arch. For masonry arches, a small increase in the span leads to a deformed geometry, which increases the minimum horizontal thrust. For a given arch, the maximum displacement before collapse must be determined, as well as the corresponding horizontal thrust for a given increase in span length. This approach does not exist in the published literature and will be developed in Chapter 5.

2.4.3 Acceleration loading

In addition to the collapse of an arch due to static loads or displacements, numerous researchers have explored the resistance of an arch to lateral accelerations, such as those due to an earthquake. Oppenheim (1992) explored this topic in detail, by treating a four-bar chain model of an arch as a dynamical system. Assuming that the hinges would only occur in particular locations, he derived an equation of motion for an arch of a given thickness and angle of embrace. This approach provides information about the onset of mechanism-motion, and the behaviour of the different portions of the arch as the mechanism rotates from the initial configuration until the collapse state. It can also be used to analyse an arch under non-uniform acceleration loading, including earthquake loading with random values of ground acceleration and frequency. Most valuably, Oppenheim explored the potential energy of the system and demonstrated that formation of the initial mechanism is not sufficient to cause collapse. The mechanism will recover before collapse, until the point when the maximum potential energy is reached. This is a promising method of analysis for masonry structures in earthquake loading, and will be discussed in Chapter 8. However, Oppenheim's approach is tedious because the equation of motion must be derived anew each time a different structure is considered. Although valuable, the applicability is not as general as a kinematic approach using least-work calculations.

Several researchers have thus used a mechanism-type analysis with calculations of least work to determine the hinge locations and the corresponding values of constant lateral acceleration to form the mechanism. Most notably, Clemente (1998a, 1998b) pursued this approach. Clemente explored the influence of geometry on the arch behaviour under lateral loading, and investigated the location of hinges for various arch configurations. However, Clemente did not consider the possibility for a mechanism involving three hinges within the span and one hinge at the support. In his approach, Clemente assumed that one hinge will always form at each support with

only two hinges in the span (Clemente 1998b). The literature does not currently contain a clear overview of the threshold accelerations and the governing mechanisms for a variety of circular masonry arches. The problem will be explored in Chapter 6, by considering the resistance of an arch to static tilting, which is equivalent to applying a uniform horizontal acceleration in addition to the acceleration due to gravity.

2.4.4 The masonry vault

The masonry vault is a three-dimensional surface, which may sometimes be considered as a series of masonry arches in combination. Indeed, existing vaults often contain a number of cracks, which effectively divide the vault into a series of arches (Heyman 1983). The thrust of the vault will contribute to movements of the supports, and cracks will form in the vault to accommodate this movement. Numerous writers have demonstrated the safety of cracked masonry vaults and domes through an equilibrium approach based on the safe theorem of plasticity. If one state of equilibrium can be demonstrated (i.e. a thrust surface due to the applied loads can be found within the masonry) then the vault will stand under the applied loads. A typical approach is to divide the vault or dome into a series of slices and demonstrate the safety of each slice. This method can be traced to one of the earliest applications of structural analysis, carried out by Poleni in 1748 for the dome of St. Peter's in Rome (Heyman 1988).

Huerta (2001) provides an overview of the equilibrium approach to the structural analysis of masonry vaults. The method was first applied rigorously by Heyman (1966, 1967) using classical "membrane" theory. More recently, O'Dwyer (1999) and Smars (2000) have developed computer algorithms to search for equilibrium solutions in masonry vaulting. O'Dwyer's method is particularly useful for defining a "thrust surface" -- a three-dimensional version of the thrust line -- which must lie within the surface of the masonry vault. These methods are the correct approach to demonstrating a possible equilibrium solution for a masonry vault, and can be used to predict accurately the thrust of the vault. For a real structure, the engineer can interpret the cracking patterns and slice the vault accordingly for a more accurate prediction of the vault thrust.

In addition, a small number of researchers have carried out collapse analyses of masonry vaulting. Using upper-bound approaches and assuming a symmetrical collapse mechanism, Oppenheim *et al.* (1989) have successfully applied limit analysis to masonry domes. Lucchesi *et al.* (1999) presented no-tension elastic constitutive equations for masonry and developed closed-form solutions for the collapse analysis of a cylindrical masonry vault; but their approach is heavily mathematical for even the simplest geometrical cases, and is hardly practical for the assessment of real structures. Heyman (1993) investigated the overloads that may occur on a masonry vault, including the loads due to a collapsing timber roof, as well as water filling the "pockets" on top of the vault. Such overloads are unlikely, but the analysis of the strength of a vault can be carried out (conservatively) using conventional limit analysis procedures and considering the vault as a series of individual arches. However, this reduces the masonry vault to the conventional problem of a masonry arch bridge and seeks to determine what load can be carried on top of the vault. As with masonry arches, imposed displacements represent an additional threat to masonry vaulting, which engineers have not investigated sufficiently.

This dissertation investigates the circular masonry arch of constant thickness, and the results of this study can be applied directly to circular barrel vaults. The methods presented here for two-dimensional arches can also be extended in principle to consider domes, crossing vaults, and other three-dimensional vault configurations. This dissertation defines the broad patterns of structural behaviour, which should set the stage for further investigations of more complicated problems, and can be extended to arches or vaults of varying shape and thickness.

2.5 Arches on Buttresses

The goal of the current study is to assess the stability of a masonry arch supported on two buttresses. In the 19th century, several writers considered the collapse state of such a system and investigated the possibility that a fracture would occur in the supporting buttresses. These authors assumed that the arch functions as a three-pinned arch, and would collapse due to the overturning of the masonry buttresses, in a symmetrical five-hinge mechanism involving a hinge at the base of each buttress. Monasterio (ca. 1800) applied this method to the analysis of a shallow arch supported on low abutments. In Figure 2.6 the intrados hinge in the arch is clearly seen, as well

as the fracture reducing the effective mass of the buttress. There is a hinge at the extrados at the crown (point B), a hinge at the intrados (point M) and an additional hinge at the outside of the abutment (point F), so the arch-buttress combination forms a symmetrical five-hinge collapse mechanism. Notably, Monasterio considered the influence of a fracture in the supporting abutment.

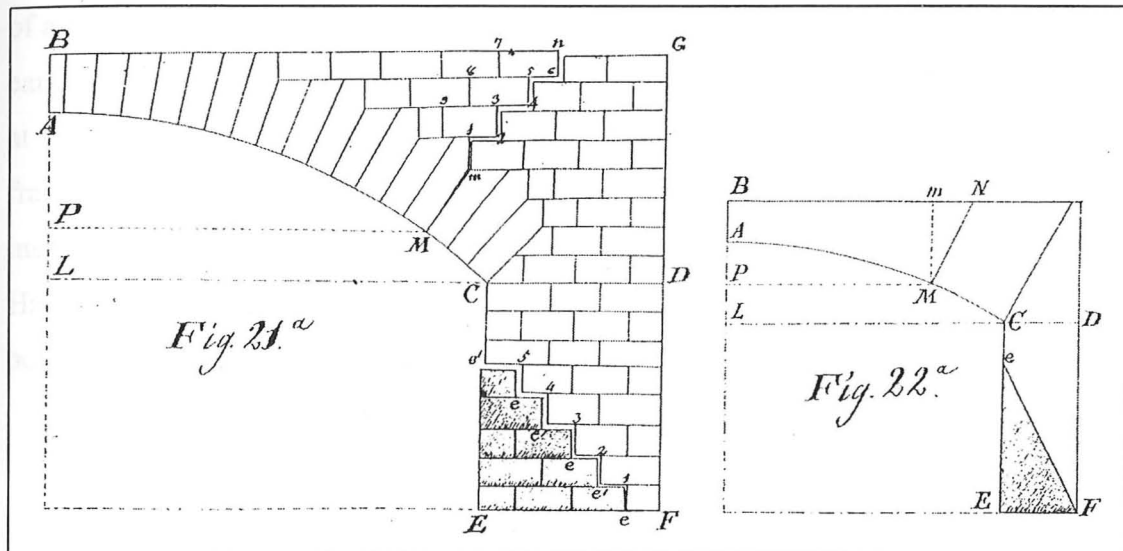


Figure 2.6 Collapse state of a buttressed arch bridge (Monasterio ca. 1800). The line AB is a line of mirror symmetry, so that the assumed collapse mechanism is a five-hinge mechanism.

In France, Gauthey (1809) and Persy (1834) considered the fracture of a buttress supporting a vault. Both assumed a straight-line fracture at an inclination of 45° , based on assumptions about the material. Persy's drawing is reproduced in Figure 2.7: line AS represents the postulated line of fracture at the collapse state.

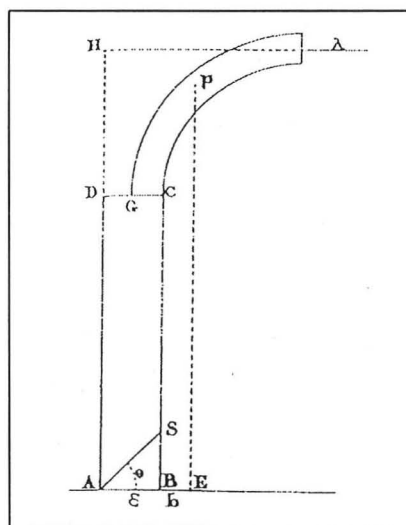


Figure 2.7 Persy's line of fracture AS at the collapse state of a buttressed arch (1834).

In the 19th century, several leading engineers considered the failure of the buttress to be a crucial concern, particularly in the design of bridges. Gauthey made the first published mention of the problem in relation to bridge collapse: "La chute d'un pont ne pourrait guère arriver sans qu'il ne se fit quelques disjonctions dans ses culées," [*"The collapse of a bridge could hardly occur without some disjunction of the abutments."*] (Gauthey 1809). In Germany, Walther (1855) investigated the possibility of a fracture in the abutments leading to a mechanism of collapse, without referencing earlier work. Figure 2.8 illustrates Walther's assumed fracture location along line KP at the failure state. Walther considered only the influence of the material above the fracture line KP in the abutment, and declared the material below the line as ineffective. (This is similar to Monasterio's earlier work illustrated in Figure 2.6.) Haupt (1853) cites Gauthey and computes the strength of a buttressed arch under a point load, considering the combined failure of the buttress and arch together.

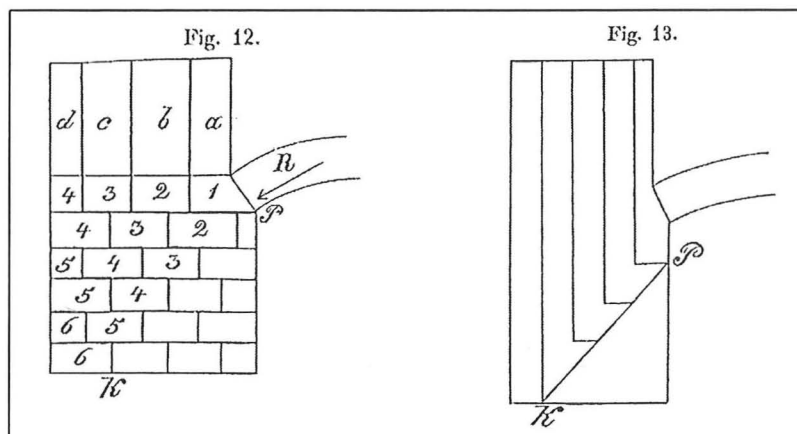


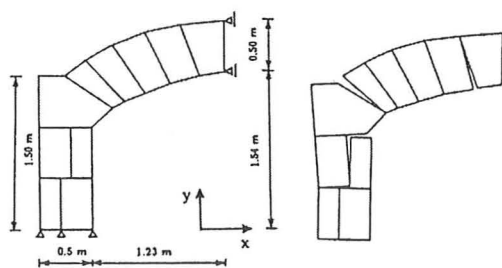
Figure 2.8 Collapse state of a buttressed arch bridge (Walther 1855). Only the buttress material above line KP is considered to be effective.

Early engineers recognised the importance of the buttress failure, which could lead to the collapse of an arch. However, engineers abandoned the rigorous study of masonry structures for nearly one hundred years, and as a result, did not investigate the collapse of buttressed arches during the 20th century. In recent years, the assessment of existing structures has led to a revived interest in the stability of buttressed arches.

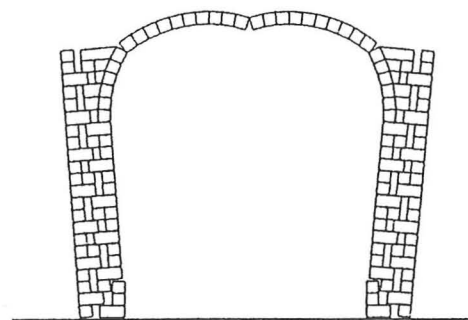
Huerta and López (1997) investigated the collapse condition of a barrel vault with leaning buttresses in a Spanish church (Fig. 1.1). The authors demonstrated a 50% increase in the horizontal thrust of the vault over its initial value due to large deformations in the structure. At the height of the vault support, the span had

increased by 370 mm (nearly 7% of the span), altering the geometry of the original structure significantly, and reducing the safety of the structure. The authors explored the effect of increased displacements, and analysed the safety of the structure against further movements. Their study applied the type of analysis explored in this dissertation and is a fruitful area for future work on the stability of buttressed arches.

Baggio and Trovalusci (1995) as well as Mamaghani *et al.* (1999) have used the discrete element method to analyse a masonry vault supported on rectangular masonry buttresses: see Figure 2.9. In both cases, they were able to predict the collapse mechanism, with three hinges in the vault, and an additional hinge at the base of the buttress, corresponding to a fractured region in the buttress. Though the method successfully identified the collapse mechanism, the use of such finite element programs is highly sensitive to the assumptions about the material properties, particularly the stiffness of the contact elements. Furthermore, the authors were concerned primarily with the values of vertical load that would cause collapse, and did not investigate the de-stabilising influence of any displacements occurring by progressive movements in the foundations. In each case, the authors increased the self-weight of the vault progressively until collapse, and did not investigate the displacements or accelerations to cause collapse. The methods presented in this dissertation are concerned with solving the problem illustrated in Figure 2.9 by using general limit analysis methods for masonry, and assuming that support displacements and horizontal acceleration are more likely to cause collapse than vertical live loading on top of the vault.



(a) After Mamaghani *et al.* (1999)
(Reproduced by permission of I. Mamaghani.)



(b) After Baggio and Trovalusci (1995)
(Reproduced by permission of P. Trovalusci.)

Figure 2.9. Buttressed arch analyses using discrete element methods

Medero *et al.* (1998) used finite-element methods to study the nave of the church in Vézelay, which Viollet-le-Duc had studied extensively. By allowing for the masonry to separate in the absence of compressive forces, the authors predicted a likely collapse mechanism and the mode of deformation in the arch. In addition, they were able to model the hinges in the vault as well as some cracking in the buttress. The analysis indicated that a fracture may form in each buttress as the structure nears the collapse state. The study used sophisticated gap elements to model the response of the mortar in the joints, but it has a number of shortcomings. In particular, the authors analysed the undeformed shape of the vaults, in an effort to explain the deformations, and did not analyse the deformed structure as it exists today. Conventional finite-element formulations have difficulty with the large-displacement behaviour and geometrical non-linearities of this type of problem. Furthermore, the results are extremely sensitive to the assumptions about the material properties and boundary conditions. Finally, the authors did not explore the implications of imposed displacements for the stability of the structure, though they conclude that the stability is "very sensitive to abutment movement" (Medero *et al.* 1998).

Viollet-le-Duc (1854) had studied the same church in the 19th century and wrote about the large deformations of the vault: see Figures 2.5 and 2.10. In this structure the vaults of the lateral naves help to support the main buttress, but the gross deformation in the central nave and the leaning of the buttresses is apparent. Medero *et al.* (1998) sought to explain the deformations with complex material models using finite-element analysis. In contrast, this dissertation assumes that the material does not deform and that the structure deforms according to rigid-body mechanics by formation of hinges between rigid elements and by support movements. The goal is to find the maximum load or displacements that would cause collapse.

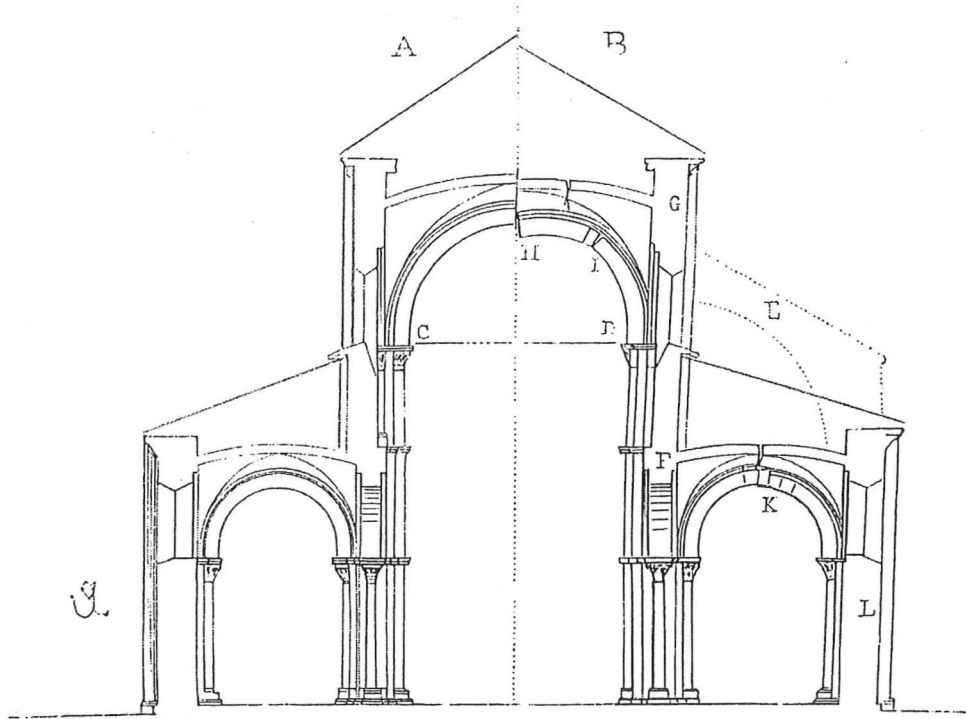


Figure 2.10 Deformed state of the Church at Vézelay, France (Viollet-le-Duc 1854). On the left as originally designed, and on the right as distorted.

Even with the simplified material assumptions of limit analysis, the structural behaviour of buttressed arches is complex. Increased deformations can lead to greatly increased internal forces. A first-order structural analysis, based on theories of small deformations, will not reveal the sensitivity to additional movements that determine the safety of the structure. Of the literature on buttressed arches, only Huerta and Lopez (1997) have considered the implications of additional movements for the stability of the structure. This is straightforward to consider because the system is statically determinate. The arch or vault has three hinges, and the thrust in the actual vault can be determined uniquely. The resistance of the abutments to this thrust can be estimated, and a clear understanding of the structural safety emerges. Finally, it is possible to impose increased displacements by artificially leaning the buttresses further, and to investigate the conditions that will lead to collapse of the structure.

Boothby (2001) has reviewed and assessed recent developments in the analysis of masonry arches and vaults, and has recognised the threat to stability posed by large displacements. Boothby concludes with the following paragraph:

Although rigid-plastic analysis does not admit movements of the springings of a roof vault at the top of the piers, this phenomenon is observable in nearly every medieval building at the top of the nave piers, due to either inadequate buttressing, or simply to the long-term loads imposed on the pier tops. *This effect is a cause of great concern in the preservation of roof vaults.* [italics added] (Boothby 2001, p. 255.)

The movements described by Boothby result from a wide range of causes, including foundation subsidence, construction defects, vibrations, etc., and they will continue to increase over the life of the structure. While Boothby seeks an explanation for the displacements, it is generally more useful to accept that movements will occur and that engineers should investigate the safe limits of these movements. As the preceding review of the literature reveals, earlier researchers have not pursued this approach, and it will be developed in this dissertation. To do so, the following chapters apply rigid-plastic analysis, assuming that the material does not deform. To investigate the safe limits of the displacements, the rigid structure is displaced and the new equilibrium conditions are examined. Imposing artificial support displacements provides insight into the stability of masonry arches supported on buttresses.

2.6 Measures of Safety

Engineers must develop measures of safety for existing masonry structures. Rankine (1858) proposed a load factor of safety for the stability of buttresses based on the resisting moment divided by the moment required for overturning. This is a rational approach, though Rankine's method is somewhat unsafe because it considers the buttress to act as a monolith, rather than being susceptible to fracture. Heyman (1969) introduced a geometrical factor of safety for masonry arches, in addition to the more conventional load factor of safety. Finally, Smars (2000) proposed a kinematic factor of safety based on the allowable support movements for a masonry arch: see Figure 2.11. The kinematic safety is determined starting from the stable state of the structure, and imposing displacements until collapse occurs. This dissertation extends Smar's method to consider the influence of displacements on the thrust capacity of buttresses and the stability of buttressed arches.

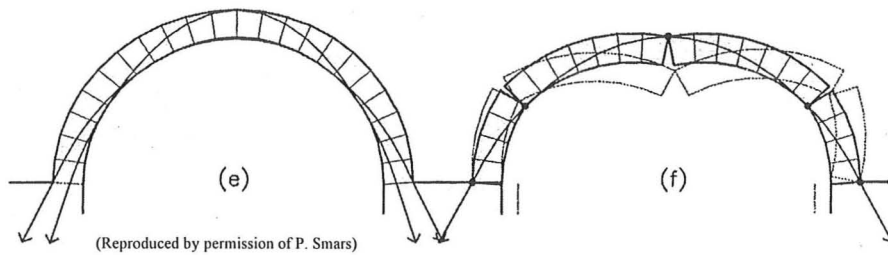


Figure 2.11 "Kinematic" safety factor for an arch on spreading supports (Smars 2000). The image on the left illustrates the minimum and maximum states of horizontal thrust for the arch as originally constructed. The image on the right is the arch at a possible collapse state due to spreading supports.

The geometric factor, load factor, and kinematic factor are the three primary measures of safety for masonry structures, and they can all be determined by the use of limit analysis. Additional measures of safety for masonry buildings are required, and guidelines have not been published for the safety assessment of arches supported on buttresses. In particular, engineers must have a procedure to follow in assessing the safety of buttressed arches, and this thesis proposes such a procedure.

Finally, there are no accepted methods for assessing the safety of buttressed arches under earthquake loading. Numerous researchers have studied the dynamic response of individual block structures and this remains an active area of research (Housner 1963; Augusti and Sinopoli 1992; Lipscombe and Pellegrino 1993; Makris and Roussos 2000). However, researchers in engineering mechanics have not sufficiently addressed the key problem for engineers in the assessment of historic masonry buildings: the dynamic response of buttressed arches to horizontal ground accelerations. This dissertation provides a basic introduction to the problem and defines a procedure for assessing the ground acceleration capacity of masonry arches supported on buttresses.

2.7 Summary

This chapter has reviewed the relevant literature and illustrated the shortcomings of the published record on the problem of buttressed arches. In summary:

- 1) Limit analysis can be used to investigate the stability conditions for masonry structures, whether in their original conformation or their current deformed state.

- 2) Elastic analysis requires many assumptions and places emphasis on the strength and stiffness of the material rather than the stability of the structure.
- 3) Historically, engineers were concerned with the capacity of buttresses to resist horizontal loads and the appearance of a fracture at the collapse state. This subject has not been investigated in the published record for over a century.
- 4) The consequences of gross deformations in arches and vaults are an important problem in the safety of masonry structures; yet few researchers have investigated the influence of support displacements on the stability of arches and buttressed arches.
- 5) In the 19th century, numerous engineers examined the collapse state of arches supported on buttresses. Today's engineers are being asked to assess the safety of such structures, though there are currently no accepted guidelines for doing so.

PART II: THE MASONRY BUTTRESS

Chapter 3 Collapse of Masonry Buttresses¹

3.1 Introduction

The safety of masonry vaulted structures depends on the ability of buttresses to support the thrust of vaults and arches. Despite the importance of the buttress stability, researchers have not studied sufficiently the capacity of masonry buttresses for horizontal thrust. This chapter investigates the collapse of a masonry buttress under lateral loads and the associated fracture in the buttress. Following Heyman's approach for leaning walls and towers (Heyman 1992), this chapter proposes a method to determine the shape of the fracture and the corresponding value of horizontal thrust required to overturn a masonry buttress.

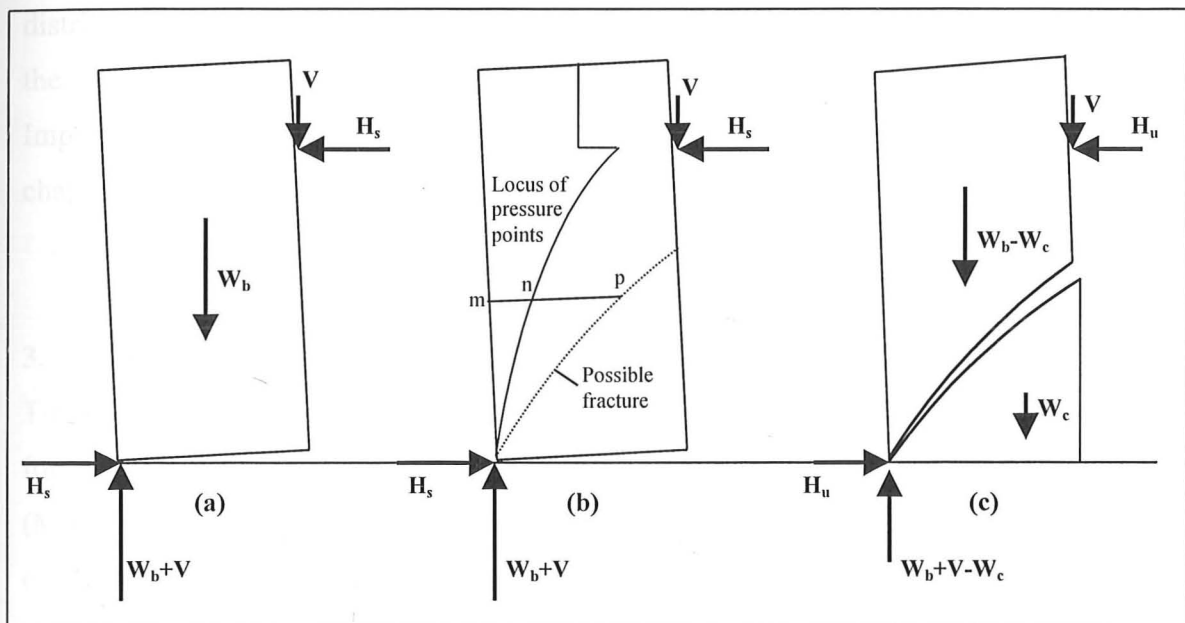


Figure 3.1 Buttress collapse by overturning due to a horizontal force: (a) Solid buttress; (b) Internal forces in solid buttress at overturning from an analysis of horizontal slices of the buttress; (c) Fractured buttress fails at lower thrust, H_u .

Figure 3.1 illustrates the problem. A buttress must resist a horizontal thrust, H , which applies an overturning moment. This is countered by a stabilising moment due to the weight of the buttress, W_b , and the weight of the vault, V . At the collapse state, a fracture will occur, and the stabilising moment will be reduced by the moment due to the weight of the ineffective region (below the fracture) of the buttress, W_c (see Figure 3.1c). The internal line of forces, often known as a line of thrust, is here called a *locus of*

¹ This chapter is the result of research carried out in open collaboration with Professors S. Huerta and J.I. Hernando at the Universidad Politécnica de Madrid in the spring of 2001.

pressure points, for reasons that will be made clear in Chapter 5. This is the locus of internal reaction points found by making a horizontal cut in the buttress and determining the location of the vertical force reaction necessary to maintain equilibrium at that level. The fracture surface at the collapse state can be estimated by defining a fracture condition in relation to the eccentricity of the locus of pressure points from the centroid of the cross-section.

In a rectangular section, the internal line of forces, called the *locus of pressure points*, must act at the one-third point in the fractured region of the buttress. This produces a line of zero axial stress where the material is assumed to separate and a fracture forms. The fracture surface is illustrated by the dotted line in Figure 3.1(b), defined by the condition $mp = 3mn$, derived from the assumption that the compressive stress distribution is linear in the fractured region. The weight of the vault, V , acts to stabilise the buttress, though the horizontal thrust, H , acts to de-stabilise the buttress. Importantly, the horizontal thrust of the arch, H , varies with geometry changes and this chapter will focus on the influence of the horizontal thrust on the stability of a buttress.

3.2 Mechanism of Collapse

To demonstrate the safety of a masonry structure, the resulting internal compression forces, or locus of pressure points, must be contained everywhere within the masonry (Moseley 1843; Heyman 1995). When the internal forces deviate sufficiently from the centroid of the cross-section, tensile stresses may cause a crack to form on the opposite side. When the thrust reaches the edge of the masonry, a “hinge” will develop, and the entire section will be cracked. Cracking is not dangerous in itself, and it is the way in which masonry structures adapt to small changes of the boundary conditions. As illustrated in Chapter 2, a masonry arch will adapt to a small movement of the abutments by forming three hinges. Increasing the spread of the abutments will form a kinematically-admissible mechanism, which will lead to the collapse state. A three-hinged arch is statically determinate, and requires a fourth hinge to form in order to provide a collapse mechanism. On the other hand, a buttress is statically determinate to begin with and needs only one hinge to collapse. The process of collapse analysis is the same for buttresses as for arches: a collapse mechanism is assumed (in this case the location of the single hinge); the equilibrium equations are written; and the collapse

load is calculated for the given mechanism. The actual collapse load will be the lowest load at which a mechanism forms, with a corresponding line of internal forces contained entirely within the masonry.

The application of limit analysis methods presupposes that the individual masonry blocks must have sufficient size. Thus, it is not possible to build a tall, load-bearing wall from very small blocks, the size of sand particles. Actual masonry buttresses typically have 10 or 20 blocks across the width of the buttress, as opposed to 100 or 1000. As the block size becomes smaller, it is more likely that the blocks will separate if they are not held in direct compression. This is precisely the case with masonry buttresses. As a consequence of the unilateral character of the material -- it is able to withstand compression but not tension -- some fracture of the buttress can be expected at collapse, similar to leaning towers or walls of masonry (Heyman 1992). At the limit of overturning, part of the buttress will remain attached to the base and a stress-free surface of fracture will form.

For masonry arches each individual voussoir is considered to be solid, and this practical assumption leads to a rational and safe analysis. The same assumption can be extrapolated to buttresses, and a horizontal slice can be considered as a "voussoir." This is a logical assumption for buttresses, which are typically built with horizontal courses of masonry. However, for buttresses it is unsafe to consider each slice as if it were a solid. If the thrust is eccentric, the material which is not in direct compression will be ineffective and will separate from the effective region of the buttress. This is analogous to the case of multi-ring brick arches. If a hinge forms on the extrados of the arch, individual bricks in the intrados will no longer be held in place by direct compression, and these bricks may fall from the arch. Similarly, regions of the buttress not in direct compression will be ineffective, and as the buttress fails due to overturning, these regions will fall from the solid buttress.

3.3 Proof of Straight Fracture

To determine the shape of the fracture at overturning, it is necessary to assume a compressive stress distribution in the unfractured region of the masonry. It is reasonable to assume a linear stress distribution in axial compression, with a fracture occurring at the location of zero stress, according to simple elastic theory. This leads to the middle-

third rule: for a rectangular cross-section, tension will occur when the normal force falls outside of the middle-third of the cross-section.

Numerous authors have made the assumption of a linear stress distribution in compression in order to solve a specific problem in masonry structures (Dupuit 1870; Castigliano 1879; Heyman 1992; La Mendola *et al.* 1993). This assumption provides a basis for solving the problem of buttress overturning. Though elastic theory is generally unhelpful for the analysis of masonry structures globally, it can be applied in isolation to very simple problems in order to gain insight into the possible stress distribution in a particular element. It is not possible to know the exact stress distribution in a masonry structure, and thus any calculation of the internal stresses can only be an approximation. However, assuming a linear stress distribution in compression can be used to gain insight into the problem. Figure 3.2 illustrates the assumption of the compressive stress distribution and the resulting location of zero stress where the material is ineffective.

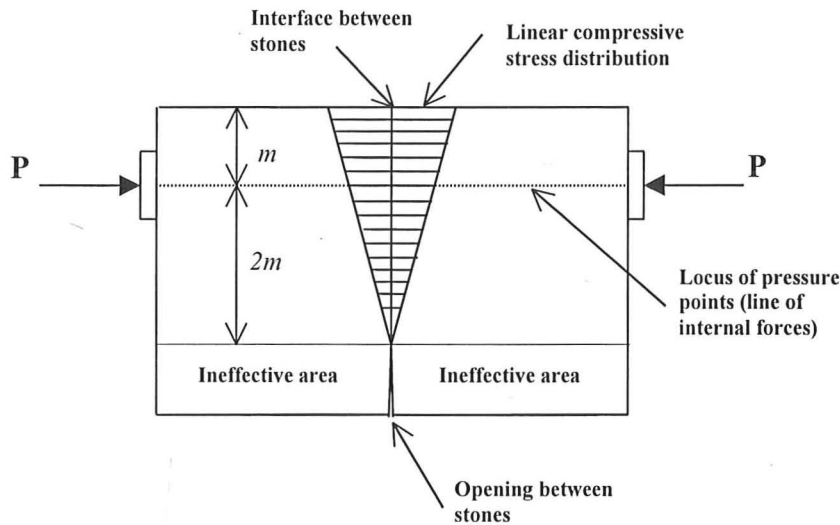


Figure 3.2. Assumption of linear compressive stress distribution under axial loading in the fractured region of a masonry buttress. In this example, two stones are held together by the axial compressive forces, P , lying outside the middle-third of the rectangular cross-section. The internal stress distribution is linear in compression, so that the internal line of forces acts at the one-third point of the triangular stress distribution. Material not in direct compression is assumed to be ineffective, and an opening is assumed to form between the stones.

The *kern* points of a section define the points at which an axial force produces zero stress at each of the extreme fibres. For a rectangular section, the kern points occur at the one-third points of the section, and therefore an axial force applied anywhere within the middle-third will produce a state of compressive stress over the entire section.

Because masonry is assumed to have no capacity for tension, the material is assumed to separate when it is no longer in direct compression, as in Figure 3.2 above.

The assumption of a linear stress distribution leads to an unexpected and elegant result for the buttress problem. In a buttress of constant width and depth, the critical line of fracture at overturning turns out to be straight, rather than curved as in Figure 3.1(c). (In three dimensions, the surface of fracture is planar.) Thus, at the failure state, the lower portion of the buttress is a triangular wedge supporting a solid, uncracked, upper portion of the buttress, with force resultants acting at the one-third point of the lower portion.

To determine the shape of the curve of fracture, the equilibrium of a horizontal slice in the lower cracked portion is examined as a free body. A thin horizontal slice of masonry is analysed as illustrated in Figure 3.3, assuming that the resultant vertical force acts at one-third of the width. The slice has a thickness of dy , and is subjected to a constant horizontal force, H , and a varying vertical force from above, W . Since the problem is regarded as two-dimensional, it is convenient to define a weight of material per unit area of the elevation, γ , which accounts for the depth (through-thickness) of the buttress and the density of the material. As usual, it is assumed that sliding will not occur.

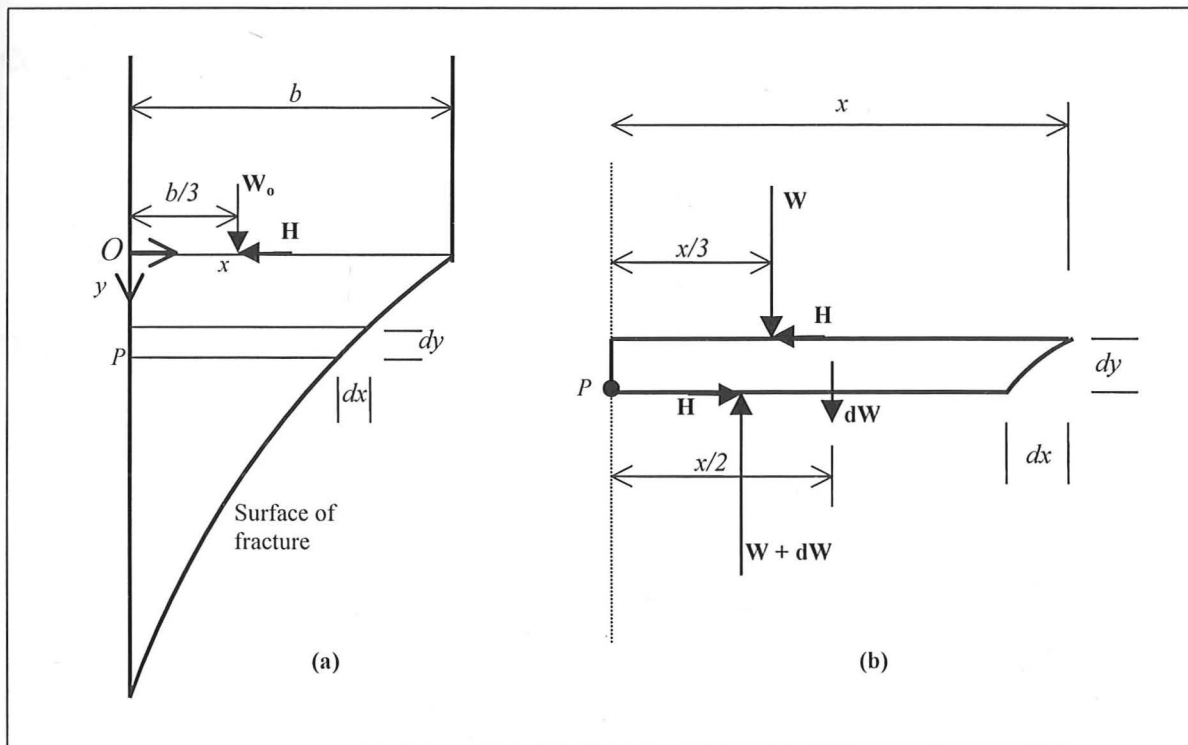


Figure 3.3. (a) Equilibrium in the lower fractured region of the buttress; (b) Equilibrium of a horizontal slice. The horizontal force, H , is applied from the right, and overturning is assumed to occur about the lower left corner. The origin O of a cartesian (x, y) co-ordinate system is shown in (a), where the fracture begins.

Enforcing moment equilibrium for the horizontal slice of width x about point P:

$$\frac{Wx}{3} + \frac{xdW}{2} = \frac{Wx}{3} + d\left(\frac{Wx}{3}\right) + Hdy \quad [3.1]$$

which becomes, on re-arrangement

$$\frac{xdW}{2} = \frac{xdW}{3} + \frac{Wdx}{3} + Hdy. \quad [3.2]$$

Simplifying and solving for W gives

$$W = \frac{x}{2} \left(\frac{dW}{dx} \right) - 3H \left(\frac{dy}{dx} \right). \quad [3.3]$$

But for a thin slice of thickness dy :

$$dW = \gamma x dy. \quad [3.4]$$

Combining [3.3] and [3.4] gives

$$W = \left(\frac{\gamma x^2}{2} - 3H \right) \left(\frac{dy}{dx} \right). \quad [3.5]$$

Differentiating [3.5] with respect to x , and combining with [3.4] gives

$$\left(\frac{\gamma x^2}{6} - H \right) \left(\frac{d^2 y}{dx^2} \right) = 0. \quad [3.6]$$

To satisfy [3.6] for general values of x ,

$$\left(\frac{d^2 y}{dx^2} \right) = 0 \quad [3.7]$$

It follows that (dy/dx) is constant and hence the curve of the fracture must be a straight line. Equation [3.6] is also satisfied by the condition

$$H = \frac{\gamma x^2}{6} \quad [3.8]$$

which corresponds to the horizontal force required to equilibrate the weight of a triangular wedge. Therefore, in the special case of no applied force from above, where $W_o=0$, the fracture is also linear.

This general finding reveals that a masonry buttress at the limit of overturning will form a planar fracture at the base. In a real buttress, the fracture line will not be perfectly straight, and will be influenced by the composition of the masonry and the interlocking of the individual stones. This section has illustrated that the fracture is *straight*, but the exact location of the fracture must also be determined in order to calculate the capacity of the buttress. The location of the fracture can be determined from the equilibrium equations for the masonry buttress.

3.4 Equations of Equilibrium

Based on the assumption of a straight line of fracture at the collapse state, equilibrium equations for the collapse of masonry buttresses can be written for the vertical buttress of Figure 3.4. An increase in the vertical applied force, V , will act to stabilise a buttress, while increasing the horizontal thrust, H , will lead to the failure of a buttress. In the case of buttresses supporting masonry vaults, the stabilising vertical load, V , is unlikely to change significantly because it is derived from the weight of the masonry in the vault. The horizontal thrust required for equilibrium of the arch, H , is obviously dependent on the geometry of the structural system, and it can change dramatically due to the leaning of buttresses or other imposed displacements, such as foundation settlements or earthquake loading. Therefore, the horizontal thrust, H , is generally the most critical loading for the stability of buttresses.

To calculate the resistance of the buttress to overturning, two equations are required to determine the critical fracture height, e , and the corresponding failure load, H . One equation results from the moment equilibrium of the entire solid about the lower left-hand corner, less the fractured region (shown in Figure 3.4b). A second equation may be derived from the equilibrium condition for the lower triangle (shown in Figure 3.4c) together with the assumed stress distribution in the fractured region of the buttress. From these two equations, the critical fracture height, e , and overturning load, H , can be determined uniquely.

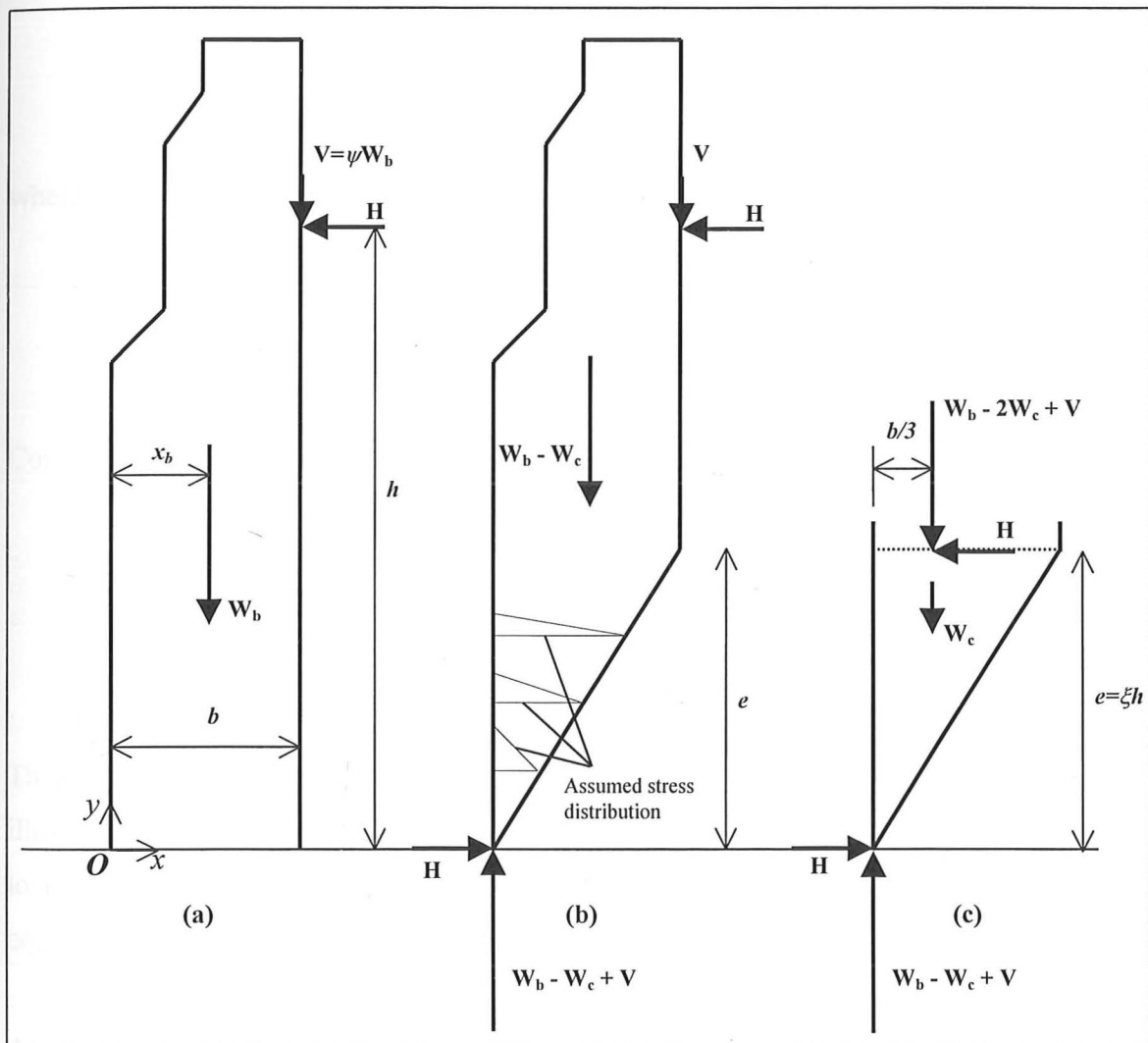


Figure 3.4 (a) Buttress geometry; (b) Equilibrium of fractured buttress; (c) Equilibrium of fractured wedge.

Assuming that the buttress is fractured, the overturning load, H , must be in equilibrium with the weight of the intact part of the buttress. For present purposes, it is convenient to

use an x, y co-ordinate system with the origin, O , at the pivot point of the buttress. The stabilising moment about O for the buttress is

$$M_s = W_b x_b + Vb \quad [3.9]$$

where x_b is the x -coordinate of the centroid of the buttress (Figure 3.4a).

Moment equilibrium about the origin (Figure 3.4b) gives:

$$M_s - W_c \left(\frac{2b}{3} \right) - Hh = 0 \quad [3.10]$$

where the weight of the ineffective detached region of the buttress is

$$W_c = \frac{bey}{2}. \quad [3.11]$$

Combining and solving for the overturning force gives

$$H = \frac{\left(M_s - \frac{b^2 ey}{3} \right)}{h}. \quad [3.12]$$

This is the general linear equation for the force that will overturn a buttress of the form illustrated in Figure 3.4(b) with a given fracture to height e . To determine the collapse load unambiguously, the critical fracture height, e , is derived by examining the internal equilibrium of the buttress in the lower, intact region.

At the limit of overturning, the internal forces in the buttress are unique, and the triangular fractured region of the buttress must satisfy force equilibrium as shown in Figure 3.4(c), in order to satisfy the "fracture" assumption of a simple triangular compressive stress distribution. The triangular wedge is loaded by the force resultants from the upper region of the buttress, applied at one-third of the width of the buttress, in order to initiate the propagation of the fracture at a height of e . The weight of the

fractured wedge, W_c , also acts at the one-third point. This results in a simple expression, which relates the force reactions at the base of the buttress to the geometry of the fractured portion of the buttress

$$(W_b - W_c + V) \left(\frac{b}{3} \right) - He = 0. \quad [3.13]$$

Substituting for W_c from [3.11] and solving for H gives

$$H = \frac{b(W_b + V)}{3e} - \frac{b^2\gamma}{6}. \quad [3.14]$$

Equation [3.14] gives a second formula for the overturning force, H , as a function of the fracture height, e .

The condition for the rotational equilibrium of the buttress [3.12] and the equilibrium conditions to produce the fracture in the lower region of the buttress [3.14], provide two independent equations to determine both the critical height of fracture, e , and the value of the overturning force, H . A specific example of a rectangular buttress will be analysed for overturning later in this chapter. The above equations constitute a general approach for solving the collapse state of a buttress by examining the unique value of internal forces at the limit of overturning. The equations above can of course be adapted to account for buttresses with varying profiles and more complex lateral loading, such as horizontal overturning forces at two different heights (for example, as a result of two flying buttresses in the case of Gothic buttresses).

This approach is valid for buttresses in which:

- 1) the lower, fractured region of the buttress is rectangular in elevation, with constant depth-density;
- 2) there are no external loads applied to the lower, fractured region of the buttress; and (as usual),
- 3) Sliding does not occur.

3.5 Limits on Sliding

Although overturning failure without sliding will govern the stability for most masonry buttresses, failure by sliding of masonry blocks may occur in certain circumstances. The sliding is assumed to occur on a horizontal plane between level courses of masonry. Sliding will be most critical at the level of the applied horizontal force, where the vertical force acting over the horizontal plane must develop sufficient friction to overcome the possibility of sliding.

To avoid sliding at the level of the applied force

$$H < (W + V)f_s \quad [3.15]$$

where W here is the weight of the buttress above the level being considered, V is the vertical component of the applied force, and f_s is the assumed static coefficient of friction. Typical values of f_s are 0.5-0.7, for stone on stone (Rankine 1858). Sliding is thus most likely to occur for a horizontal force applied near the top of the buttress, where the weight of the buttress above is minimal. The use of pinnacles on some Gothic buttresses can play an important role to prevent sliding in this instance (Heyman 1968, 1995). Though it is unlikely to occur in practice, a horizontal applied load near the base of a buttress can also lead to sliding failure rather than overturning failure.

3.6 Rectangular Buttresses

The methods described above were developed in relation to the stepped buttress shown in Figure 3.4 and can readily be applied to the simplest case of rectangular buttresses. There, the total weight of the buttress is

$$W_b = bh_b\gamma \quad [3.16]$$

where h_b is the total height of the rectangular buttress and γ is the depth-density. The horizontal co-ordinate of the centroid is

$$x_b = \frac{b}{2}. \quad [3.17]$$

Thus equation [3.12] governing the rotational equilibrium of the buttress, becomes

$$H = \left(\frac{b}{h}\right) \left(\frac{h_b b \gamma}{2} + V - \frac{b e \gamma}{3}\right). \quad [3.18]$$

Equation [3.14] becomes

$$H = b \left(\frac{h_b b \gamma + V}{3e} - \frac{b \gamma}{6}\right). \quad [3.19]$$

It is convenient now to define three dimensionless geometric factors for rectangular buttresses:

$$\xi = \frac{e}{h} \quad [3.20]$$

relating the fracture height to the height of the applied force;

$$\mu = \frac{h}{h_b} \quad [3.21]$$

relating the height of the applied force to the total height of the buttress; and

$$\psi = \frac{V}{W_b} \quad [3.22]$$

relating the vertical load, V , to the weight of the buttress, W_b .

Substituting these factors, equation [3.18] becomes

$$H = b^2 \gamma \left(\frac{1 + 2\psi}{2\mu} - \frac{\xi}{3}\right) \quad [3.23]$$

and equation [3.19] becomes

$$H = b^2 \gamma \left(\frac{1 + \psi}{3\mu\xi} - \frac{1}{6} \right). \quad [3.24]$$

From these two equations, the critical values of H and ξ can be determined. Combining [3.23] and [3.24] to eliminate H gives the following quadratic equation for ξ

$$\xi^2 - \left(\frac{1}{2} + \frac{3}{2\mu} + \frac{3\psi}{\mu} \right) \xi + \left(\frac{\psi + 1}{\mu} \right) = 0. \quad [3.25]$$

Solving [3.25] for ξ gives the location of fracture height leading to failure in a rectangular buttress. (The correct root must be between 0 and 1.) This value can then be substituted into [3.23] or [3.24] to find the critical failure load for overturning, H_u , corresponding to ξ . The critical value of ξ is independent of the scale of the buttress.

Remarkably, the fracture location does not depend on the width, b , of the buttress and depends only on the height of the applied force (the factor μ) and the relative value of the vertical load (the factor ψ). The reason for this is that all weights scale as b and all lever arms (i.e. x -coordinates of centres of gravity) also scale as b . So equation [3.25] defining the value of e is independent of b . Equation [3.25] can be solved for varying values of μ and ψ to find the corresponding fracture heights. The results are presented in Figure 3.5, and it is clear that the fracture height depends mostly on the relative value of the vertical force, ψ , and is relatively insensitive to the relative height of the applied force, μ . In fact, for the case of the vertical force equal to one half the weight of the buttress, ($\psi = 0.5$) the fracture height will occur at $\xi = 0.5$ for any value of μ (though sliding limits will exist depending on the geometry of the problem). This result may be obtained by direct manipulation of equation [3.25]. For typical values of applied vertical load ($\psi = 0$ to 0.5), the fracture height will vary between $\xi = 0.7$ to 0.5. In other words, the height of the fracture, e , will typically be 50% to 70% of the height, h , of the applied horizontal force. An increase in the applied vertical load (the factor ψ), will decrease the height of the fracture by changing the internal stress conditions in the buttress.

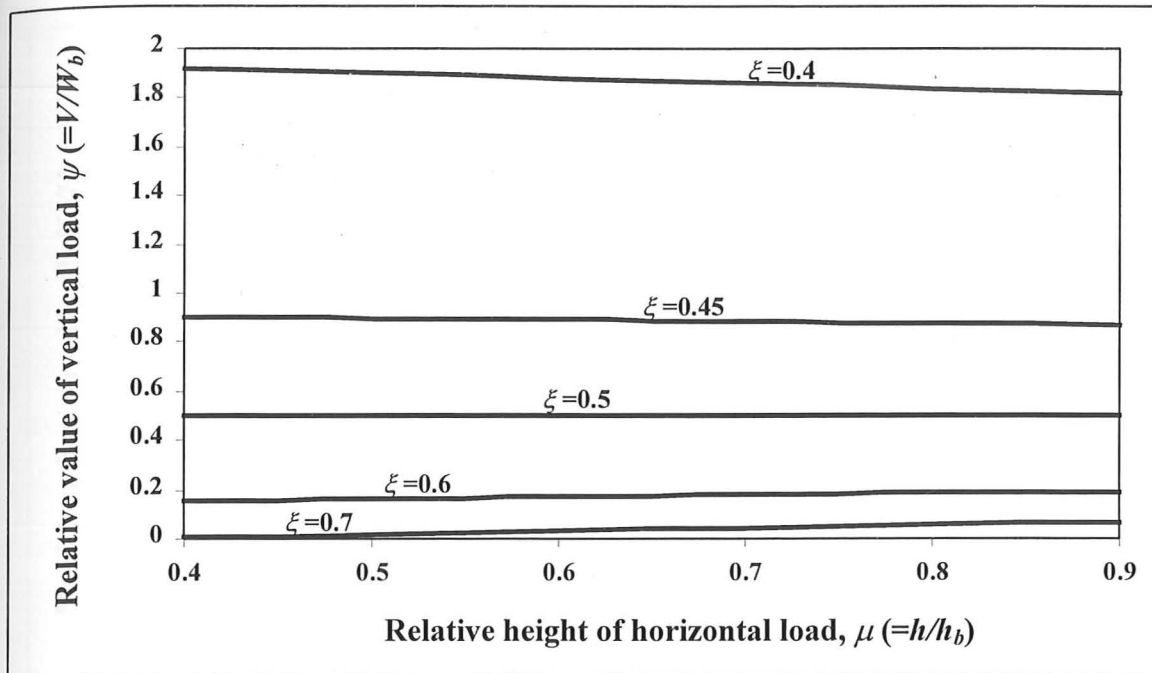


Figure 3.5. Variation in fracture height, ξ , as determined from Equation [3.25] for rectangular buttresses.

The methods presented above can be used to determine the reduction in overturning force due to the fracture, and the results are summarised in Figure 3.6. The critical failure load can be determined graphically from Figure 3.6, based on the height of the applied force, μ , and the relative value of the vertical load, ψ . The value H_s is the overturning force for a solid, unbreakable buttress, and the vertical axis of the graph provides the maximum horizontal load, H_u , as a fraction of H_s . For rectangular buttresses, the overturning force of the solid buttress is

$$H_s = b^2 \gamma \left(\frac{\frac{1}{2} + \psi}{\mu} \right). \quad [3.26]$$

The graph also illustrates the limits on sliding, which depend on the proportions of the buttress, given by the ratio h_b/b . For a static coefficient of friction of 0.7, the sliding limits are solved for various buttress proportions. The buttress may fail by sliding rather than overturning when the thrust is applied near the base of the buttress (small μ), or near the top of the buttress (as μ approaches 1).

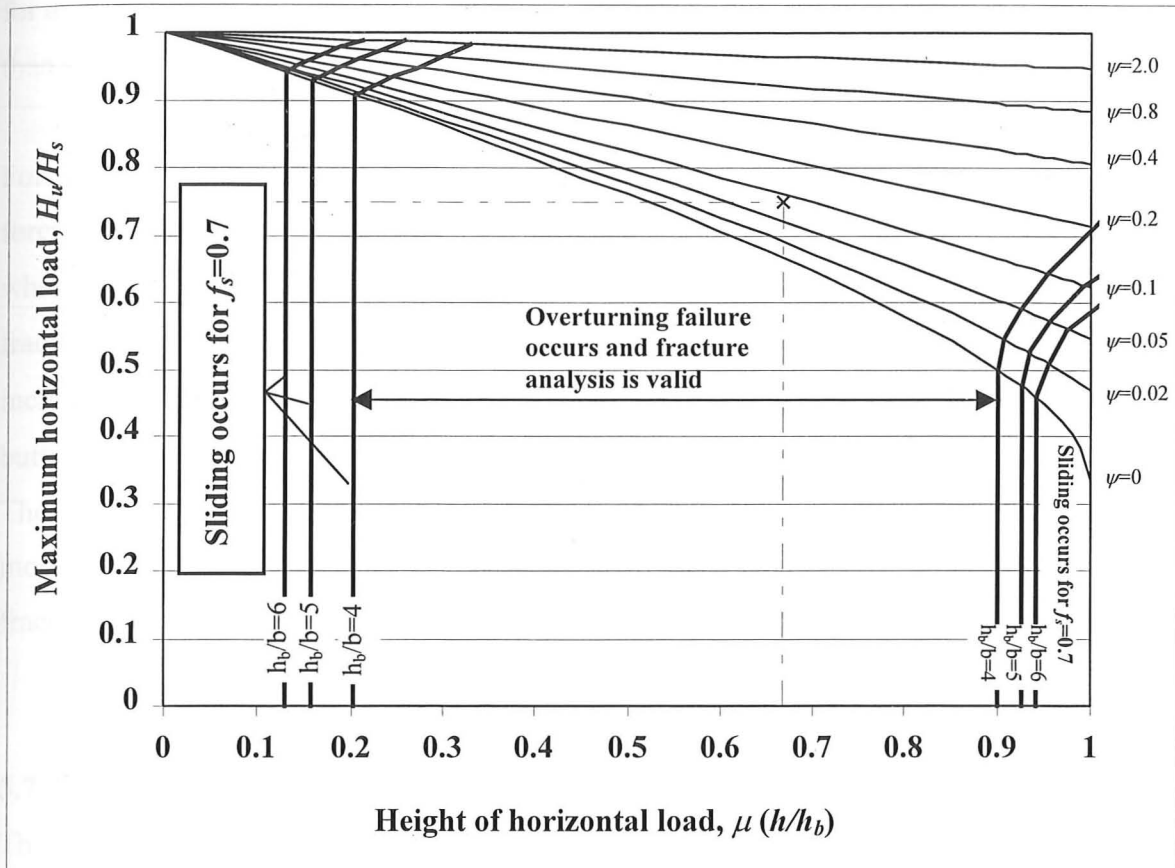


Figure 3.6. Collapse loads for rectangular buttresses under horizontal load.

To illustrate the use of Figure 3.6, a rectangular buttress with a height h_b of 12 m and a base width b of 3 m is considered. A horizontal force is applied at a height h of 8 m, so that $\mu = 0.67$. The depth of the buttress (perpendicular to the elevation shown in Figure 3.4) is uniform and equal to 1.5 m, and with a material density of 2000 kg/m^3 , the depth-density, γ , becomes 3000 kg/m^2 , or 29.4 kN/m^2 . The buttress supports a vertical load, V , of 100 kN, and the factor $\psi = 0.09$. (The vertical load V is 9% of the buttress weight, $W_b = 1060 \text{ kN}$.) From [3.26] the maximum horizontal force, H_s , for the solid buttress is 234 kN. From Figure 3.6, the ratio of H_u/H_s is found by interpolation to be approximately 0.76 for this buttress (marked by the point x on the graph). Therefore, the maximum horizontal force, H_u , is $0.76H_s$, or approximately 178 kN. The same result is found computationally by solving equation [3.25]. The critical fracture occurs at $\xi = 0.65$, corresponding to a height of $e = 5.2 \text{ m}$ for this example. Solving [3.23] or [3.24] (instead of using Figure 3.6) gives an overturning force of $H_u = 178 \text{ kN}$, which agrees with the estimate made using Figure 3.6. From [3.15], the critical sliding load is 317 kN

for a coefficient of friction of 0.7, verifying that failure will occur by overturning rather than sliding.

For this example, the fracture at the point of overturning has reduced the overturning force by approximately 25%. This reduction that can be read directly from Figure 3.6, where the vertical axis, H_i/H_s , provides the reduction in overturning force due to the fracture and the ineffective buttress material at overturning. As the applied vertical force increases (i.e. the factor ψ increases), the height of the fracture decreases, and the buttress resistance approaches the full resistance of the solid buttress, where $H_i/H_s=1.0$. The horizontal load capacity of typical buttresses is 20%-30% less than the capacity of a monolithic buttress, justifying the current study and demonstrating the importance of the fracture at the collapse state.

3.7 Non-Rectangular Buttresses

The methods presented in this chapter can be applied to other buttress forms. In such cases, the equations for external and internal equilibrium must be derived uniquely for each buttress, and solved by following the concepts of internal equilibrium and external overturning, as presented previously. In general, there are three additional buttress forms that must be accounted for:

- 1) the sloping, or leaning buttress;
- 2) the stepped, or Gothic buttress; and
- 3) the buttress, with a T-shaped cross-section, i.e. with adjoining cross walls.

The leaning buttress is discussed in detail in the next chapter, and the other two cases will be presented briefly here.

3.7.1 Gothic (stepped) buttresses

For rectangular buttresses, overturning occurs about the base of the buttress, and it is straightforward to determine the mechanism of collapse as described above. For stepped buttresses, typical of much Gothic architecture, the buttress must be examined at different levels to determine the critical location about which overturning may occur. In this case, numerous patterns of fracture can occur due to the changes in profiles. Figure 3.7(a) illustrates the simplest case, assuming that the fracture extends throughout the lowest region of the buttress. For some stepped buttresses, this simple assumption may

be unsafe and the critical fracture may occur elsewhere in the buttress. Figure 3.7(b) shows a case where the fracture occurs at the top of the first "step" in the buttress.

In a real buttress, various fracture patterns are possible and the critical fracture will depend on the construction and location of joints in the masonry. For Gothic buttresses it is advisable to make simplifying assumptions about the fracture shape and choose the most conservative location. Assuming a linear stress distribution will give a unique answer for the collapse state, but the engineer must use judgement to determine which fracture location is most critical.

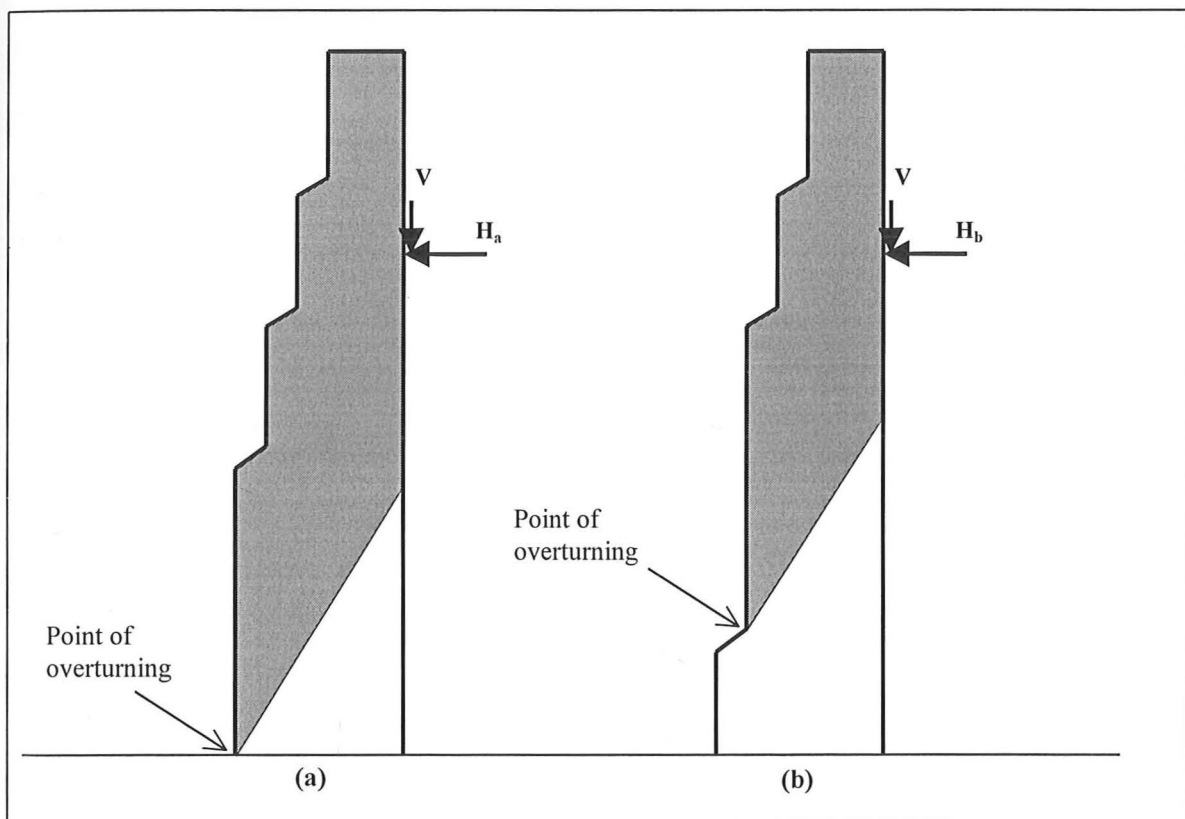


Figure 3.7. Possible fracture patterns in various Gothic buttresses at the point of overturning due to an applied horizontal thrust, H . The shaded areas represent the effective mass of each buttress that contributes to the stabilising moment to resist the applied horizontal load.

3.7.2 The T-Shaped Buttress

This chapter has considered only isolated buttresses of uniform thickness, but real buttresses are frequently attached to masonry walls so that the effective buttress section is T-shaped. In this case, the engineer must consider the contribution of the cross wall in calculating the resistance of a buttress. The problem is significantly more complex than the rectangular buttress, but can be simplified by assuming that the fracture lines are

straight: see Figure 3.8(b). The critical fracture height and overturning force can be solved with a rapidly-converging iterative calculation, which will not be presented here.

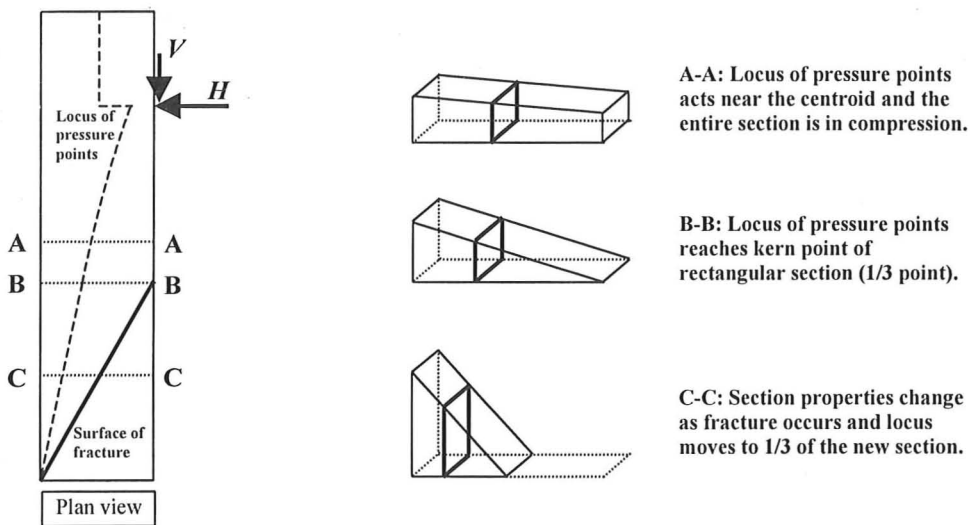


Figure 3.8(a) Assumed stress distribution in a fractured rectangular buttress at collapse.

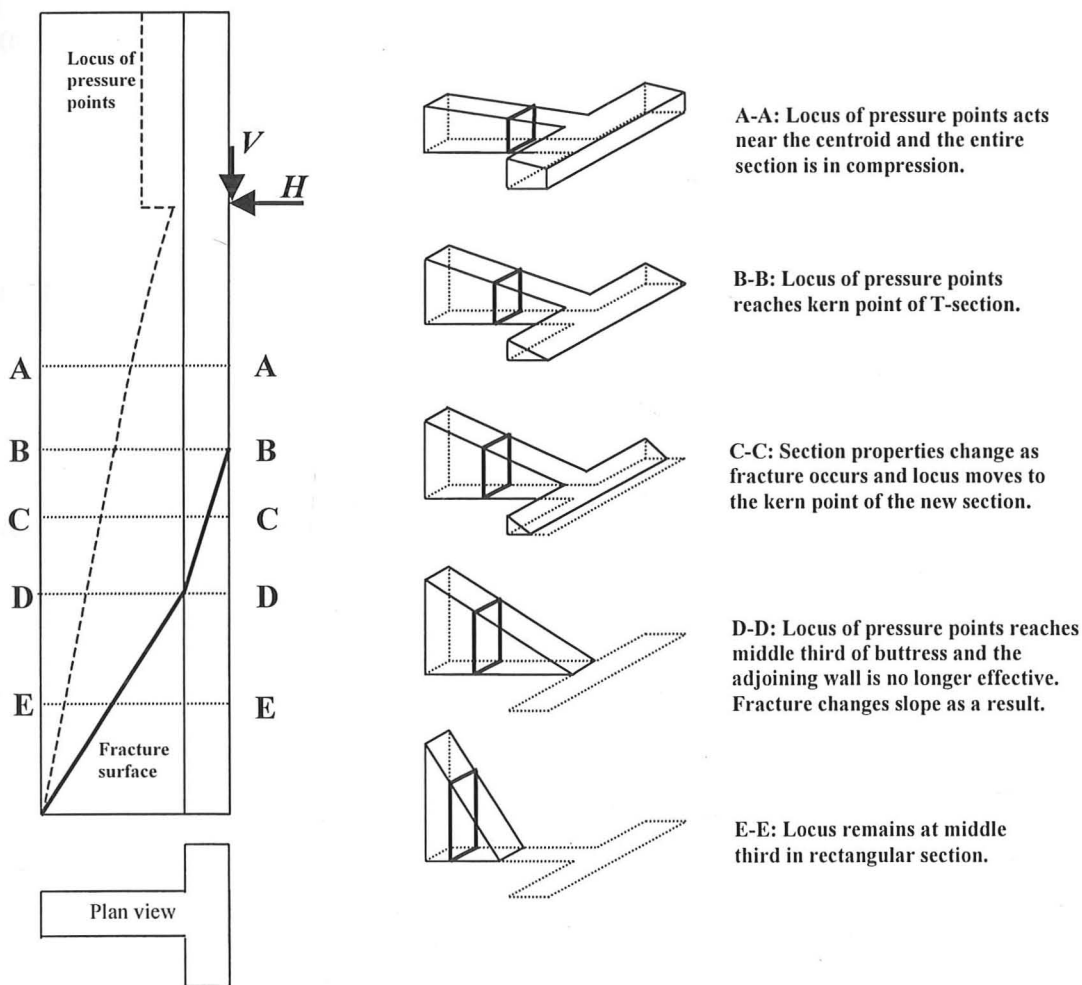


Figure 3.8(b) Assumed stress distribution in a fractured T-shaped buttress at collapse.

Depending on the form of the wall and the interlocking of the masonry, the cross-wall could be an effective part of the buttress, as in Figure 3.9(d), or the wall could be completely ineffective in contributing to the resistance of the buttress, as in Figure 3.9(a). The fracture patterns in Figures 3.9(c) and 3.9(d) are derived from the assumption of a linear compressive stress distribution in a T-section, as illustrated in Figure 3.8 on the previous page. The fracture forms initially in the wall when the pressure point reaches the kern point of the T-section. Once the fracture surface leaves the wall, the buttress section is rectangular and the pressure point acts at the one-third point of the effective section.

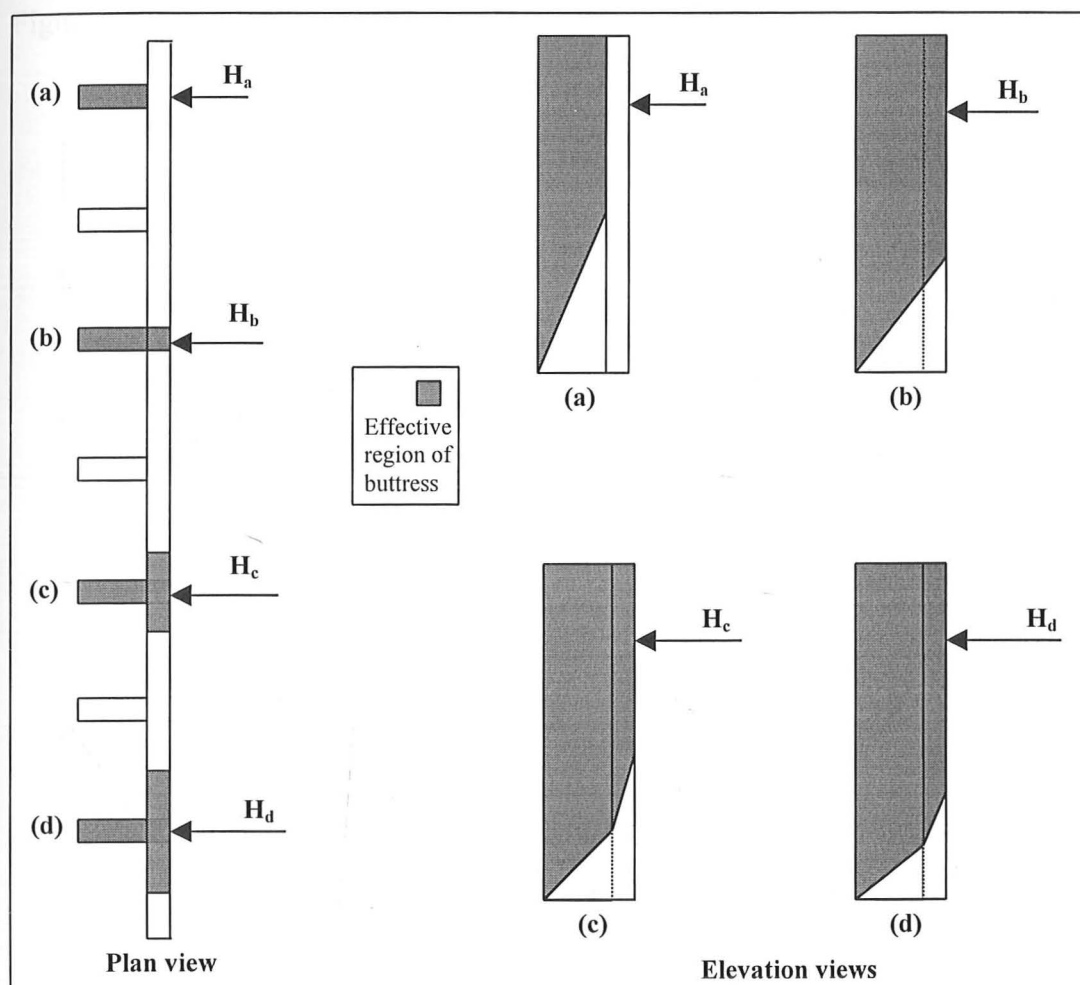


Figure 3.9. Possible contributions of cross-walls to buttress, ranging from none (a) to greatest (d).

3.8 Experimental Results

To verify the collapse mechanisms proposed in this chapter, a series of experiments have been carried out on small-scale buttresses made of plywood blocks approximately 27 mm thick. A layer of sand was glued to each block to increase the coefficient of

static friction between blocks to a level typical of stone on stone, and thus to prevent sliding. The buttresses were loaded laterally to collapse by slowly increasing the applied horizontal load. A rectangular buttress and a T-shaped buttress were tested, each with a height of 72.8 cm and a width of 18.2 cm. Each buttress was tested alone as in Figure 3.10(a), and tested again with an imposed load of 500g (11%-14% of buttress weight) on top of the buttress to model the stabilising contribution of the weight of the arch as in Figure 3.10(b). In each case, failure occurred by overturning, with a fracture in the lower region of the buttress. Further details on the experiments are presented in Appendix B, including the predictions of the collapse mechanisms for each experiment. Figures 3.10 and 3.11 present each buttress after collapse has occurred by overturning.

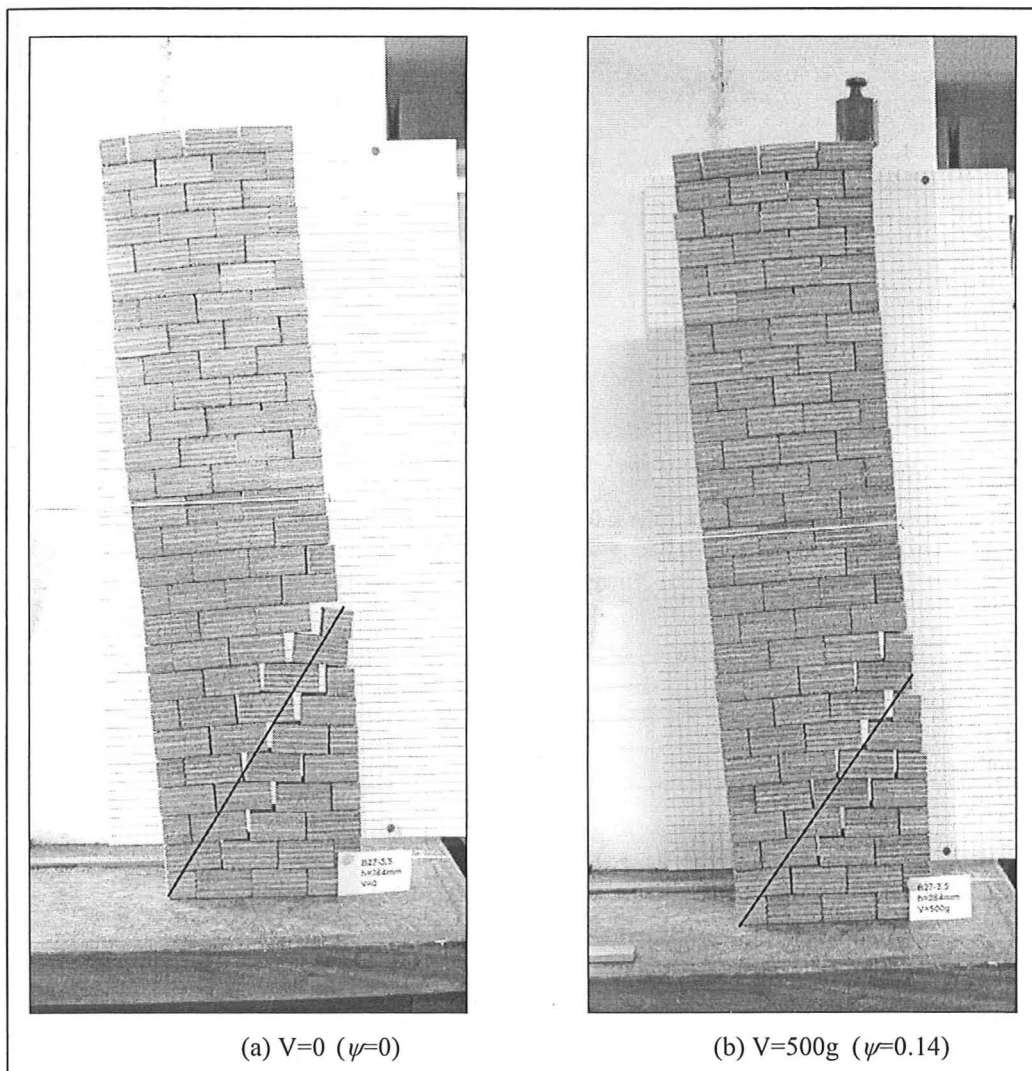


Figure 3.10. Test on rectangular buttress with $h/b=4$ and $\mu=0.5$ with a solid line for the fracture predicted by the method of section 3.6. The horizontal load is applied from the left by the white string, and the buttress is shown in the post-collapse configuration after it has reached its maximum capacity.

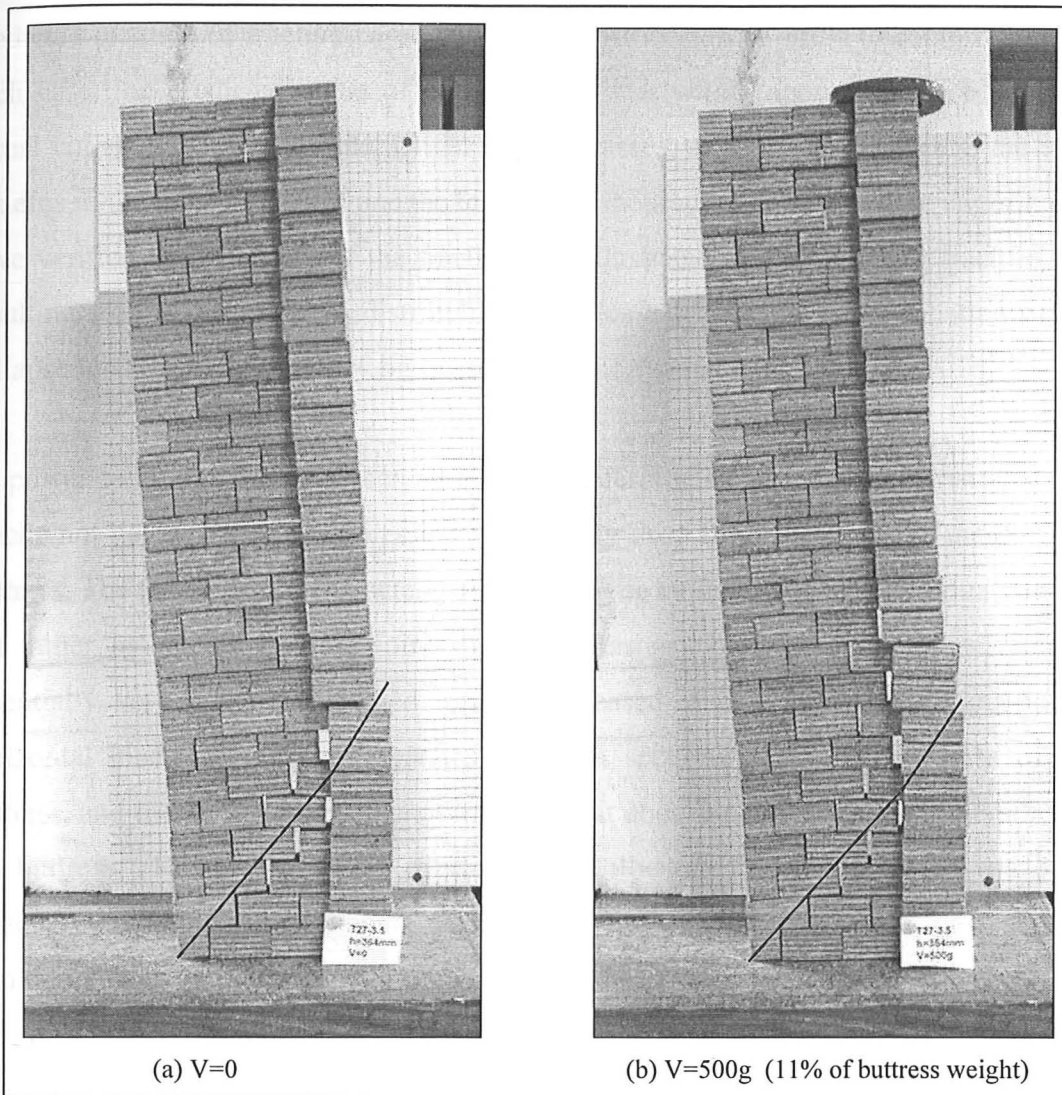


Figure 3.11 Test on T-shaped buttress with $h_t/b=4$ and $\mu=0.5$ with a solid line for the predicted fracture. The horizontal load is applied from the left by the white string, and the buttress is shown in the post-collapse configuration after it has reached its maximum capacity.

Test Number	B27.5.0	B27.5.500	T27.5.0	T27.5.500
Vertical load, V	V=0	V=500g	V=0	V=500g
Theoretical prediction of thrust, H_u	H=667g ($\xi=0.72$)	H=955g ($\xi=0.62$)	H=1023g	H=1279g
Experimental Result, H_{test}	H=710g	H=920g	H=980g	H=1230g
Thrust to overturn solid buttress, H_s	878g	1128g	1360g	1596g
H_u/H_{test}	0.94	1.04	1.04	1.04

Table 3.1 Experimental results versus calculated results for model buttresses.

For the rectangular buttress and the T-shaped buttress, the experiments verified the predicted location of fracture based on a linear distribution of stress in compression. In each case, the predicted value of collapse load was within approximately 6% of the actual collapse load: see Table 3.1. In real buttresses, as in the experiments, the joint patterns in the masonry determine the location of the fracture. These simple experiments have verified the existence of the fracture and illustrated that the straight fracture line resulting from a linear stress distribution provides a reasonable approximation of the collapse load of actual masonry buttresses under horizontal load.

As postulated in the theory presented in this chapter, the experiments demonstrated that blocks not held in direct compression will simply drop from the effective mass of the buttress. The failure is not characterised by sliding or by failure of the individual blocks, but rather by opening of the joints between masonry blocks. The buttress remains essentially vertical as the applied load is increased, and at the point of maximum horizontal load, the buttress separates into two sections: the effective mass of the buttress, and the ineffective wedge of material that does not contribute to the stability of the buttress. Failure occurs by overturning as illustrated in Figures 3.10 and 3.11. Dozens of additional experiments on model buttresses of varying sizes gave similar results, though only four such experiments have been presented here. The experiments provide support for the theory developed in this chapter, though further experiments are necessary to verify the limits to the theory presented here.

3.9 Summary

The methods presented in this chapter provide a straightforward approach to predicting the collapse load for horizontal buttresses under lateral load. This chapter has presented several key ideas:

- 1.) The horizontal thrust of an arch or vault acts to de-stabilise a masonry buttress, while the vertical forces act to stabilise the buttress. Methods to assess buttress capacity against overturning forces should focus on the value of the horizontal thrust.

- 2.) The overturning collapse of a masonry buttress involves the formation of a surface of fracture, which reduces the collapse load by reducing the stabilising moment of the buttress. Horizontal thrusts calculated on the basis of an assumed monolithic buttress are unsafe.
- 3.) The surface of fracture can be calculated by assuming a linear distribution of compressive stress and by supposing that a crack forms when the resultant internal force exits the kern of the section (middle-third for rectangular cross-sections). The problem is statically determinate and involves the solution of two equations with two unknowns, representing the thrust and fracture height.
- 4.) Based on these assumptions, the fracture surface at collapse is *planar* for rectangular buttresses. This result can be observed in actual buttresses at collapse due to overturning.
- 5.) In real buttresses the fracture depends on the composition of the masonry, and the planes of failure are likely to make a zig-zag line along the existing joint surfaces. The method of straight-line fracture presented in this paper gives an approximate solution to the problem. Complex buttress forms require additional simplifying assumptions or more complex analysis.
- 6.) Adjacent vertical walls may contribute greatly to the buttress stability and should be considered in the case of buttresses combined with cross walls. The engineer must judge the contribution of the cross walls based on the interlocking of masonry blocks in each particular case.

Chapter 4 Leaning Buttresses

4.1 Introduction

Outward leaning is the greatest threat to the stability of a buttress. Most masonry buttresses exist in a state of leaning, which increases throughout the life of the structure. In general, the lean of a buttress may be due to any or all of the following:

- Deformation and subsidence in the foundations during construction;
- Construction defects or small movements between stones;
- Elastic deformation of the masonry and mortar (usually very small);
- Additional subsidence due to changes in the soil conditions (caused by consolidation of the soil, enhanced by changes in the water table, adjacent excavations, long term creep of the foundations, etc.);
- Ratcheting movements of the stones due to vibrations of the structure (from earthquakes, bell-ringing, wind loading, etc.);
- Seasonal effects of temperature and moisture over long periods of time; etc.

As the buttress leans, the eccentric loading on the foundations can cause additional leaning, which will continue to increase during the life of the structure. The present work is not primarily concerned with the source of the displacements; rather it seeks to find the magnitude of displacements that would cause collapse. The lean of the buttress causes an increase in the span of the vault or arch, which will increase the thrust of the arch. In some cases, the increased thrust of the arch may exceed the decreased horizontal thrust capacity of the leaning buttress.

A leaning buttress overturns at a lower load than the same buttress in a vertical position, due to the horizontal shift of the centroid of the buttress. Even small amounts of leaning will significantly alter the equilibrium conditions. For buttressed vaults, a small amount of leaning in the buttress, such as 1° from vertical, will alter the line of thrust and increase the applied thrust of the vault (Huerta and López 1997). The previous chapter examined the collapse state of the buttress and the occurrence of a straight fracture at collapse. This chapter extends these findings to consider a leaning buttress. This chapter determines the influence of leaning on the fracture location and the value of thrust at collapse. Finally, methods for assessing the safety of existing, leaning buttresses are presented.

4.2 Shape of Fracture for Leaning Buttresses

For leaning masonry walls or towers loaded only by their own weight, Heyman (1992) demonstrated that the fracture would take on a slight curvature at the point of overturning, as illustrated in Figure 2.4 in the literature review. A buttress leaning outwards (i.e. away from the applied load) may develop a fracture that curves slightly below the straight-line fracture. Thus it is safe to approximate the fracture as a safe line for a buttress leaning away from the applied load, since any effective material neglected by the straight-line assumption will contribute to the stability of the buttress. A buttress sloping inwards (i.e. towards the applied load) may develop a fracture that curves above the straight line. Thus, it may be slightly unsafe in this case to assume that the fracture acts as a straight line, but for practical purposes it is a reasonable assumption. Remarkably, experiments by Vicat on masonry towers in 1832 demonstrated a sloping buttress that developed a straight-line fracture at the collapse state: see Figure 4.1. This result illustrates that the assumption of a straight-line fracture is appropriate for sloping or leaning buttresses.

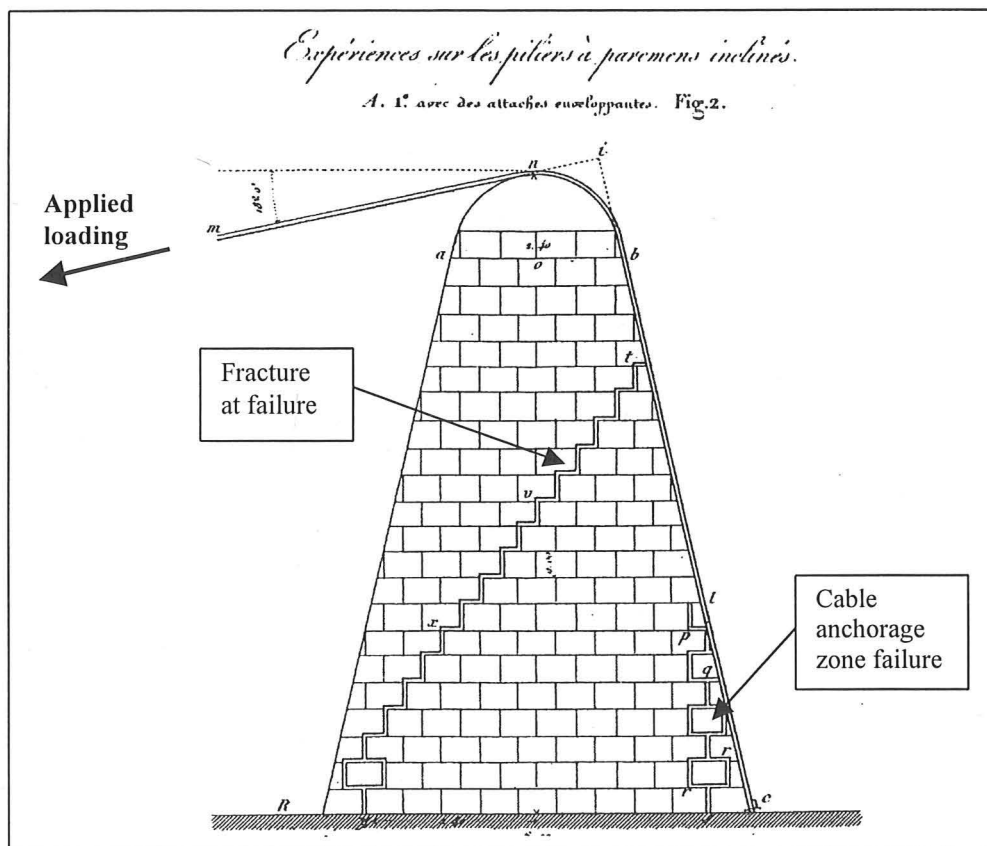


Figure 4.1 Experiments on masonry towers for suspension bridges (Vicat 1832). As in Figure 2.2, the tower served as the anchorage for the cable, which extended around the top of the tower. The applied load is equivalent to an inclined load at the top of the tower, similar to the thrust of a vault, where the load of the cable applies both a vertical and horizontal load to the top of the tower.

4.3 Leaning Rectangular Buttresses

Typical buttresses lean less than 2° , and the tower of Pisa leans by approximately 5° . The critical question for leaning buttresses is to determine if the location of the line of fracture will shift substantially as a result of small angles of leaning. The collapse analysis for rectangular buttresses presented in Section 3.6 can be modified for a buttress with a small angle of inclination, ϕ , measured from the vertical. All other variables and dimensions are as outlined in the previous chapter and as shown in Figure 4.2. The rotation is assumed to occur about the outer corner at the base of the buttress, point O , and the usual small angle approximations are applied.

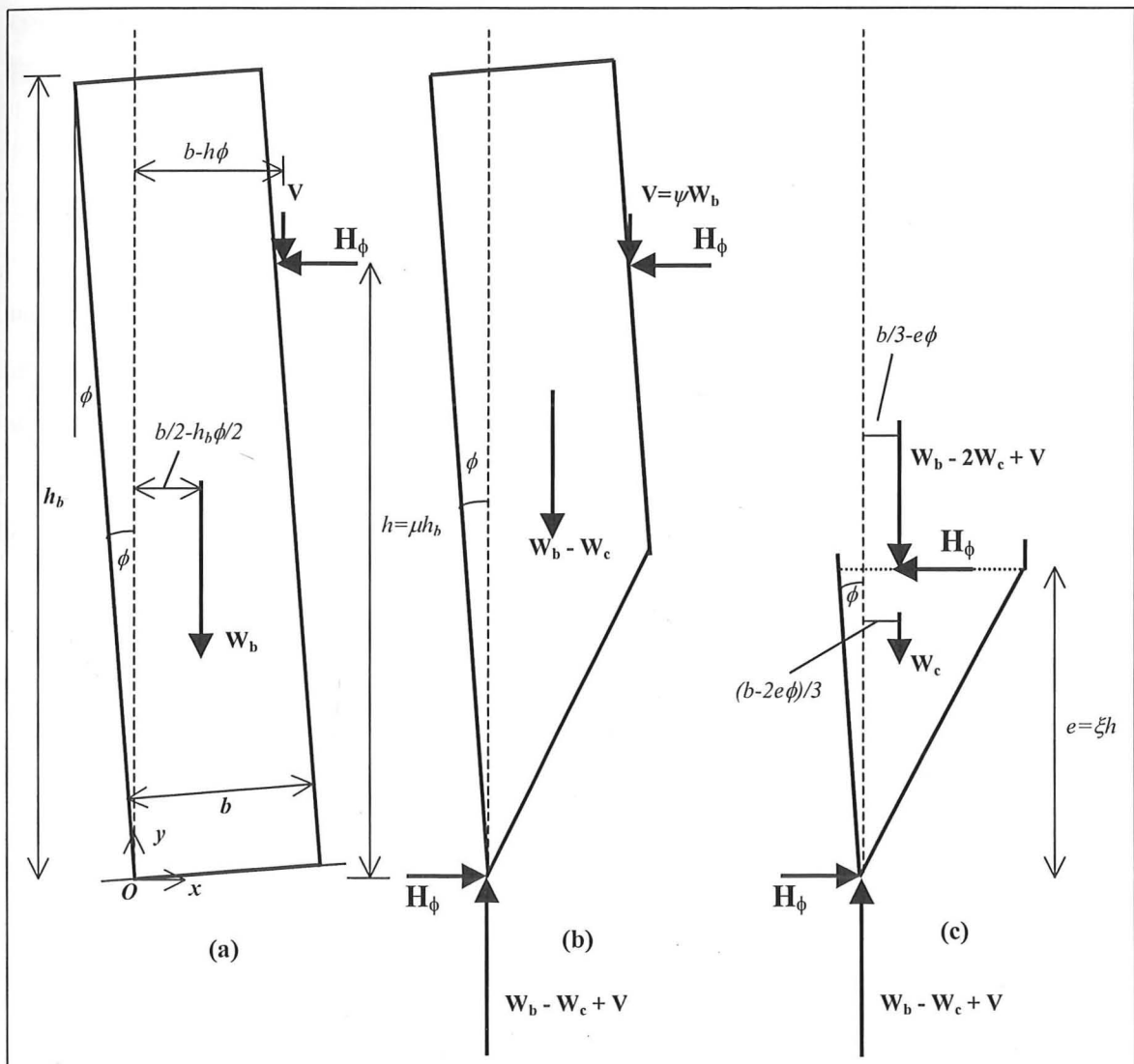


Figure 4.2 (a) Leaning rectangular buttress assuming that the rigid support has rotated; (b) Equilibrium of effective buttress; (c) Equilibrium of fractured wedge as a free body.

As a result of leaning by a small angle, ϕ , the stabilising moment of the unfractured buttress about the origin becomes

$$M_{s\phi} = W_b \left(\frac{b - h_b \phi}{2} \right) + V(b - h\phi) \quad [4.1]$$

where the usual small-angle assumptions are made, and the angle of lean, ϕ , is given in radians. The height of the horizontal thrust is assumed to remain constant as the buttress leans. The buttress is assumed to begin in a vertical position, and then rotate about the outer edge of the buttress on a rigid foundation, as in Figure 4.2(a).

As in the previous chapter, two equations can be derived from the equilibrium conditions: the overturning condition for Figure 4.2(b), and the fracture condition for Figure 4.2(c). The overturning condition is governed by

$$H_\phi = \left(\frac{b}{h} \right) \left(\frac{h_b b \gamma}{2} + V - \frac{be\gamma}{3} - \phi \left(\frac{h_b^2 \gamma}{2} + V - \frac{e^2 \gamma}{6} \right) \right) \quad [4.2]$$

which can be compared to equation [3.18] for the vertical buttress. Equation [4.2] is the same as [3.18], but with a new term containing ϕ , so that [4.2] reduces to [3.18] when $\phi=0$.

Equilibrium of the leaning fractured wedge shown in Figure 4.2(c) gives

$$H_\phi e = (W_b - 2W_c + V) \left(\frac{b}{3} - \phi e \right) + W_c \left(\frac{b - 2e\phi}{3} \right) \quad [4.3]$$

which becomes

$$H_\phi = b \left(\frac{h_b b \gamma + V}{3e} - \frac{b\gamma}{6} - \phi \left(h_b \gamma + V - \frac{2be\gamma}{3} \right) \right). \quad [4.4]$$

Again, equations [4.3] and [4.4] reduce to [3.14] and [3.19] for the vertical rectangular buttress (i.e. when $\phi=0$).

By introducing the dimensionless factors for rectangular buttresses given in [3.20]-[3.22], equation [4.2] becomes

$$H_{\phi} = b^2 \gamma \left(\frac{1+2\psi}{2\mu} - \frac{\xi}{3} - \phi \left(\frac{h_b}{b} \right) \left(\psi + \frac{1}{2\mu} - \frac{\mu\xi^2}{6} \right) \right) \quad [4.5]$$

which likewise reduces to [3.23] for $\phi=0$. Similarly [4.4] becomes

$$H_{\phi} = b^2 \gamma \left(\frac{1+\psi}{3\xi\mu} - \frac{1}{6} - \phi \left(\frac{h_b}{b} \right) \left(\psi + 1 - \frac{2\mu\xi}{3} \right) \right) \quad [4.6]$$

which likewise reduces to [3.24] for $\phi=0$.

As before, these two equations for H_{ϕ} provide a means of determining both H_{ϕ} and the critical fracture height, ξ . Combining [4.5] and [4.6] to eliminate H_{ϕ} gives the following quadratic equation for the fracture height:

$$\xi^2 \left(1 + 2\mu \left(\frac{h_b}{b} \right) \phi \right) - \left(\frac{1}{2} + \frac{3}{2\mu} + \frac{3\psi}{\mu} - 3\phi \left(\frac{h_b}{b} \right) \left(\frac{1}{2\mu} - 1 \right) \right) \xi + \left(\frac{\psi+1}{\mu} \right) = 0. \quad [4.7]$$

This is a modification of [3.25], with new terms containing ϕ in two of the coefficients. Solving [4.7] for ξ gives the location of fracture height leading to failure in a rectangular buttress leaning by a small angle, ϕ . As before, the correct root must be between 0 and 1. This value can then be substituted into [4.5] or [4.6] to find the critical overturning load, H_{ϕ} . The purpose of this analysis is to determine the influence of the buttress lean, ϕ , on the critical fracture height ξ .

Equation [4.7] has been solved for typical buttresses by varying the values of μ , ψ , h_b/b , and ϕ to determine the sensitivity of the solution to each variable. The buttress proportion, h_b/b , is considered for values of 4 and 6. The height of the applied load, μ , is considered for values of 0.5 and 0.7. Finally, the vertical load factor, ψ , varies from 0.1 to 1, i.e. where the applied vertical force V is 10% to 100% of the buttress weight. The buttress lean, ϕ , is considered between 0° and 5° . The results for equation [4.7] are presented in Figures 4.3 and 4.4 for the varying values.

For all cases, the critical fracture height, ξ , is remarkably constant and is insensitive to the angle of lean. The value of the thrust height, μ , has very little effect on the fracture height just as in Figure 3.5, though the vertical load factor, ψ , can lead to minor increases in the fracture height for small values of vertical load.

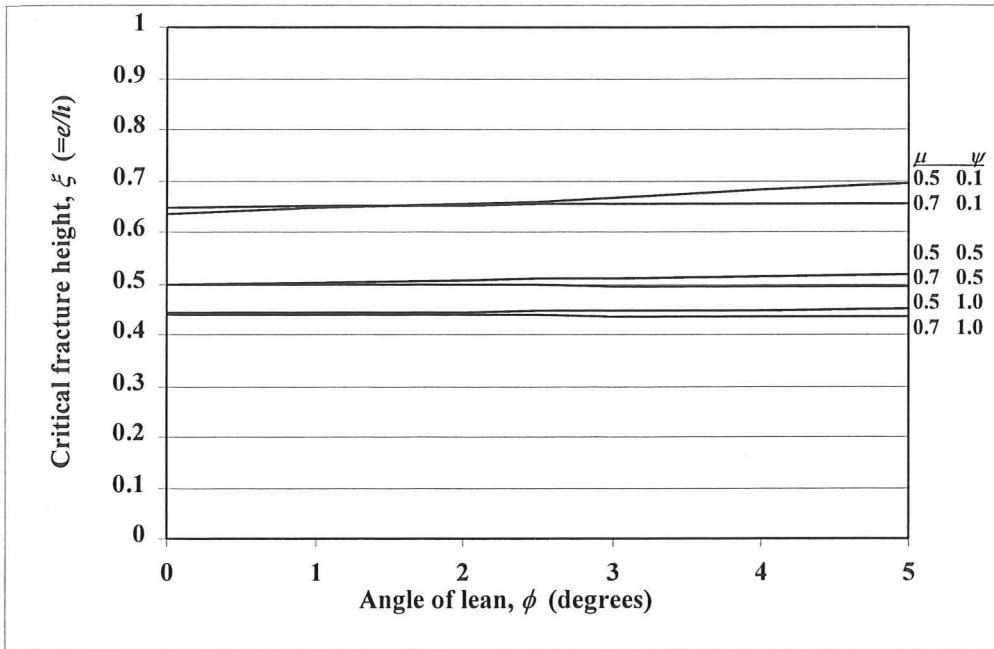


Figure 4.3 Variation in fracture height for a leaning rectangular buttress ($h_1/b=4$).

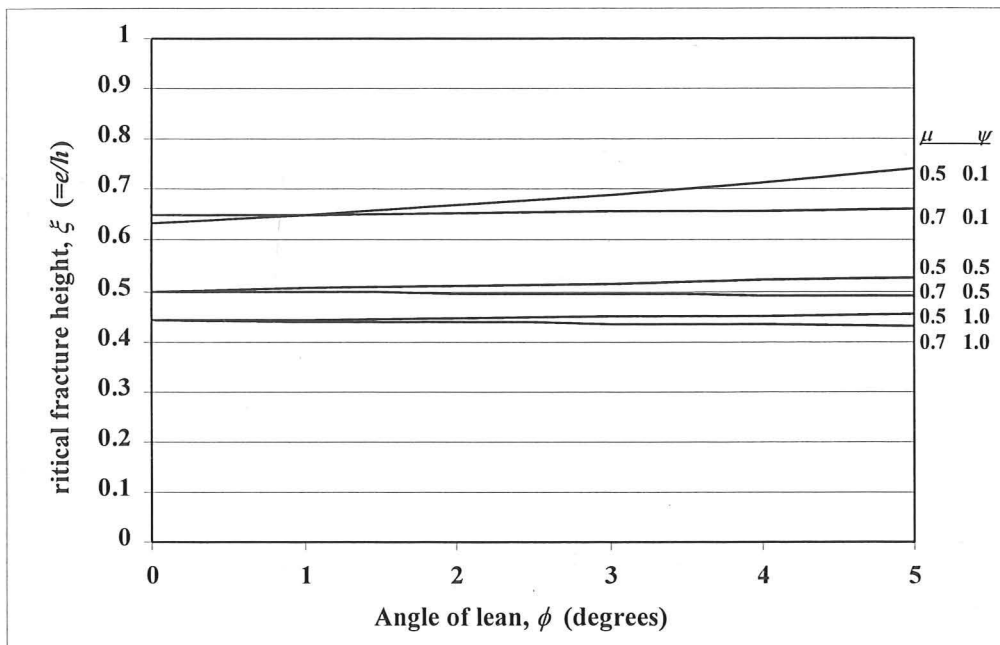


Figure 4.4 Variation in fracture height for a leaning rectangular buttress ($h_1/b=6$).

For most buttresses, the current lean will be less than 2° , and for these values it is reasonable to assume that the critical fracture height, ξ , remains constant as the buttress leans. Thus, in order to assess the collapse load for a leaning buttress, the critical fracture height can be determined for the vertical buttress, and can then be assumed to remain constant as the buttress leans outward.

4.4 Thrust Capacity of Leaning Buttresses

The reduction in thrust capacity for a leaning rectangular buttress is given by equation [4.5] or [4.6]. From both equations it is apparent that the reduction is linear with ϕ for small values of ϕ . The equation for overturning can be expressed as:

$$H_\phi = H_u - H_{reduction} \quad [4.8]$$

where H_u is the overturning load given by [3.23] for the unique value of ξ from [3.25]. From [4.5] the reduction due to leaning is then

$$H_{reduction} = b^2 \gamma \phi \left(\frac{h_b}{b} \right) \left(\psi + \frac{1}{2\mu} - \frac{\mu \xi^2}{6} \right). \quad [4.9]$$

The ξ^2 term gives a very small contribution to the reduction, because it represents the change in the restoring moment of the "lost" wedge, which is small because its centroid is close to the origin. Therefore we shall neglect this term. This is a safe assumption, since including this term would reduce the capacity further. Hence the reduction can be approximated as

$$H_{reduction} \cong b h_b \gamma \phi \left(\psi + \frac{1}{2\mu} \right) \quad [4.10]$$

This reduction is directly proportional to the angle of lean, ϕ , which must be provided in radians due to the small angle assumptions made, as stated earlier. The buttress can resist a maximum lean, ϕ_{max} , before collapse, at which point the buttress cannot resist any thrust and $H_\phi=0$. This point is given by

$$\phi_{\max} = \frac{\left(\frac{1 + 2\psi}{2\mu} - \frac{\xi}{3} \right)}{\left(\frac{h_b}{b} \right) \left(\psi + \frac{1}{2\mu} \right)}. \quad [4.11]$$

Equations [4.8] to [4.11] are summarised in Figure 4.5 for a hypothetical rectangular buttress.

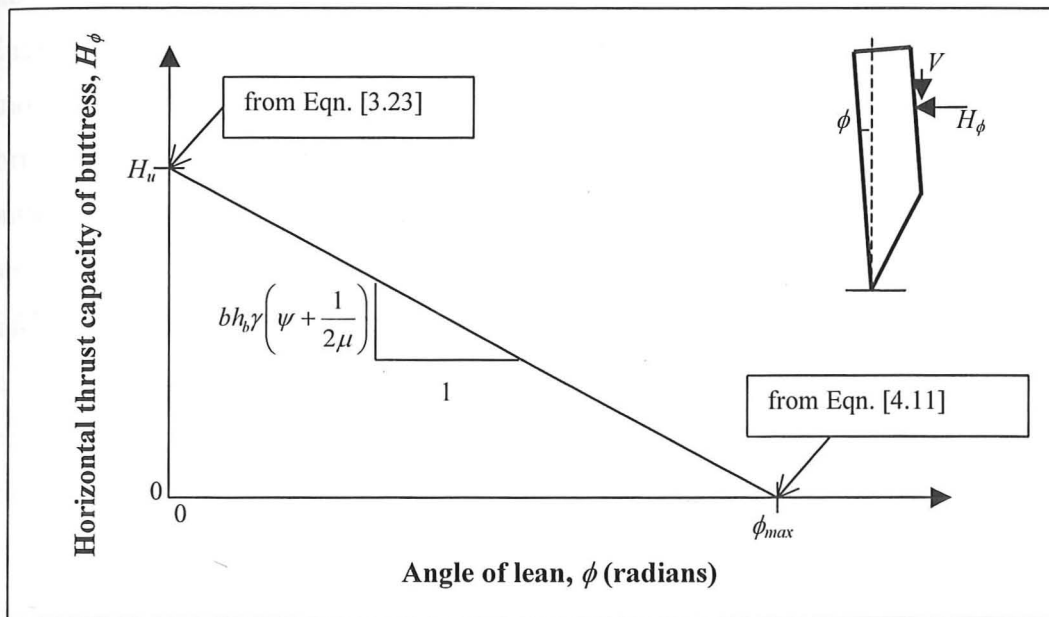


Figure 4.5 Thrust capacity for a leaning rectangular buttress.

Following the approach presented in this section, the same relation between the angle of lean and the capacity of the buttress can be derived for more complex buttress shapes, such as Gothic buttresses as in Figure 3.7. Regardless of the shape of the buttress, there is a reduction in the resistance of a buttress to horizontal thrust that is proportional to ϕ . The capacity of the buttress comes only from the stabilising moment due to its effective mass, and the stabilising moment is reduced linearly with ϕ for small angles of lean.

The preceding analysis has determined the fracture for failure of the vertical buttress, and assumed that the fracture location is not altered as the buttress leans. The maximum angle of lean, ϕ_{\max} , represents the threshold at which the fractured buttress will overturn for zero horizontal load. This value will vary for the same buttress

depending on the value of the stabilising vertical load, V , and the centroid of the effective buttress, which depends on the height of the fracture. The maximum angle of lean will not occur in practice; it is merely useful for defining the slope of the reduction in the resistance of the buttress as a result of leaning, thereby indicating the sensitivity of H to the changes in ϕ . This will be illustrated with reference to an example later in this chapter.

4.5 Safety of Buttresses

Engineers must evaluate the safety of existing arches supported on buttresses of a known inclination. The structure will be standing, but due to the geometry changes the thrust of the arch is larger than its original, design value, while the capacity of the buttress for resisting thrust is less than it was originally. A structural engineer who has been asked to assess the safety of the structure will need to have some criterion of safety by which to judge the structure. This section introduces several possible ways of defining, or thinking about, the suitable factors of safety. Obviously, the methods must consider the dimensions of the buttress, the magnitude of the applied loads, and the influence of the buttress inclination on the safety of the buttress. Several general methods will be presented for vertical, upright buttresses, and then extended to consider the influence of leaning.

Two leading engineers of the 19th century proposed a geometrical coefficient of safety based on the location of the reaction at the base of the buttress in relation to the centroid of the buttress (Moseley 1843; Rankine 1858). More recently, Huerta and López (1997) proposed a geometrical safety factor obtained by relating the force reaction in the buttress to the distance from the edge of the buttress. This is analogous to the geometrical factor of safety proposed by Heyman (1982) for masonry arches. While this is a straightforward and revealing method of measuring safety, it does not directly consider the safety against the applied horizontal force. Because the vertical load, V , is a constant stabilising force, and the horizontal thrust, H , is a variable destabilising force, it is more logical to focus on the horizontal load to determine the safety of an existing buttress. To achieve this, two measures of buttress safety are here proposed:

- 1) Pressure point factor; and
- 2) Load factor for collapse.

To determine the pressure point factor for a buttress, the *reaction point* at the base of the buttress must be examined. This reaction point is measured from the outer edge of the buttress, about which overturning may occur, using co-ordinate η as defined in Figure 4.6.

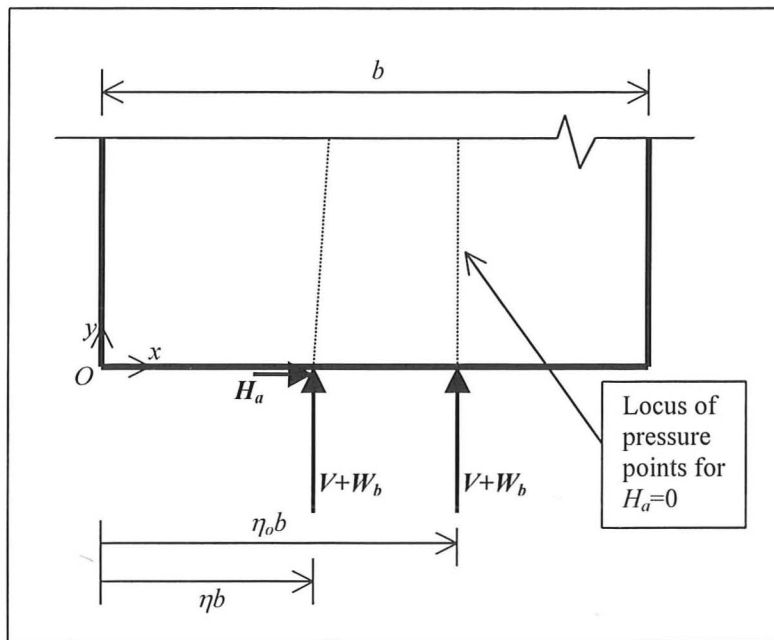


Figure 4.6. Reaction point, ηb , at the base of the buttress for an applied horizontal thrust, H_a . The thrust is applied from the right, and the vertical load, V , is applied at the right-hand edge. If no horizontal thrust is applied ($H_a=0$), the reaction point occurs at the resultant of the vertical loads, $\eta_o b$. The origin is defined as the point O about which overturning may occur.

For a vertical buttress with no horizontal load applied, the weight of the buttress and the vertical force act at an initial reaction point of

$$\eta_o = \left(\frac{W_b x_b + Vb}{b(W_b + V)} \right). \quad [4.12]$$

As the applied horizontal load, H_a , is increased from zero, the reaction point occurs at

$$\eta = \eta_o - \left(\frac{H_a}{W_b + V} \right) \left(\frac{h}{b} \right) \quad [4.13]$$

where x_b is the horizontal location of the centroid of the buttress measured from the outer edge. As long as the buttress remains solid, the relationship between the reaction point at the base of the buttress varies linearly with respect to the applied horizontal load, H_a . The general form of equation [4.13] is plotted in Figure 4.7, for the rectangular buttress example presented in the previous chapter. If the buttress did not fracture, the maximum applied horizontal force would increase to the value of H_s , the overturning force for the solid buttress, which would occur when the reaction point arrives at the edge of the buttress ($\eta=0$).

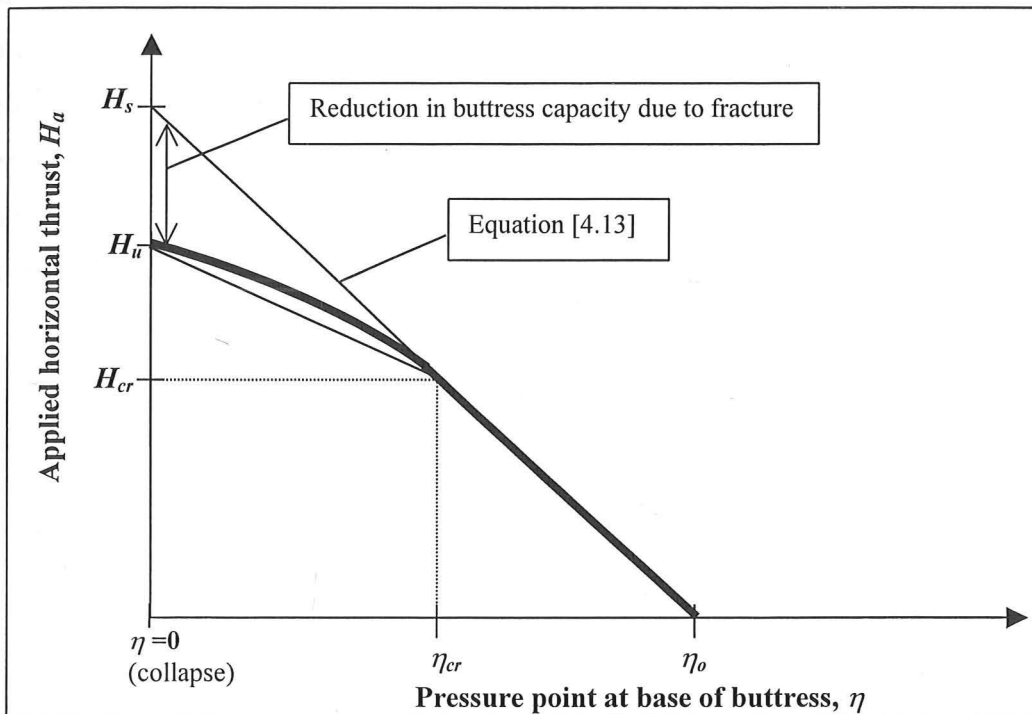


Figure 4.7. Movement of pressure point at base of buttress as horizontal thrust is increased (see Fig. 4.6.)

As the applied horizontal load is increased, the reaction point, η , moves toward the outer edge of the buttress. When η falls outside the kern point, η_{cr} , (i.e. η becomes less than $1/3$ for a rectangular cross-section), some stones will become ineffective, and the resulting fracture will reduce the stabilising moment of the buttress. This occurs when the applied load exceeds H_{cr} , which corresponds to the first cracking at the base of the buttress. The value of H_{cr} can be calculated by considering the

horizontal force required to produce the reaction point at the kern point of the section. For a rectangular cross-section, the kern point occurs at $b/3$, and the horizontal force to initiate cracking is

$$H_{cr} = \left(x_b - \frac{b}{3} \right) \left(\frac{W_b}{h} \right) + \frac{2Vb}{3h}. \quad [4.14]$$

Equation [4.14] is valid for any form of buttress with a rectangular base. The weight, W_b , acting at a centroid, x_b , is measured from the point about which overturning is considered, as in Figure 3.4(a). When the applied force exceeds H_{cr} , the stabilising moment is reduced due to the loss of masonry outside of the compression zone as described in Chapter 3. Thus the linear equation [4.13] no longer relates the applied horizontal load and the reaction point at the base of the buttress. The required horizontal force decreases until the failure load, which can be found from the methods described in the previous chapter. The shape of this nonlinear curve will vary depending on the buttress form, and the exact shape of the curve is not of great importance. The most important consideration is the value of applied load to initiate cracking, H_{cr} , as well as the ultimate load for collapse, H_u . Between these two values it is safe to assume a straight line for simplicity, as drawn in Figure 4.7. The analyst needs only to compute the thrust for initial cracking, H_{cr} , and the thrust at collapse, H_u . The reaction point at the base can then be approximated for any value of horizontal thrust.

To define the safety under a given applied load, H_a , the resulting value of η is compared to the initial value η_o , i.e. the value of η before any horizontal load is applied to the buttress. This provides a "pressure point" factor of safety, which is

$$SF_{\text{pressurepoint}} = \frac{\eta_o}{\eta_o - \eta}. \quad [4.15]$$

Thus, if the reaction point has reached the edge of the buttress, $\eta=0$, the factor of safety will have reduced to 1.0 (i.e. no safety) and the buttress will be on the verge of

collapse. For small values of horizontal force, the reaction point occurs close to the vertical resultant, η_o , and the safety against overturning becomes high.

In a safe working state, the pressure point coordinate, η , will be greater than the pressure point coordinate at which cracking begins, η_{cr} . In conventional terms, the thrust line will fall within the middle-third of a rectangular section. Once the fracture develops, the capacity of the buttress decreases, and the eccentric load on the foundations will cause the buttress to lean additionally. To ensure a safe design, the force resultant at the base of the buttress should lie within the middle-third for a rectangular section. More generally, the force resultant should lie between the kern points, so that the entire section acts in direct compression.

This can be illustrated with reference to the example of the 12 m high rectangular buttress discussed in Chapter 3, which supports a vertical load of 100 kN. The buttress is 3 m wide at the base, 1.5 m in thickness, and weighs 1060 kN. If no leaning is present, then $\eta_o=0.54$ from [4.12] for this example. The buttress begins to fracture when the reaction point, η , falls below the kern point, $\eta_{cr}=0.33$. This occurs at a horizontal thrust of $H_{cr}=91$ kN, as found from [4.14].

If the buttress supports a horizontal thrust of 80 kN, then $\eta=0.36$ for the rectangular buttress from [4.13], and the buttress will remain uncracked according to the analysis presented here. From equation [4.15], the factor of safety is therefore 2.9 for the thrust of 80 kN.

An additional measure of safety is the conventional load factor

$$SF_{load} = \frac{H_u}{H_a} \quad [4.16]$$

computed by dividing the horizontal load capacity of the buttress, H_u , by the applied thrust, H_a . For the current example, the buttress will fail due to an applied thrust of approximately $H_u=178$ kN (determined in section 3.6), and therefore has a factor of safety against failure of 2.2 for the applied thrust of 80 kN. In the rare event of sliding

failure, the analyst can apply the load factor against the critical horizontal load for sliding failure as defined in Section 3.5, rather than overturning failure.

This section has considered only the case of vertical buttresses, and the proposed measures of safety can now be modified to account for the influence of leaning.

4.6 Safety of Leaning Buttresses

For a vertical buttress, the stabilising moment is given by [3.9], but a leaning buttress will be less stable, depending on the height of the stabilising vertical forces. The vertical forces act at a resultant height of

$$\bar{y} = \frac{W_b y_b + Vh}{W_b + V} \quad [4.17]$$

where y_b is the vertical centroid of the solid buttress, and h is the height of the applied vertical load, V , as in Figure 4.2.

The effect of a small angle of lean, ϕ , is to reduce the stabilising moment due to the reduction in the moment arm about the pivot O by the distance of $\phi\bar{y}$. In addition to the usual small angle assumptions, this also assumes that the height of the horizontal thrust remains constant. The adjusted stabilising moment is therefore

$$M_{s\phi} = M_s - \phi\bar{y}(W_b + V) \quad [4.18]$$

where the stabilising moment for the vertical buttress M_s is found from [3.9]. This is a general version of [4.1] for a buttress of any form, with known weight and location of centroid. Equation [4.18] can be adapted accordingly by reducing the stabilising moment, M_s , and the critical value of horizontal load can be computed as before.

To confirm the safety of an existing buttress, and to investigate the influence of additional leaning, the location of the reaction point at the base of the buttress, η , can

be considered as in the previous section. As a buttress leans by an angle ϕ (in radians), the reaction point coordinate becomes

$$\eta_\phi = \eta_o - \frac{\bar{y}\phi}{b} \quad [4.19]$$

where \bar{y} is computed from [4.17].

The general form of equation [4.19] is plotted in Figure 4.8, both for a vertical buttress, and also for the same buttress leaning by an angle ϕ . The effect of leaning is to shift the entire curve to the left as a result of the horizontal movement of the buttress centroid. It is clear that the leaning buttress will develop a fracture at a lower value of H_{cr} , and will fail at a lower value of horizontal thrust. The new values of H_u and H_{cr} as a result of the lean, are H_ϕ and $H_{\phi cr}$, respectively. The kern point of the section does not change, and therefore the reaction point for the onset of cracking, η_{cr} , is reached for a lower value of horizontal thrust, $H_{\phi cr}$.

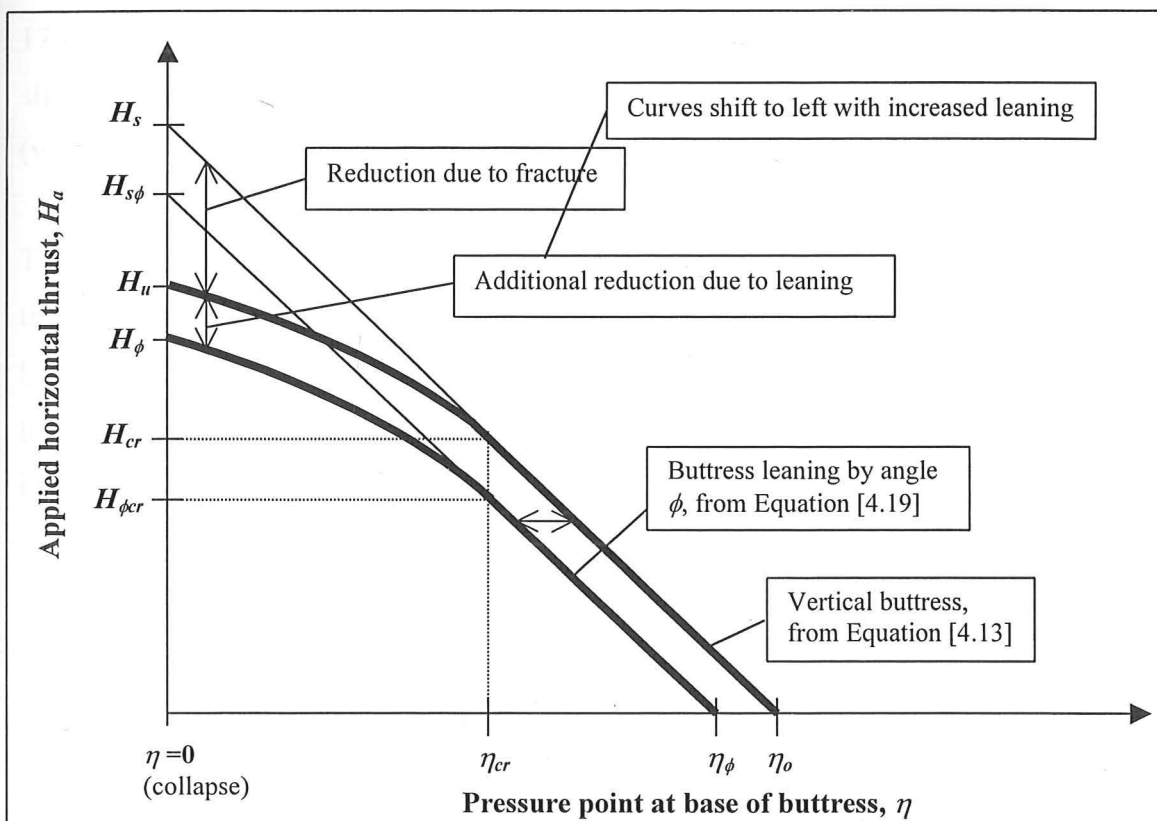


Figure 4.8. Influence of leaning on buttress reaction and capacity. The pressure point at the base of the buttress moves toward the edge as the horizontal load is increased. The presence of buttress leaning shifts the entire curve to the left.

Further insight can be gained by considering the angle of lean at which cracking will begin for the given applied load. This is computed from

$$\phi_{cr} = \frac{b(\eta - \eta_{cr})}{\bar{y}} \quad [4.20]$$

Again the previous example of the rectangular buttress can be used to illustrate the influence of buttress leaning. For this example, the vertical centroid of the buttress acts at a height of $y_b = 6.0$ m, and considering the applied vertical load of 100 kN at a height of $h = 8$ m, the resultant vertical centroid is $\bar{y} = 6.17$ m from [4.17]. For a horizontal load of 80 kN, the pressure point coordinate $\eta = 0.36$ and the rectangular buttress will begin cracking when the buttress leans by 0.015 radians ($=0.8^\circ$) according to [4.20].

If the buttress exists in a state of leaning with $\phi = 0.017$ radians ($=1^\circ$), then the thrust capacity of the buttress will be reduced by approximately 16 kN from [4.10]. This is a reduction in strength of nearly 10% from the thrust capacity of the vertical buttress of 178 kN. The new pressure point, η_ϕ , will be 0.32 from [4.19] and the buttress will be slightly cracked under the horizontal thrust of 80 kN. In general, wider buttresses (with lower ratios of h_b/b) will be less sensitive to the effects of leaning.

The same load factor of safety from [4.16] can be used, but the value of H_u must be the reduced capacity of the buttress as a result of the lean. The capacity of the leaning buttress, H_ϕ , is found from [4.8]-[4.10] as described previously. For the buttress leaning by 1° , the capacity of the buttress is reduced to approximately 160 kN, from its original value of 178 kN. For an applied horizontal thrust of 80 kN, the load factor of safety is reduced to 2.0, as opposed to 2.2 for the vertical buttress.

4.7 Comparison of Safety Factors

Moseley (1843) and Rankine (1858) were the first to propose measures of safety based on limiting the position of the thrust resultant in relation to the edge of the buttress. Rankine defined the position of the thrust measured from the centre of the

section, which he called the *stability of position*. He proposed that this distance should be limited to $b/6$ in the case of buttresses (i.e. with the thrust just passing through the outside of the middle third). Interestingly, Rankine allowed values as high as $3b/8$ (i.e. only $b/8$ from the edge of the cross-section) for retaining walls and other structures that did not support the thrust of arches. Rankine's method can be used to compute a geometrical safety factor, which can be compared to the two safety measures proposed in the previous section. To find this "Rankine" factor of safety, the width of the section, b , is divided by twice the deviation of the thrust from the centre of the section. Thus, a buttress on the verge of cracking would have a "stability of position" of $1/6$, and a "Rankine" safety factor of 3. In relation to the pressure point, η , at the base of the buttress, the Rankine safety factor is expressed as:

$$SF_{Rankine} = \frac{1}{1 - 2\eta} \quad [4.21]$$

for buttresses of rectangular cross-section.

This measure of safety provides significantly different results depending on the buttress being considered, and it can be compared to the two other methods proposed in this chapter. Generally, the load factor for collapse is the most conservative, and the two geometrical measures from [4.15] and [4.21] provide higher numerical measures of safety. This can be illustrated by the example of the rectangular buttress discussed earlier.

All three measures provide a very high safety for low values of horizontal thrust, but as the thrust increases, the load factor provides the lowest numerical measure of safety. For the rectangular buttress example discussed earlier under an applied thrust of 80 kN, the load factor from [4.16] is 2.2, while the pressure point factor based on [4.15] is 2.9, and Rankine's proposed measure gives a safety factor of 3.6. The results are plotted in Figure 4.9 for horizontal thrust values ranging from zero up to the collapse state (when the safety factor against collapse is 1.0).

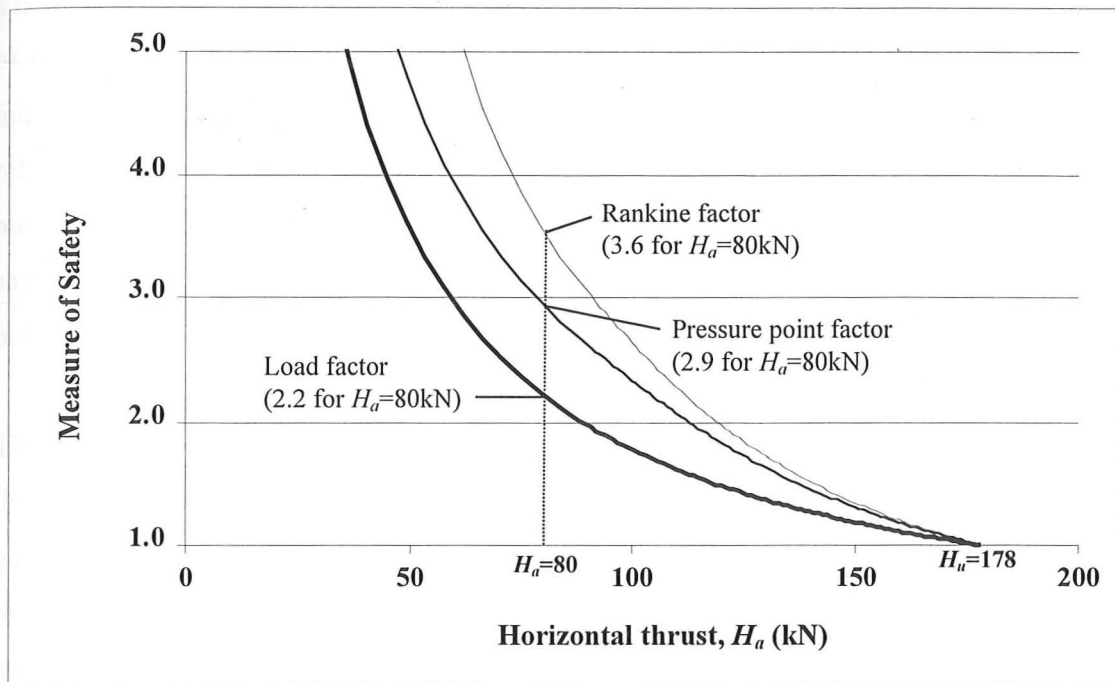


Figure 4.9. Safety factors for the rectangular buttress example from Chapter 3. ($h_b=12$ m, $b=3$ m, $h=8$ m, $\gamma=29.4$ kN/m², $V=100$ kN, $H_{cr}=91$ kN, $H_u=178$ kN)

As the buttress leans, each curve will shift to the left, reducing the safety factor. For the same buttress leaning by 1° , the load factor for collapse is reduced to 2.0, and the pressure point factor is reduced to 2.4, while the geometrical safety factor from Rankine is reduced to 2.8. The results of these comparisons are summarised in Table 4.1 below.

	Load Factor (Eqn. [4.19])	Pressure Point (Eqn. [4.15])	Rankine (Eqn. [4.21])
Vertical buttress ($\phi=0^\circ$) ($H_a=80$ kN, $V=100$ kN)	2.2	2.9	3.6
Leaning buttress ($\phi=1^\circ$) ($H_a=80$ kN, $V=100$ kN)	2.0	2.5	2.8
Vertical buttress ($\phi=0^\circ$) ($H_a=80$ kN, $V=200$ kN)	2.8	3.4	5.6
Leaning buttress ($\phi=1^\circ$) ($H_a=80$ kN, $V=200$ kN)	2.5	2.8	4.0

Table 4.1. Comparison of safety measures for the rectangular buttress example

The measures of safety have been computed for the same buttress with twice the value of vertical load, V , and are presented in Table 4.1. The addition of vertical load greatly increases the geometrical factor of safety, since it considers the pressure point in relation to the centroid of the section, regardless of the value of vertical load. The two measures of safety proposed in this chapter are a more consistent measure of the safety of the buttress, because they consider only the de-stabilising effects of the horizontal load.

This chapter has proposed three different measures of the safety of a buttress. All three give a numerical value of 1.0 when the buttress is on the point of collapse, but in general, they give different results leading up to the collapse state. There is no single recommended measure of safety, though the load factor and the pressure point factor appear to be more useful than Rankine's proposal. The use of a load factor is a simple and familiar concept, and it gives the lowest numerical values of the three measures of safety. Though this is the easiest measure to apply, the load factor is not advisable as the only measure of safety for buttresses. For this reason, curves such as Figure 4.7 and 4.8 should be constructed in order to assess the safety of an existing buttress. These curves, combined with the pressure point factor of safety given by equation [4.15], provide a greater understanding of the capacity of a buttress for increased horizontal loading. Of course, all of the measures should be determined for the current angle of inclination of the buttress.

The measures of safety presented in this chapter have concentrated on the influence of the applied horizontal load, though some authors have applied a "load factor" to the applied force, thus increasing the stabilising vertical load as well (see for example Aragon 1909). This may be an unsafe approach, since only the horizontal component of force is de-stabilising and applying a load factor to the vertical component of force (typically the dead load of the structure) will not increase the safety of the structure. Thus, efforts to define the safety of buttresses should focus on the implications of increased horizontal thrust and increased leaning, both of which are detrimental to the stability of the buttress.

4.8 Summary

This chapter has investigated the change in equilibrium conditions in a buttress as a result of leaning. Furthermore, this chapter has presented two straightforward methods to define the safety of the buttress. The first is based on the location of the reaction point under increasing horizontal thrust, and the second is a conventional load factor of safety.

The following conclusions can be drawn:

- 1) At the collapse state, the height at which the diagonal fracture line intersects the inner edge of the buttress does not move significantly due to leaning of the buttress. The resistance of the buttress to horizontal loads and the height of the critical fracture can be determined for the vertical buttress, and the height of the fracture can be assumed to remain constant as the buttress leans.
- 2) The resistance of the buttress decreases due to the horizontal shift of the vertical centroid of the buttress as the buttress leans. For small angles of lean, ϕ , the capacity of the buttress will decrease *linearly* with ϕ as the buttress leans away from the applied thrust.
- 3) It is useful to define the location of the pressure point at the critical section of the buttress (usually at the base, but possibly in a higher region for a stepped buttress). The sensitivity of the buttress to increased loading can be examined by investigating the movement of the internal pressure point as the horizontal thrust increases.
- 4) The internal pressure point will also shift linearly with ϕ as a result of small angles of lean, and can be used to investigate the sensitivity of the buttress to increased leaning.
- 5) The conventional load factor for collapse (i.e. H_u/H_a) will provide the lowest measure of safety and is a simple and convenient way to define the safety of buttresses.
- 6) By taking into account the stabilising effect of any vertical load applied at the inner edge of the buttress, the pressure point factor gives a more accurate measure of safety than a conventional geometrical safety factor as suggested originally by Rankine's "stability of position."

PART III: THE MASONRY ARCH

Chapter 5 The Masonry Arch on Spreading Supports

5.1 Introduction

As the buttresses lean outwards, the arch will deform relative to its original conformation. Thus, a buttress supporting an arch at a height of 10 m will cause a span increase of 0.34 m (0.17 m on each side) for a lean of only 1° . As discussed in the literature review, this is a common problem for masonry vaults supported on buttresses; but hitherto engineers have not studied the influence of increased buttress leaning on the equilibrium of the arch. In particular, researchers have not determined the increase in the thrust of the arch as a result of support movements.

This chapter investigates the influence of the spreading of supports on masonry arches. The arch is considered to be a circular segment of uniform thickness supported on rigid abutments, which translate horizontally and so de-stabilise the arch (Figure 5.1). This is equivalent to an arch supported on leaning buttresses, in which the span of the arch increases. Computations are presented to determine the minimum possible thickness for circular arches, and to investigate the change in internal forces as a result of spreading supports. In most masonry buildings, arches and vaults are constructed with fill on top, which provides an alternative force path for the thrust of the arch. Therefore, this chapter assumes the arch springing to be just above the fill.

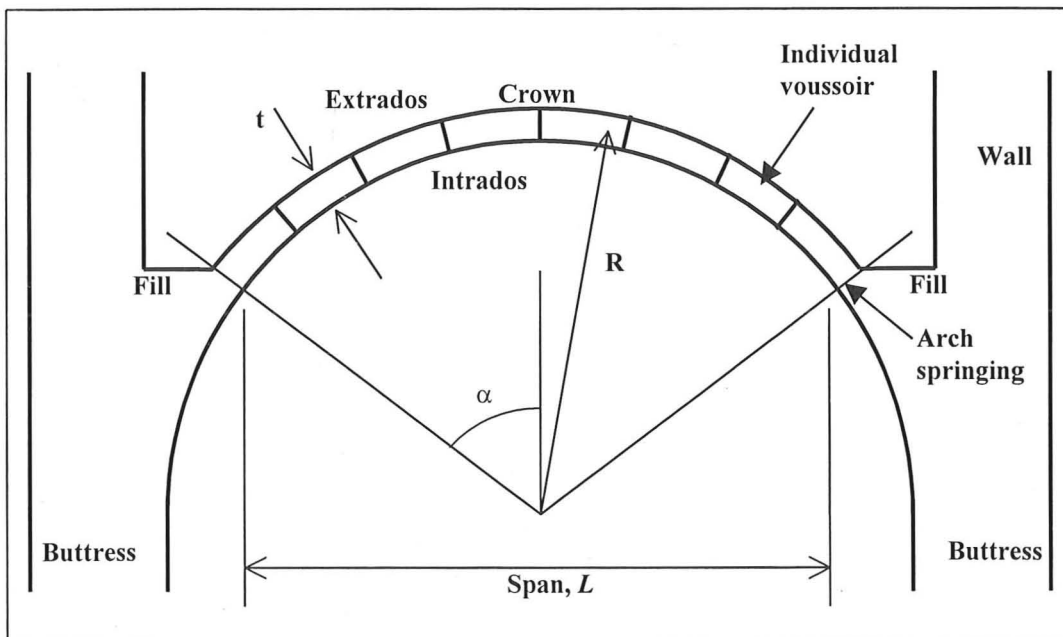


Figure 5.1 Definition of geometry for a voussoir masonry arch.

5.2 Least-Thickness Analysis

Investigations into the stability of arches on spreading supports have revealed a historical error in the analysis of circular arches. For the circular arch of absolute *minimum* thickness, the required span increase to cause collapse is zero, since the arch is exactly on the point of collapse without any movements of the supports. Solving this problem has revealed that previous investigations into the minimum required thickness of circular arches have been incorrect. This section will explain this historical error, before returning to the central focus of this dissertation: the destabilising effect of displacements on masonry structures. The findings from the minimum-thickness analysis are relevant to the problem of the arch on spreading supports, and it is worthwhile to discuss the least-thickness problem in some detail.

The minimum required thickness for circular arches under their own weight is a classical problem in masonry structures, in which a symmetrical five-hinge mechanism limits the thickness of the arch: see Figure 5.2. In 1729, Couplet gave a solution based on incorrect hinge locations, in which he assumed the intrados hinges to occur at 45° (Heyman 1972). Couplet and other researchers estimated the minimum thickness necessary by seeking the internal line of thrust due to the self-weight of the arch. By assuming that the thrust line at the hinge locations must be tangential to the intrados of the arch, Heyman determined that the minimum thickness ratio is:

$$\frac{t}{R} \cong 2 \frac{(\beta - \sin \beta)(1 - \cos \beta)}{\beta(1 + \cos \beta)} \quad [5.1]$$

where the variables t , R , and β are defined in Figure 5.2 below (Heyman 1969). A plot can be made of t/R as a function of β , and from it the unique value of β for any given t/R may be read. Then a second equation must be solved in order to determine the limiting value of α for the given thickness. Heyman (1969) presents a plot of t/R as a function of α .

An alternative approach to this problem is to use a "work-balance" equation. For given values of t/R and α , a symmetrical five-hinge mechanism can be postulated, with the intrados hinges located at $\pm\beta$ from the apex, where β is arbitrary. When an

infinitesimal motion of this mechanism takes place, the total work done by gravity will be zero if the correct value of t/R has been chosen. If this is not the case, the calculation can be repeated with different values of t/R and β until the zero-work, i.e. static equilibrium condition, has been found. Then the entire calculation can be repeated until the minimum value of t/R has been found. Values of t/R as a function of α determined by Heyman do not agree exactly with the results of the "work-balance" method outlined above. This presents a paradox, even though the discrepancies are too small to worry a structural engineer (i.e. only 1.4% error for $\alpha=90^\circ$).

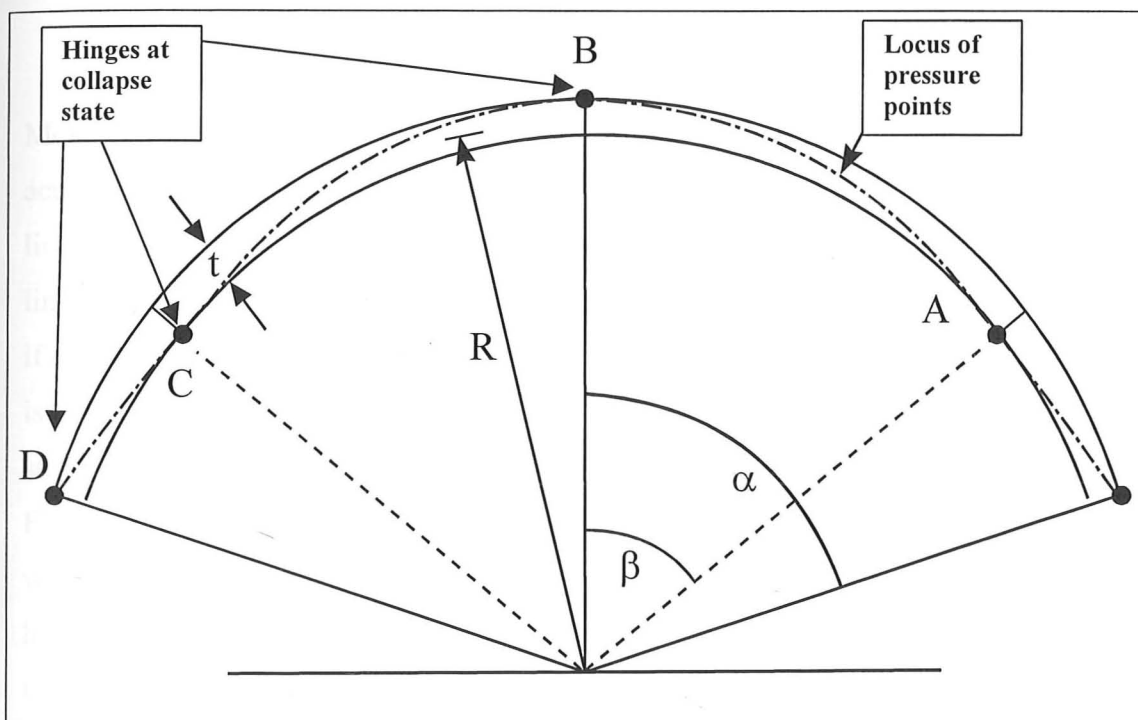


Figure 5.2 Circular arch at minimum thickness ratio, $(t/R)_{min}$. This is a symmetrical five-hinge mechanism, though in practice, slight asymmetries will exist and four hinges are sufficient for collapse. The four-hinge collapse mechanism must have hinge rotations of alternating sign in order to be kinematically admissible.

It turns out, perhaps surprisingly, that the assumption of a thrust line that is tangential at the intrados hinge is not precisely correct. To explain why this is the case, Figure 5.3 presents the static equilibrium of a very thin voussoir, defined by two radial cuts, near the location of the intrados hinge at point A in the arch of Figure 5.2. The weight of the slice is dV . If $dV=0$, the thrust line would pass through the two lower corners of the thin voussoir; i.e. it would be tangential at the intrados. But it is not possible for the resultant force (thrust line) to be tangential at the intrados when the force dV is non-zero. This discrepancy occurs as a result of the centre of mass of each voussoir being located away from the computed thrust line.

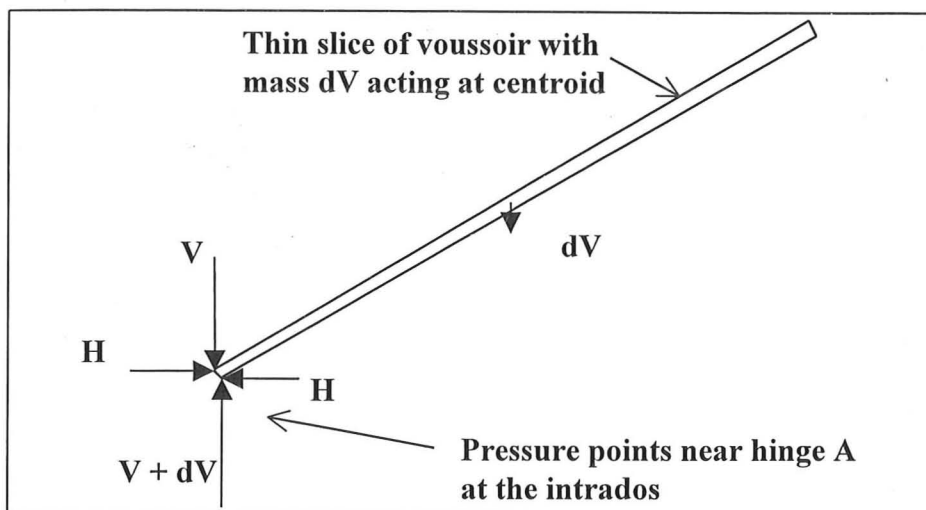


Figure 5.3 Static equilibrium of a thin voussoir near the intrados hinge location.

Moseley (1843) described the difference between the line of thrust and the line of action of the forces, which must pass through the centre of mass of each voussoir. A line of thrust would be precisely correct only if the load were applied exactly on the line; i.e., if it were a chain loaded with hanging weights. This discrepancy is avoided if one thinks of the thrust line as a *locus of pressure points*, where each pressure point is the location of the resultant force on a radial "cut" needed to keep a segment of the structure in equilibrium. In the case of masonry arches, a thin voussoir (shown in Figure 5.3) is held in equilibrium by the resulting thrusts on either side of the slice, which act on the pressure points of the voussoir. An arch in a state of minimum thrust has three hinges, and is therefore statically determinate. It is possible to construct a unique locus of pressure points for the arch, shown as the dashed line in Figure 5.2; and this locus is indeed tangential to the intrados at angle $\pm\beta$. The locus of pressure points here is equivalent to Moseley's (1843) *line of resistance* as well as the *druckkurve* defined rigorously by Milankovitch (1907).

By ignoring the path of internal forces in the arch, and applying work calculations as described above to determine the stability of the arch, the critical thickness ratio is found to be 0.1075 for an arch subtending 180° . The intrados hinges occur at $\beta = 54.5^\circ$, rather than at 58.9° as predicted by Heyman's equation [5.1]. This result agrees exactly with the calculation of the locus of pressure points at the state of minimum thickness described in the previous paragraph and determined statically by Milankovitch (1907). This represents a slight increase in the required thickness over

the value of 0.1060 determined by Heyman (1969). The historical solutions to this problem are presented in Table 5.1 below. The solutions by Couplet and Heyman predicted smaller thickness ratios than are possible, and were therefore unsafe calculations. Only Pétit (1835) computed a slightly larger thickness than necessary, based on his very close approximation of the minimum thickness, although he does not provide the location of the intrados hinges for his calculation.

	Minimum t/R	β , degrees	% t/R difference
Current study (2002)	0.1075	54.5	-
Heyman (1969)	0.1060	58.9	-1.4%
Milankovitch (1907)	0.1075	54.5	-
Pétit (1835)	0.1078	N/A	+0.3%
Couplet (1729)	0.1010	45.0	-6.0%

Table 5.1. Historical solutions for minimum thickness of a semicircular arch ($\alpha=90^\circ$).

Figures 5.4 and 5.5 plot the minimum required thickness for arches of various angles of embrace. Heyman's approximate solution differs only slightly, and would fit within the thickness of the line for the exact solution plotted in Figure 5.4. By plotting on logarithmic scales, Figure 5.5 shows that the approximation

$$\left(\frac{t}{R}\right)_{\min} \cong \frac{\alpha_{\max}^4}{48} \quad [5.2]$$

is an excellent approximation up to $\alpha=60^\circ$ (1.05 radians).

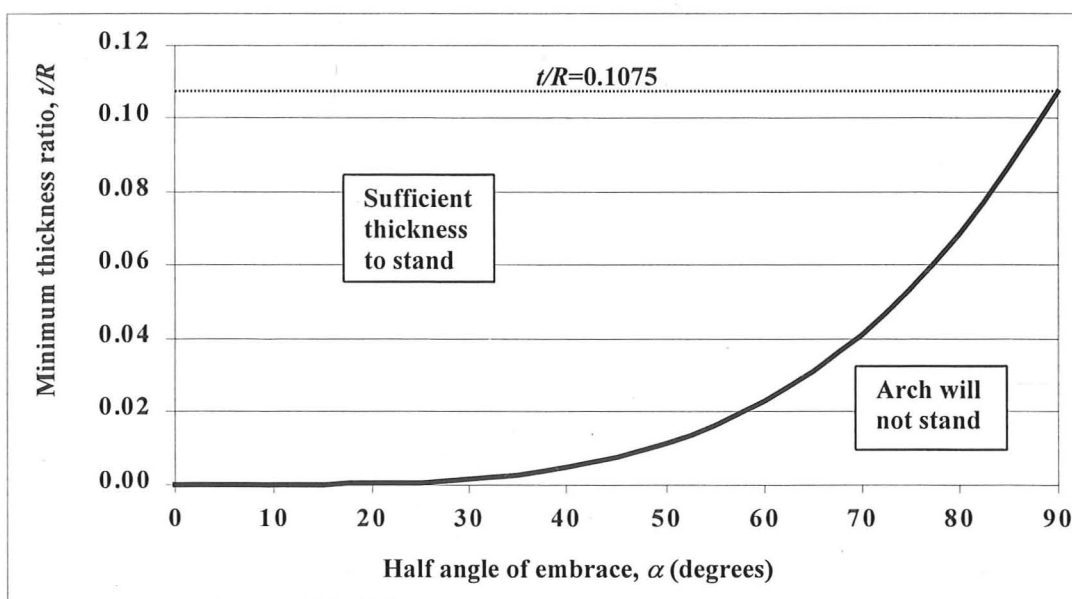


Figure 5.4. Minimum thickness of circular arches for varying angles of embrace.

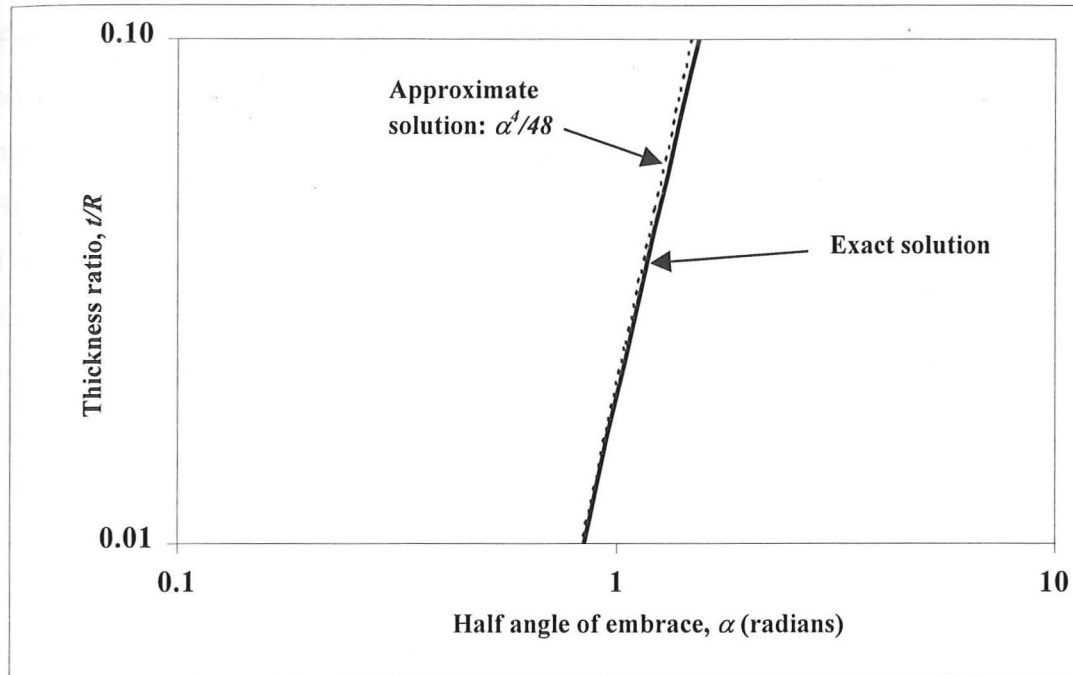


Figure 5.5. Minimum thickness of circular arches on log-log scale comparing the exact solution with an approximate solution based on a power-series expansion.

This approximation is the first term of a power series expansion of Heyman's equation for minimum thickness and it is a reasonable estimate of the minimum thickness for a circular arch. Importantly, this is a "safe" approximation of the minimum thickness required for a circular arch, because it estimates slightly larger thickness ratios than are necessary to stand.

Circular arches of very small thickness can stand with a total angle of embrace less than 60 degrees. Much greater thickness is required for larger angles of embrace, and the effect of α on the required thickness increases steeply. For practical purposes, most arches subtend a total angle larger than 80 degrees ($\alpha=40^\circ$), so the values presented in Table 5.2 are most relevant to building construction.

Half embrace, α	40°	50°	60°	70°	80°	90°
Minimum t/R	0.0047	0.0113	0.0228	0.0413	0.0687	0.1075
Intrados hinge, β	27.4°	33.6°	39.5°	45.0°	49.9°	54.5°

Table 5.2. Minimum thickness ratios and hinge locations for varying angles of embrace.

This analysis has determined the minimum thickness to stand, which will serve as a limit on the thickness ratios for further discussion of circular arches.

5.3 Thrust of Arches

The thrust of arches is another classical problem in masonry structures. A perfectly constructed arch supported on rigid supports can resist a range of thrust values between the maximum thrust and minimum thrust (Swain 1927, Heyman 1966, 1995). However, most arches exist in a deformed state due to movements of the supports. The arch thrust causes the abutments to spread apart, increasing the span of the arch. *As soon as the abutments spread apart, the arch exists in a state of minimum thrust.* The smallest outward movement of the abutments will cause the arch to form three hinges (A, B, and C in Figure 5.6), and the abutment thrust can then be determined uniquely from the geometry and the location of the hinges. In this case there are intrados hinges at A and C, and an extrados hinge at B. There are no *extrados* hinges at the abutments, as t/R is larger than the minimum required for the given value of α , and thus the arch can safely stand. (For small angles of embrace, the *intrados* hinges will form at the abutments.) If the span continues to increase, the arch will deform according to rigid-body kinematics. The crown of the arch (point B) will descend and the thrust will increase due to the change in geometry. Importantly, as the abutment spreads, the vertical force reaction at the support will remain constant, and the horizontal thrust will increase.

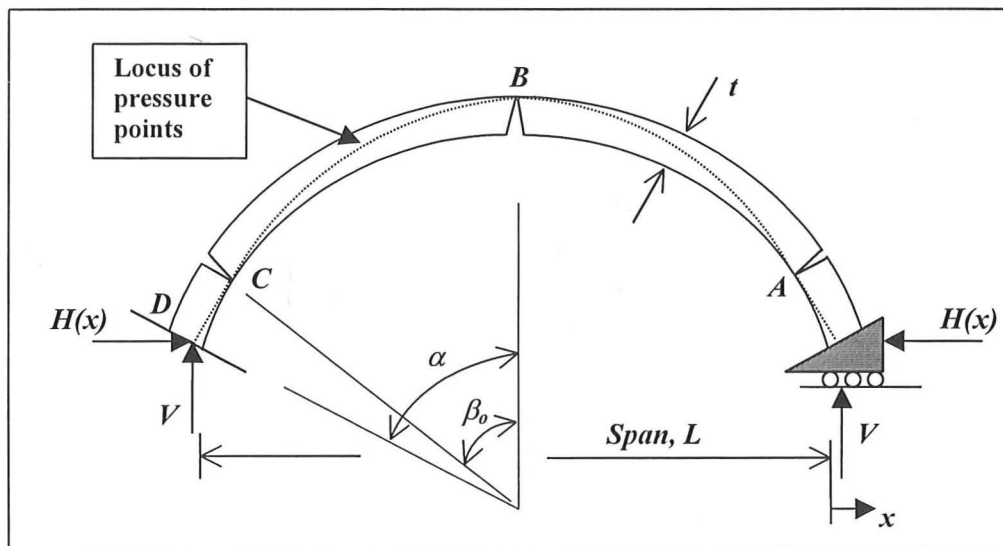


Figure 5.6 Circular arch segment with spreading abutments at state of minimum thrust (corresponding to small, positive values of x).

At the state of minimum thrust, the extrados hinge B occurs at the crown. (It is assumed that the hinge will form exactly at the apex of the arch, though in practice a keystone often prevents this from happening and the extrados hinge occurs very near

the crown on either side.) Two intrados hinges occur at an angle β_o measured from the vertical on each side of the crown. As the supports move together or apart, the arch will deform as a mechanism and the value of the horizontal thrust will change substantially. The change in horizontal thrust due to horizontal support movement is plotted qualitatively in Figure 5.7.

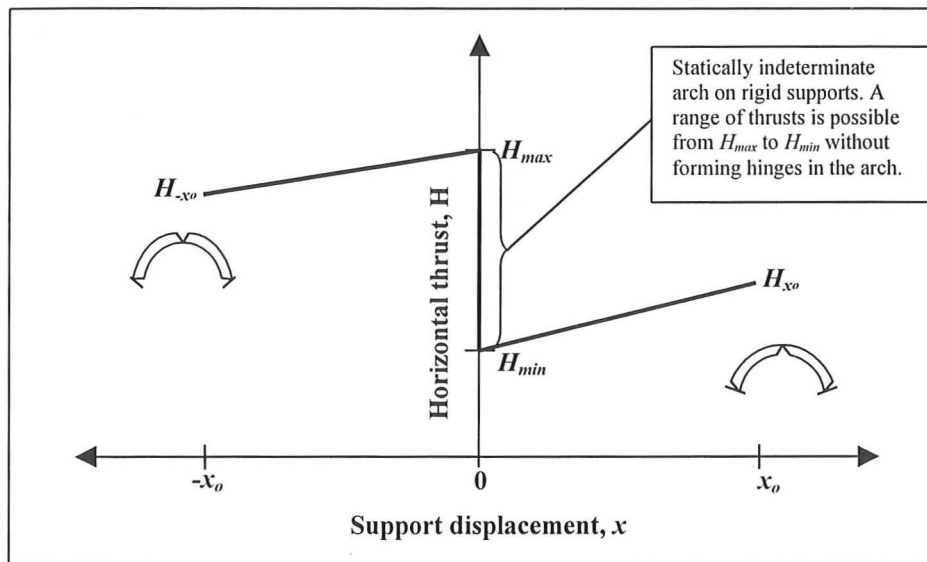


Figure 5.7. Change in horizontal thrust of a voussoir arch with support movement. Hinge locations are indicated in the inset sketches for displacement in each direction.

A perfectly-fitted voussoir arch on rigid supports is statically indeterminate and a range of horizontal thrust values is possible between the minimum and maximum thrust (Heyman 1967, 1996). If the supports move closer together, the arch will immediately move to the state of maximum thrust, H_{max} , and will form hinges to accommodate the movement. But if the supports move apart, the arch will immediately move to the state of minimum thrust, H_{min} , and will form three hinges to accommodate the movement. As the supports continue to move, the arch will continue to deform as a mechanism and the thrust will change as the geometry of the arch changes. Moving the supports apart causes the crown of the arch to descend and increases the thrust of the arch. Moving the supports together causes the crown of the arch to rise and decreases the thrust of the arch: see Figure 5.7. When the arch supports have spread apart by a distance x_o the minimum thrust of the arch will become H_{x_o} , which is greater than the absolute minimum thrust, H_{min} . Likewise, if the arch supports have moved together by a distance x_o the maximum thrust of the arch will become H_{-x_o} , which is less than the absolute maximum thrust, H_{max} . In each case,

it is possible to compute the value of horizontal thrust uniquely if the hinge locations in the arch are known. This chapter is concerned only with positive values of x , corresponding to the problem of spreading supports, and seeks to determine the exact hinge locations and the value of thrust as the arch supports spread apart.

The value of the minimum thrust can be found by examining the equilibrium conditions for the central region of the arch as shown in Figure 5.8.

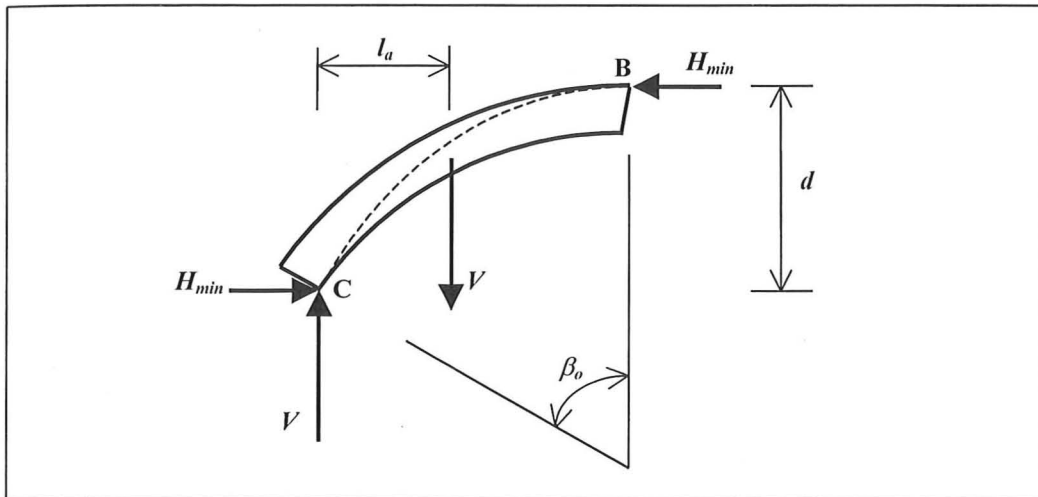


Figure 5.8. Equilibrium of central region of a masonry arch, acting under its own weight, at the state of minimum thrust, H_{min} , due to a very small outward movement of the supports. The arch is symmetrical, so this analysis can be applied to section BC or section AB of the arch.

Taking moments about point C of Figure 5.8, it is straightforward to write an equation for the horizontal thrust as a function of the intrados hinge location β . For an arch of any shape the minimum thrust H_{min} is

$$H_{min} = \frac{Vl_a}{d} \quad [5.3]$$

where the weight of the half arch V , the rise d and the horizontal centroid l_a are all a function of the initial hinge location β_o and the shape of the arch (i.e. the thickness ratio t/R for circular arches). To determine the minimum thrust, the correct hinge location, β_o , is the hinge location with the *maximum* value of thrust from the central region ABC. Coulomb was the first to note that the *minimum* thrust occurs for the hinge location, β_o , which *maximises* the equation for minimum thrust (Heyman 1972). For example, the horizontal thrust from the central arch region ABC is plotted in

Figure 5.9 for the semi-circular arch of minimum thickness, $t/R = 0.1075$ and the critical hinge location β_o occurs at 54.5° (as in Table 5.2).

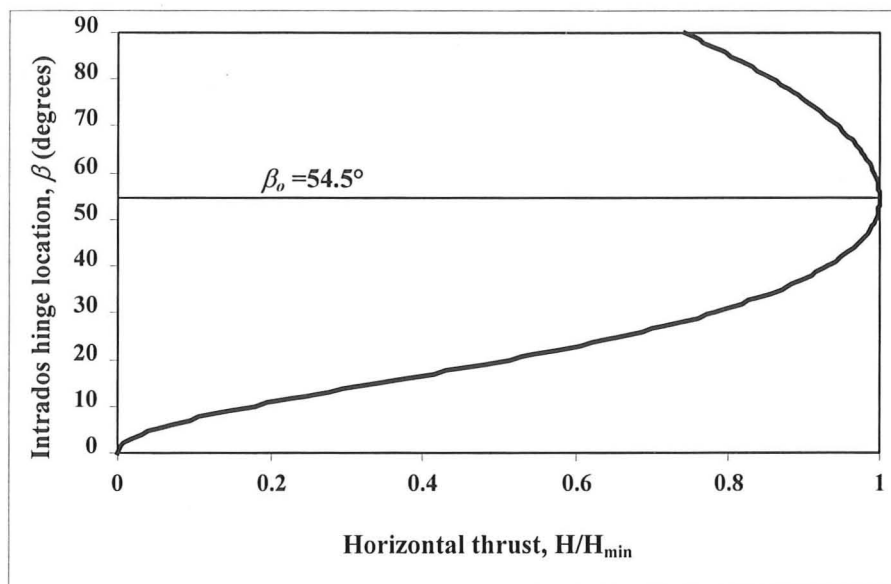


Figure 5.9. Horizontal thrust from the central region (ABC) of a semi-circular arch with $t/R = 0.1075$ as a function of the location of the intrados hinge β . Not all hinge locations are statically admissible, but the maximum value will correspond to the correct hinge location for the state of minimum thrust. This curve corresponds to the thrust from equation [5.3] for a circular arch, and is normalised by the correct value of minimum thrust, H_{min} .

This provides a simple means of determining the hinge location for an arch on spreading supports and the value of the corresponding minimum thrust. The analyst must consider each possible intrados hinge location, and the hinges will form in the location that maximises the thrust of the arch.

For a circular arch segment, each thickness ratio t/R has a corresponding initial value of β_o , as plotted in Figure 5.10. This is due to the relationship between the circular shape of the arch and the approximately parabolic shape of the locus of pressure points. For arches subtending an angle 2α less than $2\beta_o$, the hinge β_o will form at the support, at an angle α from the crown of the arch. Figure 5.10 is demonstrated with reference to the minimum thickness ratio, $t/R = 0.1075$, for a semi-circular arch. If the arch subtends α larger than 54.5° , the intrados hinge will form at $\beta_o = 54.5^\circ$ when the supports move apart. If α is less than 54.5° for an arch of $t/R = 0.1075$, the intrados hinges will form at the supports.

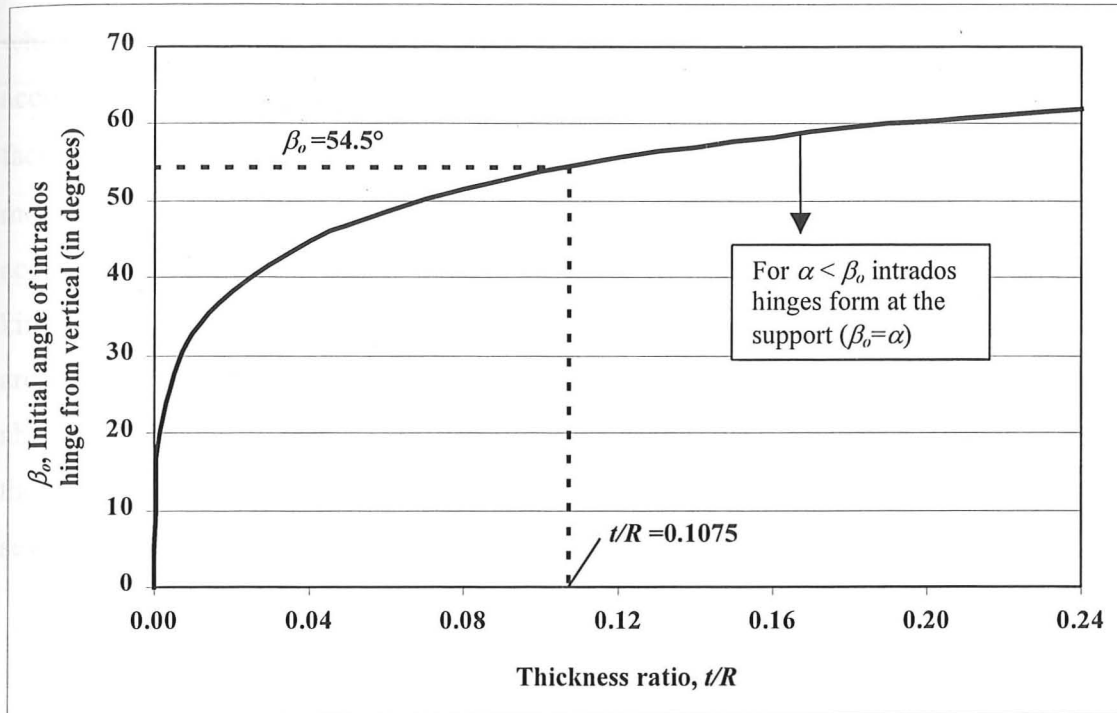


Figure 5.10. Intrados hinge location corresponding to minimum thrust for circular arches.

As illustrated in the previous section, an arch of thickness ratio $t/R = 0.1075$ will be on the point of collapse for a total angle of embrace of 180° ($\alpha = 90^\circ$). An arch of the same thickness ratio would safely stand for an angle subtending 120° ($\alpha = 60^\circ$), and the value of the minimum thrust would be identical. The intrados hinge occurs at $\beta_0 = 54.5^\circ$ in both cases, since α is greater than β_0 . But if the arch of $t/R = 0.1075$ subtended a total angle of 100° ($\alpha = 50^\circ$), the intrados hinges would form at the supports, and the minimum thrust would be slightly lower.

5.4 Failure Mechanism for Spreading Supports

An arch on spreading supports will fail in one of two ways: a symmetrical five-hinge mechanism similar to the arch of minimum thickness as in Figure 5.2; or a three-hinge mechanism by snap-through if the thickness is sufficiently large. It is necessary to determine the exact mode of failure and the maximum value of span increase in order to determine the thrust from the arch as the supports move apart. Researchers have not previously addressed this problem, though it is of primary importance for assessing the safety of masonry arches and vaults.

For most arches, failure will be governed by the five-hinge collapse mechanism, in which the central portion of the arch is a three-hinged arch, which deforms to accommodate the span increase. The problem is greatly complicated by one simple fact: as the span increases, the intrados hinge location β_o may change position and move toward the crown of the arch. Most significantly, a given span increase can be accommodated by several possible hinge locations. Smars illustrated that various kinematic mechanisms occupy the same statically admissible domain for a voussoir arch, though he did not discuss the implications of this fact in the context of spreading abutments (Smars, 2000). In other words, various equilibrium states are possible and the arch can adopt a different deformed shape for each. This remarkable fact raises several issues:

- 1) A deformed arch can move safely between various equilibrium states due to imposed movements, such as earthquake vibrations.
- 2) The thrust in the arch is determined by the hinge locations and the corresponding dip of the arch at the crown due to the increased span.
- 3) In the case of spreading abutments, it is not possible to calculate the exact collapse condition without starting from a known equilibrium state.

The critical question is to determine the intrados hinge location at failure, which can be used to calculate the increase in span and the change in geometry that will cause collapse. Without knowing the exact hinge location at failure, there are multiple equilibrium configurations with different hinge locations and different span increases, which satisfy the collapse condition. Collapse will occur by a five-hinge mechanism when the thrust from the central region of the arch ABC exceeds the stability limit for the supporting region CD (shown in Figure 5.6). Each possible hinge configuration has a differing value of dip at the crown of the arch and a different span increase at failure. This departs from the usual assumptions of small displacements for limit analysis, since the geometry of the structure changes significantly. To solve the problem of spreading abutments, it is necessary to begin from a known equilibrium configuration, and follow the equilibrium state of the structure as it deforms until collapse. The MATLAB program ArchSpread, included in Appendix B, carries out such a calculation in the following steps:

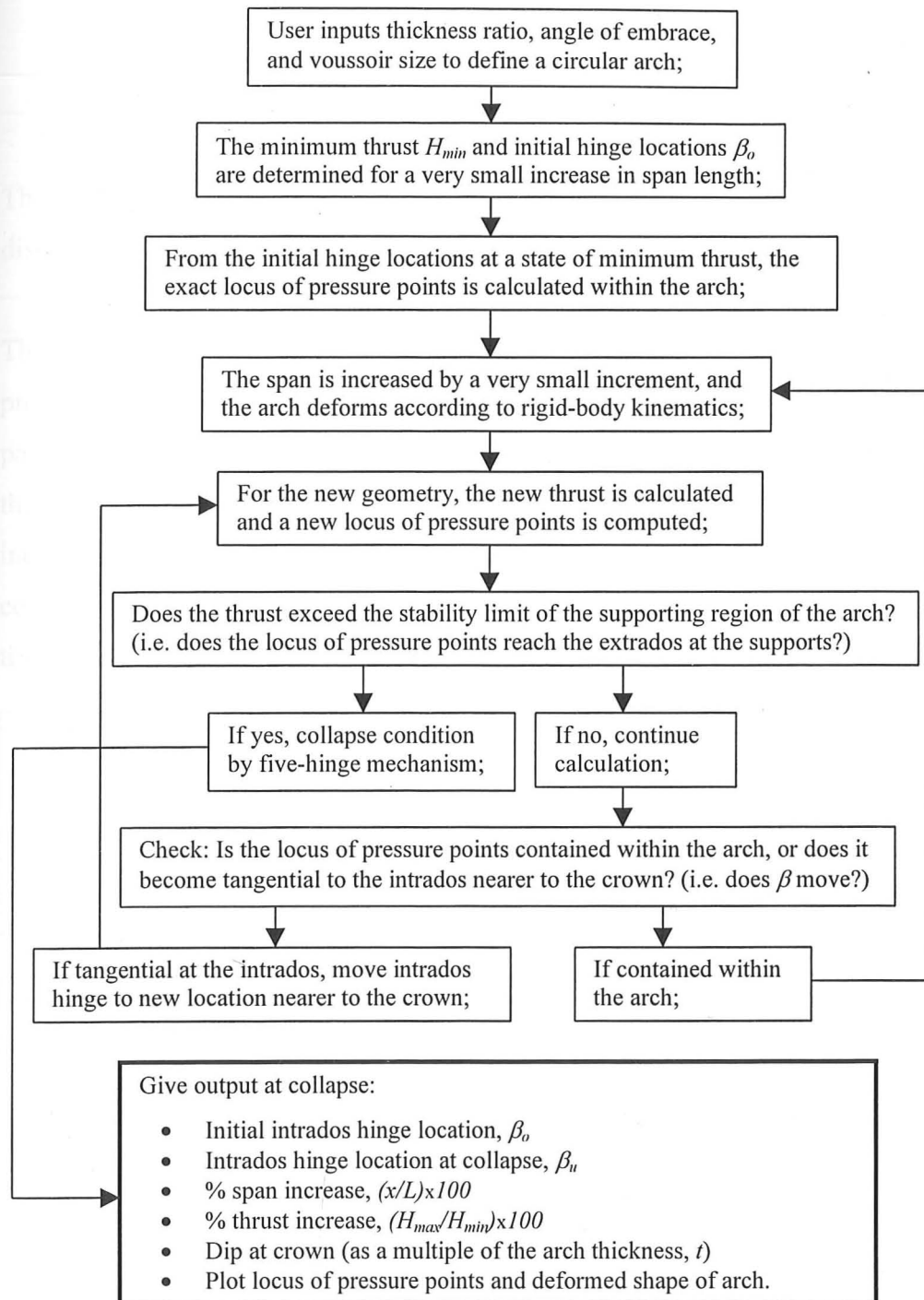


Figure 5.11 Algorithm to determine the collapse state of an arch on spreading supports.

The three-hinge "snap-through" failure will occur only for arches of very large thickness ratios and small angles of embrace. For this to occur, the locus of pressure points must be a horizontal line tangential to the arch intrados at the abutment. Snap-through by a three-hinge mechanism will occur for arches subtending a half angle of embrace:

$$\alpha \leq \cos^{-1} \left[\frac{1 - \frac{t}{2R}}{1 + \frac{t}{2R}} \right] \quad [5.5]$$

This limit is outside the geometrical range for circular arches and the present discussion, though the snap-through mechanism may be critical for some flat arches.

The governing failure mechanisms for circular arches on spreading supports are presented in Figure 5.12, as determined from the program ArchSpread. The lowest part of the curve is the region of least thickness, where the minimum thrust is equal to the maximum thrust. As the thickness increases, the maximum thrust at collapse increases. The ArchSpread program was used to determine the thickness ratios for the collapse state at which the maximum thrust from the arch, H_{max} , is 1.5, 2.0, and 5.0 times greater than the initial minimum thrust, H_{min} , defined in Figure 5.8.

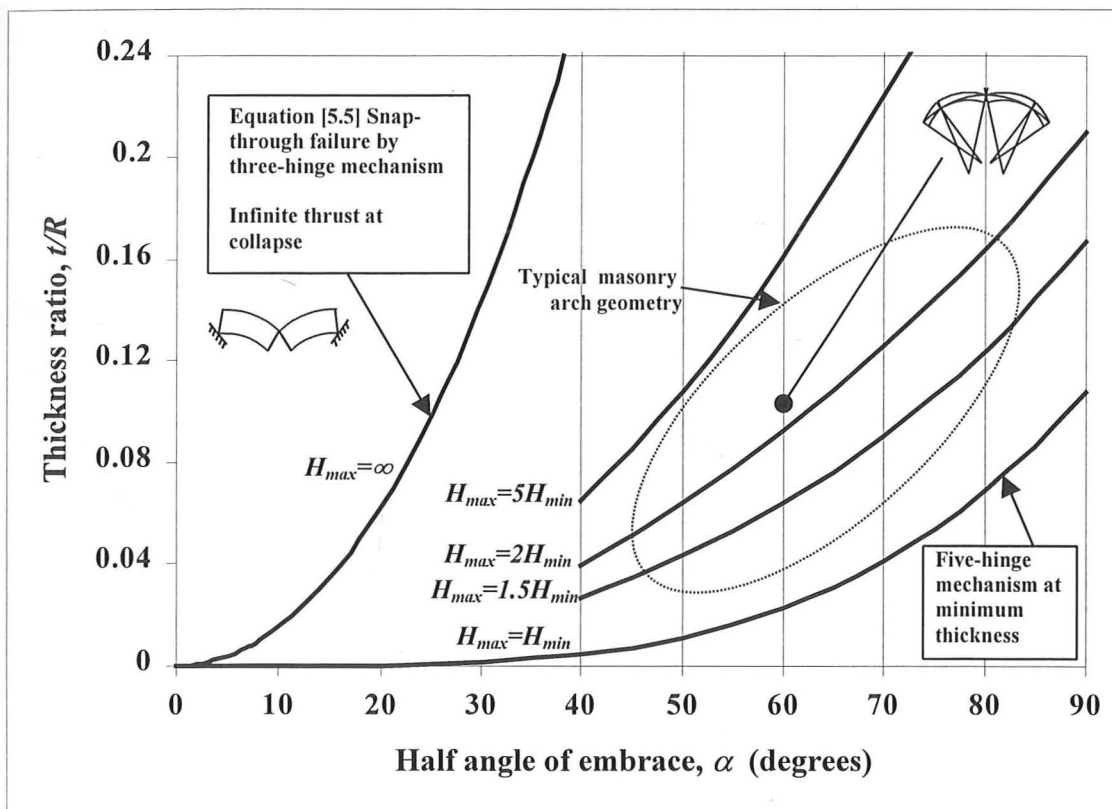


Figure 5.12. Collapse mechanisms and associated horizontal thrust for circular arches on spreading supports. The maximum horizontal thrust from the arch at collapse is defined as H_{max} , a multiple of H_{min} .

This analysis illustrates that in the case of spreading abutments, most arches will fail due to a five-hinge mechanism. As the thickness increases, the failure mechanism approaches a snap-through failure and the thrust increases significantly prior to

$$\alpha \leq \cos^{-1} \left[\frac{1 - \frac{t}{2R}}{1 + \frac{t}{2R}} \right] \quad [5.5]$$

This limit is outside the geometrical range for circular arches and the present discussion, though the snap-through mechanism may be critical for some flat arches.

The governing failure mechanisms for circular arches on spreading supports are presented in Figure 5.12, as determined from the program ArchSpread. The lowest part of the curve is the region of least thickness, where the minimum thrust is equal to the maximum thrust. As the thickness increases, the maximum thrust at collapse increases. The ArchSpread program was used to determine the thickness ratios for the collapse state at which the maximum thrust from the arch, H_{max} , is 1.5, 2.0, and 5.0 times greater than the initial minimum thrust, H_{min} , defined in Figure 5.8.

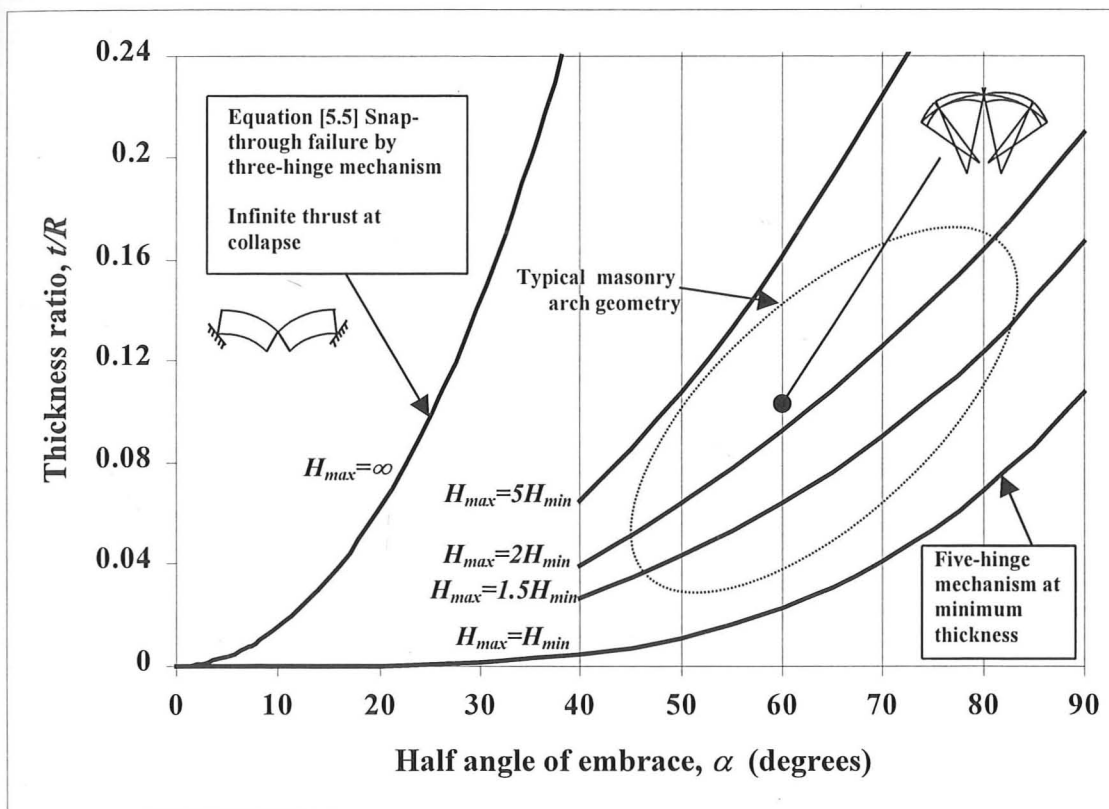


Figure 5.12. Collapse mechanisms and associated horizontal thrust for circular arches on spreading supports. The maximum horizontal thrust from the arch at collapse is defined as H_{max} , a multiple of H_{min} .

This analysis illustrates that in the case of spreading abutments, most arches will fail due to a five-hinge mechanism. As the thickness increases, the failure mechanism approaches a snap-through failure and the thrust increases significantly prior to

collapse. This is of great importance in assessing the safety of arches supported on buttresses, where the thrust of the arch may exceed the capacity of the buttress (to be shown in Chapter 7). This is particularly true in the case of leaning buttresses, which cause the span of the arch to increase and can lead to the collapse of a buttressed arch.

5.5 Spread Limits at Collapse

Circular arches subtending angles of 80° to 180° ($\alpha=40^\circ$ to 90°) have been analysed using the program ArchSpread (described in Figure 5.11) for various thickness ratios to determine the maximum spread of the abutments before collapse occurs. Some of the results are shown in Figures 5.13 and 5.14. Each curve begins with the least possible thickness ratio (from Table 5.2), and the collapse state is computed for larger thicknesses. As a practical limit, arches are not investigated beyond the region where the maximum thrust is greater than five times the minimum thrust at collapse.

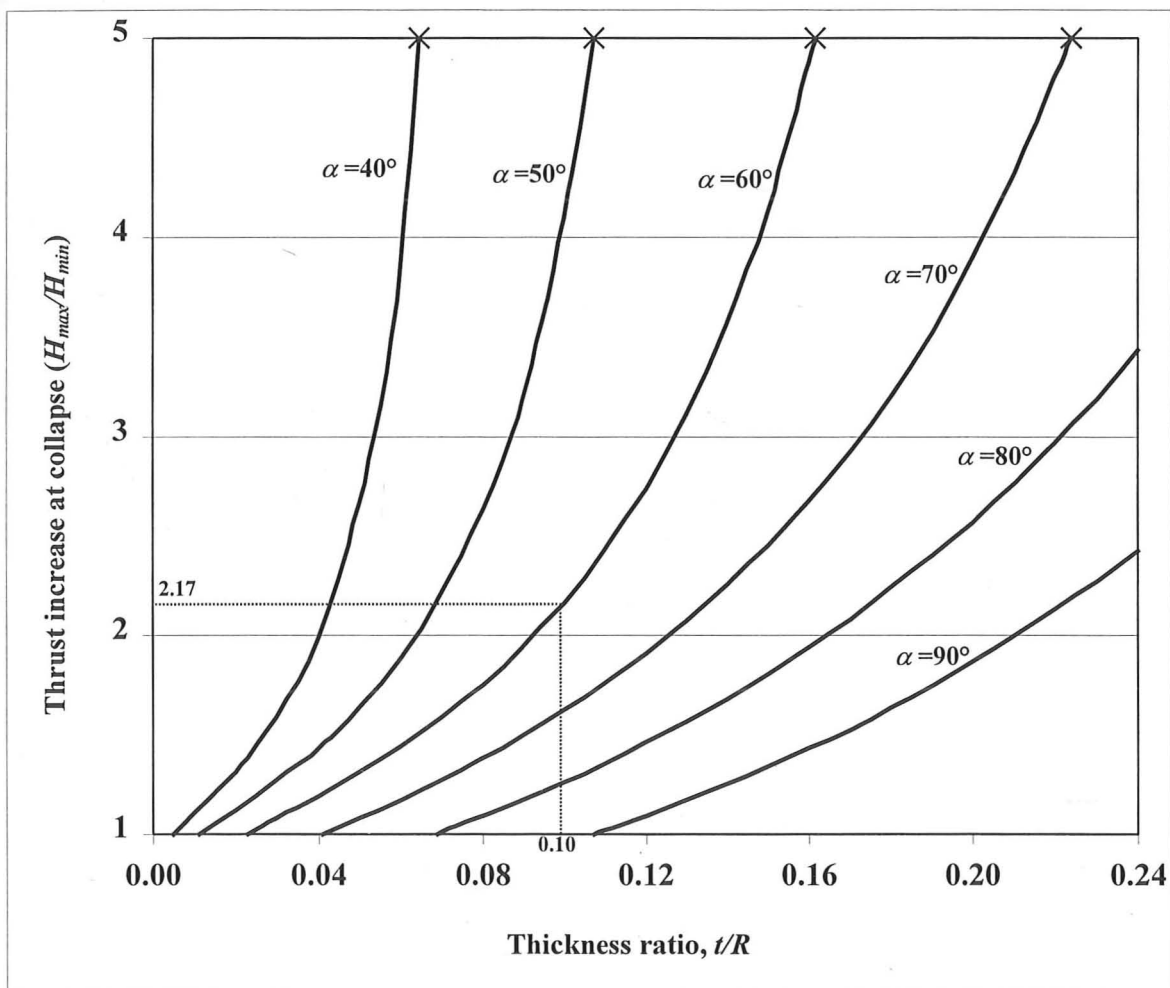


Figure 5.13. Thrust increase at five-hinge collapse for circular arches of varying geometry. For example, an arch subtending 120° ($\alpha=60^\circ$) with $t/R=0.10$ will collapse by a five-hinge mechanism with a thrust of $2.17H_{min}$.

The corresponding values of span increase to cause collapse are presented in Figure 5.14. For arches with smaller angles of embrace, the curves are truncated at the point where the maximum thrust is equal to five times the minimum thrust. For circular arches, the percentage of span increase to cause collapse is approximately linear in relation to increasing thickness ratios.

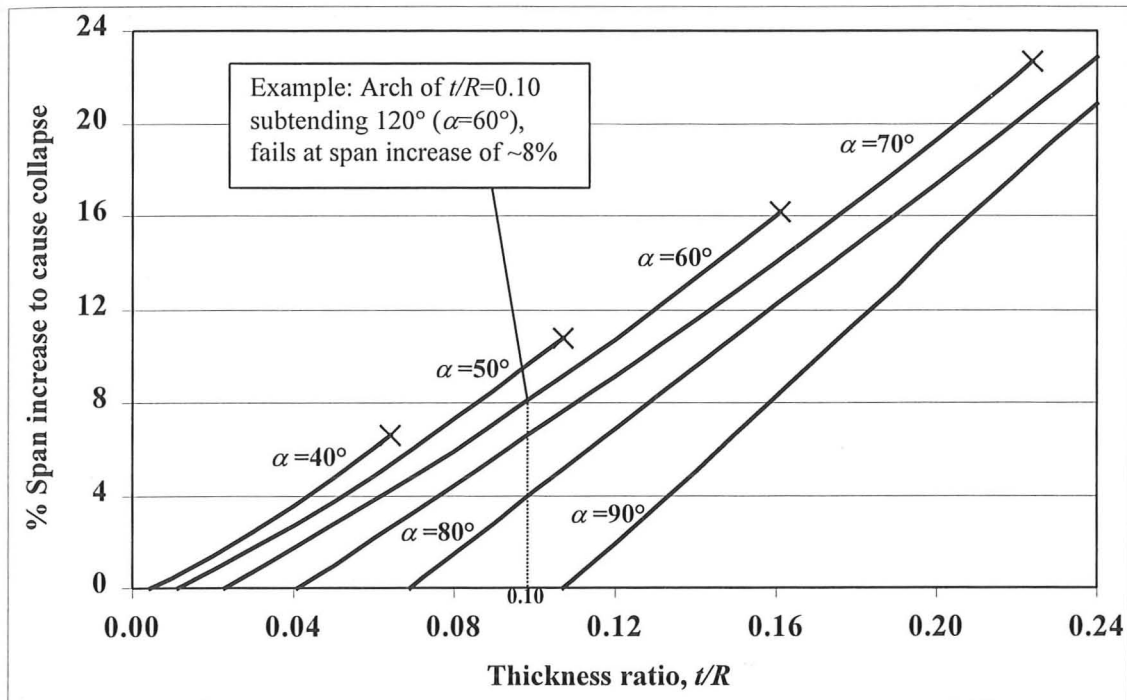


Figure 5.14 Maximum span increase at collapse for circular arches. Some plots are terminated when the thrust of the arch at collapse is equal to five times the minimum thrust. These points are marked by "x" and correspond to the same points on Figure 5.13.

In each case, the intrados hinge begins at the initial hinge location, β_o , and moves toward the crown of the arch as the supports are moved apart. At the collapse state when five hinges form, the intrados hinges have moved to a critical location β_u . The implications of this hinge movement will be discussed in the next section and illustrated by the experimental results at the end of this chapter. The movements of the hinges from the initial hinge location, β_o , to the hinge location at collapse, β_u , are summarised in Figure 5.15 for arches subtending angles of embrace of 40° , 60° , and 80° . As the angle of embrace becomes smaller the intrados hinge is more likely to move by a large amount before collapsing. As before, the curves for small angles of embrace are truncated when the maximum thrust becomes five times the minimum thrust. The voussoir size is taken as 0.1° to provide a theoretical limit for the problem and allow the intrados hinges to move smoothly as the arch deforms.

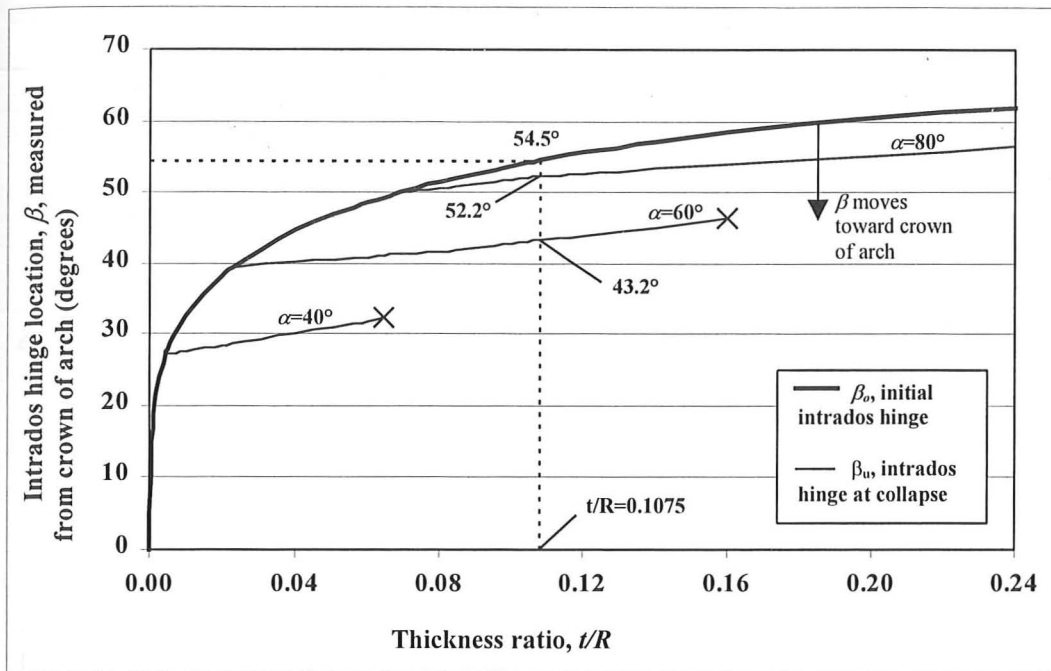


Figure 5.15. Summary of intrados hinge movements from initial hinge location, β_o , to final hinge location at the collapse state, β_u , assuming the voussoir size is 0.1° .

To explain Figure 5.15, we return again to the example of a circular arch with a thickness ratio of $t/R = 0.1075$. If the arch subtends a total angle of 160° ($\alpha = 80^\circ$), the hinge moves from the initial location of $\beta_o = 54.5^\circ$ to $\beta_u = 52.2^\circ$ at the collapse state. But if the arch subtends a smaller angle of embrace of 120° ($\alpha = 60^\circ$), the hinge begins at 54.5° as before, but moves all the way to 43.2° from the crown at the collapse state. This demonstrates that the intrados hinge locations may move substantially as the arch deforms to the collapse state. This will now be demonstrated with reference to a specific example in order to demonstrate the influence of the voussoir size.

5.6 Effect of Voussoir Size

The results presented in Figures 5.12 to 5.15 are based on arches with small voussoirs (of angle 0.1°), in order to provide theoretical limits for the problem. This is, of course, much smaller than the voussoir angles used in practice, so it is of interest to know how the results would change for large voussoir sizes. To investigate the effect of larger voussoir size on the stability of arches on spreading supports, an arch subtending a total angle of embrace of 120° ($\alpha = 60^\circ$) with a thickness ratio of $t/R = 0.10$ has been analysed using the ArchSpread program. The program output is illustrated in Figure 5.16 for an arch with 1° voussoirs. In addition, the same arch has been analysed for voussoir sizes of 0.1° , 5° , and 10° : see Table 5.3 for a summary.

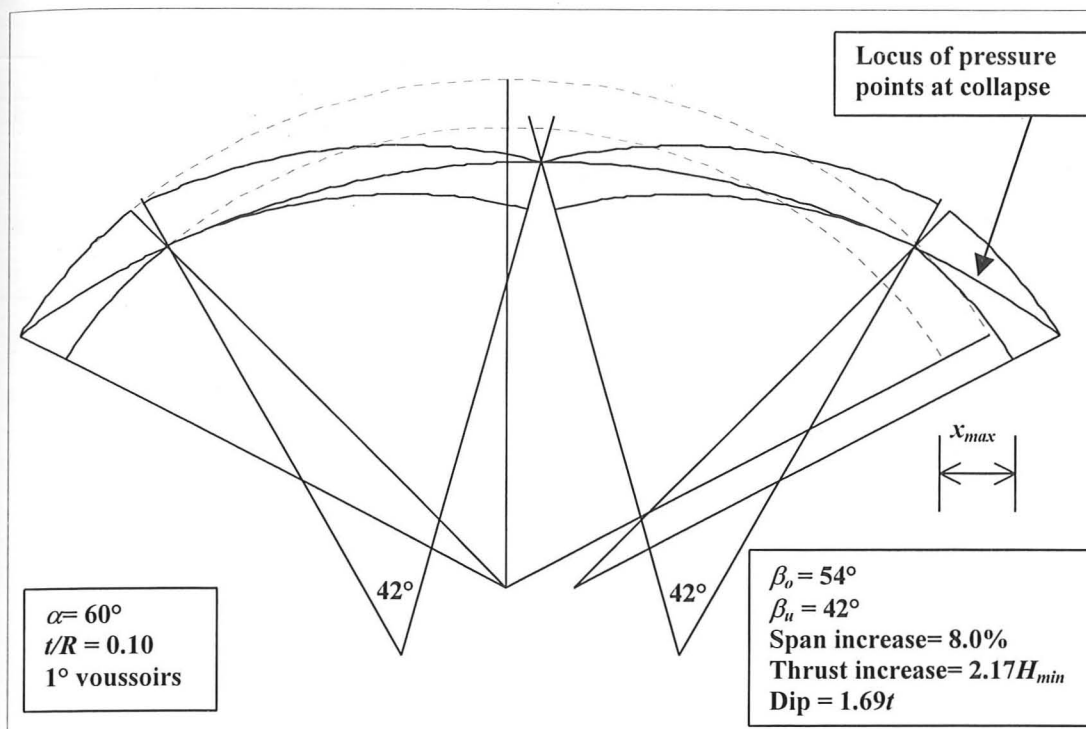


Figure 5.16 Symmetrical collapse mechanism for an arch on spreading abutments ($t/R=0.10$; $\alpha=60^\circ$; voussoir angle $=1^\circ$).

Voussoir size	0.1°	1°	5°	10°
Initial hinge, β_o	53.8°	54°	55°	50°
Collapse hinge, β_u	42.7°	42°	40°	40°
Span increase (%)	8.2	8.0	8.6	9.3
Thrust increase ($\times H_{min}$)	2.16	2.17	2.02	2.03
Dip at crown (xt)	1.73	1.69	2.09	2.54

Table 5.3 Collapse state for an arch subtending 120° ($\alpha=60^\circ$) and $t/R=0.10$ with varying voussoir sizes.

The different response due to varying voussoir sizes is summarised in Figure 5.17, which plots the increasing thrust as the span increases. The slight difference between the arches of 1° and 0.1° voussoirs is due to the difference in the hinge location β at the collapse state. The 1° voussoir arch fails when $\beta=42^\circ$, while the 0.1° voussoir arch continues to deform until $\beta=42.7^\circ$. The 5° - and 10° -voussoir arches both fail at $\beta=40^\circ$, and can resist slightly larger span increases. Most significantly, the lowest line on the curve is the thrust if the initial hinge is artificially constrained at $\beta=53.8^\circ$, and does not move to the final position of approximately 42° . The intrados hinge movement leads to increased thrusts as the span increases, which may be significant in some cases. The effect of the hinge movement is an important factor in the response of arches to moving supports, and engineers should be aware of this possibility.

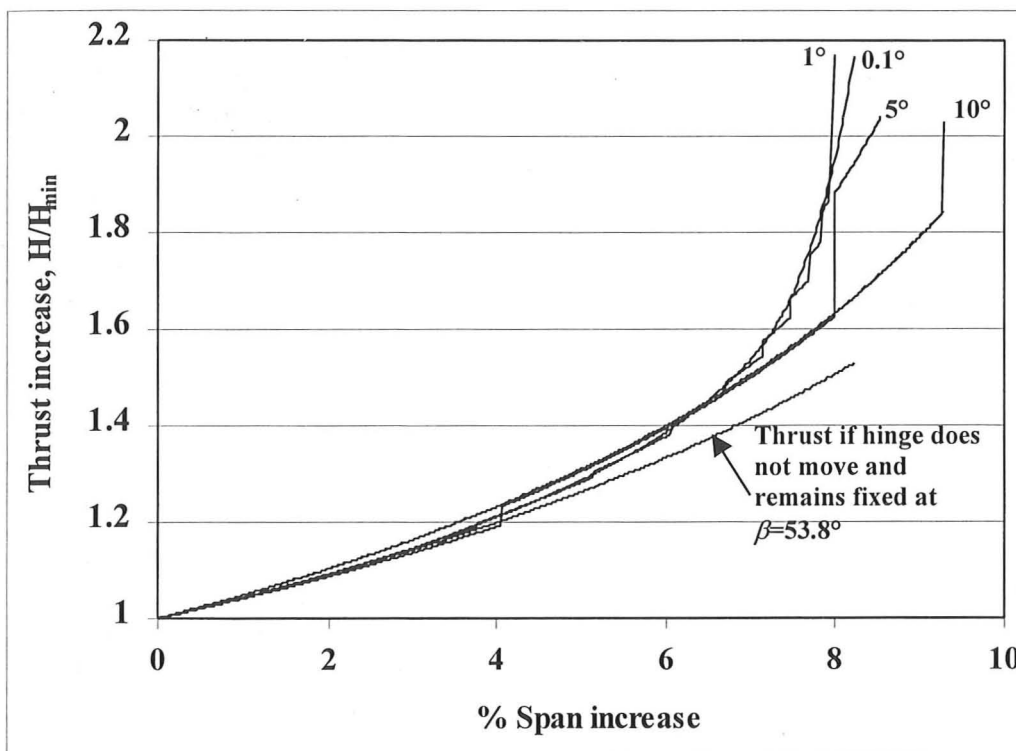


Figure 5.17. Thrust increase with span increase for various voussoir sizes ($\alpha=60^\circ$, $t/R=0.10$).

The importance of the hinge movement is illustrated by the "stepped" effect of the thrust increase. As the hinge moves from one voussoir to the next, the sudden change in geometry -- corresponding to the hinge moving inwards by one voussoir -- causes discontinuities in the thrust increase. In actual arches, this geometrical change can lead to a dynamic effect, where the arch adjusts to the shifting hinge and the crown drops suddenly. This effect may reduce the safety of arches by causing collapse at smaller span increases than those predicted by the analysis applied in this chapter.

In summary, defining the arch as finite voussoirs has several important effects:

- 1) Larger voussoirs limit the possible hinge locations. For smaller voussoirs, the intrados hinge at β can move more smoothly from one voussoir to another. Large voussoirs require sudden changes in the geometry of the arch to adjust to the changing hinge locations.
- 2) Using larger voussoirs generally increases the capacity of the arch for abutment spreading, although not always. Increasing the size of the voussoir can "strengthen" the arch by preventing the movement of the intrados hinge, or in some cases can cause premature collapse if the hinge location is limited.
- 3) As the intrados hinge moves position, larger voussoirs will cause sudden changes in geometry and sudden increases in horizontal thrust. This can introduce dynamic effects into arches with spreading abutments.

5.7 Experimental Results

Small scale experiments have been conducted in order to investigate the collapse mechanisms of arches on spreading supports. Two model arches were made from voussoirs cast as individual concrete blocks, 50mm in radial thickness. Arch1 had a radius of 220mm and a thickness ratio, t/R , of 0.23, with voussoirs of approximately 11° . Arch2 had a radius of 385mm and a thickness ratio, t/R , of 0.13, with voussoirs of 10° . Both arches were tested to collapse by spreading the supports, and the results are presented in Figures 5.18-5.21 and in Table 5.4.

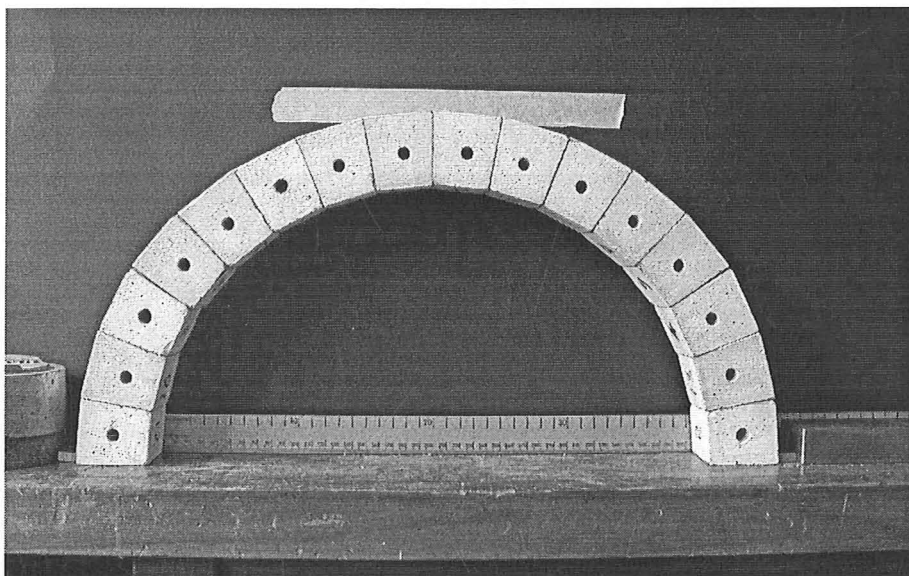


Figure 5.18. Undeformed masonry arch of approximately 11° blocks (Arch1: $t/R=0.23$, $\alpha=90^\circ$).

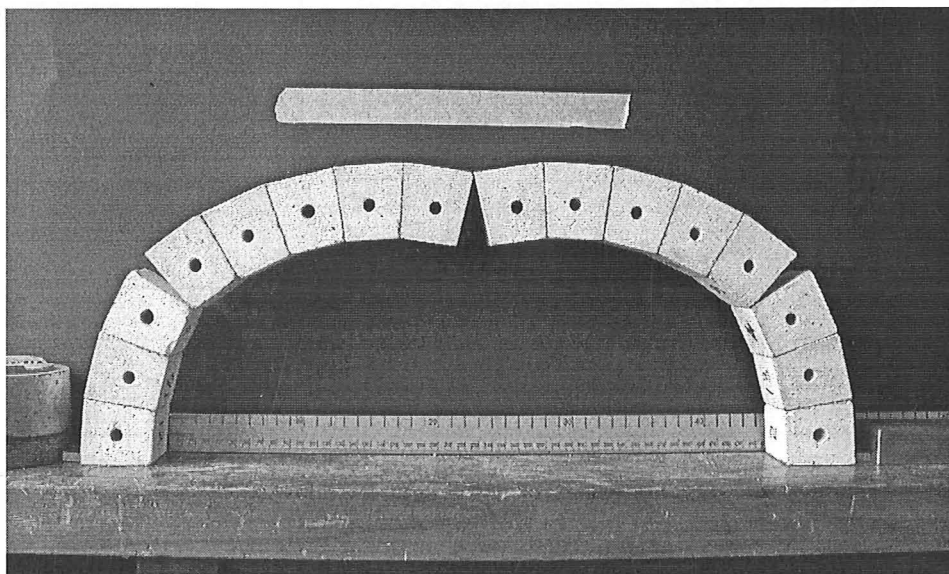


Figure 5.19. Deformed Arch1 on spreading supports just before collapse.

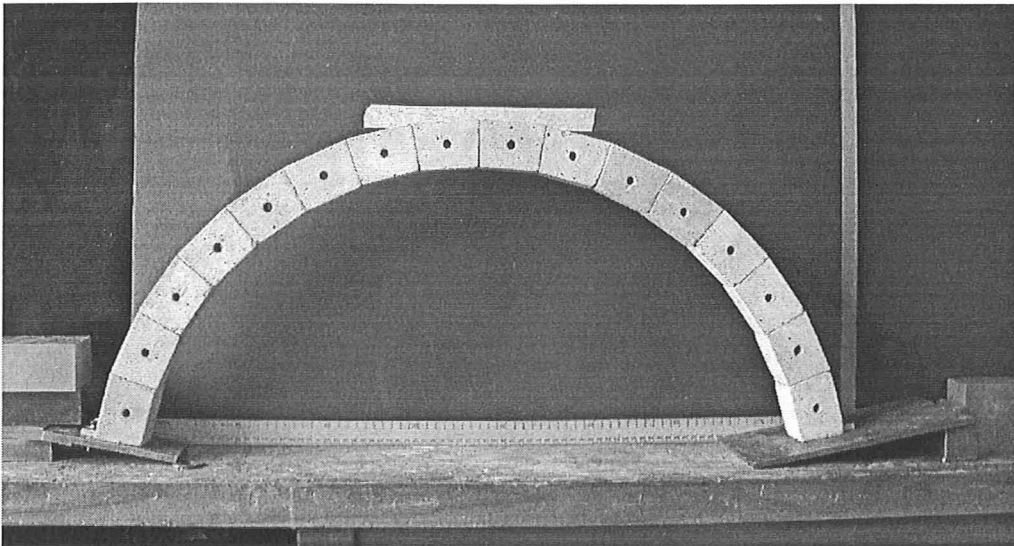


Figure 5.20. Undeformed masonry arch of 10° blocks (Arch2: $t/R=0.13$, $\alpha=80^\circ$).

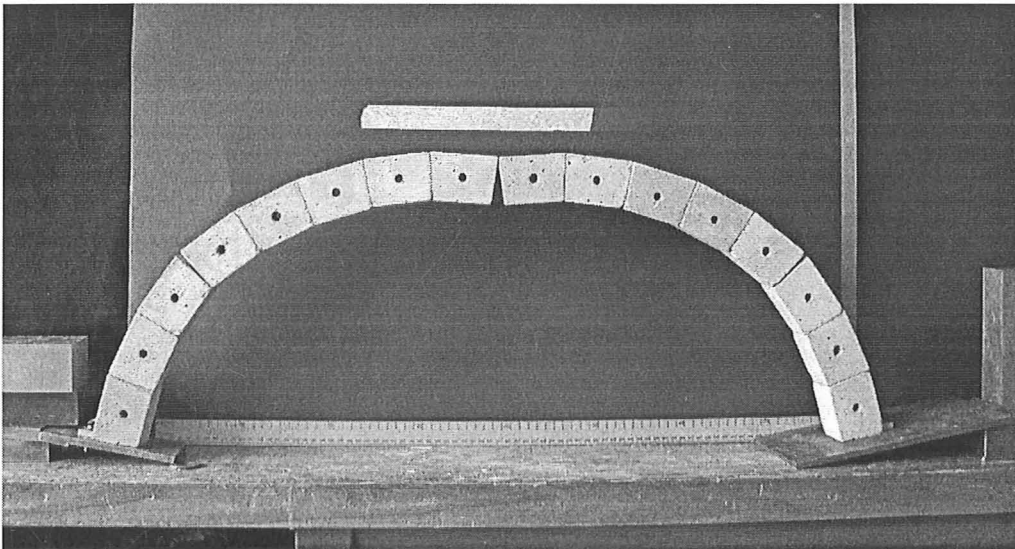


Figure 5.21. Deformed Arch2 on spreading supports just before collapse.

	Arch1: $t/R = 0.23$ (voussoir size $\sim 11^\circ$, $\alpha=90^\circ$)			Arch2: $t/R = 0.13$ (voussoir size of 10° , $\alpha=80^\circ$)		
	Predicted	Test	% diff.	Predicted	Test	% diff.
Initial hinge, β_o	56°	56°	0%	60°	60°	0%
Collapse hinge, β_v	56°	56°	0%	50°	50°	0%
% Span increase just before collapse	16.9%	15.4%	-8.9%	8.8%	7.8%	-11.4%
Dip at crown just before collapse	$1.0t$	$0.8t$	-20%	$1.2t$	$0.8t$	-33%

Table 5.4. Predicted response and experimental results for arches on spreading supports.

In each case, the methods presented in this chapter correctly predicted the final collapse mechanism. In the first arch, the intrados hinges remained in their initial configuration and did not move as the support spreads. In the second arch, the hinges occurred at 60° initially, and then moved to the next voussoir (at 50°) before reaching the final collapse state. In both arches, collapse occurred by a four-hinge mechanism when the thrust from the central region of the arch exceeded the stability conditions for one of the supporting regions of the arch (i.e. the locus of pressure points arrives at the extrados at the support). For perfectly symmetrical arches, the collapse is a five-hinge mechanism as predicted by the program ArchSpread, but in practice, very small asymmetries cause collapse by a four-hinge mechanism.

Importantly, the theoretical approach presented in this chapter predicts slightly larger support movements than the movements measured just before collapse. For Arch1 and Arch2 the actual support movements were less than the predicted support movements for collapse by 8.9% and 11.4%, respectively. The explanation for this discrepancy is due to the nature of the collapse mechanism and the imperfect modelling of the blocks. As the arch approaches the collapse state, the thrust from the central region is nearly equal to the resistance of the supporting region of the arch. Any small movement will lead to changes in the stability of the system and premature collapse of the arch. In particular, small vibrations will lead to the collapse of the arch and therefore it is highly difficult to reach the theoretical limit for spreading of the supports. Furthermore, the edges of the blocks were not perfectly defined and thus the hinge locations could not occur exactly at the edge of the blocks as assumed in the analysis. This could have been avoided by using carefully machined steel voussoirs, but this would not have modelled the reality of masonry structures, which are inexact in their construction. Finally, the slight asymmetry of real structures may cause collapse to occur prematurely by a four-hinge mechanism rather than a perfectly symmetrical five-hinge mechanism.

5.8 Summary

This chapter has analysed the specific problem of a circular arch segment on spreading abutments, and the following points are significant:

- 1) The arch of minimum thickness for a given angle of embrace can be determined exactly with a work-balance calculation, or from the exact equations for thrust in a circular arch.
- 2) The Heyman (1969) equation for minimum thickness is not precisely correct, and can underestimate the minimum thickness by a small amount (about 1% for a semicircular arch).
- 3) The conventional "thrust line" is not precisely tangential to the arch at the intrados hinge. A locus of pressure points -- a more precise concept -- can be constructed by making "cuts" in the structure and finding the "pressure point" where the resultant axial forces pass through the joint between voussoirs to satisfy equilibrium. The locus of pressure points is equivalent to the "line of resistance" defined by Moseley (1843).
- 4) Each thickness ratio has an initial position of the intrados hinge, β_0 , where the initial hinges will occur in the case of spreading abutments (provided that the total angle of embrace is greater than $2\beta_0$).
- 5) For the problem of spreading abutments, the method presented here predicts that circular arches will collapse due to the formation of a five-hinge mechanism. Though this mechanism is symmetrical, only four hinges are required for collapse to occur so the actual collapse mechanism may not be exactly symmetrical due to slight asymmetries in practice.
- 6) The vertical force reaction at the arch support remains constant, but the horizontal thrust increases substantially as the supports move apart.
- 7) As the supports move horizontally, the intrados hinge in a circular arch will move toward the crown, altering the geometry of the arch and further increasing the thrust of the arch prior to collapse.
- 8) A given span increase may be accommodated by a number of possible equilibrium configurations, each with different hinge locations and different deformed shapes. To determine the collapse condition the analyst must begin from a known equilibrium configuration.
- 9) For spreading abutments, typical masonry arches may exert a thrust up to five times the minimum thrust before they collapse.
- 10) The theoretical span increase to cause collapse is approximately linear in relation to the thickness ratio for a circular arch.

- 11) The size of individual voussoirs can alter the response of the arch to spreading supports; and finite voussoirs can cause sudden changes in geometry as the intrados hinge "jumps" between voussoirs.
- 12) Actual arches collapse at slightly lower span increase than predicted due to the precarious nature of the collapse mechanism and the imperfect "corners" of the voussoirs, which do not form hinges exactly at the edge as theorised.
- 13) The collapse of masonry arches on spreading abutments is a complex problem, with uncertainties in the exact collapse mode due to uncertainties in the hinge locations in the arch.
- 14) Only circular arches of constant thickness have been considered here, but the general procedure can be adapted to arches of any shape and thickness.

Chapter 6 The Masonry Arch under Lateral Acceleration

6.1 Introduction

As the previous chapter demonstrated, masonry arches can be analysed as rigid-block assemblies that collapse due to instability of the structure rather than failure of the material. In addition to the threat of support movements, earthquake loading can apply large horizontal accelerations, which may de-stabilise a masonry arch. This chapter investigates the resistance of the circular masonry arch to constant horizontal acceleration, combined with the vertical acceleration due to gravity. This is equivalent to tilting an arch on a plane until the arch collapses, and the critical angle of tilt gives the minimum value of lateral acceleration to cause the arch to collapse. Thus, an analysis of tilting arches provides an initial approximate procedure for the equivalent static analysis of masonry structures in earthquake loading. This provides insight into the relative stability of various arch geometries, and can be used to investigate the change in internal forces as a result of lateral acceleration. In general, the seismic performance of vaulted masonry buildings is poorly understood, and this chapter provides a basic introduction to the response of arches to lateral acceleration by defining the governing mechanisms for circular arch segments.

For vertical loading due to gravity, the internal line of forces (the locus of pressure points) is contained within the arch initially. As the arch is tilted, the internal forces shift to account for the horizontal component of acceleration. Eventually, the line of forces cannot be contained within the thickness of the arch, hinges form, and the arch becomes a mechanism with four hinges, commonly called a four-bar chain (Fig. 6.1).

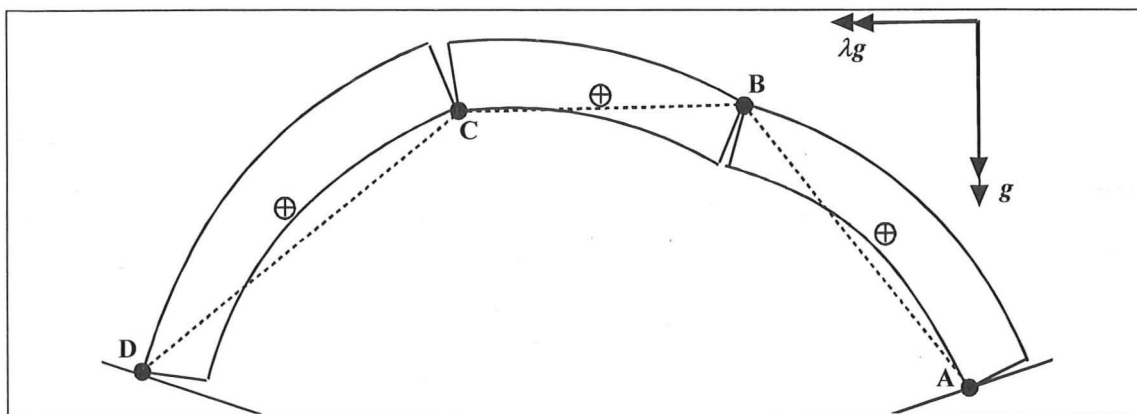


Figure 6.1 Hinge formation and the collapse of an arch as a four-bar chain due to lateral acceleration.

In the previous chapter, it was necessary to determine the exact locus of pressure points in order to find the critical hinge locations throughout the history of deformation. For an arch on spreading supports, the geometry of the structure continues to change and a new equilibrium state must be found for the new geometry at each stage. The arch on spreading abutments involves large support displacements and the structure changes continuously to adapt to the new geometry. For the current problem, the initial (circular) geometry of the arch is unchanged as the arch tilts, and the critical loading to cause collapse can be solved directly from a work calculation based on an infinitesimal motion. This follows Heyman's upper-bound approach for the limit analysis of masonry arches, and the critical collapse mechanism must be found for the applied loading.

6.2 Method of Analysis

To determine the minimum constant horizontal acceleration for collapse, it is first necessary to postulate a failure mechanism, and determine the amount of work required to form the mechanism. To ensure that the correct hinge locations are found, it is necessary to check other possible mechanisms, and to verify that the correct mechanism requires the smallest value of lateral acceleration. At the collapse state, the masonry arch requires four hinges to form – two hinges at the extrados, B and D, and two hinges at the intrados, A and C – as shown in Figure 6.2. Clemente (1998a) demonstrated that the hinge at point D will always form at the extrados of the support. The location of the three other hinges, C at the intrados, B at the extrados, and A at the intrados, must be found by iterative calculations. For this dissertation, a uniform horizontal acceleration is applied to the structure, and the calculation is independent of the uniform density of the material. The combined action of the vertical acceleration of gravity with the horizontal acceleration is equivalent to a resultant acceleration acting at an angle of Γ from the vertical.

As in the previous chapter, the arch is a circular segment with a centreline radius of R , thickness t , and angle of embrace 2α . The only loading is due to the self-weight of the arch. The hinge locations for A, B, and C are defined by the angles a , b , and c measured from the horizontal line at the geometric centre of the arch. The four hinges divide the arch into three rigid segments, each with a centre of mass M_i , for $i = 1, 2, 3$.

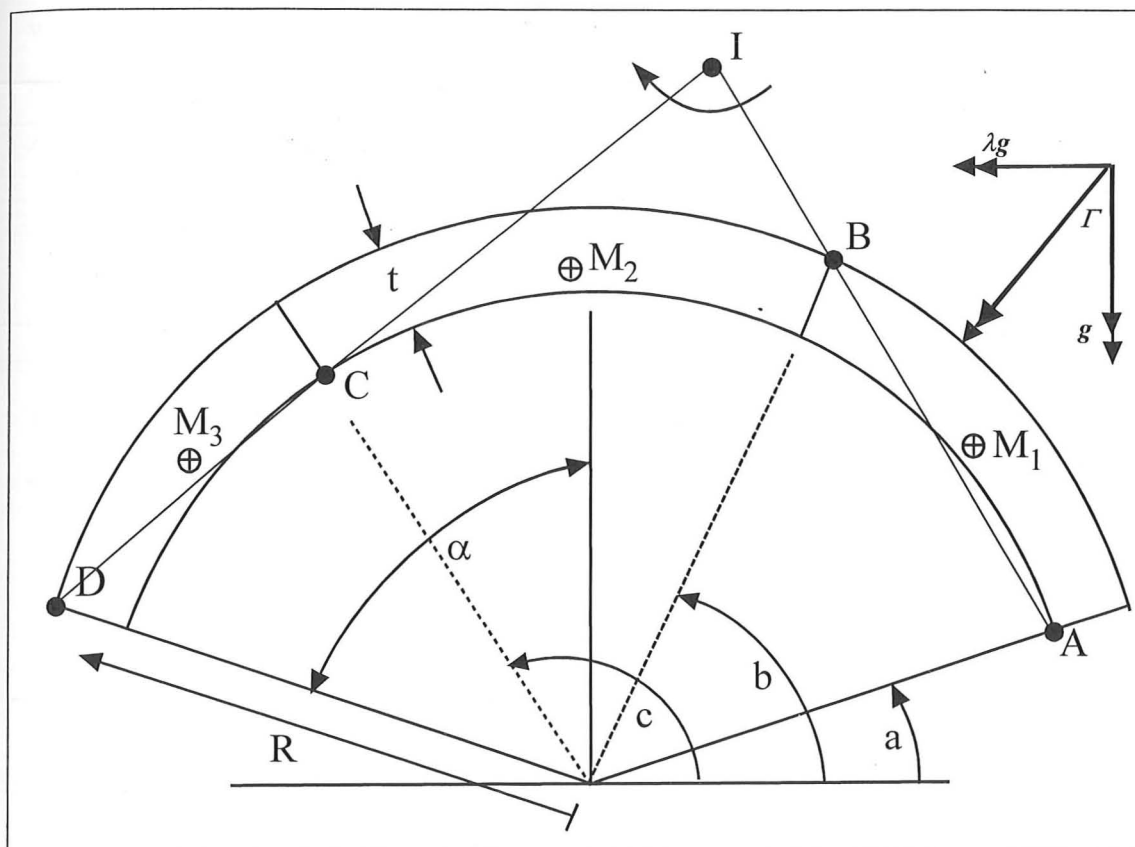


Figure 6.2. Geometry of a circular masonry arch with four hinges due to horizontal acceleration.

The lateral acceleration is defined as a factor, λ , multiplied by the acceleration of gravity, g . The lateral acceleration λg and the vertical acceleration g , are related by Γ , where:

$$\tan(\Gamma) = \frac{\lambda g}{g} = \lambda. \quad [6.1]$$

The angle Γ is equivalent to the inclination at which the equivalent lateral acceleration would be applied if the entire structure were tilted on a plane. Based on the initial assumptions of rigid blocks which can form hinges at any location between voussoirs, there is no energy dissipated within this system, and therefore the sum of internal work done is zero. The work equation relating the horizontal and vertical displacements, u_i and v_i , of each centre of mass, to the total work done by the acceleration is:

$$\sum_{i=1,2,3} M_i g v_i + \sum_{i=1,2,3} M_i \lambda g u_i = 0 \quad [6.2]$$

which states that the sum of vertical work plus the sum of horizontal work must equal zero (i.e., external work must equal internal work). Rearranging [6.2], and solving for λ yields:

$$\lambda = -\frac{\sum_{i=1,2,3} M_i v_i}{\sum_{i=1,2,3} M_i u_i} \quad [6.3]$$

The factor λ is defined as the sum of the vertical gravitational work divided by the sum of the horizontal work. From [6.1], the equivalent angle of tilt Γ is:

$$\Gamma = \tan^{-1}(\lambda). \quad [6.4]$$

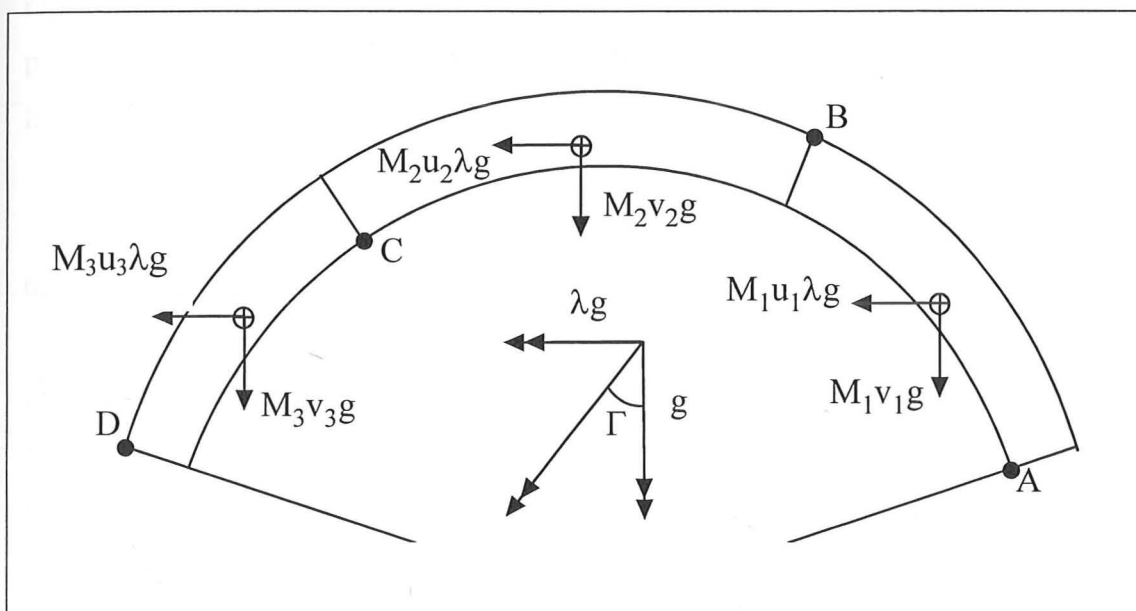


Figure 6.3. Equivalent tilted arch and work done by components due to the applied acceleration

To determine the minimum lateral acceleration factor to produce a collapse mechanism, λ_{min} , the work calculation is summarised in the following steps:

- 1) For assumed hinge locations A, B, C, and D, determine the centre of mass of each segment, and the location of the instantaneous centre, I, for the central portion. (Figure 6.2).
- 2) Apply a small rotation to segment BC of the arch, and calculate the corresponding rotations of the two remaining arch segments. (The mechanism has one degree of freedom, so the relative rotations are defined by the rotation of one component.)

- 3) Based on the relative rotations of each segment, compute the small vertical and horizontal displacements, v_i and u_i , of each centre of mass, M_i .
- 4) Compute the vertical and horizontal components of work done as the sum of the displacements multiplied by the masses, including the unknown λ (Figure 6.3).
- 5) The value of horizontal acceleration, λ , is computed from [6.3] by dividing the total vertical work by the total horizontal work.
- 6) Store the current value of λ and repeat the calculation for all kinematically admissible positions of hinges A, B, and C.
- 7) The hinge locations resulting in the lowest value of λ identify the collapse mechanism and the corresponding value of λ_{min} .

This process is carried out by the program ArchTilt, written in MATLAB and attached in Appendix A, in which the user inputs the angle of embrace and thickness ratio, and the program performs the algorithm described above. The program output provides the hinge locations A, B, and C for the critical mechanism and the minimum lateral acceleration, λ_{min} .

6.3 Collapse Mechanisms

The previous chapter demonstrated that the symmetrical five-hinge mechanism governs for small thickness ratios, suggesting that a similar mechanism will govern for angles of embrace slightly less than the maximum possible angle of embrace. But in this case, essentially the same failure mechanism will occur, though the hinge locations will rotate by the angle of tilt, Γ , to new positions. Thus, it is the same problem of the minimum thickness arch, with the axes of the coordinate system rotated by the angle Γ . This is equivalent to building in the arch foundation by an angle of 2Γ (Figure 6.4), because each support would rotate by Γ from the original position. The support with the extrados hinge D is fixed, so the opposite support would rotate around the arch by an angle of 2Γ . Of course this simplified approach is only valid for the unique case of the circular arch, in which the entire arch can be "rotated" without altering the mechanics or the geometry of the problem. Importantly, only four hinges are needed for collapse to occur, so that the entire five-hinge mechanism does not have to form. Thus, it is valid to apply a four-hinge collapse mechanism, derived from the geometry of the five-hinge mechanism.

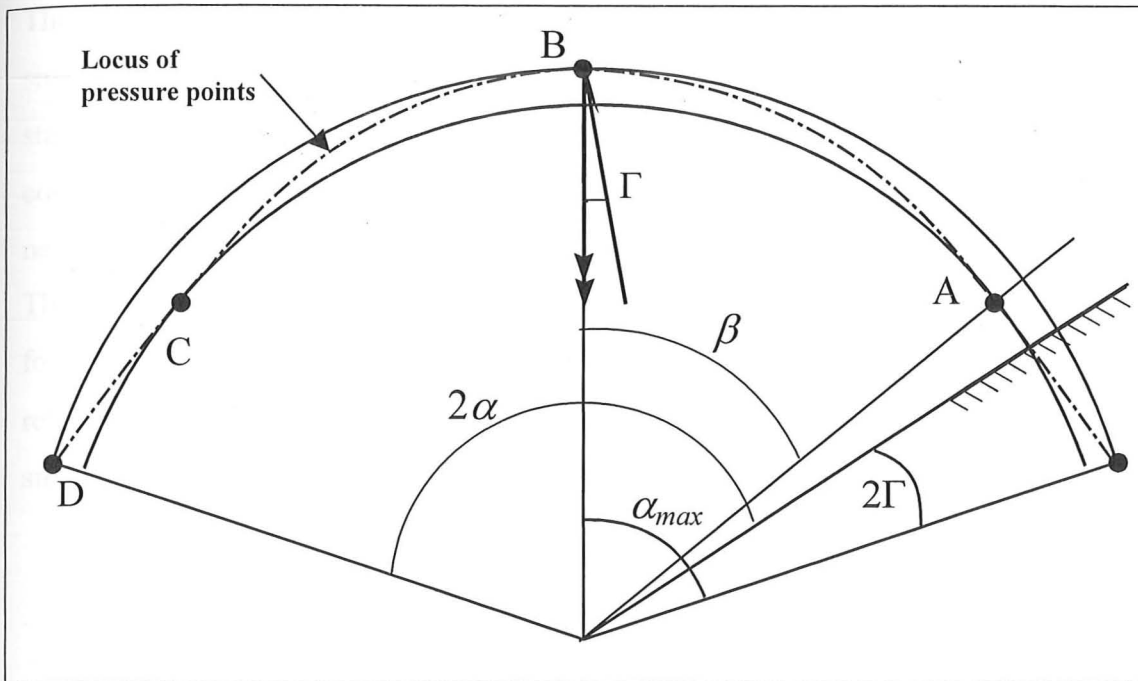


Figure 6.4. Minimum thickness arch rotated through an angle, Γ .

If the minimum thickness arch is rotated through Γ clockwise, a symmetrical arch of the same thickness will be on the point of collapse under an acceleration vector angled at Γ . This mechanism holds true until the point when 2Γ exceeds the hinge location of the right-hand abutment. After this point, the hinge at A will form at the support, and not in the span of the arch. This will occur for an angle of tilt:

$$\Gamma = \frac{\alpha_{max} - \beta}{2} \quad [6.5]$$

where β is the angle of the intrados hinge from the crown at the maximum angle of half embrace, α_{max} , for the given thickness ratio.

For arches with small thickness ratios and large angles of embrace, the relationship between Γ and α will be linear with a slope of -1 , until the point that the angle α forms at the support, when the slope will increase due to greater resistance to lateral loading. Until this point, three of the hinges occur in the span, with only one hinge at the support. After this point, a hinge forms at each support and two hinges form in the span.

The minimum thickness arches presented in Table 5.2 have been considered for smaller angles of embrace than the critical angle, α_{max} , at which they will no longer stand. For each thickness, the minimum required lateral acceleration to induce collapse is summarised in Figure 6.5. This graph plots the minimum angle of tilt, Γ , necessary for collapse of arches with various thickness ratios and angles of embrace. The thickness ratios presented in Figure 6.5 range from 0.011 to 0.108, and are plotted for total angles of embrace from 80° up to 180° ($\alpha=40^\circ$ to 90°). As postulated, the relationship between Γ and α is linear with slope -1, and then rises more steeply for smaller angles of embrace when the hinges A and D form at the supports.

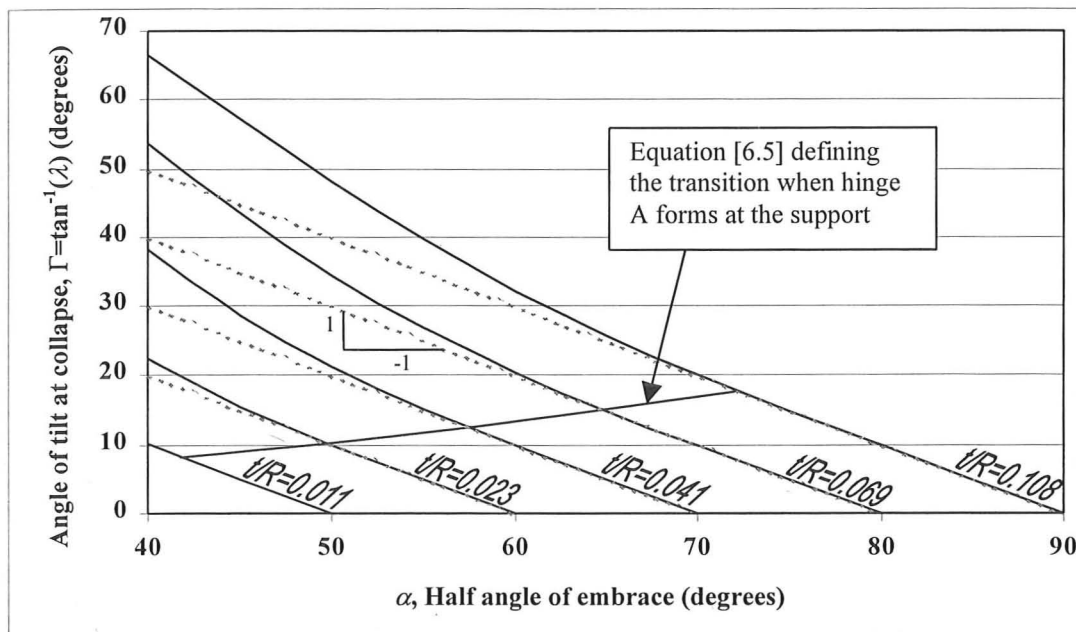


Figure 6.5. Maximum angle of tilt for circular arches of various thickness ratios.

The behaviour is consistent regardless of the thickness, suggesting that a general rule for determining the threshold acceleration of circular arches can be derived. For an arch of given t/R and angle of embrace 2α , it is possible to approximate the critical angle Γ , which will cause the onset of a collapse mechanism. This approximation is shown as the set of dashed lines in Figure 6.5. The direct relationship between α and Γ means that if the angle of tilt, Γ , is zero for α_{max} , then the Γ for a given α is simply:

$$\Gamma \geq \alpha_{max} - \alpha. \quad [6.6]$$

The minimum thickness ratio, which will collapse at the maximum possible angle of embrace, α_{max} , can be approximated by the equation:

$$\left(\frac{t}{R}\right)_{\min} \cong \frac{\alpha_{\max}^4}{48} \quad [5.2]$$

where α_{max} is given in radians, as presented previously in Chapter 5. Rearranging and solving for the maximum angle of embrace, α_{max} , yields:

$$\alpha_{\max} \cong \left[\frac{48t}{R}\right]^{1/4} \cong 2\left[\frac{3t}{R}\right]^{1/4} \quad [6.7]$$

For a given t/R ratio, this can be used to approximate the maximum angle, α_{max} , at which an arch of that thickness would stand. Combining [6.5] and [6.7] gives:

$$\Gamma \geq 2\left[\frac{3t}{R}\right]^{1/4} - \alpha \quad [6.8]$$

where Γ and α are given in radians. This equation can be applied to existing arches of known angle of embrace and thickness ratio, to determine the approximate critical angle of tilt for collapse to occur. For example, a circular arch subtending an angle of 130° ($\alpha=1.13$ radians), with a thickness ratio of 0.09, would have an approximate Γ of 0.31 radians, or 18° according to equation [6.8]. From [6.1], this value corresponds to $\lambda=0.32$, or a lateral acceleration of 0.32g. The exact solution from the ArchTilt program is Γ_{cr} of 0.37 radians, or 21° , corresponding to a lateral acceleration of $\lambda=0.38g$. This approximation provides a conservative estimate of the minimum lateral acceleration necessary to form a collapse mechanism in a circular arch. The minimum lateral acceleration for collapse is summarised in Figure 6.6 below, from the tangent of the Γ values in Figure 6.5.

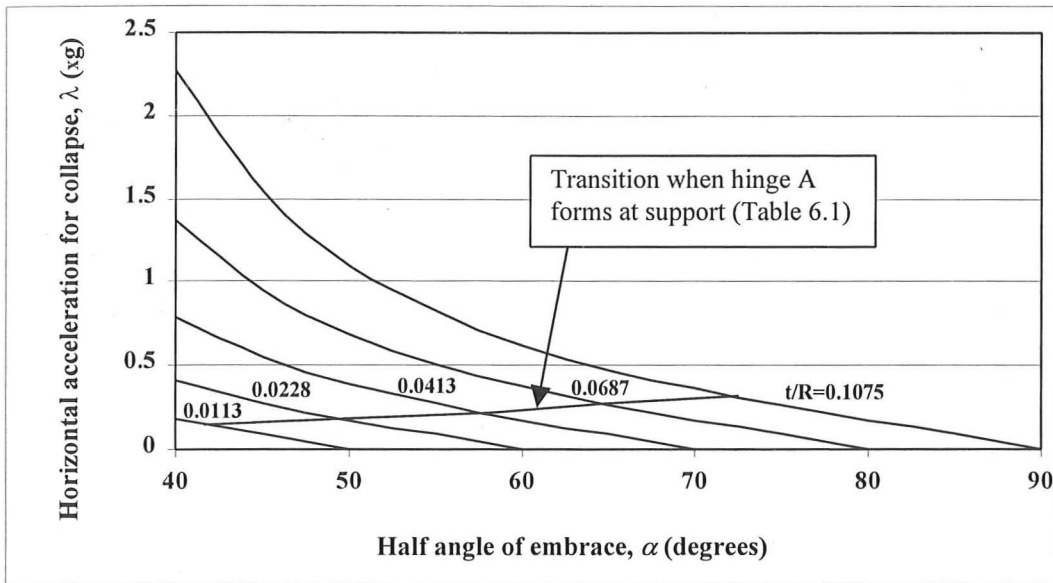


Figure 6.6 Value of horizontal acceleration for collapse of a circular arch. The simple approximation described in this chapter is tangent to each curve for small values of acceleration, as in Figure 6.5.

Typical arch geometries range from $t/R = 0.04$ to 0.10 and $\alpha = 60^\circ$ to 80° . For these cases, the horizontal acceleration for collapse is less than $0.5g$, which is within the range of peak ground accelerations experienced in a strong earthquake. The values presented here are simply a threshold acceleration for the formation of the collapse mechanism. Below this acceleration the arch translates as a rigid body, as will be discussed in Chapter 8 regarding seismic safety. An arch can sustain values of horizontal acceleration greater than λg if the acceleration is applied for a short period of time, but such a situation has not been analysed in the current dissertation.

The key values from Figures 6.5 and 6.6 are presented in Table 6.1.

Thickness ratio	0.011	0.023	0.041	0.069	0.108
α_{max} (degrees)	50°	60°	70°	80°	90°
β_o , initial intrados hinge (degrees) (from Table 3.2)	33.6°	39.5°	45.0°	49.9°	54.5°
Angle of tilt Γ (degrees) when hinge A forms at the support (from eqn. [4.5])	8.0°	10.0°	12.5°	15.0°	17.5°
Horizontal acceleration λ for hinge A at the support	0.14	0.18	0.22	0.27	0.32
Half embrace α (degrees) when hinge A forms at the support	42.0°	50.0°	57.5°	65.0°	72.5°

Table 6.1. Values for the transition between the four-hinge mechanism with a hinge at each support, and the four-hinge mechanism with only one hinge at one support.

6.4 Critical Hinge Locations

For circular arches, the hinge locations of the critical failure mechanisms follow a very clear pattern. For small angles of embrace, at which the arch is very stable, the hinge A always forms at the right abutment. Thus, the angle at which A forms is simply $90-\alpha$. The central hinge B is typically close to A for very stable configurations, but as the angle of embrace increases and the necessary angle of tilt Γ decreases, the hinge B tends toward the centre of the arch (90°). Similarly, as the angle of embrace increases, the angle at which C forms continues to increase. This behaviour is illustrated in Figure 6.7 for a circular arch with a thickness ratio of 0.108, in which the angle of each hinge location is measured from the horizontal line below the right abutment. The plot terminates when α reaches $\alpha_{max}=90^\circ$, the angle of embrace at which the circular arch can no longer stand under vertical loading for the given thickness.

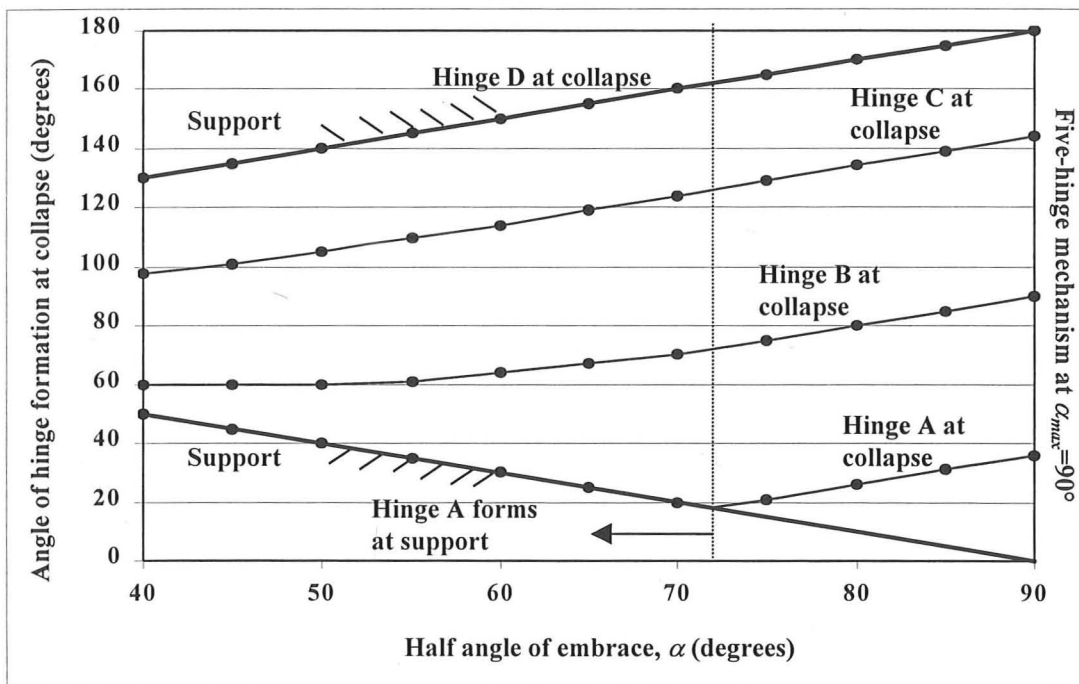


Figure 6.7. Critical hinge locations for collapse of a circular arch with $t/R = 0.108$ under constant horizontal acceleration.

Thus, a circular arch demonstrates two different collapse mechanisms. The first mechanism is a typical four-bar chain, of the type investigated by Oppenheim (1992), in which two of the hinges always form at the abutments. The second mechanism of collapse occurs as the angle of embrace approaches the maximum allowable angle for the given thickness, and the mechanism corresponds to part of a symmetrical five-hinge mechanism for the arch of least thickness. In the case of the five-hinge

mechanism, only four hinges are necessary for failure, and the angle A, formerly at the right support of the arch, moves into the span. The change in the type of governing mechanism is illustrated by the abrupt change in slope in the location of hinge A, as illustrated in Figure 6.7. This occurs when the angle $90-\alpha$ equals the critical angle of tilt Γ . After this point (which occurs at $\alpha=72.5^\circ$ in Figure 6.7), the distance between the hinges A, B, and C remains constant and the same mechanism merely rotates around the circular arch. This continues until the maximum angle of embrace is reached, at which point the mechanism will be symmetrical with B occurring at 90° , and hinges A and C equidistant on either side of B (at an angle of β). For the semicircular arch of minimum thickness, the critical intrados hinges occur 55° from the crown of the arch, so the angle $a=35^\circ$ and $b=145^\circ$ for the case of $\alpha=90^\circ$.

6.5 Thrust at Collapse

As the lateral acceleration is applied to the arch, the force reactions at each support can change significantly. The reactions on the far side of the arch (hinge D) increase, while the reactions on the near side of the arch (hinge A) decrease. For an arch on buttresses, the far side of the arch (hinge D) is most interesting because the lateral accelerations will tend to destabilise the buttress on that side. The support reactions at the collapse state have been computed for varying arch geometries: see Figure 6.8.

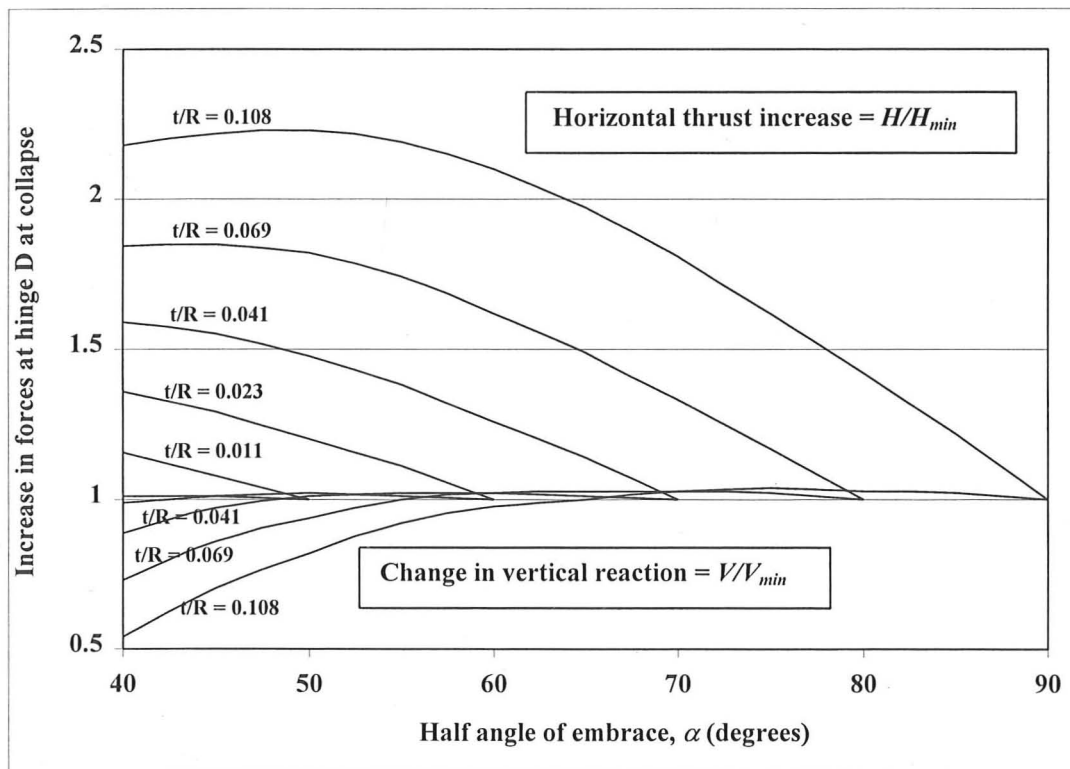


Figure 6.8. Change in support reactions at hinge D at collapse due to constant lateral acceleration.

As the lateral acceleration is applied, the horizontal thrust on the far support increases significantly over the minimum thrust, H_{min} . Interestingly, the vertical reaction at the support remains largely constant for angles of embrace greater than 120 degrees ($\alpha=60^\circ$). For typical arch geometries the vertical reaction remains constant and the horizontal thrust increases in a nearly linear fashion. The increase in horizontal thrust may be significant for some arches supported on buttresses, particularly due to the lowered resistance of the buttress as a result of the lateral acceleration. This will be discussed in the next chapter for the analysis of arches supported on buttresses.

The reactions at the hinge on the near side of the arch (hinge A) are reduced considerably by the lateral acceleration, but remain compressive for all of the cases considered. As long as compression force reactions exist at the hinge, the assumption of failure by a four-hinge mechanism is appropriate. Tensile forces would separate the hinge and invalidate the assumption of failure by a four-hinge mechanism.

6.6 Effect of Voussoir Size

To illustrate the ArchTilt program and to investigate the effect of voussoir size on the stability of arches, an arch subtending a total angle of embrace of 120° ($\alpha=60^\circ$) with a thickness ratio of $t/R=0.10$ is considered. In addition, the same arch is analysed for voussoir sizes of 1° , 5° , and 10° . The results for each different voussoir size are summarised in Table 6.2.

Voussoir size	1°	5°	10°
Collapse hinges (a-b-c)	30° - 64° - 116°	30° - 65° - 110°	30° - 60° - 100°
Lateral acceleration, λ (xg)	0.58	0.59	0.66
Equivalent angle of tilt, Γ	30.1°	30.7°	33.5°
Thrust increase at hinge D (H/H_{min})	2.01	2.03	2.11

Table 6.2. Collapse state for an arch subtending 120° with $t/R=0.10$ for varying voussoir sizes.

Constructing an arch with larger voussoirs limits the possible hinge locations and generally increases the capacity of the arch for horizontal acceleration. In theory, a 10-degree voussoir arch can sustain 10% higher lateral accelerations than an arch with small voussoirs. All of the results presented in this chapter are based on arches of 1-degree voussoirs, which allow the hinges to form in the critical locations. Based on the comparison between various voussoir sizes, this is a conservative approach.

6.7 Summary

This chapter has identified the governing collapse mechanisms and illustrated the effect of varying the arch geometry on the resistance to lateral acceleration. The study of circular arches with constant thickness has established the patterns of behaviour for arches under constant horizontal acceleration, and the general approach can be extended to arches of varying shapes and varying thickness. The following conclusions can be drawn:

- 1) Under increasing horizontal acceleration, a masonry arch will undergo rigid-body motion until a threshold value of acceleration, λg , is reached, which is sufficient to form a four-hinge mechanism.
- 2) This approach verifies the minimum-thickness analysis of the previous chapter. The arch of minimum thickness will collapse for zero horizontal acceleration, or $\lambda=0$.
- 3) The critical value of λg increases with an increase in thickness or a decrease in the angle of embrace.
- 4) For a relatively stable arch with a large thickness ratio and a small angle of embrace, two of the four hinges will form at the arch abutments, and the other two hinges will form within the span of the arch.
- 5) As arches become less stable (smaller thickness ratios or greater angles of embrace), the failure mechanism will become more symmetrical and three of the hinges will form in the span of the arch.
- 6) For typical arch proportions, the relationship between angle subtended and critical angle of tilt, Γ , is linear. This provides a conservative method for estimating the horizontal acceleration to cause collapse for a given arch.
- 7) Under horizontal acceleration, the equivalent static thrust of the arch may increase by a factor of about two before the collapse mechanism is reached.
- 8) Larger voussoir sizes will increase the resistance of the arch to lateral accelerations compared with arches of small voussoirs.

PART IV: THE BUTTRESSED ARCH

Chapter 7 Collapse of Buttressed Arches

7.1 Introduction

This chapter combines the results from preceding chapters to investigate the collapse state of arches supported on buttresses. Three general loading situations can lead to the collapse of buttressed arches: applied loads, applied support displacements, and applied ground accelerations. The present chapter investigates the collapse of buttressed arches due to applied displacements and applied lateral acceleration. The goal of this study is to determine the general patterns of behaviour and the likely failure modes for buttressed arches.

7.1.1 Applied loading

Using principles of limit analysis, it is straightforward to determine the collapse state of a rigid-block structure due to an applied load. The hinge locations are postulated, and a work calculation is performed to determine the maximum applied load, P . The critical collapse mechanism will occur for the lowest value of applied load which forms a kinematically admissible mechanism (Heyman 1969; Livesley 1978). For an arch on masonry buttresses, the analyst must consider collapse mechanisms involving a combined arch-buttress mechanism, including the possibility of a fracture surface in the buttress, as in Figure 7.1.

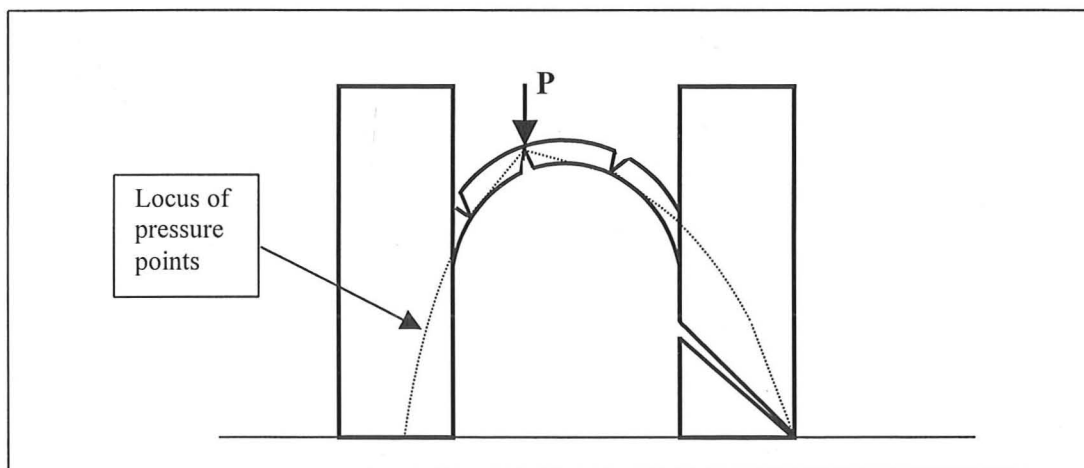


Figure 7.1 Collapse of a buttressed arch due to a point load and the self-weight of the masonry

If the buttress were so massive as to provide effectively rigid abutments to the arch, collapse of the arch could be considered in isolation. But in other cases, a combined

Chapter 7 Collapse of Buttressed Arches

7.1 Introduction

This chapter combines the results from preceding chapters to investigate the collapse state of arches supported on buttresses. Three general loading situations can lead to the collapse of buttressed arches: applied loads, applied support displacements, and applied ground accelerations. The present chapter investigates the collapse of buttressed arches due to applied displacements and applied lateral acceleration. The goal of this study is to determine the general patterns of behaviour and the likely failure modes for buttressed arches.

7.1.1 Applied loading

Using principles of limit analysis, it is straightforward to determine the collapse state of a rigid-block structure due to an applied load. The hinge locations are postulated, and a work calculation is performed to determine the maximum applied load, P . The critical collapse mechanism will occur for the lowest value of applied load which forms a kinematically admissible mechanism (Heyman 1969; Livesley 1978). For an arch on masonry buttresses, the analyst must consider collapse mechanisms involving a combined arch-buttress mechanism, including the possibility of a fracture surface in the buttress, as in Figure 7.1.

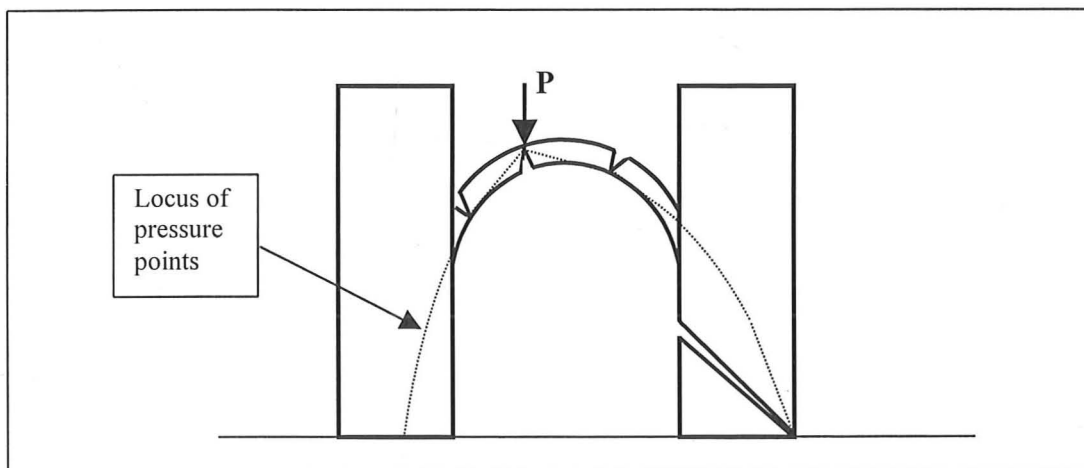


Figure 7.1 Collapse of a buttressed arch due to a point load and the self-weight of the masonry

If the buttress were so massive as to provide effectively rigid abutments to the arch, collapse of the arch could be considered in isolation. But in other cases, a combined

"arch-buttress" mode may lead to lower values of the collapse load than for the arch alone. For masonry buildings, a concentrated load on top of the vault is unlikely, though Heyman (1993) has demonstrated that this can occur in the event of a heavy roof collapsing onto the arch or vault below. This dissertation does not investigate the influence of applied loads, since previous researchers have investigated this topic in detail. For buttressed arches, it is sufficient to state that engineers must consider mechanisms involving the failure of the buttress by the formation of a fracture surface, as discussed in Chapters 3 and 4 and as illustrated in Figure 7.1.

7.1.2 Applied displacements

Applied displacements are a significant threat to the safety of buttressed arches. Various kinds of displacement may de-stabilise the structure, and this chapter will focus on the most common pathology: outward leaning of the buttresses. As the buttresses lean, the change in geometry alters the equilibrium conditions. The thrust capacity of the buttress decreases and the thrust of the arch increases due to the displacements. The current chapter considers the collapse state of the buttressed arch system by combining the results of Chapters 3, 4, and 5. The goal is to demonstrate the conditions for the failure of the system as a result of leaning buttresses and determine in a given case which component is more likely to fail first: the buttress or the arch.

7.1.3 Applied accelerations

Seismic loading can cause the collapse of buttressed arch systems as a result of ground accelerations (Croci 1998; Spence and D'Ayala 1999). The current chapter presents a simple method for determining the minimum constant lateral acceleration to form a collapse mechanism. This is a preliminary step in understanding the response of a rigid-block structure to earthquake loading. Chapter 6 developed this approach for the circular arch, and this chapter extends the analysis to circular arches supported on buttresses. The goal is to provide a general methodology for assessing the stability of buttressed arch systems, based on the calculation of the minimum horizontal acceleration to form a collapse mechanism. This is not an exact or full method for analysing the seismic response of buildings, rather it is a method for determining the influence of geometry on the resistance to horizontal acceleration.

7.2 Geometry of Buttressed Arches

Traditional masonry structures are built in a wide variety of forms, with different buttressing systems and endless variations in vaulting geometry. This dissertation adopts the simplest possible form: circular arches supported on rectangular buttresses. This system is typical of barrel vaults supported on rectangular masonry walls, or of individual masonry arches supported on individual buttresses. The chosen geometry of circular arches and rectangular buttresses is applied only to illustrate the general patterns of behaviour and the likely causes of collapse. In practice, each individual structure is unique and the analyst should apply the general methods to the specific structure being considered.

The current chapter investigates two particular extreme configurations for buttressed arches (Figure 7.2). In each case, the width, b , of the buttress at its base is regarded as the unit of length.

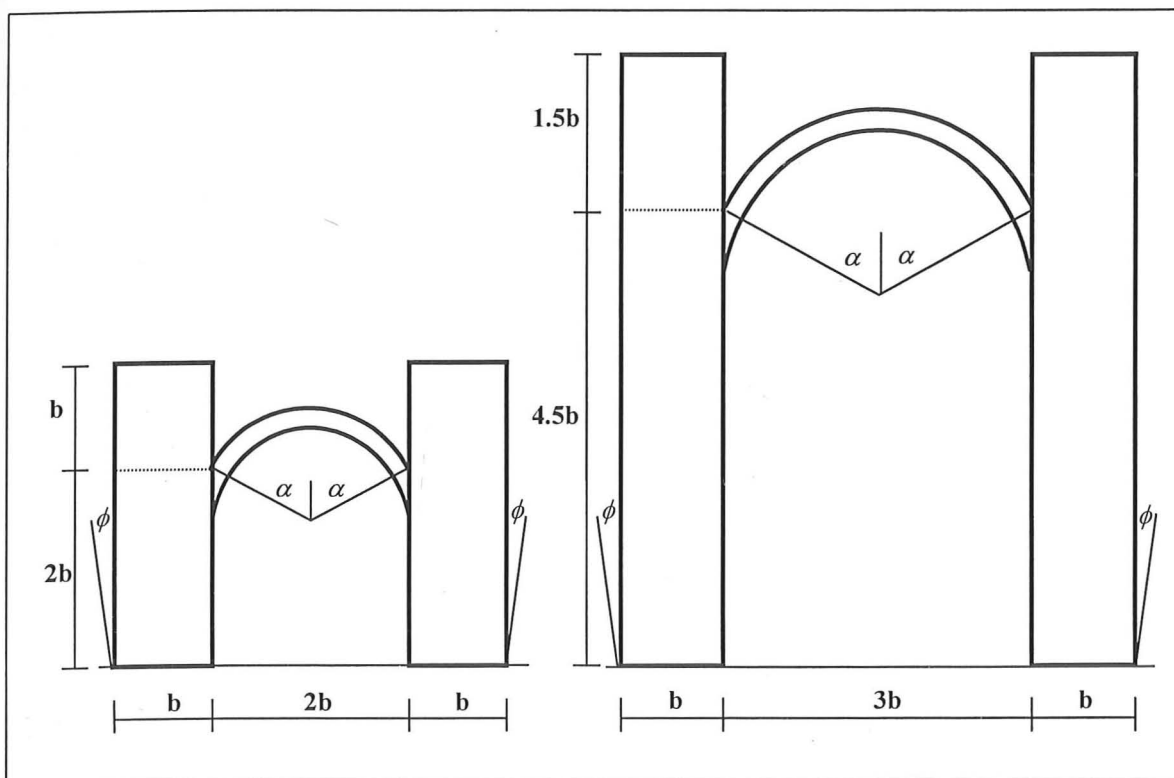


Figure 7.2: a) Buttressed arch Case A

b) Buttressed arch Case B

Case A is a highly conservative configuration, with the buttress width equal to half the span, and the height of the arch support equal to the span. Furthermore the buttresses are very conservative with a height to width ratio of three. Case B is more daring, and is

approximately the same as the proportions of the high transverse arches and slender buttresses of the Sainte-Chapelle in Paris (Heyman 1996). The span of the arch is three times the width of each buttress, and the height of the arch is 1.5 times the span of the arch. In addition, the buttresses of Case B are much more slender than Case A, with a height to width ratio of six. For both cases, the half angle of embrace, α , and the thickness ratio, t/R , are variable as in Chapters 5 and 6. Thus, the buttress systems of Case A and Case B can be investigated for a wide variety of arch geometries. Each case will be analysed for collapse due to outward leaning of the buttresses as well as applied horizontal acceleration in the following sections.

7.3 Arch on Leaning Buttresses

Many buttressed arches and vaults have collapsed throughout history, for example the partial collapse of the dome of the Hagia Sophia and the partial collapse of vaulting bays in many Gothic cathedrals. In most cases, the arch or vault collapses and the buttresses remain standing. The current section analyses the collapse on account of the lean of buttresses, and seeks to explain the collapse of vaulting and the apparent resilience of buttresses.

As the buttresses lean, the span of the arch increases. Chapter 4 demonstrated that the capacity of buttresses for horizontal thrust decreases linearly with the rotation ϕ as the buttress leans. The arch will deform to accommodate the span increase, and the change in geometry will lead to increased values of horizontal thrust, as discussed in Chapter 5. In the case of buttressed arches, the progressive increase in the rotation of the buttresses will lead to increasingly unfavourable conditions until the arch collapses. To assess the safety of a buttressed arch, the engineer must determine if the arch will collapse first, or if the capacity of the buttress will be exceeded by the increased thrust of the arch. This section proposes a method for analysing the problem.

For arches with small thickness/radius ratios, Chapter 5 demonstrated that collapse will occur for small values of span increase. For larger thickness ratios, the arch can resist greater span increases and will provide greater increases in horizontal thrust before collapsing. As the thickness/radius ratios increase further, eventually the arch thrust is

sufficient to cause the buttress to fail, and the failure of the buttress will lead to collapse of the arch. The program ArchLean, written in Matlab and included in Appendix A, analyses the problem for a prescribed geometry of the arch-buttress combination by increasing the lean of the buttress until the arch collapses. The program is illustrated here with reference to the buttress configurations of Cases A and B (Figure 7.2) For an angle of embrace of 120° ($\alpha=60^\circ$), the collapse state is determined for varying values of the thickness ratio, t/R . The results are presented in Figures 7.3 and 7.4 for thickness ratios ranging from 0.05 to 0.20.

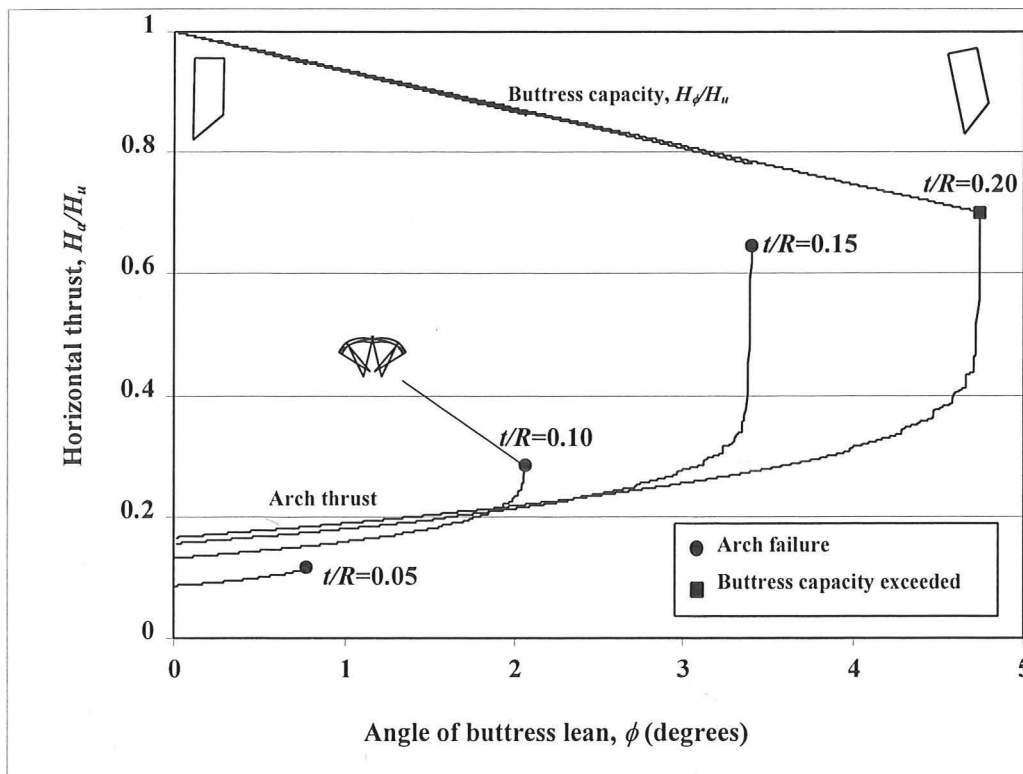


Figure 7.3 Collapse state for buttressed arch Case A due to leaning buttresses ($\alpha=60^\circ$). The problem is analysed using the program ArchLean, for an arch constructed of 1° voussoirs in each case.

The change in horizontal thrust is plotted in Figures 7.3 and 7.4, normalised by the maximum thrust capacity of the vertical buttress, H_u . The horizontal axis is the angle of inclination of the buttress in degrees. Sketches indicate the left-hand buttress configuration at $\phi = 0^\circ$ and $\phi = 5^\circ$, respectively. The arch of thickness ratio 0.10 is illustrated at the point of collapse due to excessive span increase.

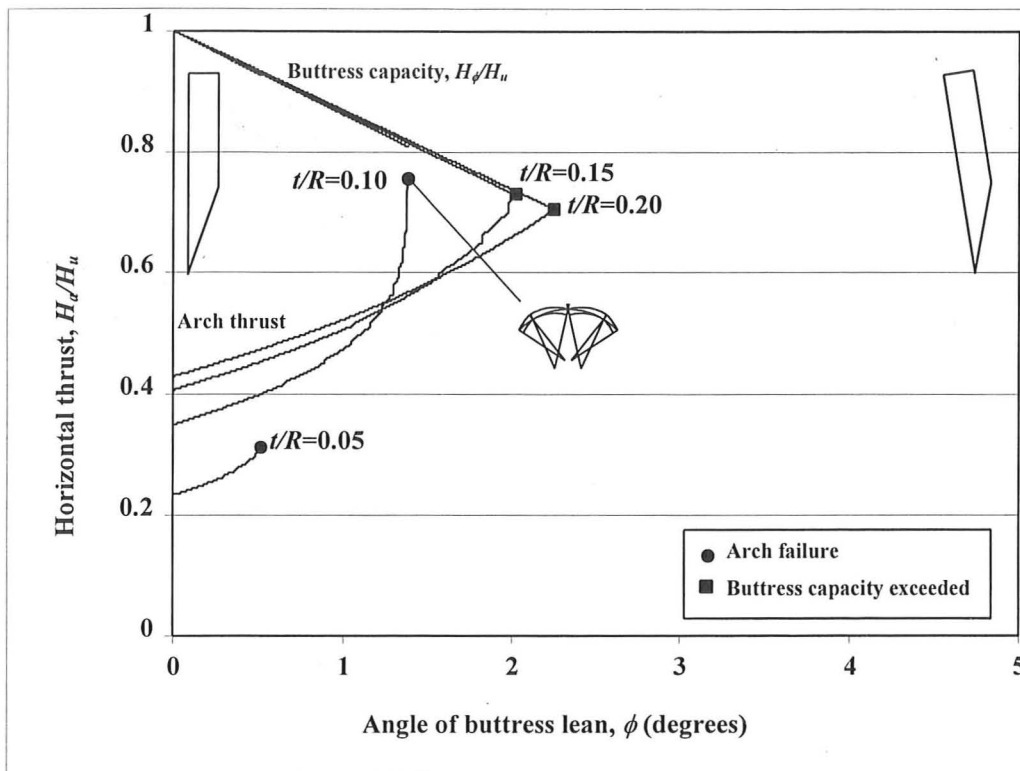


Figure 7.4 Collapse state for buttressed arch Case B due to leaning buttresses ($\alpha=60^\circ$). The problem is analysed using the program ArchLean, for an arch constructed of 1° voussoirs in each case.

For a given geometry, the program ArchLean calculates the resistance of the vertical buttress to horizontal loads based on the methods presented in Chapter 3. The buttress lean, ϕ , is slowly increased, thereby decreasing the resistance of the buttress and increasing the span of the arch. The new geometry increases the thrust of the arch, which is computed with the algorithm presented in Chapter 5. In all cases the arches have been analysed for 1° voussoirs, so that the intrados hinge can move freely as the span increased (as in Figure 5.16).

The program terminates when one of the two collapse scenarios occurs: either the "strong-buttress" or the "weak-buttress" collapse mode. Each failure mode is defined as:

- 1) Strong-buttress: Failure occurs when the arch reaches the maximum span increase for the given geometry, and the arch collapses, leaving the buttresses intact (illustrated as \bullet on Figures 7.3 and 7.4). In this case, the buttresses are "strong" enough to resist the increased thrust of the arch, but the arch collapses due to the span increase. All five hinges of the symmetrical collapse mechanism occur in the arch. This failure mode occurs for smaller thickness ratios in general.

- 2) Weak-buttress: Failure occurs when the buttress capacity for horizontal thrust is exceeded, the buttress rotates additionally, and the arch collapses (illustrated as ■ on Figures 7.3 and 7.4). In this case the buttresses are too "weak" to resist the increased thrust of the arch, and collapse occurs when the buttress gives way. At this point, the arch will collapse, relieving the horizontal thrust on the buttress, and the buttress will remain standing. The symmetrical collapse mechanism has three hinges in the arch and one hinge at the outer edge of each buttress.

These two failure modes will be used to describe the collapse of buttressed arch systems due to outward leaning of the buttresses.

For Case A, the capacity of the vertical buttress is more than five times the initial minimum thrust of the arch: see Figure 7.3. As the buttresses lean, the arch will collapse before the thrust capacity of the buttress is exceeded for most thickness values, i.e. in a "strong-buttress" failure mode. But at very high thickness ratios, such as $t/R = 0.20$, the capacity of the buttress may be exceeded. In this case the buttress is unable to resist the thrust of the arch, and the buttress fails according to the theory presented in Chapters 3 and 4. When the arch thrust exceeds the buttress capacity, a five-hinge mechanism forms in theory, with one hinge at the base of each buttress and three hinges in the central arch. In practice, only four hinges are required for collapse, and any asymmetry will cause one buttress to give way first. The buttress will begin to rotate outwards freely, and the arch will collapse. As a result, the horizontal thrust acting on the buttress becomes zero, and the buttress remains standing. Thus, for high thickness ratios, failure will occur by a "weak-buttress" mode. The geometry of the buttressed arch of Case A is highly conservative (as evidenced by the much higher capacity of the buttress in comparison to the thrust of the arch), so the system is able to withstand considerable angles of tilt without collapse. The conservative design of the buttresses means that in most cases failure will occur in the arch before the capacity of the buttress is reached.

For Case B, the capacity of the buttress is approximately three times the initial minimum thrust of the arch: see Figure 7.4. The springing of the arch is more than twice as high as the springing in Case A, and small angles of tilt will lead to larger increases in the span length for the arch. In addition, the buttresses are more slender and the higher centre of gravity will lead to greater reductions in the capacity as the buttress leans (since the capacity of the buttress decreases as the vertical centroid shifts

horizontally). This is reflected in the greater negative slope (by a factor of about 2) of the buttress resistance for Case B compared to Case A. The relative slenderness of Case B is apparent, and the arch will collapse at less than 2° of buttress leaning for most thickness ratios. For thickness ratios above 0.10, the buttress capacity will be exceeded and the arch will collapse when the leaning buttresses give way, i.e. "weak-buttress" failure will occur. Thus, in Case B, weak-buttress failure is more likely due to the more daring design of the buttressing system.

From these two examples, the behaviour of the structural system is clear. For most arch thickness ratios, "strong-buttress" failure will occur and the arch will collapse before the buttress. But for large thickness ratios, the thrust of the grossly-deformed arch may exceed the capacity of the leaning buttress, in which case the buttress will give way and the arch will collapse in a "weak-buttress" failure. In all cases, the buttress will remain standing after the collapse of the arch, due to the absence of the thrust from the arch. Thus, deformation of the buttress by leaning will lead to the collapse of the arch, but the removal of the thrust from the arch ensures that the buttress survives. For the buttress to overturn in static conditions, the centroid of the buttress must approach the horizontal coordinate of the hinge about which overturning will occur. This is not possible because the arch will collapse well before the buttress resistance approaches zero horizontal thrust. (This is the maximum amount of leaning a buttress can withstand, defined as ϕ_{max} in Chapter 4, equation [4.11].)

In order to investigate the influence of the angle of embrace of the arch on the behaviour of the system, additional values of α have been considered. Cases A and B have been analysed for angles of embrace 2α of 120° and 160° ($\alpha=60^\circ$ and 80° , respectively), with the thickness ratio varying from the minimum thickness (as determined in Chapter 5) up to a very large value of $t/R=0.20$. The results have been summarised in Figure 7.5, which illustrates that greater angles of embrace will lead to collapse for smaller values of buttress leaning. (This follows from the results of Chapter 5 illustrated in Figure 5.14.) In each of the two specific buttress systems A and B it is possible to determine the threshold thickness beyond which the buttress capacity will be exceeded. For Case A it is $t/R=0.156$, and for Case B it is $t/R=0.104$ for $\alpha=60^\circ$, as indicated on Figure 7.5.

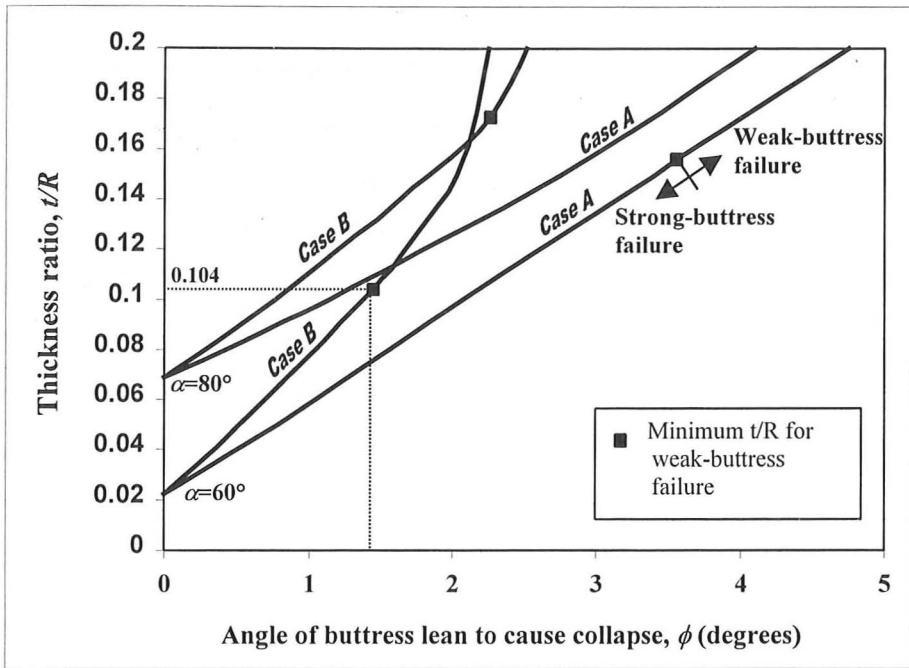


Figure 7.5 Comparison of collapse states due to leaning buttresses for Case A and B.

This threshold thickness is presented for a range of angles of embrace in Figure 7.6, marking the limit between the two failure modes depending on the geometry of the arch.

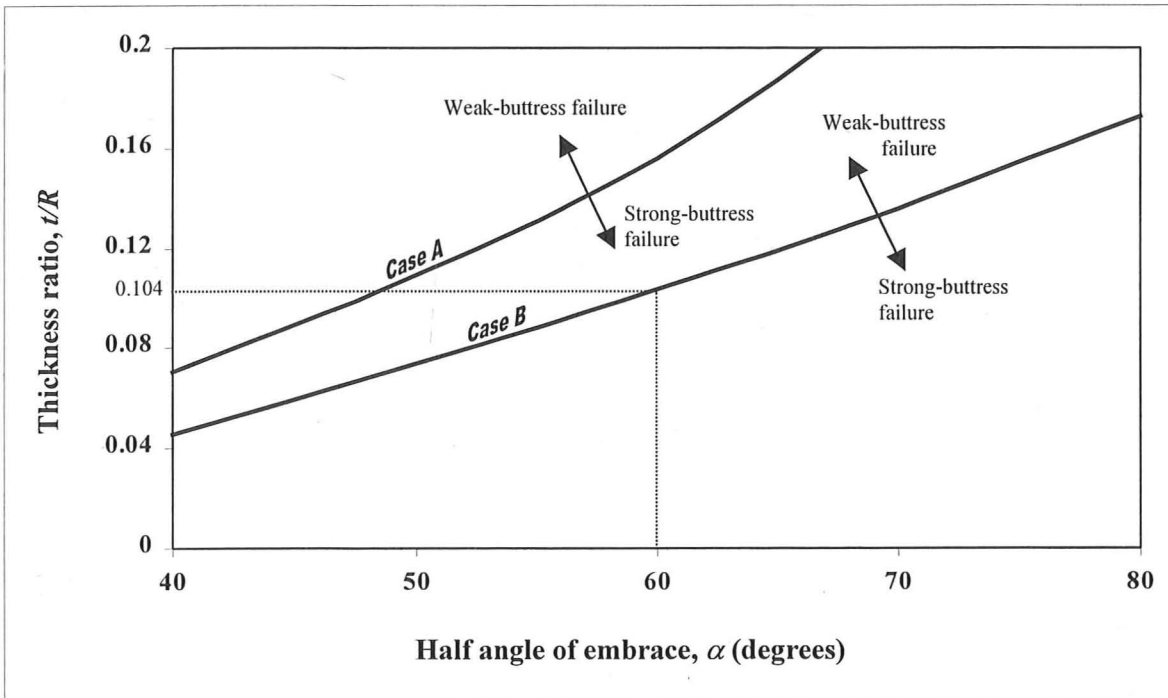


Figure 7.6 Minimum thickness for the thrust of the deformed arch to exceed the capacity of the leaning buttress, i.e. threshold thickness between "weak-buttress" and "strong-buttress" failure. For example, an arch subtending 120° ($\alpha=60^\circ$) will fail by weak-buttress collapse when the thickness ratio is greater than $t/R=0.104$.

The experimental results in Chapter 5 demonstrated that an arch on spreading supports will actually collapse for slightly smaller span increases than those predicted by analysis. For the current problem this suggests that collapse will occur at slightly lower values of lean than predicted, because the grossly-deformed arch will exist in a precarious state. Any small movement would lead to the collapse of the arch. In actual structures any shift in the buttress due to the formation of the fracture or a sudden increase in leaning could lead to the collapse of the arch at lower values of lean than predicted. Methods for assessing the safety of buttressed arches will be discussed in detail in the next chapter.

In summary, for collapse due to leaning buttresses the arch may collapse before the buttress capacity is reached, in a mode defined here as strong-buttress failure. Alternatively, failure may occur by a "weak-buttress" mode, in which the horizontal thrust capacity of the buttress is exceeded. For relatively tall buttresses, such as those presented in Case B, collapse of the arch may occur for a small amount of leaning, even less than 1° , for typical arch geometries. In both cases, the arch will collapse and the buttress will remain standing, since the arch will no longer exert a horizontal overturning force. The following section analyses the same buttressed arch structures under combined acceleration due to gravity and constant lateral acceleration.

7.4 Collapse Due to Horizontal Acceleration

Seismic loading presents a significant threat to many buttressed arches. Engineers have not determined the general conditions for the collapse of such structures and this section is a first attempt to do so. The previous chapter investigated the critical hinge locations and the collapse conditions for circular arches under constant horizontal acceleration. This section extends the same approach to circular arches on rectangular buttresses. The application of a constant horizontal acceleration, λg , is statically equivalent to tilting the entire structure on an inclined plane at angle Γ , as explained in Chapter 6.

Two possible collapse mechanisms are illustrated in Figure 7.7 for a buttressed arch acting under its own weight at the minimum value of constant horizontal acceleration for collapse, λg . For buttressed arches, horizontal acceleration can cause collapse by a

combined arch-buttress mechanism (A-B-C-D), with a hinge at the outer edge of the buttress. This is similar to the situation described in Chapter 6 for circular arches, except that the extrados hinge D now occurs at the base of the buttress instead of at the arch support (as in Figure 6.2) for the arch with a rigid abutment.

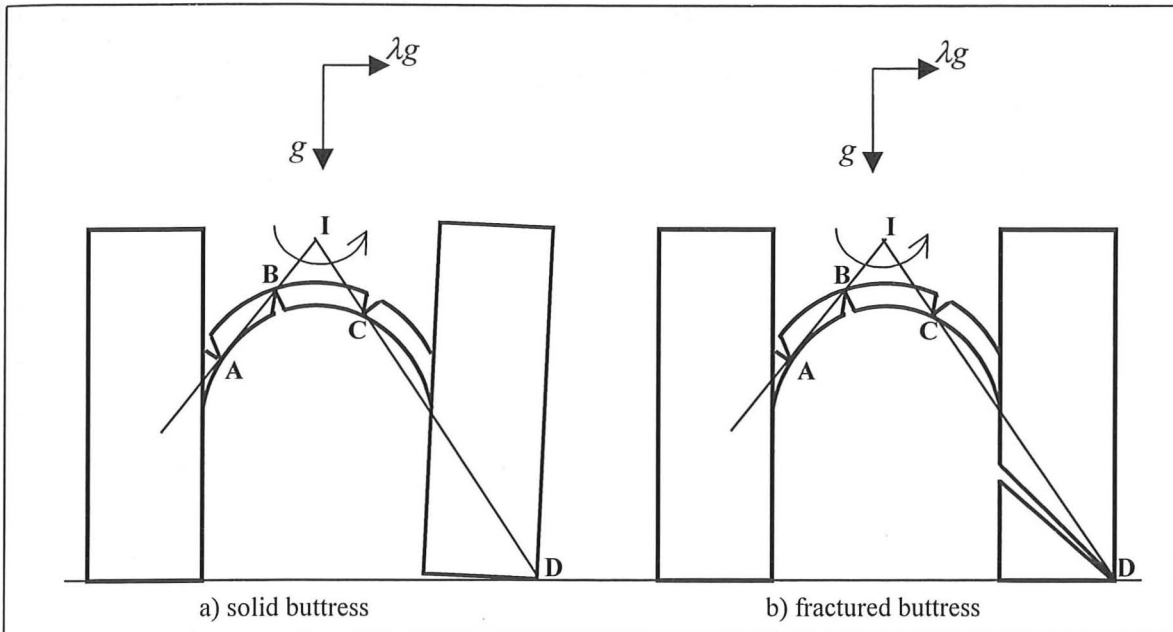


Figure 7.7 Collapse mechanisms for buttressed arches under horizontal acceleration. The instantaneous centre, I, of the central portion can be used to calculate the relative rotation of each segment.

The mechanism of Figure 7.7(a) assumes the buttress remains solid at the collapse state. This assumption may be unsafe, since the buttress is likely to fracture at the overturning limit, as in Figure 7.7(b). The previous chapter demonstrated that the horizontal thrust of the arch will increase due to the lateral acceleration while the vertical reactions will remain relatively constant. In addition, Chapter 4 demonstrated that the fracture location does not move substantially due to small values of leaning, and the same assumption can be extended to small values of horizontal acceleration here. (This is a reasonable assumption for angles of "tilt" -- or applied acceleration Γ -- up to 20° , which corresponds to a horizontal acceleration of $0.36g$.) Therefore it is valid to determine the fracture location for the vertical buttress due to the maximum horizontal thrust, and assume that the same fracture will form due to horizontal acceleration. Of course this is an approximate method for estimating the location of the fracture, but it provides an approach to understanding a possible collapse state for buttressed arches under constant lateral acceleration. For the current analysis the buttresses are assumed to be vertical, rather than leaning, and the system is analysed in an undeformed configuration.

The Matlab programs SolidTilt and ButtressTilt were written to analyse the buttressed arches of Figure 7.7(a) and (b) respectively. (The full code is presented in Appendix A for both programs.) As with the program ArchTilt used in the previous chapter, the algorithm searches for the critical hinge locations to give the minimum value of horizontal acceleration at collapse, λg . In each case, the hinge D is assumed to act at the base of the outer buttress and the program determines the critical location of the arch hinges A, B, and C and computes the corresponding value of λ for collapse.

The programs have been used to analyse the buttressed arch systems of Cases A and B. Each case has been analysed for an arch embracing 120° (i.e. $\alpha=60^\circ$) with varying thickness ratios. The results are presented in Figures 7.8 and 7.9 considering the buttress as a solid and as fractured, respectively. For small values of thickness ratio, with t/R slightly greater than $(t/R)_{min}$, the arch will collapse by a four-hinge mechanism contained entirely within the arch and not involving the buttress. As the thickness ratio increases, the maximum horizontal acceleration is limited by the combined arch-buttress failure mechanism of Figure 7.7. The heavier lines indicate the critical mechanism for collapse of the buttressed arch system, and the dashed lines illustrate the collapse limit for the arch and the buttress independently.

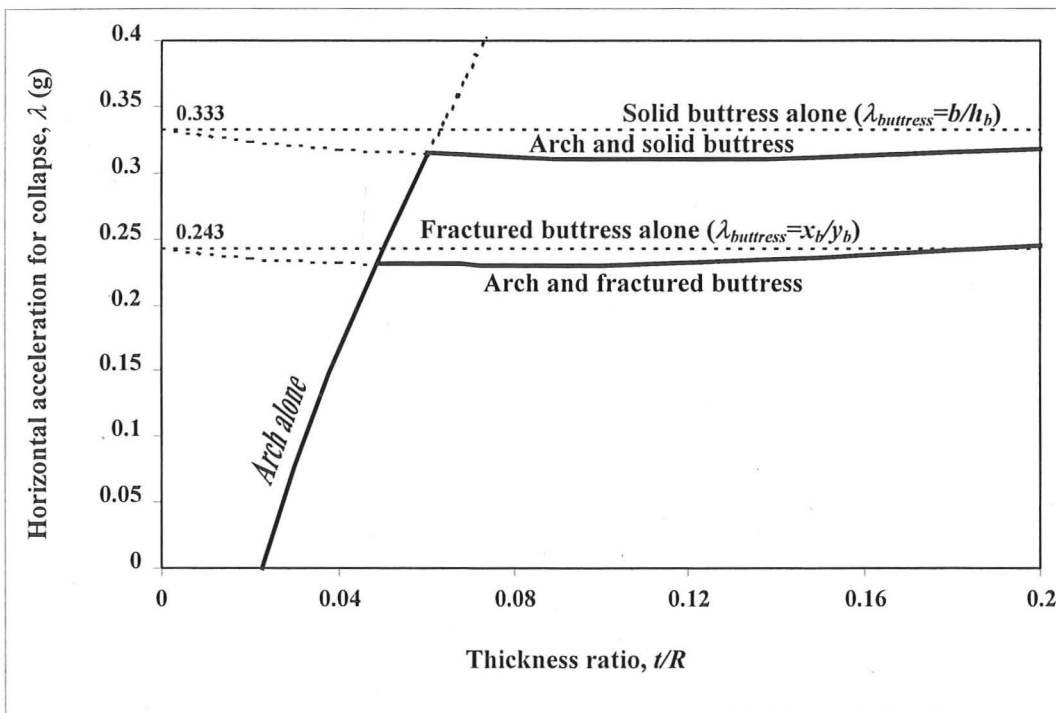


Figure 7.8. Collapse of buttressed arch Case A due to horizontal acceleration ($\alpha=60^\circ$).

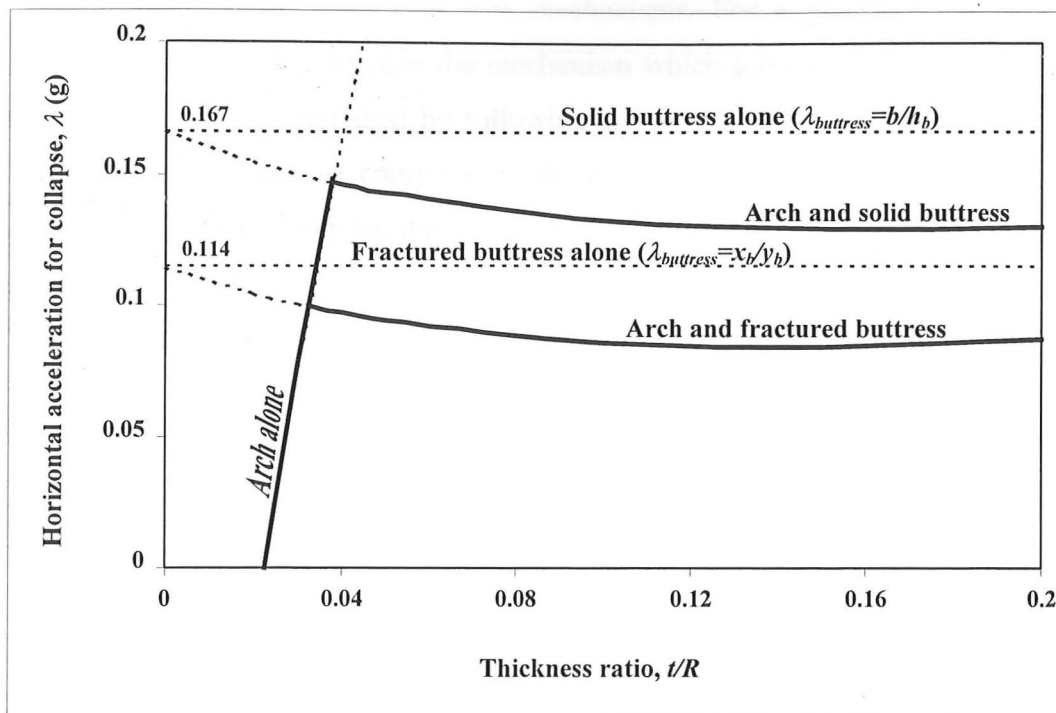


Figure 7.9. Collapse of buttressed arch Case B due to horizontal acceleration ($\alpha=60^\circ$)

Figures 7.8 and 7.9 illustrate the significance of the buttress for the seismic resistance of buttressed arches. For small arch thickness ratios, the arch will collapse independently of the buttress, as in the strong-buttress failure mode for arches on leaning buttresses in the previous section. However, as the thickness ratio increases, the governing failure mechanism will involve the buttress and the buttressed arch collapse mechanism will form at much lower values of horizontal acceleration than would be the case for the arch alone, i.e. an arch supported on rigid abutments. This is similar to the "weak-buttress" scenario in the previous section. Interestingly, higher thickness ratios for the arch lead to lower values of horizontal acceleration to form the combined arch-buttress mechanism. This reflects the influence of the mass of the arch, which can reduce the stability of the structure under horizontal acceleration. In addition, the influence of the buttress fracture has a significant effect on the resistance of the buttressed arch. For both cases, the mechanism involving the fractured buttress will occur for a horizontal acceleration approximately 30% lower than the mechanism with the solid buttress. Finally, it is important to note that the conservative geometry of Case A requires more than twice the value of horizontal acceleration than Case B to form the collapse mechanism for most thickness ratios.

Based on this analysis, a simple method can be developed for assessing the value of the acceleration for onset of buttressed arch mechanisms. For a given buttressed arch system, the analyst must determine the mechanism which governs the collapse of the arch alone. (This is accomplished by following the methods presented in Chapter 6.) This mechanism can then be compared to the combined arch-buttress mechanism of Figure 7.7(a). The mechanism for the fractured buttress results in a lower estimate of the onset acceleration for collapse than the solid buttress, and is a safer approximation. The minimum horizontal acceleration for the buttressed arch can be approximated by the minimum horizontal acceleration for the fractured buttress alone. In this case, the minimum acceleration is:

$$\lambda_{\text{buttress}} = \frac{x_b}{y_b} \quad [7.1]$$

where x_b and y_b are the horizontal and vertical coordinates of the centres of gravity for the effective mass of the buttress (measured from an origin at the outer edge about which overturning occurs). For a rectangular solid buttress, this value is simply the width of the base divided by the height, or b/h_b . For more complex buttress shapes and to consider the influence of the buttress fracture, the centres of gravity must be calculated. For the fractured buttresses of Case A and Case B, the minimum horizontal accelerations, $\lambda_{\text{buttress}}$, are 0.243g and 0.114g. (These should be compared to the values for the solid buttresses of 0.333g and 0.167g in Figures 7.8 and 7.9.)

As in the previous section, the formation of this mechanism will cause the arch to collapse first, as section ABC collapses in what is essentially a snap-through failure. In most cases, the buttress would then recover without collapsing. To determine the conditions for collapse under actual ground accelerations, it is necessary to carry out a detailed study of the dynamics of motion and the potential energy of the system. As discussed in the previous chapter, the value of horizontal acceleration λ is a minimum threshold which must be surpassed in order for the mechanism to form. This will be discussed in further detail in the following chapter, on methods for appraising the safety of existing buttressed arch structures.

7.5 Discussion

This chapter has investigated the collapse state for buttressed arches. The particular case of a circular arch supported on rectangular buttresses can be used to gain a wider understanding of the collapse state for buttressed arches of more general geometry. In addition to the conventional collapse analysis due to an applied load, engineers should consider two significant threats to the stability of this structural system: the outward leaning of the buttresses and the influence of horizontal ground acceleration.

The resistance of buttressed arch structures to horizontal ground acceleration, as analysed above, has been restricted to cases where the buttresses are vertical; but the analysis can be extended to the case of leaning buttresses. The main conclusion to be drawn from Figures 7.8 and 7.9 is that the minimum horizontal acceleration for collapse is largely determined by the geometry of the buttress system. Buttress leaning will shift the horizontal centroid of the buttress closer to the point of overturning, thereby reducing the minimum value of acceleration, $\lambda_{buttress}$, and causing the collapse mechanism to form at a lower value of ground acceleration. Hence, the leaning buttress will be more likely to collapse in a seismic event.

This chapter has presented two particular extreme cases in the geometry of buttressed arches: the highly conservative Case A and the more daring Case B. These cases provide boundaries on the usual geometry for circular arches supported on rectangular buttresses. The next chapter will analyse a case study of an existing circular barrel vault supported on masonry walls, which provides a specific example of the somewhat idealised general cases presented in this chapter. Even for the extreme cases of Case A and Case B, the structural behaviour of both systems is essentially the same. For small values of arch thickness the arch will fail first, in a failure mode termed "strong-buttress" failure. For larger values of arch thickness the buttress capacity may be exceeded by the thrust of the arch, causing a failure described as the "weak-buttress" collapse. Both types of collapse are possible, and which will occur depends on the geometry of the system.

Most importantly, this section has demonstrated that engineers should make a careful study of the collapse conditions for the arch or vault alone, as well as for the buttress alone. These studies can be taken together to elucidate the collapse conditions for the

combined buttress-arch system. In most cases, the arch is likely to collapse regardless of the buttress capacity, and the buttress will not be ruined by the collapse of the arch. The historical evidence of many collapsed vaults, which have left the buttresses intact, supports this conclusion. In these cases, new vaults have often been reconstructed on the original buttresses, suggesting that the buttresses typically remain intact. This would suggest that failure is often due to the "strong-buttress" mode of collapse.

For the specific case of seismic loading, it is necessary to consider a collapse mechanism involving the combined arch and buttress. However, the mechanism for the collapse of the buttress alone, in isolation, is a close approximation to the minimum horizontal acceleration required for collapse of the buttressed arch as a combined mechanism. Thus it is useful to consider the buttress and arch individually, as in the problem of leaning buttresses. In all cases considered here, the minimum horizontal acceleration to form a mechanism is less than 0.5g, which is a typical value of peak ground accelerations in seismic events. For example, Spence and D'Ayala (1999) have reported peak ground accelerations of up to 0.55g for the Umbria-Marche earthquake of 1997, which caused the collapse of significant masonry structures in Italy including several bays of vaulting in the Basilica of St. Francis in Assisi. Therefore, the collapse mechanism described in this chapter for buttressed arches may form in a moderate earthquake and engineers should be concerned about the safety of such structures.

7.6 Summary

This chapter has examined the collapse state of an arch supported on buttresses, and several conclusions may be drawn. In the case of leaning buttresses:

- 1) Engineers should consider the possible collapse state of buttressed arches due to outward inclination of the buttresses.
- 2) For a range of geometrical configurations, the arch may collapse before the buttress capacity is reached, in a mode defined here as strong-buttress failure. For strong-buttress failure, collapse will occur in a symmetrical five-hinge mechanism, with the central three hinges in the arch, and the two outer hinges at the arch support. As with the arch on spreading supports, the actual collapse mode is likely to be a four-hinge mechanism, due to any small asymmetry in the construction, rather than a symmetrical five-hinge mechanism.

- 3) Alternatively, failure may occur by a "weak-buttress" mode, in which the horizontal thrust capacity of the buttress is exceeded. In this case, the two outer hinges occur at the critical failure location at the outer edge of the buttresses. Again, only four hinges are required for collapse, so the failure of one buttress is sufficient to cause the arch to collapse.
- 4) For relatively tall buttresses, such as those presented in Case B, collapse of the arch may occur for a small amount of leaning, even less than 1° , for typical arch geometries.
- 5) In the case that the buttress capacity is exceeded, the arch will collapse and the buttress will remain standing, since the arch will no longer exert a horizontal overturning force. Thus, even in the case of "weak-buttress" failure, the buttress will not collapse.

For the buttressed arch under constant horizontal acceleration:

- 1) Engineers should consider the possible collapse state due to horizontal acceleration, which presents a significant threat for buttressed arches. Even in geographic regions of low seismic activity, this analysis is meaningful because it provides a measure of the stability of a buttressed arch.
- 2) The critical collapse mechanism is the mechanism that forms for the lowest value of constant horizontal acceleration.
- 3) For arches with small thickness ratios, the critical collapse mechanism will occur entirely within the arch. In this case, collapse will be governed by a four-hinge mechanism as determined in Chapter 6 for circular arches and the arch can be assumed to be supported on rigid abutments. (This is similar to the "strong-buttress" mode for leaning buttresses.)
- 4) For arches of larger thickness ratios, the minimum value of horizontal acceleration will form a combined collapse mechanism with three hinges in the arch and one extrados hinge at the support.
- 5) In the event of a combined arch-buttress mechanism, the existence of a fracture in the buttress will reduce the minimum acceleration to form a mechanism. In the case of rectangular buttresses, this minimum acceleration may be reduced by more than 30% in comparison to a solid buttress.
- 6) For typical masonry buttressed arch configurations, it is likely that the arch will collapse first and the buttress will remain standing in the event of collapse due to lateral acceleration.
- 7) The critical mechanism will form at a horizontal acceleration less than $0.5g$ for most buttressed arches, which is well within the range of actual peak ground accelerations in seismic events.

Chapter 8 Safety of Buttressed Arches

8.1 Introduction

Most buttressed arches exist in a deformed state and engineers must assess the safety of the structure as it now stands. Previous chapters have demonstrated that the *buttress* is not typically in danger of collapse, though numerous situations may threaten the stability of the *arch*. The current chapter proposes various methods for assessing the safety of a buttressed arch and presents a simple case study to illustrate the proposed safety measures.

To assess the safety of a buttressed arch, the analyst must investigate three problems:

- 1) the safety of the arch;
- 2) the safety of the buttress; and
- 3) the safety of the arch and buttress together as a system.

This chapter outlines a general approach and various options for evaluating the safety of a buttressed arch. The methods are explained and illustrated with reference to a masonry church in India, which will be analysed following the methods outlined in this dissertation. The safety measures here focus on the problem of leaning buttresses, although methods are also proposed for assessing safety under seismic loading.

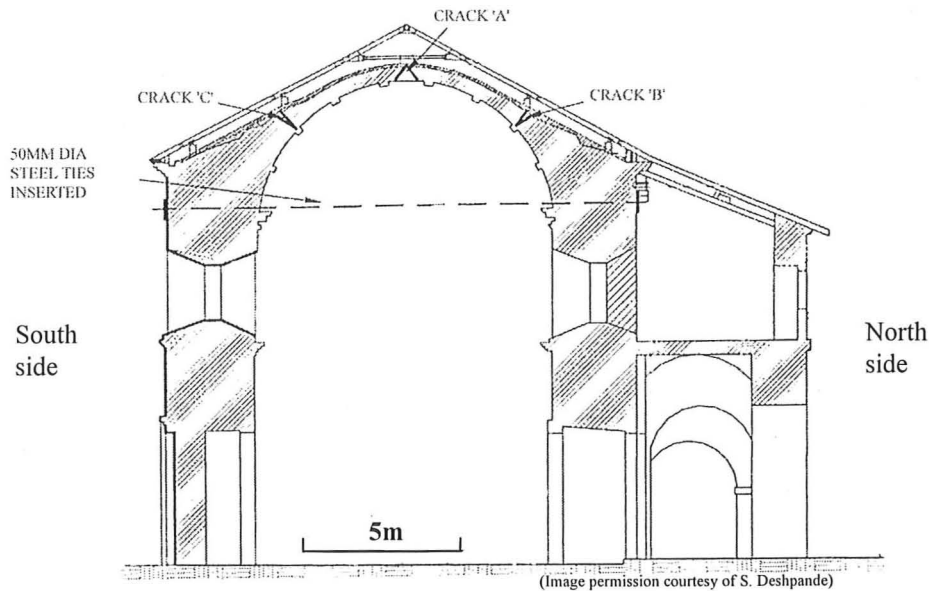
8.2 Case Study: Church at Goa, India

The 16th century Capella da Nossa Senhora do Monte in Old Goa is one of the first monuments built by the Portuguese in the Indian subcontinent, and it has important historical significance. Deshpande and Savant (2001) recently carried out restoration work and added exposed steel ties to reduce the thrust of the vault on the masonry walls. The structure of this church provides a simple case study to illustrate the methods presented in this dissertation. This chapter will examine the safety of the structure and seek to determine if the addition of steel ties across the vault was indeed necessary.

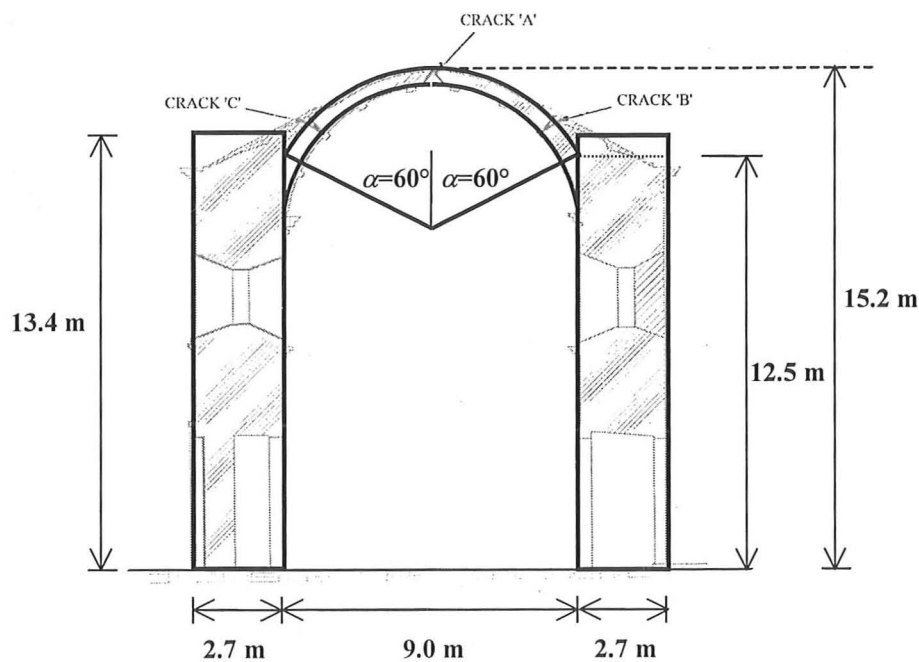
8.2.1 Structural Description

The chapel consists of a barrel vault supported on rectangular masonry walls, and is constructed entirely of laterite stone derived from weathered basalt. The vault spans

approximately 9.0 m and is supported on solid walls of approximately 2.7 m thickness: see Figure 8.1. The barrel vault on the rectangular walls can be analysed for a 1-metre wide section along the nave, which is approximately equivalent to an arch supported on rectangular buttresses. To determine the magnitude of the forces in the structure, the unit weight of the material is assumed to be 25 kN/m^3 .



a) Actual geometry of structure, showing the wooden roof above the masonry vault and the location of cracking (hinges) in the vault.



b) Idealised geometry of structure, assuming the buttressing walls are rectangular and the vault is circular of constant thickness.

Figure 8.1. Capella da Nossa Senhora do Monte, Goa, India (after Deshpande and Savant 2001).

In the current configuration, the South wall of the church (shown on the left in Figure 8.1) is leaning by nearly 0.1 m at the top of the wall, which is equivalent to a lean of approximately 0.4° (Deshpande and Savant 2001). The North wall is supported by the adjacent structure and remains nearly vertical. As a result of the leaning of the South wall, the span of the vault has increased and the vault has deformed. As predicted in earlier chapters, the vault has accommodated the increase in span by forming three hinges (A, B, and C in Figure 8.1). For the purposes of the current chapter, which aims to demonstrate the various measures of safety for a buttressed arch, the structure will be approximated as a circular arch supported on rectangular buttresses to simplify the analysis: see Figure 8.1b. To simplify the problem further, the weight of the timber roof will be neglected for the current analysis. In addition, the effect of various openings in the walls, including several doorways and a number of circular openings, will not be considered. A thorough structural analysis would account for these factors, and would use a more accurate geometrical approximation of the arch and the buttress. The current study aims to determine the general equilibrium conditions, which can be quantified by using the various measures of safety proposed later in this chapter, and does not purport to be an exact analysis of the problem. Indeed, it will be demonstrated that an approximate analysis can be used to define the safety to sufficient accuracy.

8.2.2 The Arch at Goa

The vault is circular with a radius of approximately 5.0 m and a thickness of approximately 0.5 m. The vault can be approximated as a circular arch subtending 120° with a thickness ratio of $t/R = 0.1$, as in Figure 8.1(b). For a 1-metre wide section of the vault at Goa in its original conformation, the minimum thrust is found to be 39 kN, corresponding to intrados hinge locations at 54° from the crown. (The thrust and hinge locations are calculated following the procedure developed in Chapter 5.) The computed hinge locations of 54° compare well to the actual hinges in the vault, which are located approximately 50° from the crown. The vertical reaction at each support due to the weight of the vault is approximately 64 kN per metre width. An arch of this geometry was analysed in Chapter 5 for the problem of spreading supports, and the collapse state has been illustrated in Figure 5.16. For collapse due to spreading supports, the span must increase by approximately 8%. For the span of the vault at Goa of 9.0 m, this corresponds to a span increase of 0.72 m, which may be compared

to the current increase of 0.1 m. At this collapse state, the thrust would have increased to approximately 2.2 times the initial minimum thrust of the arch, corresponding to a maximum possible horizontal thrust of 86 kN at the point when the vault will collapse due to spreading supports.

8.2.3 The Buttress at Goa

The buttresses are assumed to be rectangular, with a width of 2.7 m at the base and a height of 13.4 m, giving a h_b/b ratio of 5.0. The springing of the arch is assumed to be at a height of $h = 12.5$ m, so that $\mu = 0.9$. The weight of the buttress is 905 kN per metre width, so considering the vertical reaction of the arch, $V = 64$ kN, gives $\psi = 0.07$ (where $\psi = V/W_b$). The capacity of the buttress for horizontal thrust is then determined from equations [3.23]-[3.26]. The maximum horizontal thrust for the vertical buttress is approximately $H_u = 69$ kN, corresponding to a fracture height of $e = 8.7$ m. The reduction in thrust capacity as the buttress leans is approximately 10 kN per degree of leaning (from equation [4.10] or Figure 4.5). Therefore, in the existing state with a lean of 0.4° , the buttress capacity has been reduced to $H_\phi = 65$ kN from 69 kN. To prevent failure of the buttress by sliding, the weight of the buttress above the springing is 61 kN and the weight of the arch provides a vertical force of 64 kN. Assuming a static coefficient of friction of 0.7, sliding will occur for horizontal forces greater than 88 kN, from equation [3.15]. Therefore the buttress will fail by overturning before sliding.

The adjacent structure to the North provides additional support to the North wall, and therefore the North wall can be assumed to remain vertical. The South wall is currently leaning by 0.4° , and the analysis here will assume that the South wall will continue to lean further, thereby endangering the structure and possibly leading to collapse.

8.2.4 The Buttressed Arch at Goa

The analysis of the arch on spreading supports and the leaning buttress is combined and presented in Figure 8.2. The South buttress is assumed to lean progressively up to collapse, increasing the span of the arch; while the North buttress remains vertical. The program ArchLean has been adapted for the problem of only one leaning buttress,

and has determined that collapse will occur when the South buttress leans by slightly more than 2.0° . At this point, the thrust of the arch exceeds the capacity of the South buttress and the arch will collapse due to the failure of the buttress. Thus, the failure state is a "weak-buttress" mode, as described in Chapter 7. In the current state, with the South buttress leaning by 0.4° , the thrust of the arch has increased to 41 kN, from its initial value of 39 kN. The collapse state of the church at Goa due to the leaning of the South buttress is illustrated in Figure 8.2.

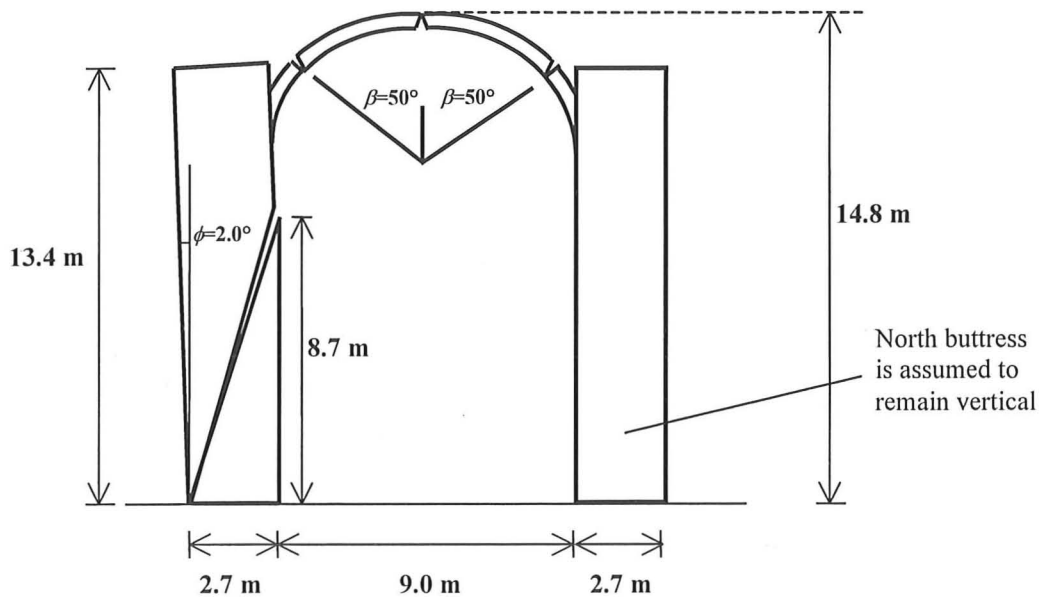


Figure 8.2. Collapse state of the church at Goa due to leaning of the South buttress. When the buttress has leaned outward by 2° , the thrust from the distorted vault will exceed the thrust capacity of the buttress and the vault will collapse. At this point, the crown of the vault has descended by 0.4 m and the thrust of the arch will have increased from 41 kN to 52 kN.

The relationship between the horizontal thrust in the structure and the leaning of the South buttress is illustrated in Figure 8.3. The current state of the structure can be compared to the final collapse state due to the thrust of the arch exceeding the capacity of the leaning South buttress. For comparison, another plot is given for the same structure but with the actual arch replaced by an arch of smaller thickness ratio ($t/R = 0.05$). In this case, analysis shows that the arch would collapse well before the thrust exceeds the capacity of the buttress and that the failure mode would be of the "strong-buttress" kind. This section has described the collapse condition for the church at Goa due to the outward leaning of the South buttress. The following sections apply measures of safety to the church, as well as a general procedure for assessing the safety of buttressed arches.

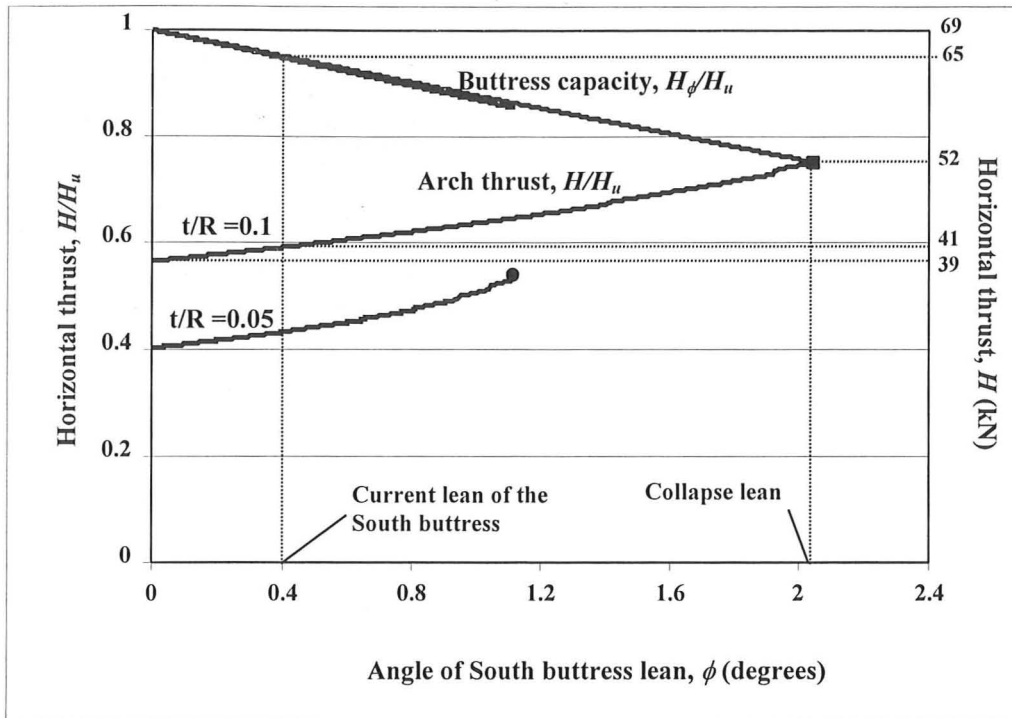


Figure 8.3 Changing horizontal thrust as the South buttress leans for the church at Goa. Collapse occurs when the buttress leans by just over 2° , and the thrust of the deformed arch exceeds the capacity of the leaning buttress. If the arch were half the thickness ($t/R = 0.05$), then the arch would collapse before exceeding the buttress capacity, at a buttress lean of 1.1° (shown by the lowest curve).

8.3 Load Factor for Collapse

For an arch supported on buttresses, the most obvious measure of safety is a simple load factor applied to the thrust of the arch. The load factor is equal to the horizontal thrust capacity of the leaning buttress H_ϕ divided by the thrust of the arch, or

$$SF_{load} = \frac{H_\phi}{H}. \quad [8.1]$$

For the church at Goa as originally built, the vertical buttress has a thrust capacity of 69 kN, and the arch provides a minimum thrust of 39 kN, so the initial load factor of safety against collapse is 1.8. As the buttress has increased its lean over several centuries, the load factor has reduced. This can be appreciated from Figure 8.3, where the buttress capacity is decreasing and the applied thrust is increasing. For the church in its present state with a lean of 0.4° , the buttress capacity is 65 kN and the applied thrust is approximately 41 kN due to the deformation of the arch. Thus, the load factor of safety has been reduced from 1.8 to 1.6 due to the current lean of the buttress. If the

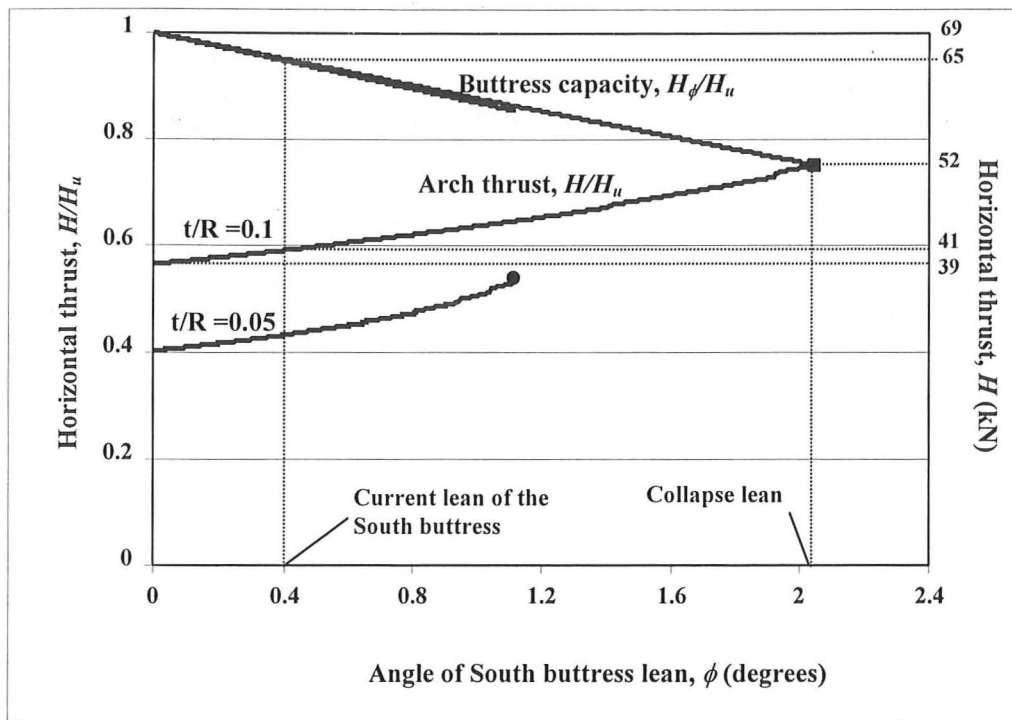


Figure 8.3 Changing horizontal thrust as the South buttress leans for the church at Goa. Collapse occurs when the buttress leans by just over 2° , and the thrust of the deformed arch exceeds the capacity of the leaning buttress. If the arch were half the thickness ($t/R = 0.05$), then the arch would collapse before exceeding the buttress capacity, at a buttress lean of 1.1° (shown by the lowest curve).

8.3 Load Factor for Collapse

For an arch supported on buttresses, the most obvious measure of safety is a simple load factor applied to the thrust of the arch. The load factor is equal to the horizontal thrust capacity of the leaning buttress H_ϕ divided by the thrust of the arch, or

$$SF_{load} = \frac{H_\phi}{H}. \quad [8.1]$$

For the church at Goa as originally built, the vertical buttress has a thrust capacity of 69 kN, and the arch provides a minimum thrust of 39 kN, so the initial load factor of safety against collapse is 1.8. As the buttress has increased its lean over several centuries, the load factor has reduced. This can be appreciated from Figure 8.3, where the buttress capacity is decreasing and the applied thrust is increasing. For the church in its present state with a lean of 0.4° , the buttress capacity is 65 kN and the applied thrust is approximately 41 kN due to the deformation of the arch. Thus, the load factor of safety has been reduced from 1.8 to 1.6 due to the current lean of the buttress. If the

lean of the buttress were to increase steadily to 2° , the thrust of the arch and the carrying capacity of the buttress would be equal at 52 kN per metre; and the arch would collapse. At the collapse state, when the thrust of the arch equals the capacity of the buttress, the load factor is 1.0 (i.e. there is no reserve of safety).

It is important to recall from Chapter 7 that the load factor measurement of safety is not valid in the event of a "strong-buttress" failure, in which the arch collapses first. This can be illustrated for the Goa church by assuming a smaller thickness ratio for the arch. Thus, if the thickness ratio were 0.05 instead of its actual value of 0.10, the arch would collapse before the buttress fails (as shown by the lower curve in Figure 8.3). In this case, the thrust capacity of the buttress would still be 1.6 times greater than the thrust from the arch at the point when the arch collapses. Thus, the load factor for the thrust of the arch is only rationally applicable to a "weak-buttress" failure, in which the thrust of the deformed arch can exceed the capacity of the buttress. For the actual church at Goa, the arch could exert a thrust as high as 88 kN before collapsing due to spreading supports, which is greater than the thrust capacity of the buttress. Therefore collapse will occur due to a "weak-buttress" failure, and the load factor of safety of 1.6 is a valid measure of the safety against collapse.

8.4 Pressure-Point Factor

The pressure-point factor described in Chapter 4 for buttresses is an additional measure of the influence of the horizontal overturning force. This measure considers the reaction point at the critical section of the buttress and investigates the location of this reaction point as the horizontal force increases and as the buttress leans outwards. (Sections 4.5-4.7 present the concept of the pressure-point and the influence of applied loads and increased leaning on the location of the reaction point in the buttress.) The pressure-point co-ordinate η is measured from the outer edge of the buttress about which overturning would occur, and can be compared to the initial reaction point co-ordinate η_o if the buttress did not support any horizontal thrust. For the church at Goa, the hypothetical reaction at the base of the South buttress for zero horizontal force occurs at $\eta_o = 0.53$. For a given lean and applied thrust, the reaction point η can be used to define the safety as

$$SF_{\text{pressurepoint}} = \frac{\eta_o}{\eta_o - \eta} \quad [4.15]$$

as presented for buttresses in Chapter 4. When the buttress is vertical ($\phi = 0^\circ$) and the initial horizontal thrust of the arch is applied ($H_a = 39$ kN), the reaction point at the base of the Goa buttress is $\eta = 0.35$, which lies within the middle third of the buttress. In its current state of leaning, the horizontal thrust of the arch has increased to 41 kN and the reaction point at the base has moved to $\eta = 0.29$. This reaction point is computed for the leaning buttress by assuming that cracking has begun and that some of the buttress is no longer effective, since the reaction point is outside of the middle third. The pressure-point factor is summarised for the church at Goa in Table 8.1.

Angle of lean, ϕ	Thrust of arch, H	Reaction point, η	Pressure-point Factor
0°	0 kN	0.53 (η_o)	∞
0°	39 kN	0.35	2.9
0.4°	41 kN	0.29	2.2
$\phi_u = 2.0^\circ$	52 kN	0	1.0 (i.e. collapse)

Table 8.1. Pressure-point factor for the church at Goa.

In its undeformed state, the church at Goa had a pressure-point factor of 2.9, suggesting considerable safety. But with the slight lean of the South buttress to its current state of 0.4° , the reaction point at the base shifts from 0.35 to 0.29, decreasing the pressure-point safety factor to 2.2.

Just as with the load factor for collapse of the buttress, the pressure-point factor is only valid in the case of weak-buttress failure. If the arch collapses before the capacity of the buttress is reached, the reaction point at the base of the buttress cannot be used to assess the safety of the structure. For example, if the vault at Goa were half the thickness, with $t/R = 0.05$, the vault would collapse before the capacity of the buttress is exceeded. In this case, the pressure-point safety factor would be 2.3, indicating that the buttress could withstand higher values of thrust; yet the arch would collapse before the capacity of the buttress is exceeded. Thus, the pressure-point safety factor is only valid when the horizontal thrust capacity of the buttress is exceeded and failure is governed by a "weak-buttress" collapse.

8.5 Safety Assessment of an Arch on Leaning Buttresses

The previous measures of safety have been concerned only with the value of the horizontal thrust applied to the buttress. However, in the event of a "strong-buttress" failure, the horizontal thrust capacity of the buttress is irrelevant (so long as it is greater than the maximum possible thrust from the arch). In this case, the safety factors presented above are irrelevant and positively misleading.

To determine the safety of an arch supported on leaning buttresses, the analyst must first investigate the arch and buttress independently and then together as a system. The most common structural problem for buttressed arches is the progressive outward leaning of the buttress. This dissertation has presented the general procedure to analyse this problem, although each individual structure will require a slightly different approach. To assess the safety of this structural system against collapse due to excessive leaning of the buttresses, the analyst should follow the approach summarised below in Figure 8.4.

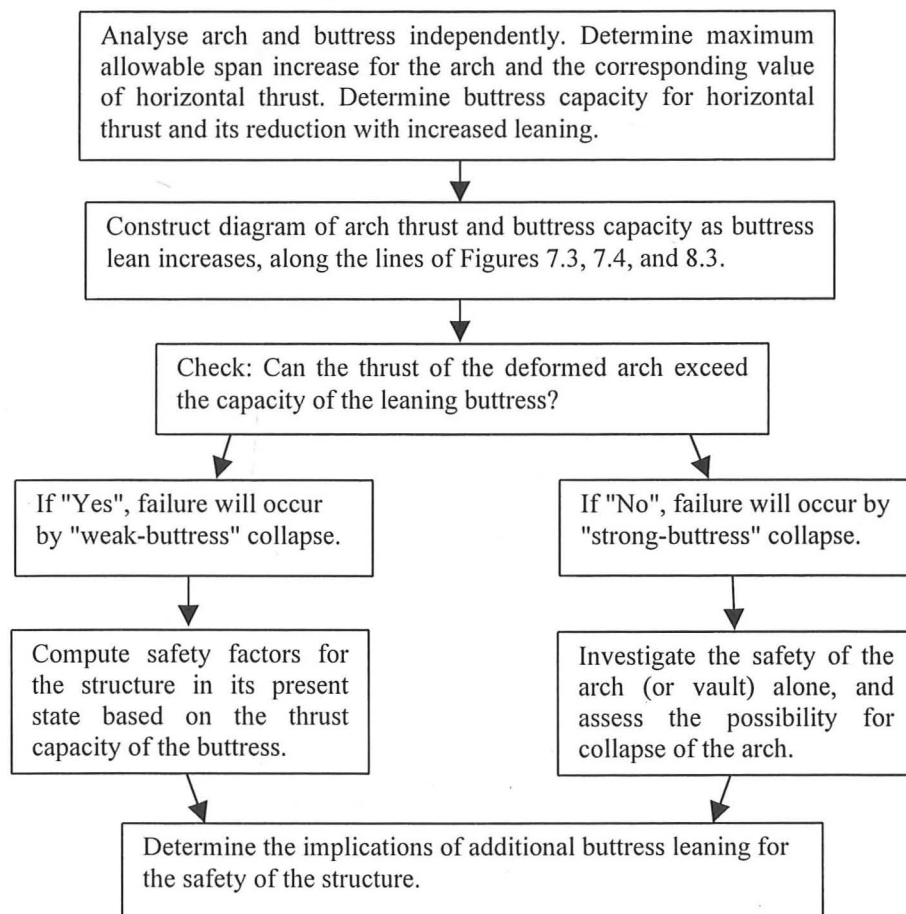


Figure 8.4. Analysis procedure for assessing the safety of an arch supported on leaning buttresses.

Thus, there is no single measure to determine the safety of an arch supported on leaning buttresses and the engineer must use judgement to assess the implications of additional buttress leaning. This will depend largely on the type of failure expected and the conditions of the particular structure. In general, there are two types of failure for an arch on leaning buttresses: strong-buttress and weak-buttress. In addition, it may sometimes be useful to think of an intermediate mode of failure between the two. Each particular case requires an understanding of the current state of the structure and the implications of future movements on the safety of the structure. The best way to assess the structure is to produce a diagram summarising the changing capacity of the buttress and the thrust of the arch in relation to the lean of the buttress, as illustrated in Figure 8.5.

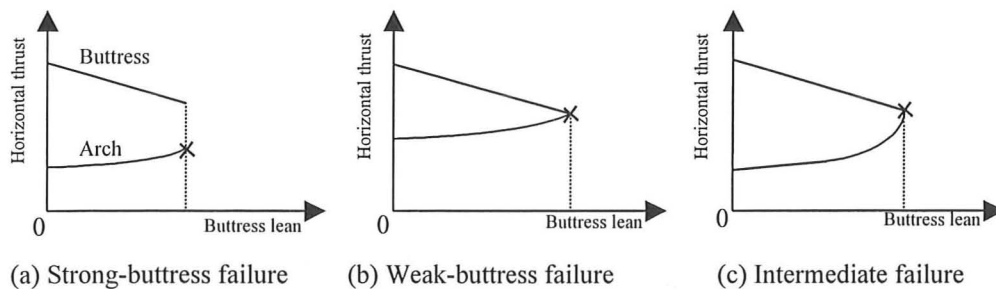


Figure 8.5. Three types of failure for an arch supported on leaning buttresses. The horizontal axis presents the inclination of the buttress and the vertical axis presents the change in horizontal thrust as the buttresses lean outwards. The arch collapse state is marked by "x".

For each of these cases, additional leaning of the buttresses will have different implications. For example, the intermediate mode of failure is characterised by a sharp increase in the thrust of the arch (Figure 8.5c), in which case the maximum safe angle of buttress lean should be well below this region of the curve. Thus, although the two curves intersect, as in the weak-buttress case, the portion of the plot for small angles of inclination may be like the strong-buttress case.

This procedure for safety assessment can now be applied to the specific example of the church at Goa. Because failure occurs by a weak-buttress mode, the two measures of safety presented in this chapter can be applied to gain insight into the implications of increased buttress leaning. For comparison, the load factor and pressure-point

factor are plotted in Figure 8.6 for the church at Goa as the angle of buttress lean increases.

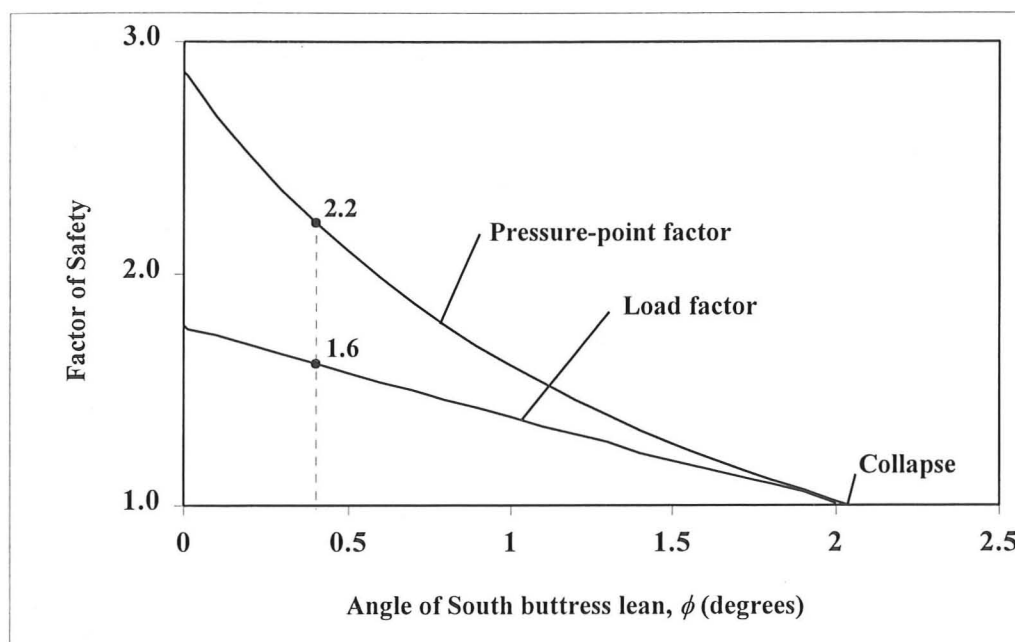


Figure 8.6. Comparison of safety factors for the church at Goa.

The load safety factor and pressure-point factor are both equal to 1.0 at the collapse state, though in general the load factor gives consistently lower values of safety. From this comparison, it is clear that the load safety factor is superior to the geometric safety factor. The pressure-point factor gives higher (i.e. more conservative) estimates of the safety and is much more difficult to calculate. Determining the geometric safety factor for different values of buttress leaning requires a computation of the progression of cracking and the movement of the reaction point up until the collapse state. The load safety factor is a very simple calculation, with immediate physical meaning in relation to the failure of the buttress. To assess the safety of the buttress against horizontal loads, the load factor of safety is the preferred method. However, the pressure-point factor can be used to assess serviceability issues for the structure, such as the danger of a fracture in the buttress due to the eccentric loading on the buttress (as discussed in Chapters 3 and 4).

For the church at Goa, the load factor suggests a level of safety of approximately 1.6. This factor is derived for the general structure in its current state, acting under only its own weight. Furthermore, this analysis did not consider the reduced weight of the

buttress due to the presence of doorways and other openings in the masonry wall. Finally, this analysis assumes that the North buttress remains vertical and does not lean as the thrust increases. If the North buttress and South buttress were to lean apart at the same angle, then the arch would collapse for a smaller angle of buttress lean of approximately $\phi = 1.2^\circ$. Thus, an analysis taking into account these factors would reduce the measure of safety further. The pressure-point factor suggests a higher level of safety, but the pressure-point is located at $0.29b$, outside the middle third, suggesting that the walls may be fractured due to the eccentricity of the thrust at the base of the buttress. Is this a reasonable level of safety for this structure? The structure is clearly approaching a precarious state and additional leaning may lead to collapse. Although the church has survived for over 400 years, the current state of leaning is approaching a dangerous level, and a factor of safety of 1.6 is not sufficient to ensure the long-term survival of the structure. In summary, there is significant uncertainty in the exact collapse state, and engineers should exercise caution to ensure that the structure does not approach the conditions for collapse.

8.6 Seismic Safety

The previous measures of safety have only considered the threat of collapse due to the outward leaning of the buttresses. In addition to this common pathology, buttressed arches may collapse due to ground accelerations resulting from seismic activity. The previous chapter outlined a method for determining the minimum constant horizontal acceleration to form a collapse mechanism, and this can be used as a first attempt to assess the stability of existing buildings.

The simplified geometry of the church at Goa has been analysed using the methods outlined in Chapter 7 for constant horizontal acceleration. The horizontal acceleration is assumed to be parallel to the arch and normal to the nave of the church. The minimum acceleration to form a collapse mechanism for the Goa church geometry is summarised in Figure 8.7 for a range of vault thickness ratios, and the actual configuration of the church with a thickness ratio of 0.10 is illustrated by the vertical chain-dotted line. If the buttresses are assumed to be solid -- i.e. unfractured in the sense of Chapter 3 -- and the thickness ratio of the arch is 0.10, then a collapse

mechanism will form at a horizontal ground acceleration of approximately 0.13g. But if the critical buttress is assumed to fracture, the minimum horizontal acceleration is reduced to 0.07g.

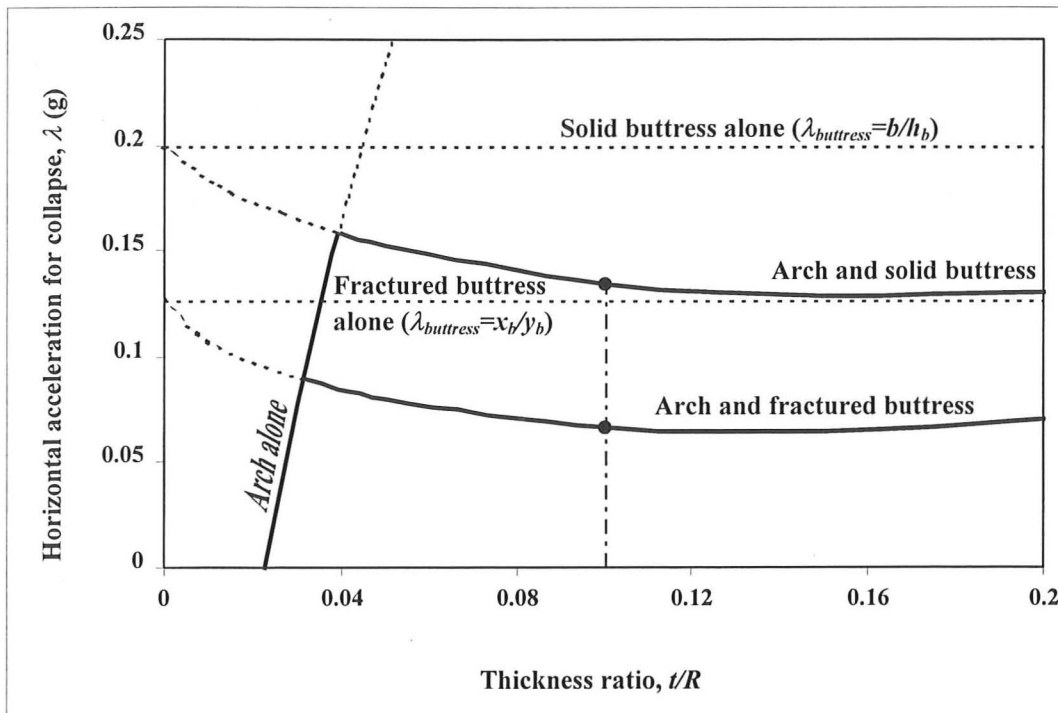


Figure 8.7. Minimum horizontal acceleration to form a collapse mechanism for the undeformed geometry of the church at Goa.

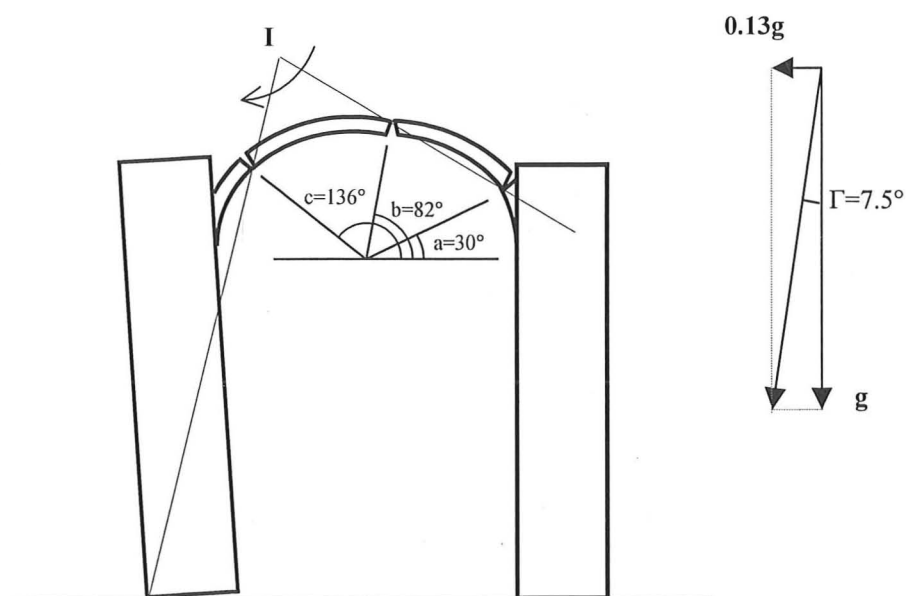


Figure 8.8. Collapse state of the church at Goa due to constant horizontal acceleration of 0.13g. The South buttress is assumed to remain solid, and three hinges form in the arch at the collapse state. The collapse state has been determined using the program SolidTilt, and the structure has been analysed in its undeformed state using work calculations based on an infinitesimal motion.

Figure 8.8 illustrates the collapse mechanism due to constant horizontal acceleration, assuming that the buttress remains solid. In this case, the minimum horizontal acceleration to form a collapse mechanism is $0.13g$, corresponding to an acceleration angled at $\Gamma = 7.5^\circ$ from the vertical. (As described in Chapter 6, the angle Γ , equivalent to the angle of "tilt" if the entire structure were tilted on a horizontal plane, is simply $\tan\lambda$.) As demonstrated in Chapter 6, for small angles of Γ , the hinges in a circular arch will shift by the angle Γ from their initial positions. The arch at Goa has initial hinge locations at $\beta_o = 54^\circ$, which would correspond to $a=36^\circ$, $b=90^\circ$, and $c=144^\circ$ in the notation of Chapter 6. The angle of applied acceleration of $\Gamma = 7.5^\circ$ simply shifts each of these hinges by 8° around the circular arch (rounded from 7.5° to 8° since the program assumes 1° voussoirs). Thus, the hinges at B and C shift by 8° to $b=82^\circ$ and $c=136^\circ$. The intrados hinge A can only move 6° before reaching the support, so it occurs at the support, or $a=30^\circ$.

Figure 8.9 illustrates the collapse mechanism due to constant horizontal acceleration, assuming that the buttress fractures due to excessive horizontal thrust found using the program ButtressTilt. In this case, the minimum horizontal acceleration to form a collapse mechanism would be reduced to $0.07g$, corresponding to an acceleration angled at $\Gamma = 4^\circ$ from the vertical.

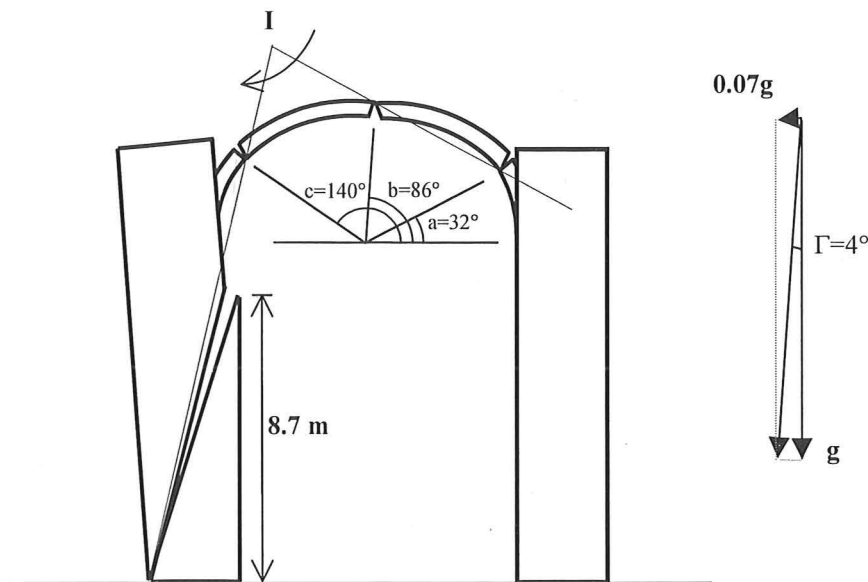


Figure 8.9. If the South buttress is assumed to fracture as predicted under a constant vertical load and an increasing horizontal load, the church will collapse for a lower value of horizontal acceleration. As before, three hinges would form in the arch at the collapse state, though the reduced buttress mass would lower the threshold acceleration to $0.07g$.

In this case, the smaller angle of applied acceleration ($\Gamma=4^\circ$), shifts each of the hinges by 4° around the circular arch. Thus, the hinges A, B, and C move by 4° from their initial configuration of $a=36^\circ$, $b=90^\circ$ and $c=144^\circ$ to $a=32^\circ$, $b=86^\circ$ and $c=140^\circ$. In general, the value of the minimum horizontal acceleration to form a collapse mechanism is not very sensitive to the hinge locations, so for practical purposes it is possible to assume reasonable hinge locations and analyse the corresponding mechanism.

To assess the safety of a structure under seismic loading, the engineer must consider the geographical location and the seismic activity of the region. For the church at Goa, the minimum values of acceleration for the onset of the mechanism are extraordinarily low, given the seismicity of the Indian subcontinent. Bhatia *et al.* (1999) have identified the region as a Moderate Damage Risk Zone (Zone III), which can expect earthquakes of Modified Mercalli intensity VII. In this zone, typical peak ground accelerations on rock are $0.10g$, though this can be amplified by local soil conditions. This result supports the conclusion that the church at Goa exists in a precarious state. The values for minimum horizontal acceleration to form a collapse mechanism have been computed for the vertical buttress and would be slightly lower for the leaning state of the South buttress. For example, the minimum horizontal acceleration for the solid buttress would be reduced to $0.19g$ from $0.20g$ due to the shift in the horizontal centroid as a result of leaning by 0.4° . The postulated collapse mechanism under lateral acceleration loading is assumed to involve the South buttress, since the North buttress is supported by the adjacent structure: see Figure 8.1(a).

For the case of the fractured south buttress under lateral acceleration, the result does not mean that the structure will actually *collapse* due to a horizontal acceleration of $0.07g$, but that the acceleration is sufficiently large to *form* a collapse mechanism. For arches supported on buttresses, it is relatively straightforward to compute the value of minimum constant acceleration to form a collapse mechanism. For more complex masonry structures, such as large cathedrals, the analysis would be more difficult, but is possible using thrust-line techniques for static equilibrium under combined vertical and horizontal loading.

For a complete analysis of the seismic response of a masonry structure, it is necessary to consider the potential energy of the system and the approximate acceleration spectrum of the seismic event. This requires a time-history analysis of the input accelerations to determine the response of the mechanism. Oppenheim (1992) has illustrated such an approach for the masonry arch independently, and it would be straightforward to extend his analysis to an arch on buttresses using the mechanisms presented in this dissertation. A complete dynamic study is beyond the scope of the current work, although the principles will be presented briefly here.

A masonry structure will undergo rigid-body motion for a peak horizontal acceleration less than the minimum horizontal acceleration λ_{min} to form a mechanism. The structure can sustain accelerations higher than this value if applied for a short period of time, which do not impart sufficient kinetic energy to bring the structure to collapse. The structure will collapse when the mechanism has rotated sufficiently and the maximum potential energy of the mechanism is reached. If the maximum potential energy is not reached, then the structure may "recover" and return to its initial configuration. This concept is illustrated by the acceleration pulse curve presented in Figure 8.10. The critical mechanism can be determined from an equivalent static analysis as described in Chapters 6 and 7. The dynamic response of this critical mechanism can then be analysed for varying acceleration pulses of finite-time duration. Each acceleration magnitude λ_i will correspond to a finite time period t_i in order to impart sufficient energy to cause collapse. These values can be computed for $\lambda_i > \lambda_{min}$ and a general curve similar to Figure 8.10 can be constructed for each mechanism. This curve can then be compared to expected seismic events in the region in order to assess the danger of collapse due to horizontal ground acceleration.

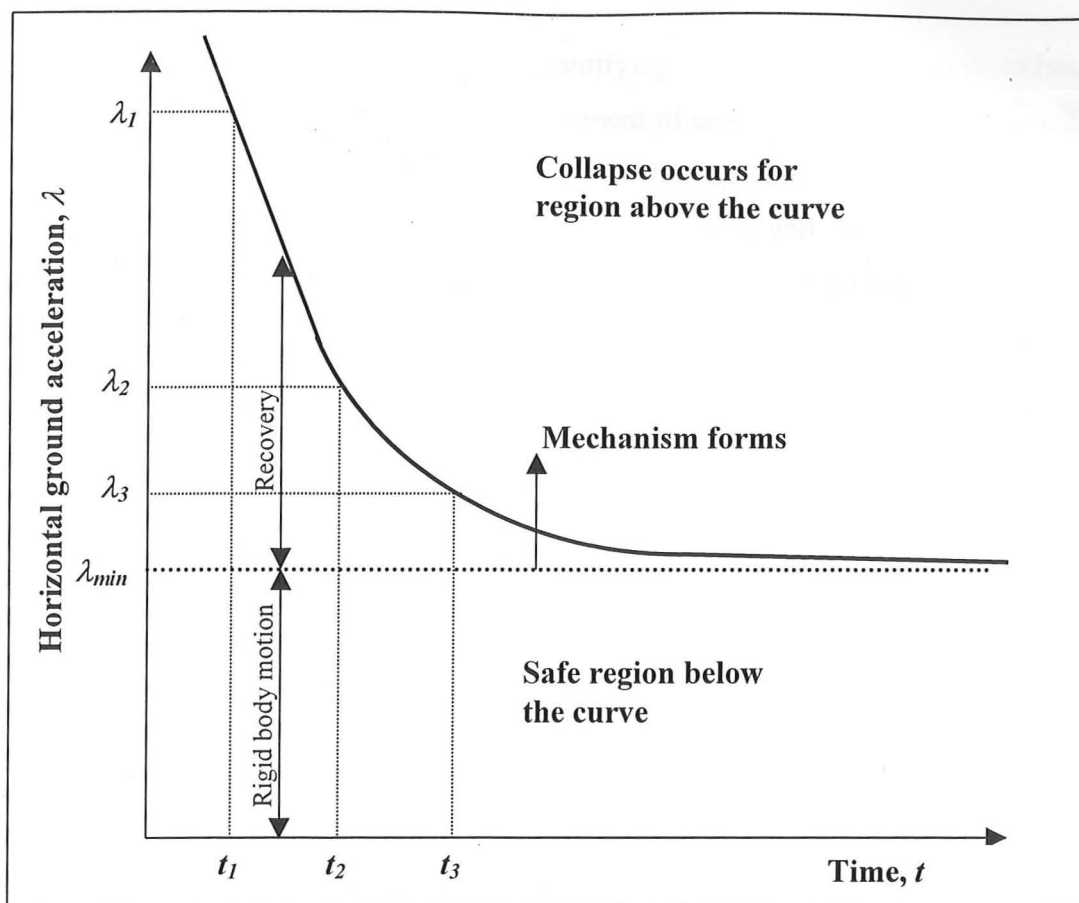


Figure 8.10. Concept of acceleration pulse curve for an assumed mechanism of collapse in a masonry structure.

The seismic analysis of structures involves a great deal of uncertainty, but the methods presented here can be used to carry out risk assessments of existing structures. This dissertation has presented methods for determining the critical mechanism for collapse of a masonry arch on buttresses; and additional research is required to examine the dynamic response of this mechanism to idealised acceleration loading. This can be useful to further understand the general stability of a structure, as in the example of the church at Goa. Furthermore, this approach can be extremely valuable for comparative studies of different structures within a geographical area. A comparative study of masonry vaulted structures in Italy may have identified the Basilica of St. Francis of Assisi as a vulnerable structure prior to the 1997 Umbria-Marche earthquake. Such a study could be useful for future assessment of seismic risk among families of masonry structures in a region.

8.7 Maintenance and Repair

This chapter has illustrated methods of quantifying the safety of buttressed arches to provide guidance for engineers in the assessment of existing masonry buildings. The example of the church at Goa has demonstrated that the church recently existed in a precarious state and justifies the decision by Deshpande and Savant (2001) to add steel ties across the vault in order to reduce the thrust on the supporting walls.

The maintenance and repair of masonry structures is not the focus of this dissertation, but it merits a brief discussion. This dissertation has argued that current displacements are an important consideration in the long-term safety of a masonry structure. It follows that a proper maintenance program requires a regular accurate survey to record the current geometry of the structure, and particularly the outward lean of the walls and buttresses. These measurements can be repeated and monitored over long periods of time, in order to provide valuable information about the relative safety of the structure. In the case of the leaning tower of Pisa, careful measurements provided engineers with the knowledge that the tower was progressing towards collapse and thus enabled them to intervene successfully (Burland 2001). Such measurements are most valuable when they are documented over a long period of time to provide engineers with an indication of the rate of change of movements in the structure.

There are numerous methods of reinforcing or repairing masonry structures; and the discussion here will be limited to the specific case of an arch supported on leaning buttresses. For severely deformed buttressed arches, Huerta (1997) has argued for the advantages of inserting exposed tension ties to reduce the thrust of the arch on the walls or buttresses. This solution is inexpensive, reversible, completely effective, and it may indeed provide visual reassurance to the occupants of a severely deformed building. Another way of repairing inclined buttresses or walls is to remove a thin wedge of material at the base of the buttress in order to bring the wall back to its vertical position. This was a technique practised by master masons in past centuries, and it is an effective method for straightening a wall or buttress without reconstructing the entire structure: see for example the work by Scott (1879) at St. Alban's cathedral. Such a method could also be applied to buttresses supporting masonry arches or vaults, although it would be necessary to provide temporary support for the arch or vault during the repairs.

8.8 Summary

This chapter has presented general methods for assessing the safety of a buttressed arch and the following conclusions can be drawn:

- 1) There is no single measure for the safety of an arch on leaning buttresses to encompass the complexity of the problem. To understand the safety of the structure, engineers should analyse the arch and buttress individually, and produce a diagram as in Figure 8.3 or 8.5 illustrating the influence of increased buttress leaning.
- 2) For collapse due to weak-buttress failure, the load factor of safety is the simplest method of measuring safety and is here recommended. However, this method is invalid if collapse occurs by strong-buttress failure, in which the arch collapses before the capacity of the buttress has been reached.
- 3) A calculation of the existing equilibrium condition has revealed that the church at Goa existed in a vulnerable state and that the recent decision to insert steel ties was justified.
- 4) The ability of a masonry structure to withstand constant horizontal acceleration provides an additional measure of the stability of masonry structures. This analysis can be used to assess the likelihood of collapse for an individual structure, or it can be used to study the relative safety of a group of structures in order to highlight those at greater risk of collapse.
- 5) A complete assessment of the seismic vulnerability of a masonry structure requires a detailed study of the dynamics and potential energy of the system. This type of analysis should focus on the critical mechanism that has been identified from the static analysis of the masonry structure under constant horizontal acceleration.
- 6) Long-term monitoring of the geometry is an essential component of the assessment and maintenance of masonry structures.

PART V: CONCLUSIONS

Chapter 9 Conclusions

9.1 Summary of Results

Traditional masonry structures can be analysed as rigid-block structures that may collapse due to applied loading, long-term displacements, or ground accelerations. Hitherto, researchers have focussed on understanding the load capacity of masonry structures, and have not sufficiently investigated the importance of displacements or ground accelerations. For traditional masonry buildings, such as a masonry vault supported on buttresses, collapse is more likely to occur due to excessive displacements or ground accelerations than on account of an applied load.

9.1.1 The Masonry Buttress

Overturning failure will typically govern the collapse of masonry buttresses under lateral loads. For failure due to overturning, a fracture will develop at collapse and the capacity of the buttress to resist horizontal loads will be reduced substantially. A simple approximate method for computing the shape of this fracture finds that it is always a straight line for rectangular buttresses. This provides the analyst with a straightforward approach for estimating the horizontal thrust capacity of a buttress. For a buttress leaning away from the applied load, the buttress capacity reduces linearly with the angle of lean. For leaning buttresses, the location of the fracture at the collapse state does not change considerably from the theoretical fracture location for a vertical buttress. Thus, the analyst can estimate the capacity of the vertical buttress to horizontal loads and reduce this capacity in accordance with the current angle of lean.

9.1.2 The Masonry Arch

Two specific problems have been analysed for the circular masonry arch: the arch on spreading supports and the arch under base motion due to uniform horizontal acceleration. The arch on spreading supports is a complex problem and the exact collapse mode is difficult to ascertain. Various statically admissible mechanisms exist for a given increase of span (i.e. different hinge locations can satisfy the same geometry change). An algorithm has been presented for following the history of distortion in an arch under spreading abutments and in all cases the thrust of the arch is found to increase as the supports spread apart. When the abutments begin to move apart, the arch

forms a three-hinge mechanism with an extrados hinge at the apex and two hinges on the intrados. As the abutments spread further, the intrados hinges migrate towards the centre. Eventually, two more hinges will form at the supports and collapse of the arch will occur by a symmetrical five-hinge mechanism for typical arch geometries. The vertical reaction of the arch remains constant throughout, while the horizontal reaction can increase substantially.

An equivalent static analysis of masonry arches can be used to determine the critical collapse mechanism due to uniform horizontal acceleration. Masonry arches will collapse due to the formation of a four-hinge mechanism with a predictable pattern of hinge locations for different geometries. In general, circular masonry arches with moderate thickness ratios have significant capacity for horizontal acceleration before forming a collapse mechanism.

9.1.3 The Buttressed Arch

In practice it is common to have an arch supported on leaning buttresses. The angle of lean may increase steadily over time, due primarily to foundation settlements; and the structure will eventually collapse. There are two general modes of collapse for this system: "weak-buttress" failure, in which the arch thrust will exceed the capacity of the buttress, and "strong-buttress" failure, in which the arch collapses before the thrust capacity of the buttress is exceeded. In both cases the arch will collapse and the buttress will remain standing.

For collapse due to horizontal acceleration, a buttressed arch may form a four-hinge collapse mechanism for much lower values of acceleration than for an arch alone. Generally, this mechanism involves three hinges in the arch and one hinge at the base of the buttress. Equivalent static analysis to determine the critical collapse mechanism can be used to assess the stability of a particular structure or compare the safety of a number of structures within a geographical region.

9.1.4 Measures of Safety

Engineers should apply several different measures of safety in order to gain an overall understanding of the safety of a masonry structure. This dissertation has proposed two primary measures of safety for the case in which the buttress capacity is exceeded by

the thrust of the arch: a load factor and a pressure-point factor. These measures are not applicable if the arch collapses in a "strong-buttress" failure mode; in which case the engineer must determine the limit of safe displacements depending on the specific case under consideration.

9.2 Future Work

This dissertation has outlined analysis methods for the collapse of masonry arches supported on buttresses. To illustrate the approach, the discussion has been limited to circular arches on rectangular buttresses. There is significant research to be carried out in extending these methods to more complex masonry structures and in validating the methods proposed by means of further experiments.

There are three broad areas for future work based on the findings of this dissertation:

- 1) The results can be extended to more complex structural forms.
 - The failure of buttresses must be analysed for more complex buttress forms, such as buttressed walls or multiple flying buttresses loading a pier.
 - The failure of arches can be extended to various arch geometries, such as pointed arches or arches of varying thickness.
 - The analysis for arches can be extended to three-dimensional vaults, such as spherical domes or crossing vaults, by analysing individual slices of the vault as independent arches. This could lead to a general theory for the collapse of masonry domes on spreading supports.
 - The collapse of buttressed arches can be extended to consider more complex forms, such as multiple span arches, as in the case of large churches or cathedrals with lateral naves. The method could also be extended to buttressed domes under constant horizontal acceleration to simulate earthquake loading in an elementary way.
- 2) Systematic studies of actual structures and model tests are necessary to verify the theoretical approach proposed in this dissertation.
 - Actual structures can be analysed to develop an understanding of the levels of safety in existing structures. In particular, this approach would be valuable within a geographical region to compare the safety of masonry structures and identify those structures which may be at greater risk of collapse.

- Buttress failure under horizontal loads may occur in a combined sliding-overturning mechanism, similar to the experiment by Vicat (1832) illustrated in Figure 2.2. Future work is necessary to investigate and define the possibility of this type of mechanism, which may occur for lower values of horizontal load than calculated for the sliding mechanism alone.
- Model testing can be carried out on small-scale masonry structures to verify the modes of collapse proposed in this dissertation, particularly for more complex structural forms.
- For seismic analysis, accurate model testing is difficult due to scaling effects. Model testing can be used for simple analyses, such as the minimum constant horizontal acceleration, but large-scale structures are necessary to understand the seismic response of actual buildings. In this case, actual buildings should be instrumented in seismic zones and monitored over long periods of time. In addition, previous vault collapses, such as the partial collapse of the dome of Hagia Sofia and the Basilica of St. Francis in Assisi, could be analysed using the methods presented in this dissertation in an attempt to explain historical failures.

3) Engineers must develop more complex methods for the collapse analysis of rigid-block structures.

- There are no satisfactory computer programs for analysing rigid-block structures as presented in this dissertation. Linear-programming methods are promising, but do not exist in a commercially available form at present.
- For seismic analysis, more complex analytical methods are required to determine the response of the mechanism to a given pattern of ground acceleration. Possible collapse mechanisms must be identified and analysed for their response to specific patterns of horizontal acceleration. In particular, the potential energy of the rotated mechanism must be investigated to determine if the structure will collapse or return to its initial state.
- The analysis of more complex systems will require new computer programs to analyse the stability of rigid-block systems. An ideal program would compute a range of possible internal thrust-lines in the initial state and allow the user to impose support displacements and ground accelerations. The solution procedure should be based on equilibrium solutions derived from kinematically-admissible displacements, rather than from finite-element solutions based on the "stiffness" or elasticity of the masonry material.

PART VI: APPENDICES

APPENDIX A: COMPUTER PROGRAMS

A.1 PROGRAM ArchSpread

FOR COMPUTING THE COLLAPSE OF CIRCULAR ARCHES ON SPREADING SUPPORTS

```
% User defines arch geometry
halfembrace = input('alpha:');
alpha = (pi/180)*(halfembrace);
t_over_R = input('ratio of t/R:');
v = input('voussoir size (degrees):');

% Initialise thrust and other variables
thrustmin = [0];
spread = [0];
spreadmax= [10];
thrustmax = [1];
fail = [0];
thrustincrease = [0];
acrit=[0];
vrads=v*(pi/180);

% Coordinate system is XY with origin at the centre of circle
X_O=[0];
Y_O=[0];
phi=[0];

% Assign arbitrary thickness to R
% Compute half-thickness h and thickness t from given ratio and R
R = [100];
t = R*t_over_R;
h = t/2;
L = (2*R-t)*sin(alpha);

% Compute inner radius and outer radius for use in centroid
calculations
r1 = R-h;
r2 = R+h;
rad = (r1^3 - r2^3)/(r1^2 - r2^2);

% Find coordinates at crown, the hinge at the extrados due to the
span increase
XC = [0];
YC = R+h;

% Find coordinates of D, the extrados at the support
XD = (R+h)*sin(alpha);
YD = (R+h)*cos(alpha);

% Angle a must be a whole number between the support and the crown
amin = [0];
amax = amin + (halfembrace);
bmax=halfembrace/v;

for b = 1 : bmax
    a = amin + b*(amax-amin)/bmax;

-% Compute angle in radians and find coordinates of a
```

```

arads = (pi/180)*a;
XA = (R-h)*sin(arads);
YA = (R-h)*cos(arads);

% Find x-coordinate of centre of gravity of arch segment AC
Cent_1 = (4/3)*rad*(sin(arads/2))/arads;
XM = Cent_1*sin(arads/2);
M = arads*(r2^2-r1^2)/2;

% Compute value of thrust
rise = (YC-YA);
thrust = (M*(XA-XM))/(rise);

    if thrust > thrustmin
        thrustmin=thrust;
        ainit=a;
    end
end

% Print critical hinge location (from crown) and minimum thrust
ainit
thrustmin

% Now impose displacements and find new position and new thrust
% Impose horizontal displacements only

% Search possible hinge locations

% Find coordinates at crown due to the span increase
XC = [0];
YC = R+h;

% Compute angle in radians and find coordinates of intrados hinge
% Round to nearest voussoir
n=(ainit/v);
o=(halfembrace/v);
q=[0];

p=(n-q)*v;
prads = (pi/180)*p;
XA = (R-h)*sin(prads);
YA = (R-h)*cos(prads);

% Find weight of arch segment AC
C1 = (4/3)*rad*(sin(prads/2))/prads;
XM1 = C1*sin(prads/2);
YM1 = C1*cos(prads/2);
M1 = prads*(r2^2-r1^2)/2;

% Compute maximum horizontal thrust for hinge location

% Find x-coordinate of centre of gravity of arch segment DA
C2 = (4/3)*rad*(sin((alpha-prads)/2))/(alpha-prads);
XM2 = C2*sin((alpha+prads)/2);
M2 = (alpha-prads)*(r2^2-r1^2)/2;

%Compute maximum thrust supported by section DA
Hmax = (M2*(XD-XM2) + M1*(XD-XA))/(YA-YD);

% Compute initial length and orientation of line AC
LAC = (((XA-XC)^2+(YC-YA)^2)^.5);

```

```

phiac = atan((YC-YA)/(XA));

% Determine maximum amount of spreading before snapthrough occurs
XCMAx=LAC-XA;

% Now begin to displace crown
for c=1:1000

% Give output of thrustincrease=100 if program does not converge
    if c>999
        thrustmax=100*thrustmin;
        acrit=p;
        break
        break
    end

% Search for critical position of crown at the collapse state
XC = -XCMAx*c/1000;

% Verify that snap-through has not occurred
    if LAC^2>(XA-XC)^2
        YC = ((LAC^2-(XA-XC)^2)^.5)+YA;
    end

% Angle rotated so far is phiac-phiic
phiic=asin((YC-YA)/LAC);
phi=phiac-phiic;

%Find new origin O'
X_O=XA-r1*sin(prads-phi);
Y_O=YA-r1*cos(prads-phi);

% Compute new centroid for curved section AC (based on small angles)
C1 = (4/3)*rad*(sin(prads/2))/prads;
XM1=X_O+C1*cos(pi/2-prads/2+phi);
YM1=Y_O+C1*sin(pi/2-prads/2+phi);

% Compute value of thrust
rise = (YC-YA);
thrust = (M1*(XA-XM1))/(rise);
increase=thrust/thrustmin;

% Store results of thrust increase and span increase for plot at end
results(c)=increase;
xvalue(c,1)=-200*XC/L;

% Make sure snap through has not occurred
    if YC<YA
        if YA<YD
            thrustmax=1000*thrustmin;
            acrit=p;
            break
            break
            break
        end
    end

%Check for failure condition if locus reaches the extrados at support
    if YA>YD
        if thrust>Hmax
            thrustmax=Hmax;
        end
    end

```

```

                acrit=p;
                break
                break
                break
                end
            end

% Now check hinge location to see if it wants to move

% Check for hinges all the way up to the crown
Rd=r1;

f=[1];
Cv = (4/3)*rad*(sin(f*vrad/2))/(f*vrad);
Xv = X_O+Cv*cos(pi/2-prads+f*vrad/2+phi);
Yv = Y_O+Cv*sin(pi/2-prads+f*vrad/2+phi);
m = vrad*(r2^2-r1^2)/2;

% Find orientation of voussoir from horizontal
sum=pi/2-prads+f*vrad+phi;

% Find radius of pressure point one voussoir away from intrados hinge
Rf = ((M1-f*m)*(XA-X_O)+thrust*(YA-Y_O)-f*m*(Xv-
    XA))/(thrust*sin(sum)+(M1-f*m)*cos(sum));

%check for thrust line within masonry at intrados hinge
% if hinge wants to move, compute new geometry and move hinge

    if Rf<r1

%Determine span increase and dip when hinge moves for the first time
        if q<1
            spanmove=-200*XC/L;
            dipmove=(r2-YC)/t;
            thrustmove=thrust/thrustmin;
        end

        q=q+1;
        spanincrease=-200*XC/L;
        p=(n-q)*v;
        prads = (pi/180)*p;
        XA = (R-h)*sin(prads);
        YA = (R-h)*cos(prads);

% Compute maximum horizontal thrust for hinge location
        C2 = (4/3)*rad*(sin((alpha-prads)/2))/(alpha-prads);
        XM2 = C2*sin((alpha+prads)/2);
        YM2 = C2*cos((alpha+prads)/2);
        M2 = (alpha-prads)*(r2^2-r1^2)/2;
        Hmax = (M2*(XD-XM2) + M1*(XD-XA))/(YA-YD);

% Compute new length and orientation of line AC
        LAC = (((XA)^2+(r2-YA)^2)^.5);
        phiac = atan((r2-YA)/(XA));

% Compute new crown position -- end if snap-through has occurred
        if (XA-XC)>LAC
            thrustmax=Hmax;
            acrit=p;
            break

```

```

        break
        break
        end

        YC = ((LAC^2-(XA-XC)^2)^.5)+YA;
        phic=asin((YC-YA)/LAC);

% angle rotated so far is phiac-phi
phi=phiac-phi;

%Find new origin O'
X_O=XA-r1*sin(prads-phi);
Y_O=YA-r1*cos(prads-phi);

% Find weight and centroid of arch segment AC
M1 = prads*(r2^2-r1^2)/2;
C1 = (4/3)*rad*(sin(prads/2))/prads;

% Compute new centroid for curved section AC (based on small angles)
XM1=X_O+C1*cos(pi/2-prads/2+phi);
YM1=Y_O+C1*sin(pi/2-prads/2+phi);

% Compute new value of thrust
rise = (YC-YA);
thrust = (M1*(XA-XM1))/(rise);

% Store results for plot at end

% Make sure snap through has not occurred
if YC<YA
    thrustmax=1000*thrustmin;
    acrit=p;
    break
    break
    break
    break
    end

% Check for thrust line (locus) leaving masonry at support
if YA>YD
    if thrust>Hmax
        thrustmax=Hmax;
        acrit=p;
        break
        break
        break
        break
        end
    end

end

end

end

% Compute locus of pressure points at failure:
% Find orientation of voussoir from horizontal

for i = 1 : (n-q+1)

% Find centroid of rotated voussoir next to hinge
Cvi = (4/3)*rad*(sin(i*vrad/2))/(i*vrad);
Xvi = X_O+(Cvi*cos((pi/2)-prads+(i*vrad/2)+phi));

```

```

mi = i*vrad*(r2^2-r1^2)/2;
sumi=pi/2-prads+(i-1)*vrad+phi;
Ri = ((M1-mi)*(XA-X_O)+thrustmax*(YA-Y_O)-mi*(Xvi-
      XA))/(thrustmax*sin(sumi)+(M1-mi)*cos(sumi));
pressure=(Ri-r1)/t;
press(i)=pressure;

%store results to plot y-value of the locus of pressure points
  against the angle from the crown
loc(i)=Ri*sin(sumi)+Y_O;
iv(i)=X_O+(Ri*cos(sumi));
radi(i)=r1*sin(sumi)+Y_O;
rli(i)=X_O+(r1*cos(sumi));
radi2(i)=r2*sin(sumi)+Y_O;
r2i(i)=X_O+(r2*cos(sumi));
end

%Plot outline of segment AD of arch
  for j = 1 : (o-n+q+1)
    sumj=pi/2-alpha+(j-1)*vrad;
    radb(j)=r1*sin(sumj);
    r1j(j)=(r1*cos(sumj));
    rad2b(j)=r2*sin(sumj);
    r2j(j)=(r2*cos(sumj));
  end

%Plot locus of pressure points in segment AD of arch
  for k = 1 : (o-n+q+1)
% Find centroid of rotated voussoir next to hinge
    Cvk = (4/3)*rad*(sin((k-1)*vrad/2))/((k-1)*vrad);
    Xvk = (Cvk*cos((pi/2)-alpha+((k-1)*vrad/2)));
    sumk=pi/2-alpha+(k-1)*vrad;
    Rk=(m*o*XD+m*XD-m*k*Xvk+thrustmax*YD)/
      (thrustmax*sin(sumk)+m*(o-k+1)*cos(sumk));
    ylocus=Rk*sin(sumk);
    xlocus=Rk*cos(sumk);

    if k>(o-n+q)
      ylocus=r1*sin(sumk);
      xlocus=r1*cos(sumk);
    end

    if k<2
      ylocus=r2*sin(sumk);
      xlocus=r2*cos(sumk);
    end

%store results to plot the locus of pressure points in x,y co-ods.
    locb(k)=ylocus;
    kv(k)=xlocus;
  end

%Plot lines on chart
  for x=1:round(XD+2)
    lined(x)=(x-1)/tan(alpha);
    xval(x)=x-1;
  end

  for z=1:round(r2+1)
    lino(z)=z-1;
    zval(z)=0;
  end

```

```

end

beta=atan(XA/YA);

for y=1:round(XA+t+1)
lina(y)=(y-1)/tan(beta);
yval(y)=y-1;
end

beta2=atan((XA-X_0)/(YA-Y_0));
wmax=round(r2*sin(beta2)+.5);

for w=1:wmax+1
lina2(w)=Y_0+(w-1)/tan(beta2);
wval(w)=X_0+w-1;
end

smax=round(r2*sin(prads-beta2)+.5);

for s=1:smax+1
linc(s)=Y_0+(s-1)/tan(prads-beta2);
sval(s)=X_0-s+1;
end

for wr=1:2
linml(wr)=Y_0;
wrval(wr)=X_0;

    if wr>1
linml(wr)=YM1;
wrval(wr)=XM1;
    end
end

% Print out final values as output
spanincrease=-200*XC/L;
thrustincrease=thrustmax/thrustmin;
dip=(r2-YC)/t;
acrit
spanincrease
thrustincrease
dip

grid on
plot(wrval, linml, iv, loc, kv, locb, r1i, radi, r2i, radi2, r1j, radb, r2j, rad2b
    , xval, lined, zval, lino, yval, lina, wval, lina2, sval, linc)
axis([Y_0, r2, Y_0, r2])
xlabel('x-Distance, cm'), ylabel('y-Distance, cm')

```

A.2 PROGRAM ArchTilt

FOR COMPUTING THE COLLAPSE OF CIRCULAR ARCHES DUE TO CONSTANT HORIZONTAL ACCELERATION

```

% User inputs arch geometry
embrace = input('two alpha:');
alpha = (pi/180)*(embrace/2);
t_over_R = input('ratio of t/R:');

theta = (pi/2) - alpha;
drads = (pi - theta);

% Initialise minimum value criterion for ratio of a to g
agmin = [100];

% Assign arbitrary thickness to R
R = [100];

% Compute half-thickness h and thickness t from given ratio and
t = R*t_over_R;
h = t/2;

% Compute inner radius and outer radius for use in centroid
  calculations
r1 = R-h;
r2 = R+h;
rad = (r1^3 - r2^3)/(r1^2 - r2^2);

% Coordinate system is XY with origin at the centre of circle
% Find coordinates of D, the hinge at the extrados at the left
  support
XD = (R+h)*cos(drads);
YD = (R+h)*sin(drads);

% Angle a must be a whole number greater than or equal to theta
amin = (90-(embrace/2))/2;
amax = amin + embrace/5;

% Angle b must be a whole number greater than amin and less than bmax
bmax = [60];

% Angle c must be a whole number less than theta + two alpha and
  greater than b
cmax = (embrace - 10 + round((180/pi)*(theta)))/2;

%Begin iteration by assuming a value of a, and checking mechanisms
  for various locations of b and c

for a = amin : amax

    bmin = a + 2;

    for b = bmin : bmax

        cmin = b + 4;

        for c = cmin : cmax

% Compute angles in radians

```

```

arads = 2*(pi/180)*a;
brads = 2*(pi/180)*b;
crads = 2*(pi/180)*c;

% Find coordinates of hinge C
XC = (R-h)*cos(crads);
YC = (R-h)*sin(crads);

% Find coordinates of hinge B
XB = (R+h)*cos(brads);
YB = (R+h)*sin(brads);

% Find coordinates of hinge A
XA = (R-h)*cos(arads);
YA = (R-h)*sin(arads);

% Find coordinates and mass of centre of gravity of arch segment AB
Clangle = brads - arads;
Cent_1 = (4/3)*rad*(sin(Clangle/2))/Clangle;
XC1 = Cent_1*cos((brads+arads)/2);
YC1 = Cent_1*sin((brads+arads)/2);
M1 = Clangle/(drads-arads);

% Find coordinates and mass of centre of gravity of arch segment BC
C2angle = crads - brads;
Cent_2 = (4/3)*rad*(sin(C2angle/2))/C2angle;
XC2 = Cent_2*cos((brads+crads)/2);
YC2 = Cent_2*sin((brads+crads)/2);
M2 = C2angle/(drads-arads);

% Find coordinates and mass of centre of gravity of arch segment CD
C3angle = drads - crads;
Cent_3 = (4/3)*rad*(sin(C3angle/2))/C3angle;
XC3 = Cent_3*cos((drads+crads)/2);
YC3 = Cent_3*sin((drads+crads)/2);
M3 = C3angle/(drads-arads);

% Find instantaneous centre I
MDC = (YC-YD)/(XC-XD);
MAB = (YA-YB)/(XA-XB);
XI = (XD*MDC - XB*MAB - YD + YB)/(MDC - MAB);
YI = MDC*(XI - XD) + YD;

% Find ratios of rotations for the mechanism being considered
gamma = [1];
phi = gamma*((XI-XC)/(XC-XD));
psi = gamma*((XB-XI)/(XA-XB));

% Equation of work
gravity_work = -(XC3-XD)*phi*M3 - (XI-XC2)*gamma*M2 +
(XA-XC1)*psi*M1;
horiz_work = (YC3-YD)*phi*M3 + (YI-YC2)*gamma*M2 + (YC1-
YA)*psi*M1;
a_over_g = -(gravity_work/horiz_work);
ag = abs(a_over_g);

%Compare output -- if the minimum acceleration is lower than previous
values, then store the current value
if ag < agmin
agmin=ag;

```

```
A_ang = 2*a;  
B_ang = 2*b;  
C_ang = 2*c;  
lamda = a_over_g;  
end  
end  
end  
  
%Compute angle of tilt, GAMMA, for the minimum acceleration  
GAMMA = (180/pi)*atan(agmin);  
  
%Print the following variables as output  
A_ang  
B_ang  
C_ang  
GAMMA  
lamda
```

A.3 PROGRAM ArchLean

FOR COMPUTING THE COLLAPSE OF CIRCULAR ARCHES ON LEANING RECTANGULAR BUTTRESSES

```

% User defines geometry of arch
halfembrace = input('alpha:');
alpha = (pi/180)*(halfembrace);
t_over_R = input('ratio of t/R:');
v = input('voussoir size (degrees):');

% Initialise thrust
thrustmin = [0];
spread = [0];
spreadmax = [10];
thrustmax = [1];
fail = [0];
thrustincrease = [0];
acrit=[0];
ycrit=[0];
vrad=v*(pi/180);
X_O=[0];
Y_O=[0];
phi=[0];

%Density of material
density=[25];

% Assign arbitrary thickness to R
% Compute half-thickness h and thickness t from given ratio and R
R = (1.5)/((1+t_over_R/2)*sin(alpha));
t = R*t_over_R;
h = t/2;
L = (2*R+t)*sin(alpha);

% Compute inner radius and outer radius for use in centroid
  calculations
r1 = R-h;
r2 = R+h;
rad = (r1^3 - r2^3)/(r1^2 - r2^2);

% Vertical reaction at support (weight of half arch)
V = density*alpha*(r2^2-r1^2)/2;

% COMPUTE CAPACITY OF BUTTRESS
% Input proportions of rectangular buttress and height of applied
  force (given here for Case B of Chapter 7)
base=[1];
height=[6];
springing=[4.5];

%Compute weight and centroid of buttress
Wb=density*base*height;
xb=base/2;

%Compute factors for rectangular buttress
mu=springing/height;
psi=V/Wb;
% Solve for maximum horizontal thrust, Hmax, by solving the quadratic
  equation
B = (-.5-3/(2*mu)-3*psi/mu);

```

```

C = (psi+1)/mu;

%Fracture height as a percentage of arch springing height
crack = (((B^2)-4*C)^0.5) - B)/2;

    if crack>1
        crack = ((-((B^2)-4*C)^0.5) - B)/2;
    end

% If there is no (real) solution between 0 and 1, end program
    if crack>1
        crack
        break
        break
    end

%Capacity of vertical buttress
thrustcapacity = density*(base^2)*((1+2*psi)/(2*mu)-crack/3);

%Compute vertical centroid of fractured buttress including V
Wc=density*springing*crack*base/2;
Wbeffective=Wb-Wc;
ybar=(Wb*height/2+V*springing-Wc*springing*crack/3)/(Wbeffective+V);

% Coordinate system is XY with origin at the centre of circle
% Find initial coordinates at crown (hinge C)
XC = [0];
YC = R+h;

% Find coordinates of D, the extrados hinge at the support
XD = (R+h)*sin(alpha);
YD = (R+h)*cos(alpha);

% Angle a must be a whole number between the support and the crown
amin = [0];
amax = amin + (halfembrace);
bmax=halfembrace/v;

for b = 1 : bmax

a = amin + b*(amax-amin)/bmax;

% Compute angle in radians and find coordinates of a
arads = (pi/180)*a;
XA = (R-h)*sin(arads);
YA = (R-h)*cos(arads);

% Find x-coordinate of centre of gravity of arch segment AC
Cent_1 = (4/3)*rad*(sin(arads/2))/arads;
XM = Cent_1*sin(arads/2);
M = density*arads*(r2^2-r1^2)/2;

% Compute value of thrust
rise = (YC-YA);
thrust = (M*(XA-XM))/(rise);

    if thrust > thrustmin
        thrustmin=thrust;
        ainit=a;
    end

```

```

end
end

% Print critical hinge location (from crown) and minimum thrust
ainit
thrustmin

% Compute pressure point at base in original configuration
nu=(1/base)*(V*base+Wb*xb-thrustmin*springing)/(Wb+V);
nunit=nu;

% Now impose displacements and find new position and new thrust
% Impose horizontal displacements only

% Search possible hinge locations

% Compute angle in radians and find coordinates of intrados hinge
% Round to nearest voussoir
n=(ainit/v);
o=(halfembrace/v);
q=[0];

p=(n-q)*v;
prads = (pi/180)*p;
XA = (R-h)*sin(prads);
YA = (R-h)*cos(prads);

% Find weight of arch segment AC
C1 = (4/3)*rad*(sin(prads/2))/prads;
XM1 = C1*sin(prads/2);
YM1 = C1*cos(prads/2);
M1 = density*prads*(r2^2-r1^2)/2;

% Compute maximum horizontal thrust for hinge location

% Find x-coordinate of centre of gravity of arch segment DA
C2 = (4/3)*rad*(sin((alpha-prads)/2))/(alpha-prads);
XM2 = C2*sin((alpha+prads)/2);
M2 = density*(alpha-prads)*(r2^2-r1^2)/2;

% Compute maximum thrust supported by section DA
Hmax = (M2*(XD-XM2) + M1*(XD-XA))/(YA-YD);

% Compute initial length and orientation of line AC
LAC = (((XA-XC)^2+(YC-YA)^2)^.5);
phiac = atan((YC-YA)/(XA));

% Determine maximum amount of spreading before snapthrough occurs
XCMAx=LAC-XA;

% Compute and store values for calculating thrust in case of
stationary hinge
ainitrads = (pi/180)*ainit;
XAinit = (R-h)*sin(ainitrads);
YAinit = (R-h)*cos(ainitrads);
Clinit = (4/3)*rad*(sin(ainitrads/2))/ainitrads;
XMlinit = Clinit*sin(ainitrads/2);
Mlinit = density*ainitrads*(r2^2-r1^2)/2;
LACinit=LAC;
phiacinit=phiac;

```

```

% Now begin to displace crown

for c=1:1000

% Give output of thrustincrease=100 if maximum spread occurs
    if c>999
        thrustmax=100*thrustmin;
        acrit=p;
        break
    end

% Search for critical position of crown at collapse
XC = -XCMAx*c/1000;
YC = ((LAC^2-(XA-XC)^2)^.5)+YA;

% Angle rotated so far is phiac-phiic
phiic=asin((YC-YA)/LAC);
phi=phiac-phiic;

%Find new origin O'
X_O=XA-r1*sin(prads-phi);
Y_O=YA-r1*cos(prads-phi);

% Compute new centroid for curved section AC measured from displaced
    origin
XM1=X_O+C1*sin(prads/2-phi);

% Compute value of thrust
rise = (YC-YA);
thrust = (M1*(XA-XM1))/(rise);

% Compute angle of tilt in degrees
tilt = -XC/springing;
lean = tilt*180/pi;

% Check to see if buttress capacity is exceeded
leanreduction=ybar*tilt*(Wbeffective+V)/springing;
leaningcapacity=thrustcapacity-leanreduction;

    if thrust>leaningcapacity
        thrust=leaningcapacity;
        nu=[0];
        break
    end

increase=thrust/thrustcapacity;
increase2=leaningcapacity/thrustcapacity;

% Store results for plot at end
results(c)=increase;
xvalue(c)=lean;
results2(c)=increase2;

%Compute and store thrust in case of hinge not moving for comparison
YCinit = ((LACinit^2-(XAinit-XC)^2)^.5)+YAinit;
phiicinit=asin((YCinit-YAinit)/LACinit);
phiiinit=phiacinit-phiicinit;
X_Oinit=XAinit-r1*sin(ainitrads-phiiinit);
Y_Oinit=YAinit-r1*cos(ainitrads-phiiinit);

```

```

XMlinit=X_Oinit+Clinit*sin(ainitrads/2-phiinit);
riseinit = (YCinit-YAinit);
thrustinit = (Mlinit*(XAinit-XMlinit))/(riseinit);
initresults(c)=thrustinit/thrustmin;

% End program if snap through has occurred
if YC<YA
    if YA<YD
        thrustmax=1000*thrustmin;
        acrit=p;
        break
        break
        break
    end
end

%Check for failure due to formation of 5-hinge mechanism
if YA>YD
    if thrust>Hmax
        thrustmax=Hmax;
        acrit=p;
        break
        break
        break
    end
end

%Now check hinge location to see if it wants to move

% Find centroid of rotated voussoir next to hinge
Cv = (4/3)*rad*(sin(vrads/2))/vrads;
Xv = X_O+Cv*cos(pi/2-prads+vrads/2+phi);
Yv = Y_O+Cv*sin(pi/2-prads+vrads/2+phi);
m = density*vrads*(r2^2-r1^2)/2;

% Find orientation of voussoir (U) from horizontal
sum=pi/2-prads+vrads+phi;

% Find radius of pressure point one voussoir away from intrados hinge
Rd = ((M1-m)*(XA-X_O)+thrust*(YA-Y_O)-m*(Xv-
    XA))/(thrust*sin(sum)+(M1-m)*cos(sum));

% Check for thrust line within masonry at intrados hinge
% If hinge wants to move, compute new geometry and move hinge

    if Rd<r1

%Determine span increase and dip when hinge moves for the first time
    if q<1
        spanmove=-200*XC/L;
        dipmove=(r2-YC)/t;
        thrustmove=thrust/thrustmin;
    end

% Move hinge at A to next voussoir
    q=q+1;
    spanincrease=-200*XC/L;
    p=(n-q)*v;
    prads = (pi/180)*p;
    XA = (R-h)*sin(prads);

```

```

YA = (R-h)*cos(prads);

% Compute maximum horizontal thrust for hinge location
C2 = (4/3)*rad*(sin((alpha-prads)/2))/(alpha-prads);
XM2 = C2*sin((alpha+prads)/2);
M2 = density*(alpha-prads)*(r2^2-r1^2)/2;
Hmax = (M2*(XD-XM2) + M1*(XD-XA))/(YA-YD);

% Compute new length and orientation of line AC
LAC = (((XA)^2+(r2-YA)^2)^.5);
phiac = atan((r2-YA)/(XA));

    if (XA-XC)>LAC
        results2(c)=Hmax/thrustmin;
        pvalue(c)=p;
        thrustmax=Hmax;
        acrit=p;
        break
    break
    break
    end

YC = ((LAC^2-(XA-XC)^2)^.5)+YA;
phic=asin((YC-YA)/LAC);

% angle rotated so far is phiac-phic
phi=phiac-phic;

%Find new origin O'
X_O=XA-r1*sin(prads-phi);
Y_O=YA-r1*cos(prads-phi);

% Find weight and centroid of rotated arch segment AC
M1 = density*prads*(r2^2-r1^2)/2;
C1 = (4/3)*rad*(sin(prads/2))/prads;

% Compute new centroid for curved section AC measured from new origin
XM1 =X_O+C1*sin(prads/2);

% Compute value of thrust
rise = (YC-YA);
thrust = (M1*(XA-XM1))/(rise);

results4(c)=thrust/thrustmin;
pvalue(c)=p;

% Make sure snap through has not occurred
if YC<YA
    if YA<YD
        thrustmax=1000*thrustmin;
        acrit=p;
        break
    break
    break
    break
    end

    if YA>YD
        if thrust>Hmax
            thrustmax=Hmax;

```

```

                                acrit=p;
                                break
                                break
                                break
                                break
                                end
                            end
                        end
                    end

% Compute locus of pressure points at failure:
% Find orientation of voussoir from horizontal

for i = 1 : (n-q+1)

% Find centroid of rotated voussoir next to hinge
Cvi = (4/3)*rad*(sin(i*vrad/2))/(i*vrad);
Xvi = X_O+(Cvi*cos((pi/2)-prad+(i*vrad/2)+phi));
mi = density*i*vrad*(r2^2-r1^2)/2;
sumi=pi/2-prad+(i-1)*vrad+phi;
Ri = ((M1-mi)*(XA-X_O)+thrust*(YA-Y_O)-mi*(Xvi-
        XA))/(thrust*sin(sumi)+(M1-mi)*cos(sumi));
pressure=(Ri-r1)/t;
end

spanincrease=-200*XC/L;
thrustincrease=thrustmax/thrustmin;
dip=(r2-YC)/t;
acrit
spanincrease
thrustincrease

%Compute new pressure point in unfractured buttress
if nu>0
nulean=ybar*tilt/base;
nu=nuinit-nulean;
end

grid on
plot(xvalue,results,xvalue,results2)
axis([0,lean+.5,0,1])
xlabel('% Buttress lean, degs'),ylabel('Thrust Increase = H/Buttress
        Capacity')

```

A.4 PROGRAM *ButtressTilt*

```

FOR COMPUTING THE COLLAPSE OF CIRCULAR ARCHES SUPPORTED ON
RECTANGULAR BUTTRESSES DUE TO CONSTANT HORIZONTAL ACCELERATION

% User defines geometry of arch
embrace = input('two alpha:');
alpha = (pi/180)*(embrace/2);
t_over_R = input('ratio of t/R:');
theta = (pi/2) - alpha;
drads = (pi - theta);

% User inputs depth-density of material here
density=[25];

% Initialise minimum value criterion for ratio of a to g
agmin = [100];

% Compute half-thickness h and thickness t from given ratio and R
R = (1)/((1+t_over_R/2)*sin(alpha));
t = R*t_over_R;
h = t/2;

% Compute span of arch
L = (2*R+t)*sin(alpha);

% Compute inner radius and outer radius for use in centroid calcs
r1 = R-h;
r2 = R+h;
rad = (r1^3 - r2^3)/(r1^2 - r2^2);

% Vertical reaction at support (weight of half arch)
V = density*alpha*(r2^2-r1^2)/2;

% COMPUTE CAPACITY OF BUTTRESS
% User inputs buttress geometry here (Case A used for example)
base=[1];
height=[3];
springing=[2];

%Compute weight and centroid of solid buttress
Wb= density*base*height;
xb=base/2;

%Compute factors for rectangular buttress
mu=springing/height;
psi=V/Wb;
% Solve for maximum horizontal thrust, Hmax, from quadratic eqn.
B = (-.5-3/(2*mu)-3*psi/mu);
C = (psi+1)/mu;
%Fracture height as a percentage of arch springing height
crack = (((B^2)-4*C)^0.5) - B)/2;

% End program if no real solution exists
if crack>1
crack = ((-((B^2)-4*C)^0.5) - B)/2;
end

if crack>1
crack
break

```

```

break
end

%Capacity of vertical buttress
thrustcapacity = density*(base^2)*((1+2*psi)/(2*mu)-crack/3);

% Coordinate system is XY with origin at the centre of circle
% Find coordinates of D, the hinge at the base of the buttress
XD = -(R+h)*cos(theta)-base;
YD = (R+h)*sin(theta)-springing;

%Compute centroid of fractured buttress
Wc=density*springing*crack*base/2;
Wbeffective=Wb-Wc;
ybar=YD+(Wb*height/2-Wc*springing*crack/3)/Wbeffective;
xbar=XD+(Wb*xb-Wc*base*2/3)/Wbeffective;

% Angle a must be a whole number greater than or equal to theta
amin = (90-(embrace/2))/2;
amax = amin + embrace/5;

% Angle b must be a whole number greater than amin and less than bmax
bmax = [60];

% Angle c must be a whole number less than theta + two alpha and
greater than b
cmax = (embrace + round((180/pi)*(theta)))/2;

%Begin iteration by assuming a value of a, and checking mechanisms
for various locations of b and c

for a = amin : amax

    bmin = a + 10;

    for b = bmin : bmax

        cmin = b + 10;

        for c = cmin : cmax

% Compute angles in radians
arads = 2*(pi/180)*a;
brads = 2*(pi/180)*b;
crads = 2*(pi/180)*c;

% Find coordinates of hinge C
XC = (R-h)*cos(crads);
YC = (R-h)*sin(crads);

% Find coordinates of hinge B
XB = (R+h)*cos(brads);
YB = (R+h)*sin(brads);

% Find coordinates of hinge A
XA = (R-h)*cos(arads);
YA = (R-h)*sin(arads);

% Find coordinates and mass of centre of gravity of arch segment AB
Clangle = brads - arads;
Cent_1 = (4/3)*rad*(sin(Clangle/2))/Clangle;

```

```

XC1 = Cent_1*cos((brads+arads)/2);
YC1 = Cent_1*sin((brads+arads)/2);
M1 = density*C1angle*(r2^2-r1^2)/2;

% Find coordinates and mass of centre of gravity of arch segment BC
C2angle = crads - brads;
Cent_2 = (4/3)*rad*(sin(C2angle/2))/C2angle;
XC2 = Cent_2*cos((brads+crads)/2);
YC2 = Cent_2*sin((brads+crads)/2);
M2 = density*C2angle*(r2^2-r1^2)/2;

% Find coordinates and mass of centre of gravity of arch segment CD
C3angle = drads - crads;
Cent_3 = (4/3)*rad*(sin(C3angle/2))/C3angle;
M3arch = density*C3angle*(r2^2-r1^2)/2;
XC3=(M3arch*Cent_3*cos((drads+crads)/2)+Wbeffective*xbar)/
(Wbeffective+M3arch);
YC3=(M3arch*Cent_3*sin((drads+crads)/2)+Wbeffective*ybar)/
(Wbeffective+M3arch);;
M3 = M3arch+Wbeffective;

% Finding instantaneous centre I
MDC = (YC-YD)/(XC-XD);
MAB = (YA-YB)/(XA-XB);
XI = (XD*MDC - XB*MAB - YD + YB)/(MDC - MAB);
YI = MDC*(XI - XD) + YD;

% Finding ratios of rotations for the given mechanism
gamma = [1];
phi = gamma*((XI-XC)/(XC-XD));
psi = gamma*((XB-XI)/(XA-XB));

% Equation of work
gravity_work = -(XC3-XD)*phi*M3-(XI-XC2)*gamma*M2+(XA-
XC1)*psi*M1;
horiz_work=(YC3-YD)*phi*M3+(YI-YC2)*gamma*M2+(YC1-YA)*psi*M1;
a_over_g = -(gravity_work/horiz_work);
ag = abs(a_over_g);

%Compare output -- if the minimum acceleration is lower than previous
values, then store the current value
if ag < agmin
agmin=ag;
A_ang = 2*a;
B_ang = 2*b;
C_ang = 2*c;
lamda = a_over_g;
end
end
end

%Compute angle of tilt, GAMMA, for the minimum acceleration
GAMMA = (180/pi)*atan(agmin);

%Print the following variables as output
A_ang
B_ang
C_ang
GAMMA
lamda

```

A.5 PROGRAM *SolidTilt*

```

FOR COMPUTING THE COLLAPSE OF CIRCULAR ARCHES SUPPORTED ON
RECTANGULAR BUTTRESSES DUE TO CONSTANT HORIZONTAL ACCELERATION
ASSUMING THAT THE BUTTRESS REMAINS SOLID AND DOES NOT FRACTURE

% User defines geometry of arch
embrace = input('two alpha:');
alpha = (pi/180)*(embrace/2);
t_over_R = input('ratio of t/R:');

theta = (pi/2) - alpha;
drads = (pi - theta);

% User inputs depth-density of material here
density=[25];

% Initialise minimum value criterion for ratio of a to g
agmin = [100];

% Compute half-thickness h and thickness t from given ratio and R
R = (1)/((1+t_over_R/2)*sin(alpha));
t = R*t_over_R;
h = t/2;

% Compute span of arch
L = (2*R+t)*sin(alpha);

% Compute inner radius and outer radius for use in centroid calcs
r1 = R-h;
r2 = R+h;
rad = (r1^3 - r2^3)/(r1^2 - r2^2);

% Vertical reaction at support (weight of half arch)
V = density*alpha*(r2^2-r1^2)/2;

% User inputs buttress geometry here (Case A used for example)
base=[1];
height=[3];
springing=[2];

%Compute weight and centroid of solid buttress
Wb= density*base*height;
xb=base/2;

% Coordinate system is XY with origin at the centre of circle
% Find coordinates of D, the hinge at the base of the buttress
XD = -(R+h)*cos(theta)-base;
YD = (R+h)*sin(theta)-springing;

%%%%%LEAVE BUTTRESS AS SOLID%%%%%%%%%%
Wbeffective=Wb;
ybar=YD+height/2;
xbar=XD+xb;
%%%%%

% Angle a must be a whole number greater than or equal to theta
amin = (90-(embrace/2))/2;
amax = amin + embrace/5;

% Angle b must be a whole number greater than amin and less than bmax

```

```

bmax = [60];

% Angle c must be a whole number less than theta + two alpha and
% greater than b
cmax = (embrace + round((180/pi)*(theta)))/2;

%Begin iteration by assuming a value of a, and checking mechanisms
% for various locations of b and c

for a = amin : amax

    bmin = a + 10;

    for b = bmin : bmax

        cmin = b + 10;

        for c = cmin : cmax

% Compute angles in radians
            arads = 2*(pi/180)*a;
            brads = 2*(pi/180)*b;
            crads = 2*(pi/180)*c;

% Find coordinates of hinge C
            XC = (R-h)*cos(crads);
            YC = (R-h)*sin(crads);

% Find coordinates of hinge B
            XB = (R+h)*cos(brads);
            YB = (R+h)*sin(brads);

% Find coordinates of hinge A
            XA = (R-h)*cos(arads);
            YA = (R-h)*sin(arads);

% Find coordinates and mass of centre of gravity of arch segment AB
            C1angle = brads - arads;
            Cent_1 = (4/3)*rad*(sin(C1angle/2))/C1angle;
            XC1 = Cent_1*cos((brads+arads)/2);
            YC1 = Cent_1*sin((brads+arads)/2);
            M1 = density*C1angle*(r2^2-r1^2)/2;

% Find coordinates and mass of centre of gravity of arch segment BC
            C2angle = crads - brads;
            Cent_2 = (4/3)*rad*(sin(C2angle/2))/C2angle;
            XC2 = Cent_2*cos((brads+crads)/2);
            YC2 = Cent_2*sin((brads+crads)/2);
            M2 = density*C2angle*(r2^2-r1^2)/2;

% Find coordinates and mass of centre of gravity of arch segment CD
            C3angle = drads - crads;
            Cent_3 = (4/3)*rad*(sin(C3angle/2))/C3angle;
            M3arch = density*C3angle*(r2^2-r1^2)/2;
            XC3=(M3arch*Cent_3*cos((drads+crads)/2)+Wbeffective*xbar)/
                (Wbeffective+M3arch);
            YC3=(M3arch*Cent_3*sin((drads+crads)/2)+Wbeffective*ybar)/
                (Wbeffective+M3arch);;
            M3 = M3arch+Wbeffective;

% Finding instantaneous centre I

```

```

MDC = (YC-YD)/(XC-XD);
MAB = (YA-YB)/(XA-XB);
XI = (XD*MDC - XB*MAB - YD + YB)/(MDC - MAB);
YI = MDC*(XI - XD) + YD;

% Finding ratios of rotations for the given mechanism
gamma = [1];
phi = gamma*((XI-XC)/(XC-XD));
psi = gamma*((XB-XI)/(XA-XB));

% Equation of work
gravity_work = -(XC3-XD)*phi*M3 - (XI-XC2)*gamma*M2 + (XA-
XC1)*psi*M1;
horiz_work = (YC3-YD)*phi*M3 + (YI-YC2)*gamma*M2 + (YC1-
YA)*psi*M1;
a_over_g = -(gravity_work/horiz_work);
ag = abs(a_over_g);

%Compare output -- if the minimum acceleration is lower than previous
values, then store the current value
if ag < agmin
    agmin=ag;
    A_ang = 2*a;
    B_ang = 2*b;
    C_ang = 2*c;
    lamda = a_over_g;
end
end
end

%Compute angle of tilt, GAMMA, for the minimum acceleration
GAMMA = (180/pi)*atan(agmin);

%Print the following variables as output
A_ang
B_ang
C_ang
GAMMA
lamda

```

APPENDIX B: EXPERIMENTAL DESCRIPTIONS

B.1 Description of Model Blocks

The blocks were cut from a plywood sheet, and coated uniformly with a layer of glue and sand to increase the coefficient of friction of the blocks. Each whole block measured approximately 51 x 51 x 27 mm, and weighed 38.4 grams on average. Each half block was approximately one half this dimension, weighing 19.4 grams on average and measuring 26 x 26 x 27 mm.

B.2 Construction of Model Buttresses

Each model buttress was constructed of alternating layers of model blocks as illustrated below in Figure B.1.



(a) Rectangular buttress

(b) T-buttress with adjoining wall

Figure B.1 Layout of blocks for each buttress experiment presented in Chapter 3.

B.3. Predictions for Buttress Experiments

Figures B.2 and B.3 illustrate the predictions for the four buttress experiments presented in Chapter 3. These predictions are based on the methods outlined in Chapter 3 for rectangular buttresses and T-shaped buttresses. All four buttresses were built to a height of 72.8 cm, with the horizontal load applied at a height of 36.4 cm.

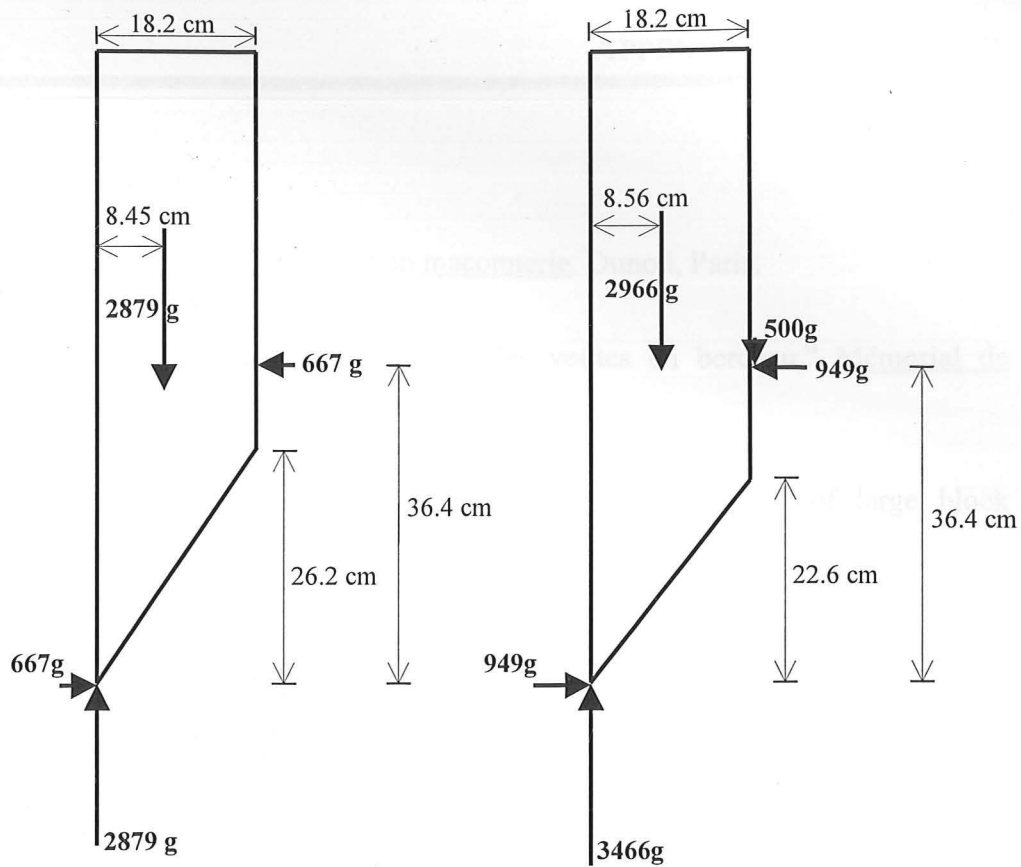


Figure B.2. Predicted fracture location and collapse state for tests on rectangular buttresses (Section 3.8).

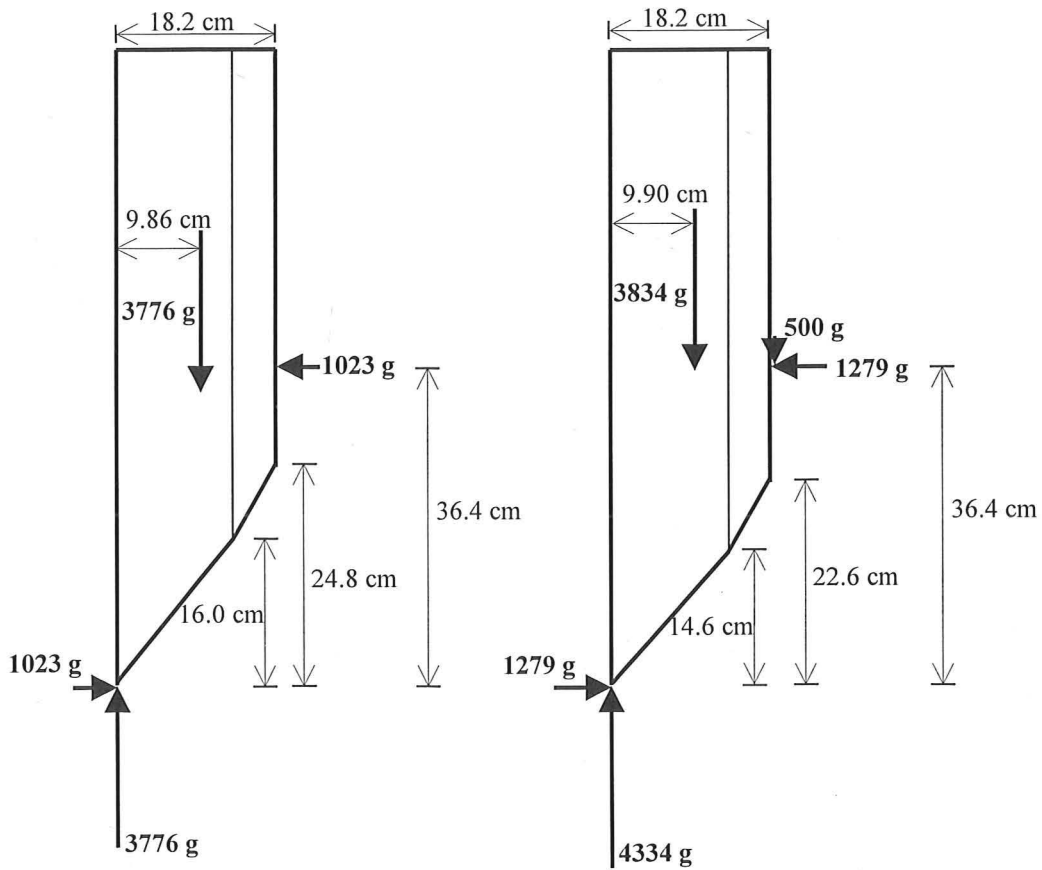


Figure B.3. Predicted fracture location and collapse state for tests on T-shaped buttresses (Section 3.8).

APPENDIX C: REFERENCES

- Aragon, E. (1909). Ponts et ouvrages en maçonnerie. Dunod, Paris.
- Audoy, (1820). "Mémoire sur la poussée des voûtes en berceau," Mémorial de l'Officier du Génie, Vol. 4, pp. 1-96, plates I-VI.
- Augusti, G. and Sinopoli, A. (1992). "Modelling the dynamics of large block structures," Meccanica, Vol. 27, 1992, pp. 195-212.
- Baggio, C. and Trovalusci, P. (1995). "Stone assemblies under in-plane actions: comparison between nonlinear discrete approaches," Computer Methods in Structural Masonry, Vol. 3, pp. 184-193.
- Bhatia, S.C., Kumar, M.R., and Gupta, H.K. (1999). "A probabilistic seismic hazard map of India and adjoining regions," GSHAP Summary Volume, Annali di Geofisica, Vol. 42, No. 6, December 1999, pp. 1153-1166.
- Bélibidor, B. F. (1729). La Science des ingénieurs dans la conduite des travaux de fortification et d'architecture civile... Nouvelle édition avec des notes par M. Navier, 1823, F. Didot, Paris.
- Boothby, T.E. and Brown, C.B. (1992). "Stability of masonry piers and arches," Journal of Engineering Mechanics, ASCE, Vol. 118, No. 2, February, pp. 367-383.
- Boothby, T.E. (1994). "Stability of masonry piers and arches including sliding," Journal of Engineering Mechanics, ASCE, Vol. 120, No. 2, 304-319.
- Boothby, T.E. (2001). "Analysis of masonry arches and vaults," Progress in Structural Engineering and Materials, Vol. 3, pp. 246-256.
- Burland, J.B. (2001). "The stabilisation of the Leaning Tower of Pisa," Ingenia, Royal Academy of Engineering, London, Vol. 10, November, 2001.

Castigliano, C.A.P. (1879). Théorie de l'équilibre des systèmes élastiques et ses applications, Augusto Federico Negro, Turin. Elastic Stresses in Structures, translated by E.S. Andrews. Scott, Greenwood and Son, London, 1919. Republished with an introduction by G.A.E. Oravas, The Theory of Equilibrium of Elastic Systems and its Applications. Dover, New York, 1966.

Clemente, P. (1998a). "Introduction to dynamics of stone arches," International Journal of Earthquake Engineering and Structural Dynamics, Vol. 27.

Clemente, P., and Raithel, A., (1998b). "The mechanism model in the seismic check of stone arches," Arch Bridges, Sinopoli, A., (Ed.), Rotterdam, pp. 123-129.

Croci, G. (1998). "The Basilica of St. Francis of Assisi after the September 1997 earthquake," Structural Engineering International, January, pp. 56-58.

Deshpande, S.C. and Savant, S. (2001). "Restoration of Capella da Nossa Senhora do Monte - Old Goa," Historical Constructions 2001, Proceedings of the 3rd International Seminar, Guimaraes, Portugal, 7-9 November, 2001, pp. 1081-1090.

Dupuit, (1870). Traité de l'équilibre des voûtes et de la construction des ponts en maçonnerie. Dunod Editeur, Paris.

Gauthey, E. M. (1809). Traité de la construction des ponts, 2 vols., F. Didot, Paris. (2nd ed., 1832; 3rd ed., 1843).

Gilbert, M. and Melbourne, C. (1994). "Rigid-block analysis of masonry structures," Structural Engineer, Vol. 72, pp. 356-361.

Harvey, W. J. (1988). "The application of the mechanism analysis to arch bridges." Structural Engineer, Vol. 66, pp. 77-84.

Haupt, H. (1853). General Theory of Bridge Construction, Appleton and Co., New York, 268 pp., 16 plates.

Heyman, J. (1966). "The stone skeleton," International Journal of Solids and Structures, Vol. 2, pp. 249-279.

Heyman, J. (1967). "On shell solutions for masonry domes," International Journal of Solids Structures, Vol. 3, pp. 227-241.

Heyman, J. (1969). "The safety of masonry arches," International Journal of Mechanical Sciences, Vol. 11, pp. 363-385.

Heyman, J. (1972). Coulomb's Memoir on Statics: An Essay in the History of Civil Engineering, Cambridge University Press, 212 pp.

Heyman, J. (1980). "The estimation of the strength of masonry arches," Proceedings of the Institution of Civil Engineers, Vol. 69, pp. 921-937.

Heyman, J. (1982). "Calculation of abutment sizes for masonry bridges," Colloquium on History of Structures, International Association of Bridge and Structural Engineers, London, 1982. (Reproduced in Heyman, J., Arches, Vaults, and Buttresses: Collected Essays, Aldershot: Variorum, Ashgate Publishing, 1996, 418 pp.)

Heyman, J. (1983). "Chronic defects in masonry vaults: Sabouret's cracks," Monumentum, Vol. 26, pp. 131-141. (Reproduced in Heyman, J., Arches, Vaults, and Buttresses: Collected Essays, Aldershot: Variorum, Ashgate Publishing, 1996.)

Heyman, J. (1988). "Poleni's problem," Proceedings of the Institution of Civil Engineers, Vol. 84, pp. 737-759.

Heyman, J. (1992). "Leaning towers," Meccanica, Vol. 27, 1992, pp. 153-159.

Heyman, J. (1993). "The collapse of stone vaulting," Structural Repair and Maintenance of Historical Buildings III, C.A. Brebbia and R.J.B. Frewer (Eds.), Southampton: Computational Mechanics Publications, pp. 327-338.

Heyman, J. (1995). The Stone Skeleton: Structural engineering of masonry architecture, Cambridge University Press, 160 pp.

Heyman, J. (1998). Structural Analysis: A historical approach, Cambridge University Press, 174 pp.

Housner, W.G. (1963). "The behavior of inverted pendulum structures during earthquakes," Bulletin of the Seismological Society of America, Vol. 53, pp. 403-417.

Huerta, S. (1990). "Diseño estructural de arcos, bóvedas y cúpulas en España, ca. 1500-1800", PhD dissertation, Escuela Técnica Superior de Arquitectura, Polytechnic University of Madrid.

Huerta, S. and López, G. (1997). "Stability and consolidation of an ashlar barrel vault with great deformations: the church of Guimarei," Structural Studies, Repairs and Maintenance of Historical Buildings, S. Sánchez-Beitia and C.A. Brebbia (Eds.), Southampton: Computational Mechanics Publications, pp. 587-596.

Huerta, S. (1999). "The medieval 'scientia' of structures: the rules of Rodrigo Gil de Hontañón," Omaggio a Edoardo Benvenuto, Genoa, Italy, 29-30 November, 1999.

Hughes, T.G. and Blackler, M.J. (1997). "A review of the UK masonry arch assessment methods," Proceedings of the Institution of Civil Engineers, Structures and Buildings, Vol. 122, August, 1997, pp. 305-315.

Kurrer, K.E. (1997). "Zur Entwicklungsgeschichte der Gewölbetheorien von Leonardo da Vinci bis ins 20. Jahrhundert," Zeitschrift für Geschichte der Baukunst, 1997, pp. 87-114.

La Hire, P. (1712). "Sur la construction des voûtes dans les édifices." Mémoires de l'Académie Royale des Sciences de Paris, Paris, 70-78.

La Mendola, L. and Papia, M. (1993). "Stability of masonry piers under their own weight and eccentric load," Journal of Structural Engineering, ASCE, Vol. 119, No. 6, pp. 1678-1693.

Lipscombe, P.R., and Pellegrino, S. (1993). "Free rocking of prismatic blocks," Journal of Engineering Mechanics, ASCE, Vol. 119, pp. 1387-1410.

Livesley, R.K. (1978). "Limit analysis of structures formed from rigid blocks," International Journal for Numerical Methods in Engineering, Vol. 12, pp. 1853-1871.

Lucchesi, M., Padovani C., Pasquinelli, G., and Zani, N., (1997). "On the collapse of masonry arches," Meccanica, Vol. 32, pp. 327-346.

Lucchesi, M., Padovani C., Pasquinelli, G., and Zani, N., (1999). "The maximum modulus eccentricities surface for masonry vaults and limit analysis," Mathematics and Mechanics of Solids, Vol. 4, pp. 71-87.

Makris, M. and Roussos, Y. (2000). "Rocking response of rigid blocks under near-source ground motions," Géotechnique, Vol. 50, No. 3, pp. 243-262.

Mamaghani, I.H.P., Aydan, O., and Kajikawa, Y., (1999) "Analysis of masonry structures under static and dynamic loading by discrete finite element method," Journal of Structural Engineering/Earthquake Engineering, Japanese Society of Civil Engineers, Vol. 16, No. 2, July 1999, pp. 75-86.

Medero Navedo, J.A., Boothby, T.E., Smith, E., (1998). "The nave of the Madeleine of Vézelay," Engineering Structures, Vol. 20, Nos. 1-2, pp. 25-36.

Melbourne, C., (Editor), (1995). Proceedings of the First International Conference on Arch Bridges, Bolton, UK, 3-5 September, 1995, 693 pps.

Milankovitch, M. (1907). "Theorie der Druckkurven." Zeitschrift für Mathematik und Physik, Vol. 55, pp. 1-27.

Milankovitch, M. (1910). "Zur Statik der massiven Widerlager." Zeitschrift für Mathematik und Physik, Vol. 58, pp. 120-128.

Monasterio, (ca. 1800). "Nueva teorica sobre el empuje de bovedas." *Unpublished Manuscript*. Library of the Escuela Técnica Superior de Ingenieros de Caminos, Canales y Puertos, Univ. Politécnica de Madrid, Spain.

Moseley, H., (1843). The Mechanical Principles of Engineering and Architecture, Longman, London.

Navier, C.L.M.H., (1826). Résumé des leçons données à l'École des Ponts et Chaussées, sur l'application de la mécanique à l'établissement des constructions et des machines. Paris.

- Ng, K.H., Fairfield, C.A., and Sibbald, A., (1999). "Finite-element analysis of masonry arch bridges," Proceedings of the Institution of Civil Engineers Structures and Buildings, Vol. 134, May, 1999, pp. 119-127.
- O'Dwyer, D., (1999). "Funicular analysis of masonry vaults," Computers and Structures, Vol. 73, pp. 187-197.
- Oppenheim, I.J., (1982). "Limit analysis of masonry domes," Proceedings of Second North American Masonry Conference, College Park, Maryland, 16 pp.
- Oppenheim, I.J., Gunaratnam, D.J., Allen, R.H., (1989). "Limit state analysis of masonry domes," Journal of Structural Engineering, Vol. 115, No. 4, April, 1989, pp 868-882.
- Oppenheim, I.J., (1992). "The masonry arch as a four-link mechanism under base motion," Earthquake Engineering and Structural Dynamics, Vol. 21, pp.1005-1017.
- Persy, N., (1834). Cours de Stabilité des Constructions à l'usage des Élèves de l'Ecole d'Application de l'Artillerie et du Génie, Lithographie de l'Ecole d'Application, Metz, France.
- Petit. (1835). "Mémoire sur le calcul des voûtes circulaires." Mémorial de l'Officier du Génie, Paris, no. 12, pp. 73-150.
- Rankine, W.J., (1858). Manual of Applied Mechanics, Charles Griffin, London.
- Sanabria, S.L., (1982). "The Mechanization of Design in the 16th Century: The Structural Formulae of Rodrigo Gil de Hontañón." Journal of the Society of Architectural Historians, Vol. 41, pp. 281-293.
- Scott, G.G., (1879). Personal and Professional Recollections. London. (New edition: Paul Watkins Publishing, London, 1995, 608 pp.)
- Seguin, (1826). "Expériences sur la pesanteur spécifique et la résistance au renversement de bâtisse". Des ponts en fil de fer. Bachelier, Paris.
- Smars, P., (2000). "Etudes sur la stabilité des arcs et voûtes," Ph.D. dissertation, Catholic University in Leuven, Belgium, March 2000, 229 pp.

Spence, R.J.S., and D'Ayala, D., (1999). "Damage assessment and analysis of the 1997 Umbria-Marche earthquake," Structural Engineering International, 3/99, IABSE, Zurich, Switzerland, pp. 229-233.

UDEC (2000), Version 3.1, Universal Distinct Element Code (UDEC): User's Guide, 1st Edition, January, 2000, Itasca Consulting Group, Minneapolis, Minnesota, USA.

Vicat, L.J., (1832). "Influence du mode d'attache des chaines sur la résistance des ponts suspendus," Annales des ponts et chaussées, Paris, pp. 394-397.

Vilnay, O., (1988). "Dynamical behaviour of three-vousoir arch," Journal of Structural Engineering, Vol. 114, No. 5, pp. 1173-1186.

Viollet-le-Duc, E.E. (1854). Dictionnaire Raisonné de L'Architecture Française. Vol. 2, "Construction," Paris.

Walther, F., (1855). "Praktisches Verfahren zur Construction der Mittellinie des Brucks in Tonnengewölben," Zeitschrift für Bauwesen, Vol. 4, pp. 384-392.

